2012

Investigation of oxidative DNA damage from ionizing radiation

Suaad Audat Abdallah
The University of Toledo

Investigation of Oxidative DNA Damage from Ionizing Radiation

By

Suaad Audat Abdallah

Submitted to the Graduate Faculty as partial fulfillment of the requirements for

the Doctor of Philosophy Degree in Medicinal Chemistry

_____

Amanda Bryant-Friedrich, Ph.D., Committee Chair

_____

Hermann v.Grafenstein, Ph.D., Committee Member

_____

Viranga Tillekeratne, Ph.D., Committee Member

_____

Dragan Isailovic, Ph.D., Committee Member

_____

Patricia Komuniecki, Ph.D., Dean College of Graduate Studies

The University of Toledo

December 2012

An Abstract of

Investigation of Oxidative DNA Damage from Ionizing Radiation

by

Suaad Audat Abdallah

Submitted to the Graduate Faculty as partial fulfillment of the requirements for

the Doctor of Philosophy Degree in Medicinal Chemistry

The University of Toledo

December 2012

Oxidative damage to deoxyribonucleic acids (DNA) caused by the direct and indirect effect of ionizing radiation and endogenously produced reactive oxygen species (ROS) can lead to mutations, carcinogenesis and cell death. Damage from ionizing radiation is partially produced by secondary low energy electrons (LEEs) that form along the ionization track. Although it has been established that LEEs can result in the formation of single and double strand breaks, the mechanism of formation of these associated lesions has not been established. It has been shown that addition of low energy electrons to DNA components leads to the formation of transient radical anions that undergo bond cleavage by dissociative electron attachment. The formation of these reactive intermediates causes the generation of carbon-centered radicals on the sugar moiety. Therefore, it is believed that carbon-centered radicals play a fundamental role in this process. One of the intermediates formed is the C2',3'-dideoxythymidinyl radical (**102**). The goal of this project is to investigate the fate of the C2',3'-dideoxy-C3'-thymidinyl radical in DNA, an intermediate of DNA-LEE interactions. Synthesis of α- and β-C3'-deoxy-3'-pivaloylthymidine (**101** and **103**, respectively) as radical precursors

of this intermediate has been completed and their efficiencies in radical generation has been evaluated. Through photolysis ($\lambda \geq 320$ nm) of these modified thymidines under anaerobic conditions, the radical of interest (**102**) was generated in the case of α-C3'-deoxy-3'-pivaloylthymidine (**103**). These findings contribute to the elucidation of the mechanistic pathways of oxidative damage to DNA by LEEs.

Oxidative damage caused by reactive oxygen species, generated from the ionization of water molecules surrounding DNA or from endogenous sources, result in formation of single and double strand breaks. The hydroxyl radical is capable of damaging the sugar phosphate backbone by abstracting hydrogen atoms from the deoxyribose moiety of DNA leading to formation of single and double strand breaks. These strand breaks are associated with the formation of electrophilic fragments capable of reaction with local nucleophiles to form DNA adducts. Since the 5'- hydrogens of deoxyribose in B-form DNA are the most accessible to solvent, they are highly vulnerable to abstraction. This event leads to the formation of the C5'-radical. Under aerobic conditions and in the presence of thiol the radical forms strand breaks terminated with a 5'-aldehyde moiety and a 3'-phosphate moiety. Oligonucleotides containing a 5'-aldehyde moiety such as **36**, are unstable and undergoe elimination to deliver the aromatic compound furfural (**67**). It was shown that furfural can form an adduct with adenine in DNA. The goal of this project is to investigate the stability and reactivity of oligonucleotides containing a 5'-aldehyde lesion and its degradation products under physiological conditions. The half-life of oligonucleotides containing a 5'-aldehyde lesion was determined to be 96 hours in single-stranded DNA. The half-life of 3',4'-didehydro-2',3'-dideoxy-5'-oxothymidine (**66**) was determined to be 13 hours under physiological

conditions. These experiments help to explain the types of adducts that form as a result of oxidative damage. These adducts can be used as biomarkers for early detection of disease such as cancer.

I dedicate this dissertation to my mother, my daughters Myes and Tasneem, my sisters Buthina, Sokina, Tahani, Sumia and to my brother Alhaj-Saleh Abdallah.

Acknowledgments:

Through this acknowledgment, I express my sincere gratitude to all of the people who have been associated with this doctoral thesis and contributed to making it a worthwhile experience. First of all, I extend my thanks to the various people who have made it possible for me to gain the required information crucial for my research. Above all, I express my thanks to my Professor Amanda Bryant-Friedrich who gave me the opportunity to engage in this valuable research and who guided me throughout the process. This thesis would not have been possible without her help, support and patience.

I would also like to express my greatest gratitude and special thanks to my mother, daughters Myes and Tasneem, sisters, and brother for their personal support and great patience at all times. My family has given me their constant support throughout my education. A special “Thank You” goes to my sister Buthina Abdallah for her undivided support and interest. She consistently inspired and encouraged me at all times, without her I would have been unable to complete my research.

I would also like to sincerely thank my committee members Dr. Hermann von Grafenstein, Dr. Viranga Tillekeratne and Dragan Isailovic who had exchanged their interesting ideas and thoughts. I would also like to thank my collegues. I am very grateful to have such a tremendous support system, which has been invaluable on both an academic and a personal level. Finally, I would like to acknowledge the academic staff of the Department of Medicinal and Biological Chemistry of the University of Toledo.

Table of Contents

Abstract ..... **iii**

Acknowledgments ..... **vii**

List of Figures ..... **xvi**

List of Tables ..... **xx**

List of Schemes ..... **xxi**

List of Abbreviations ..... **xxiv**

List of Symbols and Formulas ..... **xxvi**

1 CHAPTER ONE: Introduction and Background **1**

1.1 Ionizing Radiation (IR) **1**

1.1.1 Alpha particles (α) 1

1.1.2 Beta particles (β) 2

1.1.3 Gamma rays (γ) 2

1.1.4 X-rays 2

1.1.5 Cosmic rays 3

1.1.6 Neutron (n) 3

1.2 Interaction of IR with Biological Systems **3**

1.2.1 Direct Effect 4

1.2.1.1 Interaction of IR with DNA 4

1.2.2 Indirect Effect 6

1.2.2.1 Interaction of LEE with DNA 6

1.2.2.2 Interaction of IR with Water 7

1.3 DNA Damage by Hydroxyl Radicals (HO•) 10

1.3.1 Base Damage in DNA by Hydroxyl Radicals (HO•) 10

1.3.2 Sugar Damage in DNA by Hydroxyl Radicals (HO•) 10

1.3.2.1 C1'-Radical 11

1.3.2.2 C2'-Radical 13

1.3.2.3 C3'-Radical 14

1.3.2.4 C4'-Radical 18

1.3.2.5 C5'-Radical 21

1.4 DNA Damage by Hydrogen Atoms (H•) 24

1.5 DNA Damage by Solvated Electrons (e^-_{aq}) 25

1.6 Significance of the DNA Damage by IR 25

1.6.1 Significance of the Investigation of the C-3' dideoxy Radical Generated by LEE-DNA interaction. 26

1.6.2 Independent Generation of the Deoxyribosyl Radical 27

1.7 Relevance of the Investigation of the Oxidative Damage to C-5' 32

2 CHAPTER TWO 34

2.1 RESULTS and DISCUSSION: Synthesis and Photolysis of C3'-Modified Nucleosides 34

2.2 Design and Synthesis of Photochemical Precursors for the C2',3'-Dideoxy-C3'-thymidinyl Radical (102). 35

2.3 Investigation of the suitability of α and β-Pivaloylketone Precursors 101 and 103 for the Generation of C3' Radical 102. 39

2.3.1 Photochemical Generation of the C2',3'-Dideoxy-C3' Radical in the Presence of *tri-n*Butyltin Hydride. 40

2.3.2 Photochemical Generation of the C2',3'-Dideoxy-C3'-Radical in the Presence of Glutathione. 50

2.3.3 Photochemical Generation of the C2',3'-Dideoxy-C3'-Radical in the Absence of Hydrogen Atom Donor. 53

3 CHAPTER THREE: 57

3.1 Results and Discussion: Investigation of the 5'-Aldehyde Lesion 57

3.2 Overview of DNA synthesis 58

3.3 Oligonucleotides Synthesis 60

3.3.1 Synthesis of 5'-Modified Thymidine Building Blocks for Oligonucleotide Synthesis 60

3.3.2 Incorporation of **135** into Oligonucleotides 61

3.3.3 Synthesis of Modified Oligonucleotides Containing a 5'-Aldehyde Lesion (**144**) 65

3.3.3.1 Storage of Modified Oligonucleotide Containing 5'-Aldehyde (**144**) 67

3.3.3.2 Stability of 5'-Aldehyde Containing Oligomer (**144**) under Physiological Conditions 68

3.4 Synthesis of the Nucleoside Resulting from β-Elimination of 5'-Aldehyde Containing Oligomers 69

3.4.1 Synthesis of 3',4'-Didehydro-2',3'-dideoxy-5'-oxothymidine (**66**) 69

3.4.1.1 Stability of 3',4'-Didehydro-2',3'-dideoxy-5'-oxothymidine (**66**) 71

3.4.1.2 Reactivity of 3',4'-Didehydro-2',3'-dideoxy-5'-oxothymidine (**66**) in the Presence of Deoxyadenosine 74

3.4.1.3 Reactivity of 3',4'-Didehydro-2',3'-dideoxy-5'-oxothymidine (**66**) in the Presence of a dA Containing Oligonucleotide 75

3.5 Reactivity of Furfural 76

3.5.1 Reactivity of Furfural (**67**) in the Presence of an Excess of dA at pH = 7.4 and 37 °C 77

3.5.2 Reactivity of Furfural (**67**) in the Presence of Excess dA at pH = 2 and 37 °C 78

4 CHAPTER FOUR 81

4.1 Conclusion and Future Research Directions 81

4.1.1 Synthesis and Photolysis of C3'-Modified Nucleosides 81

4.1.2 5'-Oxidative Damage 85

5 CHAPTER FIVE 88

5.1 EXPERIMENTAL PROCEDURES 88

5.2 Materials 88

5.3 Structural Analysis 88

5.3.1 NMR Spectroscopy 89

5.3.1.1 ^{1}H-NMR 89

5.3.1.2 ^{13}C-NMR 89

5.3.1.3 ^{31}P-NMR 90

5.3.1.4 ^{1}H-NOESY-NMR 90

5.3.2 Mass Spectrometry 90

5.3.2.1 ESI-MS 90

5.3.2.2 MALDI-ToF MS 90

5.3.2.3 High Resolution Mass Spectrometry 92

5.3.3 Chromatographic Methods 92

5.3.3.1 Thin Layer Chromatography 92

5.3.3.2 Flash Chromatography 92

5.3.3.3 HPLC 92

5.3.4 Other Equipment and Devices 93

5.4 Synthesis of Nucleoside Radical Precursors 94

5.4.1 Synthesis of 3'-β-(pivaloyl)-3'-deoxythymidine (**101**) 94

5.4.1.1 5'-*O*-(*tert*-Butyldimethylsilyl)-3'-deoxy-*C*-methylenethymidine (**107**) .. 94

5.4.1.2 1-[(5-*O*-*tert*-Butyldimethylsilyl)-3-*C*-(hydroxymethyl)-2,3-dideoxy-b-D-*threo*-pentofuranosyl]thymine (**108**) 94

5.4.1.3 1-[(5-*O*-*tert*-Butyldimethylsilyl)-3-*C*-(formyl)-2,3-dideoxy-β-D-*threo*-pentofuranosyl]thymine (**109**) 95

5.4.1.4 1-[(5-*O*-*tert*-Butyldimethylsilyl)-3-*C*-(2,2-dimethyl-1-hydroxypropyl)-2,3-dideoxy-β-D-*threo*-pentofuranosyl]thymine (**110**) 95

5.4.1.5 1-[(5-*O*-*tert*-Butyldimethylsilyl)-3-*C*-(2,2-dimethyl-1-oxopropyl)-2,3-dideoxy-β-D-*threo*-pentofuranosyl]thymine (**111**) 96

5.4.1.6 1-[2,3-dideoxy-3-*C*-(2,2-dimethyl-1-oxopropyl)-2,3-dideoxy-β-D-*threo*-pentofuranosyl]thymine (**101**) 97

5.4.2 Synthesis of 3'-α-(pivaloyl)-3'-deoxythymidine (**103**) 98

5.4.2.1 1-[5-(*tert*-Butyldiphenylsilyl)-2,3-dideoxy-3-*C*-formyl-β-D-*erythro*-pentofuranosyl]thymine (**115**) 98

5.4.2.2 1-[5-(*tert*-Butyldiphenylsilyl)-2,3-dideoxy-3-*C*-(2,2-dimethyl-1-hydroxypropyl)-β-D-*erythro*-pentofuranosyl]thymine (**116**) 98

5.4.2.3 1-[5-(*tert*-Butyldiphenylsilyl)-2,3-dideoxy-3-*C*-pivaloyl-β-D-*erythro*-pentofuranosyl]thymine (**117**) 99

5.4.2.4 1-(2,3-dideoxy-3-*C*-pivaloyl-β-D-*erythro*-pentofuranosyl)thymine (**103**) 99

5.5 Synthesis of Damage products 100

5.5.1 Synthesis of C2',3'-Dideoxythymidine (**118**) 100

5.5.2 Synthesis of C2',3'-Didehydro-2',3'-dideoxythymidine (**125**) 100

5.6 Photolysis Experiments 100

5.6.1 Photochemical Generation of the C2',3'-Dideoxy-C3'-thymidinyl Radical from **103** 101

5.6.1.1 Photolysis of **103** in the Presence of *tri-n*Butyltin hydride as a Hydrogen Atom Donor 101

5.6.1.2 Photolysis of **103** in the Presence of Glutathione as a Hydrogen Atom Donor 101

5.6.1.3 Photolysis of **103** in the Absence of a Hydrogen Atom Donor 102

5.6.2 Photochemical Generation of the C2',3'-Dideoxy-C3'-thymidinyl Radical from **101** 102

5.6.2.1 Photolysis of **101** in the Presence of *tri-n*Butyltin hydride as a Hydrogen Atom Donor 102

5.6.2.2 Photolysis of **101** in the Presence of Glutathione as a Hydrogen Atom Donor 103

5.6.2.3 Photolysis of **101** in the Absence of a Hydrogen Atom Donor 104

5.7 Synthesis of C5'-modified thymidine 104

5.7.1 1-[5-*O*-(acetyl)-5-*C*-((4,4'-dimethoxytrityl)oxymethyl)-2-deoxy-β-D-*erythro*-pentofuranosyl]thymine (**134**) 104

5.7.2 1-[5-*O*-(acetyl)-5-*C*-((4,4'-dimethoxytrityl)oxymethyl)-3-H-phosphonateTriethylammonium Salt, 2-deoxy-β-D-*erythro*-pentofuranosyl]thymine (**135**) 104

5.7.3 5'-*O*-(*tert*-Butyldimethylsilyl)-thymidine (**105**) 105

5.7.4 5'-*O*-(*tert*-Butyldimethylsilyl)-3'-*O*-benzoyl-thymidine (**146**)[105] 106

5.7.5 3'-*O*-benzoyl-thymidine (**147**)[106] 106

5.7.6 3',4'-Didehydro-2',3'-dideoxy-5'-oxothymidine (**66**)[107] 107

5.8 Oligonucleotide Synthesis 108

5.8.1 Purification of Oligonucleotides 108

5.8.1.1 Oligonucleotide Purification Cartridges (OPC) (Trityl-on Method) 109

5.8.1.2 Desalting of Oligonucleotide 109

5.8.2 Quantification of Oligonucleotides 110

5.8.3 Synthesis of Modified Oligonucleotides 110

5.8.3.1 Modified Oligonucleotides Containing monomer (**134**) 110

5.8.3.2 Modified Oligonucleotides **144** 111

5.9 Stability of Modified Oligonucleotides 144 111

5.10 Stability of 3',4'-Didehydro-2',3'-dideoxy-5'-oxothymidine (66) at pH = 7.4 at 37 ºC 112

5.11 Stability and Reactivity of 66 in Presence of GSH 112

5.12 Reactivity of 3',4'-Didehydro-2',3'-dideoxy-5'-oxothymidine (66) 112

5.12.1 Reactivity of **66** in Presence of deoxyadenosine 112

5.12.2 Reactivity of **66** in Presence of Oligonucleotides Containing dA 112

5.13 Reactivity of Furfural 113

5.13.1 Reactivity of Furfural in Presence of dA at pH = 7.4 and 37 ºC 113

5.13.2 Reactivity of Furfural in Presence of Excess dA at pH = 2 and 37 ºC 113

5.13.3 Reactivity of Excess Furfural in Presence of dA at pH = 2 and 37 ºC 113

List of Figures

Figure 1-1: Reactions induced by primary ionizing radiation and secondary electrons[4] ... 5

Figure 1-2: Events induced by absorption of energy by water[11] 8

Figure 1-3: Reactions occurring after absorption of energy by water[11] 9

Figure 1-4: Reaction of a solvated electron with uracil[61] 25

Figure 1-5: Proposed pathways for phosphodiester bond cleavage of DNA via LEE[66] ... 27

Figure 1-6: Norrish Type I photocleavage of oligonucleotide containing acyl groups 29

Figure 1-7: Pivaloyl radical precursors designed to generate radicals at different positions in nucleosides and nucleotides 31

Figure 1-8: DNA adducts derived from 2'-deoxyribose oxidation 33

Figure 2-1: Photochemical generation of C2',3'-dideoxy-C3'-thymidinyl radical (**102**) from precursors **101** and **103** 35

Figure 2-2: Strategic approach to determine the feasibility of **101** and **103** as photochemical precursors of the C2',3'-dideoxy-C3'-thymidinyl radical . 41

Figure 2-3: Reversed-phase HPLC analyses of the photolysates resulting from photolysis of **103** (green), Controls (red), Standard **118** along with radical precursors **103** (blue) were injected separately 43

Figure 2-4: Reversed-phase HPLC chromatogram of the photolysates resulting from photolysis of **101** (1 mM) in 1:1 acetonitrile/water in the presence *tri-n*butyltin Hydride 45

Figure 2-5: Reversed-phase HPLC chromatogram of the photolysates resulting from photolysis of **101** (1 mM) in acetonitrile in the presence *tri-n*butyltin hydride 47

Figure 2-6: Reversed-phase HPLC chromatogram of the photolysate resulting from photolysis of **101** (1 mM) in water in the presence *tri-n*butyltin hydride. 48

Figure 2-7: Reversed-phase HPLC chromatogram of the photolysate resulting from photolysis of **101** (1 mM) in methanol in the presence *tri-n*butyltin hydride 49

Figure 2-8: Proposed mechanism for Norrish Type II photocleavage for **101** 50

Figure 2-9: Reversed-phase HPLC chromatogram of the photolysate resulting from photolysis of **103** (1 mM) in 1:1 acetonitrile/water in the presence 6 mM GSH 52

Figure 2-10: Reversed-phase HPLC chromatogram of the photolysates resulting from photolysis of **101** (1 mM) in 1:1 acetonitrile/water in the presence 6 mM GSH 53

Figure 2-11: Reversed-phase HPLC chromatogram of the photolysate resulting from photolysis of **103** (1 mM) in 1:1 acetonitrile/water in the absence of hydrogen atom donor 53

Figure 2-12: Reversed-phase HPLC chromatogram of the photolysate resulting from photolysis of **101** (1 mM) in 1:1 acetonitrile/water in the absence of hydrogen atom donor 54

Figure 3-1: Steps involved in solid-phase oligonucleotide synthesis 59

Figure 3-2: Ion-exchange HPLC chromatogram of modified oligonucleotide **138**..... 64

Figure 3-3: MALDI-ToF MS of modified oligonucleotide **138** 64

Figure 3-4: Ion-exchange HPLC chromatogram of 5'-aldehyde containing oligomer **144** 66

Figure 3-5: MALDI-ToF MS of 5'-aldehyde containing oligomer **144**..... 67

Figure 3-6: Ion-exchange HPLC chromatogram of 5'-aldehyde containing oligomer **144** after 96 hrs at pH 7.4 and 37 °C 68

Figure 3-7: Incubation of **66** in 100 mM phosphate buffer pH = 7.4 at 37 °C 71

Figure 3-8: Reversed-phase HPLC chromatogram of incubation of **66** in 100 mM phosphate buffer pH = 7.4 at 37 °C at 12 hours 72

Figure 3-9: Incubation of **66** in 100 mM phosphate buffer pH = 7.4 at 37 °C 72

Figure 3-10: Reversed-phase HPLC chromatogram after incubation of **66** in 100 mM phosphate buffer pH = 7.4 at 37 °C in the presence of 6 mM GSH after 30 minutes..... 73

Figure 3-11: Incubation of **66** in 100 mM phosphate buffer pH = 7.4 at 37 °C in the presence of 6 mM GSH..... 74

Figure 3-12: Reversed-phase HPLC chromatogram after incubation of **66** in 100 mM phosphate buffer pH = 7.4 at 37 °C in the presence of excess deoxyadenosine for 3 hours 75

Figure 3-13: Incubation of **66** in 100 mM phosphate buffer pH = 7.4 at 37 °C in the presence of excess dA..... 75

Figure 3-14: Incubation of **66** in 100 mM phosphate buffer pH = 7.4 at 37 °C in the presence of excess unmodified oligonucleotide 5'-TCTATCTATCT-3'.. 76

Figure 3-15: Reversed-phase HPLC chromatogram after the incubation of **66** in 100 mM phosphate buffer pH = 7.4 at 37 °C in the presence of an excess of unmodified oligonucleotide (TCTATCTATCT) for 24 hours..... 76

Figure 3-16: Reversed-phase HPLC chromatogram after incubation of **67** in 100 mM phosphate buffer pH = 7.4 at 37 °C in the presence of excess deoxyadenosine (dA) for 65 hours..... 77

Figure 3-17: Incubation of **23** in 100 mM phosphate buffer pH = 2.0 at 37 °C in the presence of excess deoxyadenosine (dA, **149**) 78

Figure 3-18: Reversed-phase HPLC chromatogram after incubation of **67** in 100 mM phosphate buffer pH = 2.0 at 37 °C in the presence of excess deoxyadenosine (dA) for 49 hours..... 79

Figure 3-19: Reversed-phase HPLC chromatogram after the incubation of 67 in 100 mM phosphate buffer pH = 2.0 at 50 °C in the presence of excess deoxyadenosine (dA) after 2 hours 79

Figure 5-1: The proton assignment of the deoxyribose sugar and the nucleobase moieties in thymidine 89

List of Tables

Table 3.1: Modified oligonucleotides containing diol and MALDI-ToF analyses 65

List of Schemes

Scheme 1.1: Fate of the 2'-deoxyuridin-1'-yl (**1**) radical 12

Scheme 1.2: 2-Deoxyribonolactone induced cross-link formation with human DNA polymerase β[27] 13

Scheme 1.3: Fate of the C2'-deoxyguanyl radical[33] 14

Scheme 1.4: Fate of C3'-deoxyribosyl radical proposed by Stubbe et.al.[37,34] 15

Scheme 1.5: Products of the degradation of the C3'-thymidinyl radical under anaerobic and aerobic conditions[39] 17

Scheme 1.6: DNA adducts derived from phosphoglycolaldehyde[40] 18

Scheme 1.7: Fate of C4'-thymidinyl radical 20

Scheme 1.8: M_1dG adduct of base propenal with guanine 21

Scheme 1.9: Fate of C5 '-deoxyadenosyl radical 22

Scheme 1.10: Fate of 5'-thymidinylaldehyde 23

Scheme 1.11: Adduct formation between furfural and an adenine residue in DNA 23

Scheme 1.12: Fate of 5'-(2-phosphoryl-1,4-dioxobutane) 24

Scheme 1.13: Adduct formation by trans-1,4-dioxo-2-butene with deoxycytidine..... 24

Scheme 2.1: Synthesis of compound **107**[94] 36

Scheme 2.2: Synthesis of β-C2',3'-dideoxy-C3'-pivaloylthymidine **101**[95] 37

Scheme 2.3: Synthesis of compound **115**[96,97] 38

Scheme 2.4: Synthesis of α-C2',3'-dideoxy-C3'-pivaloylthymidine (**103**)[95] 39

Scheme 2.5: Photochemical generation of the C2',3'-dideoxy-C3'-thymidinyl radical (**102**) from **103** in the presence of *tri-n*butyltin hydride 41

Scheme 2.6: Product identification from photochemical generation of the C2',3'-dideoxy-C3'-thymidinyl radical (**102**) from **101** in 1:1 acetonitrile/water in the presence of *tri-n*butyltin hydride 43

Scheme 2.7: Photochemical generation of the C2',3'-dideoxy-C3'-acylthymidinyl radical (**120**) from **101** in acetonitrile in the presence of *tri-n*butyltin hydride 45

Scheme 2.8: Photochemical generation of the C2',3'-dideoxy-C3'-thymidinyl radical (**102**) from **101** in water in the presence of *tri-n*butyltin hydride 47

Scheme 2.9: Photochemical generation of the C2',3'-dideoxy-C3'-acylthymidinyl radical (**120**) from **101** in methanol in the presence of *tri-n*butyltin hydride 48

Scheme 2.10: Photochemical generation of the C2',3'-dideoxy-C3'-thymidinyl radical (**102**) from **103** in 1:1 acetonitrile/water in the presence of GSH..... 51

Scheme 2.11: Photochemical generation of the C2',3'-dideoxy-C3'-acylthymidinyl radical (**120**) from **101** in 1:1 acetonitrile/water in the presence of GSH. 52

Scheme 2.12: Product identification from photochemical generation of the C2',3'-dideoxy-C3'-thymidinyl radical (**102**) from **103** in 1:1 acetonitrile/water in the absence of hydrogen atom donor 54

Scheme 2.13: Disproportionation between the C2',3'-dideoxy-C3'-thymidinyl radical (**102**) and *tert*-butyl radical, a proposed mechanism for formation of the reduction product **118** and the unsaturated product **125** in the absence of a hydrogen atom donor 55

Scheme 2.14: Disproportionation between the C2',3'-dideoxy-C3'-thymidinyl radical (**102**), a proposed mechanism for formation of the reduction product **118** and the unsaturated product **125** in the absence of a hydrogen atom donor 56

Scheme 3.1: Synthesis of building block **135** for DNA synthesis 61

Scheme 3.2: Incorporation of **135** into oligonucleotide using a manual coupling strategy 63

Scheme 3.3: Synthesis of 5'-aldehyde containing oligomer **144** 66

Scheme 3.4: Decomposition of **144** to **145** 68

Scheme 3.3.5: Mechanism for the decomposition of **36** to **67** 69

Scheme 3.6: Synthesis of 3',4'-didehydro-2',3'-dideoxy-5'-oxothymidine (**66**) 70

List of Abbreviations

A	Adenine
AIBN	Azo-Bis-Isobutyronitrile
BME	β-mercaptoethanol
C	Cytosine
^{13}C NMR	Carbon-13 Nuclear Magnetic Resonance Specroscopy
CPG	Controlled Pore Glass
dA	Deoxyadenosine
dC	Deoxycytidine
DEA	Dissociative Electron Attachment
DIEA	*N, N*-Diisopropylethylamine
dG	Deoxyguanosine
DNA	Deoxyribonucleic Acid
DSB	Double Strand Breaks
dsDNA	Double Strand Deoxyribonucleic Acid
dT	Thymidine
ESI-MS	Electrospray Ionization Mass Spectrometry
G	Guanine
HPLC	High Performance Liquid Chromatography

^{1}H NMR	Proton Nuclear Magnetic Resonance Specroscopy
IR	Ionizing Radiation
LEE	Secondary Low-Energy Electron
MALDI-ToF MS	Matrix-Assisted Laser Desorption Ionization Time-of-Flight Mass Spectrometry
MDSB	Multiple Double Strand Breaks
NMR	Nuclear Magnetic Resonance Specroscopy
nm	Nanometer
ROS	Reactive Oxygen Species
SE	Secondary Electrons
SSB	Single Strand Breaks
ssDNA	Single Strand Deoxyribonucleic Acid
T	Thymine
TBAF	TetraButylammonium Fluoride
TBDMS	*tert*-Butyldimethylsilyl
TBDMSCl	*tert*-Butyldimethylsilyl Chloride
TBDPSCl	*tert*-Butyldiphenylsilyl Chloride
TEAA	Triethylammonium Acetate Buffer
TEAB	Triethylammonium Bicarbonate Buffer
THF	Tetrahydrofuran
UV	Ultraviolet

List of Symbols and Formulas

AB	Diatomic molecule
Ar	Argon
CH_2Cl_2	Dichloromethane
CH_3CN	Acetonitrile
CH_3CO_2H	Acetic acid
CH_3SO_2Cl	Methanesulfonyl chloride
DCM	Dichloromethane
ddT	2',3'-Dideoxythymidine
DMF	*N,N'*-Dimethylformamid
DMTrCl	Dimethoxytrityl chloride
E	Energy
e^-	Electron
e^-_{se}	Subexcitation electrons
Et_3N	Triethylamine
$EtN(i\text{-}Pr)_2$	*N, N*-Diisopropylethylamine
eV	Electron volts
GSH	Glutathione reduced
$H^\bullet$	Hydrogen atom
H^+_{aq}	Hydronium ion

H_2O	Water molecule
H_2O^*	Excited water molecule
$H_2O^{+\bullet}$	Water radical cation
$HO^\bullet$	hydroxyl radical
hν	Energy
i-PrOH	Isopropyl alcohol
I_2	Iodine
KeV	Kiloelectron volts
M	Molar
MeOH	Methanol
MeV	Mega (million) electron volts
mM	millimolar
n-Bu_3SnH	*tri-n*butyltin hydride
NH_4OH	Ammonium hydroxide
O_2	Oxygen
PCl_3	Phosphorous trichloride
Ph	phenyl group
PhSe	Phenylselenyl group
PPh_3	Triphenylphosphine
PvCl	Pivaloyl chloride
Pyr	Pyridine
Rn	Radon
sec-BuLi	*sec*-Butyllithium

TFA	Trifluoroacetic acid
2',3'-unsat.T	2',3'-didehydro-2',3'-dideoxythymidine
λ	Wavelength of light
μL	microliter

1 CHAPTER ONE: Introduction and Background

1.1 Ionizing Radiation (IR)

Ionizing radiation (IR) is composed of particles or waves that have enough energy to liberate electrons from atoms or molecules. IR arises from both natural and man-made sources. Natural sources include cosmic rays, radon gas, generated from the decay of radium; and radioactive elements found in the earth's crust such as uranium, thorium, potassium and their radioactive decay products; and various radionuclides found naturally in food and drinks. Man-made sources include medical diagnostics and therapies such as X-rays in diagnostic radiology or the use of radiation in cancer treatments, and industrial sources such as those found at research and teaching institutions, nuclear reactors; and radio active waste.[1]

The most common types of radiation emitted from natural sources or man-made radionuclides are alpha particles, beta particles, gamma rays, x-rays, cosmic radiation, and neutron radiation.

1.1.1 Alpha particles (α)

Alpha particles are highly energetic (3-7 MeV), positively charge particles consisting of two protons and two neutrons bound together forming a particle identical to a helium nucleus. Alpha particles are emitted during radioactive decay of the heaviest radioactive elements such as uranium-238, radium-226, and polonium-210. Alpha

particles move slowly through the air due to their high mass and can be stopped by a sheet of paper. Therefore, external exposure is considered not harmful because the alpha particles lack the energy to penetrate the outer dead layer of skin. However, alpha particles are very harmful when alpha particle emitting isotopes are ingested or inhaled.[2]

1.1.2 Beta particles (β)

Beta particles are high-energy, fast moving electrons or positrons emitted from radioactive nuclei such as potassium. Beta particles can be generated from both natural and man-made sources, and are smaller than alpha particles. Beta particles are more penetrating than alpha particles into tissues or materials, but can be absorbed by plastic sheets, glass, aluminum, or layers of clothing. Beta particles are less damaging than alpha over equally traveled distances. Beta particles are most hazardous when they are inhaled or ingested.[1,2]

1.1.3 Gamma rays (γ)

Gamma rays are very high-energy photons (> 100 keV) that are emitted from radioactive nuclei along with alpha and beta particles. Gamma rays can be emitted from natural sources as well as man-made sources. Gamma rays have no charge and no mass and therefore they are very penetrating and require several inches of lead to be stopped. Gamma rays are hazardous to the entire body since they can be easily absorbed by internal organs and tissues.[1,2]

1.1.4 X-rays

X-rays are high-energy photons (100 eV-100 keV), but are lower in energy than gamma rays and are produced by the interaction of charged particles with matter. X-rays are less penetrating than γ-rays and a few millimeters of lead can stop X-rays. X-rays are

considered to be the largest source of man-maid radiation exposure due to their use in medicine and industry for examinations and inspections.[1]

1.1.5 Cosmic rays

Cosmic rays are energetic particles from deep space. They are a mixture of different types of radiation including alpha particles, electrons, protons and positrons. They can have energies above 10^{20} eV.[1]

1.1.6 Neutron (n)

The neutron is emitted by unstable nuclei and has no electric charge. It can be very penetrating. It interacts with matter causing emission of gamma and beta radiation and require heavy shielding to reduce exposure.[1]

1.2 Interaction of IR with Biological Systems

Ionizing radiation causes damage to all biological systems with DNA being one of the most important targets. IR induces mutagenicity, genotoxicity and cell death by damaging DNA. This damage includes base and sugar modifications, base release, single and double strand breaks (SSB, DSB), and clustered damage.[3] This damage is produced from the energy deposition of the primary particles in cellular medium as well as the secondary species, i.e., ions, radicals and low energy electrons (LEEs) generated along the radiation track.[4,5] These phenomena are called the direct and indirect effects of IR on DNA. In the direct effect, energy from IR deposits in the various nucleic acid components, whereas in the indirect effect energy deposition occurs in water molecules surrounding the DNA. It has been estimated that the direct effect contributes about 40% to cellular DNA damage, while water radiolysis products contribute about 60%.[3] The

chemistry involved in the interaction of ionizing radiation with DNA in the direct and indirect effect will be discussed in the following sections.

1.2.1 Direct Effect

1.2.1.1 Interaction of IR with DNA

When high-energy particles or fast charged particles produced by primary radiation such as photoelectrons or Compton electrons pass near DNA molecules, the result is DNA perturbation by rapid change of the electromagnetic field produced by the moving charge.[4] Energy transfer from IR to DNA occurs within femtoseconds of the initiating events and are divided into three groups: primary, secondary and reactive.

In primary events (**Figure 1-1**)[4], deposited radiation ionizes and excites DNA constituents (reaction **1** and **2**, **Figure 1-1**). For simplification, AB represents simple hypothetical diatomic molecule located in the cell.

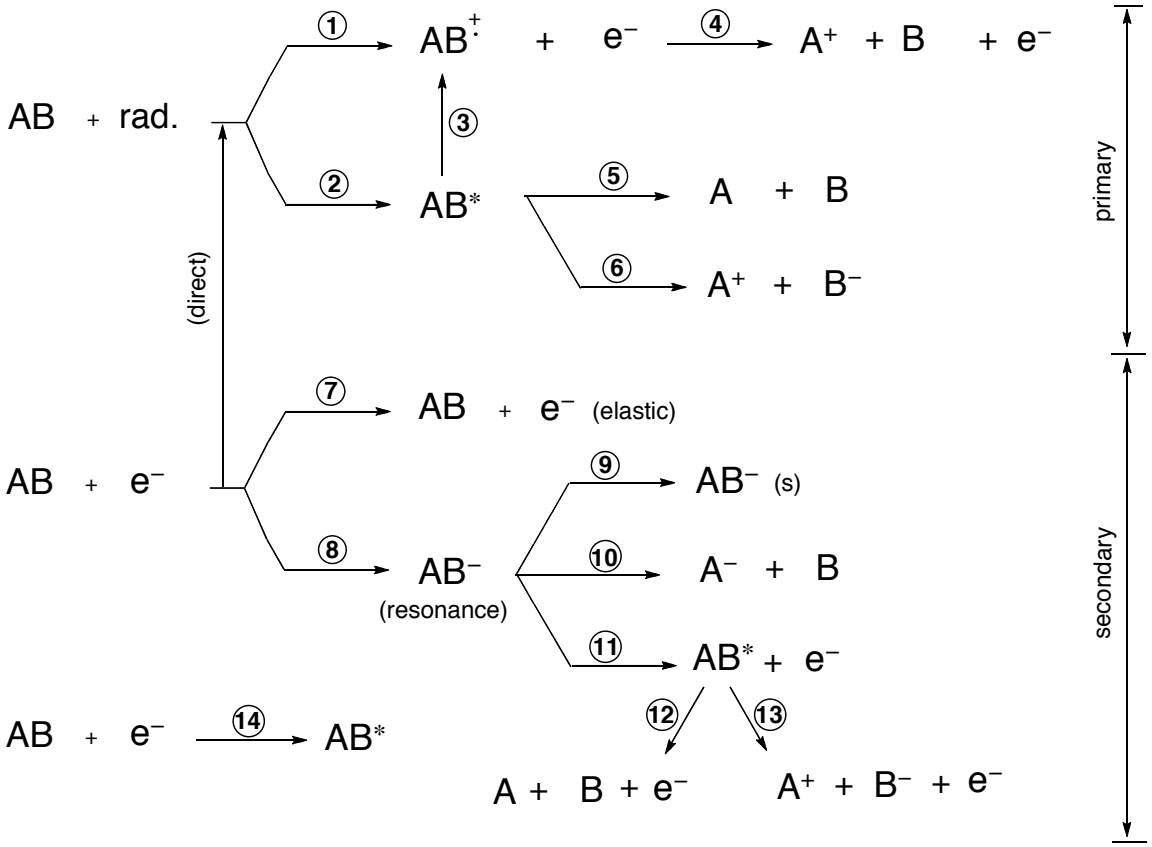

Figure 1-1: Reactions induced by primary ionizing radiation and secondary electrons[4]

During primary events 80% of the energy deposited leads to reaction 1 producing radical cations and secondary electrons (SE). The radical cation either dissociates into fragment ions and SE (reaction **4**, **Figure 1-1**)[4] or reacts with its solvation shell forming in the case of DNA base-OH adduct radicals or can release protons from the sugar moiety to form neutral radicals.[3] SE generated in reaction **1** and **4** have energies less than 30 eV with a most likely energy between 9 and 10 eV.[6-7] These SE are generated in large numbers (i.e., ~ 3 x 10^4/ MeV of deposited energy) and represent a large portion of primary radiation energy. The rest of the absorbed radiation energy (20%) produces excited molecules (reaction **2**, **Figure 1-1**), which dissociate to produce neutral species (reaction **5**, **Figure 1-1**) or ions (reaction **6**, **Figure 1-1**). Excited molecules may

autoionize if there is enough energy for its own ionization to generate more SE (reaction **3**, **Figure 1-1**).

The formation of secondary electrons is responsible for the secondary events shown in **Figure 1-1**. Secondary electrons interact with other molecules found in the cells, before their thermalization, and induce more damage, which is referred to as the indirect effect of IR on biological systems. This will be discussed later in this chapter. All reactive species formed during primary and secondary events react with all biological molecules to generate new damage products.

1.2.2 Indirect Effect

1.2.2.1 Interaction of LEE with DNA

As mentioned above, secondary low energy electrons (LEEs) with kinetic energies of 0-30 eV are generated in large amounts by ionizing radiation. The interaction of LEE with DNA results in the formation of single and double strand breaks[5,8-9]as well as base release.[10] Secondary LEEs with energies below ~ 30 eV produced from the direct effect and the ionization of water molecules interact with DNA by two pathways, resonant and nonresonant scattering.[4,5] In the nonresonant scattering mechanism, LEEs interact with DNA resulting in the reproduction of some or any of the reactions 1-6 (vertical arrow in **Figure 1-1**),[4] depending on their energies. The outcome of nonresonant scattering is single (SSB) and double (DSB) strand breaks as well as multiple double (MDSB) strand break formations through ionization, excitation and dissociation of DNA components. In the resonant scattering, LEEs cause DNA strand breaks only through the formation of transient anions (reaction **8**, **Figure 1-1**) leading to resonance stabilization (reaction **9**, **Figure 1-1**), dissociative electron attachment (DEA)

(reaction **10**, **Figure 1-1**), and vibrational and electronic excitation (reaction **11**, **Figure 1-1**), which undergoes dissociation to provide neutral and ionic atoms (reaction **12** and **13**, respectively, **Figure 1-1**). In addition, geminate recombination (reaction **14**, **Figure 1-1**) is another way to produce excited molecules and can lead to degradation via reaction **5** and **6** in, **Figure 1-1**).[4,5]

1.2.2.2 Interaction of IR with Water

When IR interacts with the water layers surrounding DNA, ionization and electronic excitation occur in about 10^{-16} seconds resulting in the formation of radical cations and subexcitation electrons (reaction **1**, **Figure 1-2**). Subexcitation electrons have sufficient energy to ionize or excite further water molecules until its energy is no longer enough to cause ionization or excitation of other water molecules. In addition to ionization, excitation of water molecules by the absorption of energy from IR is another pathway leading to the formation of water molecules in their electronic excited state (reaction **2**, **Figure 1-2**).

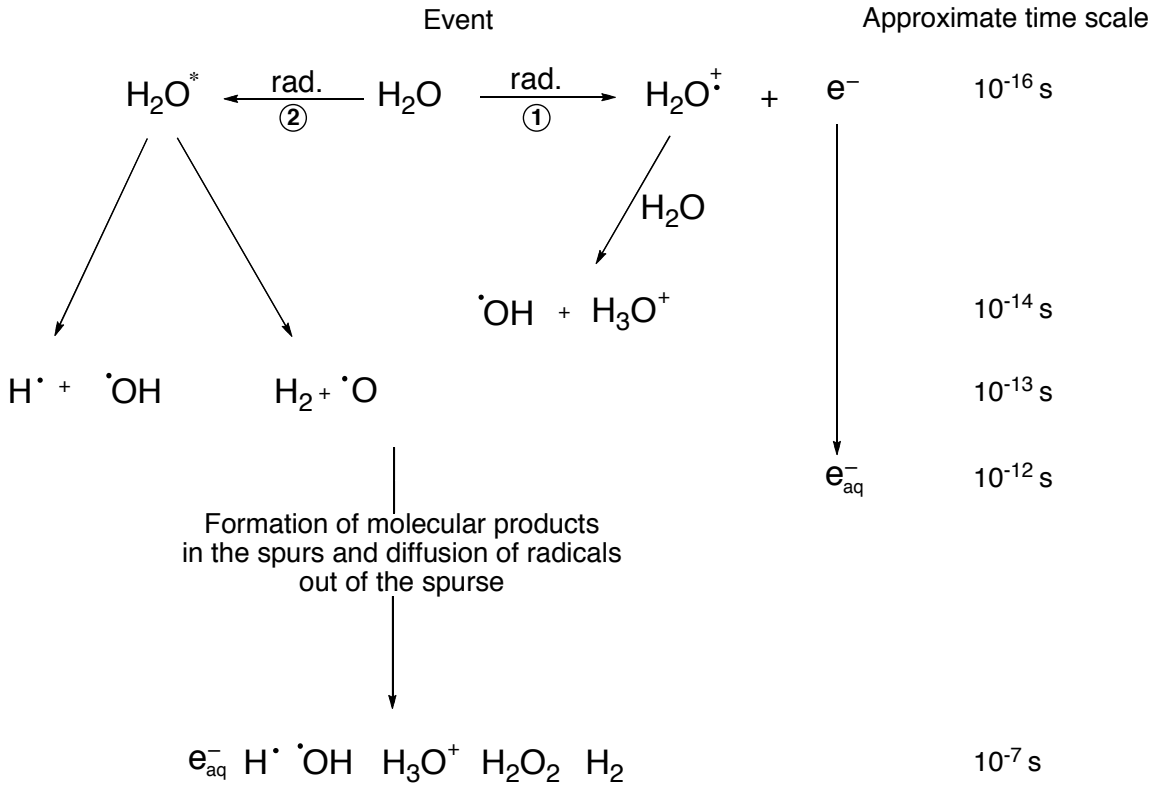

Figure 1-2: Events induced by absorption of energy by water[11]

After formation of water radical cations ($H_2O^{\bullet+}$), subexcitation electrons (e^-_{se}) and electronically excited water molecules (H_2O^*), reactions can occur within 10^{-16} to 10^{-12} seconds which are shown in **Figure 1-3** (reaction **1-4**)[11]. The water radical cation reacts with subexcitation electrons to form water molecules with high vibrational energies, which either decompose to hydrogen atoms ($H^\bullet$) and hydroxyl radicals ($HO^\bullet$), or generate hydrogen gas (H_2) and hydrogen peroxide (H_2O_2) on a time scale of 10^{-13} sec (reaction **1**, **Figure 1-3**). The water radical cation is a strong acid and rapidly loses a proton to surrounding water molecules forming hydronium ion ($H+_{aq}$) and $HO^\bullet$ (reaction **2**, **Figure 1-3**), on a time scale of 10^{-14} sec.

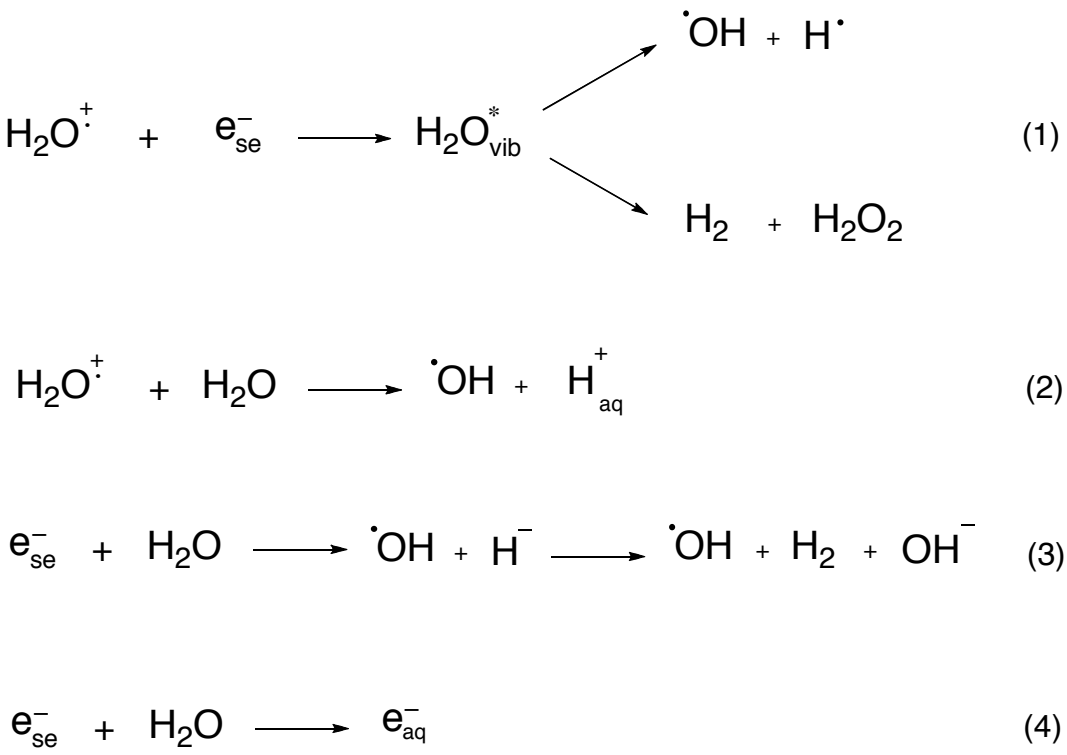

Figure 1-3: Reactions occurring after absorption of energy by water[11]

Subexcitation electrons can either undergo dissociative attachment to water resulting in the generation of hydroxyl radical, hydrogen gas and hydroxide (reaction **3**, **Figure 1-3**), or can thermalize and become solvated electrons on a time scale of 10^{-12} sec. (reaction **4**, **Figure 1-3**). Collectively, the interaction of IR with water molecules results in formation of radical cations, excited water molecules, and subexcitation electrons that further react with each other or with water molecules to produce water radiolysis products (hydrogen atom, hydroxyl radical and solvated electrons) which are capable of causing damage to all cellular components with DNA being a primary target.

1.3 DNA Damage by Hydroxyl Radicals ($HO^{\bullet}$)

1.3.1 Base Damage in DNA by Hydroxyl Radicals ($HO^{\bullet}$)

Hydroxyl radicals are generated exogenously as the result of exposure of water to IR as explained above, or endogenously through cellular metabolism, oxidative stress, chronic infection and inflammation.[12,13,14] The hydroxyl radical is a small, highly diffusible, highly reactive species with electrophilic properties that are capable of damaging the nucleobase and the sugar moiety of DNA.[15] The hydroxyl radical can add to the C-C and C-N double bonds of purines in DNA or C-C double bonds of pyrimidines. The addition of the hydroxyl radical to the double bonds of nucleobases is regioselective due to its electrophilic nature. For instance, the hydroxyl radical favors addition to the more electron rich C5 position of thymine over the less electron rich C6 position.[15,16] The hydroxyl radical can also abstract hydrogen atoms from the methyl group of thymine.[3,15]

1.3.2 Sugar Damage in DNA by Hydroxyl Radicals ($HO^{\bullet}$)

Hydroxyl radicals are highly reactive oxygen species and are capable of hydrogen atom abstraction from the five positions of the 2'-deoxyribose moiety of DNA. The resulting species are carbon-centered radicals whose reactivity depends on their environment.[17,18] The order of reactivity of $HO^{\bullet}$ toward each hydrogen atom of the 2-deoxyribose moiety was proposed based on solvent accessibility of the sugar hydrogen atoms in B-form DNA (H5' > H4' > H3' ≈ H2' ≈ H1').[19] The chemistry of each of these sugar radicals is discussed in the following sections.

1.3.2.1 C1'-Radical

The C1'-deoxyribosyl radical is an N-glycosyl radical that is generated through the abstraction of the C1'-hydrogen of the 2'-deoxyribose moiety in DNA by hydroxyl radicals generated from exogenous and endogenous sources. The fate of this radical was investigated through the independent generation of 2'-deoxyuridin-1'-yl (**1**) in single and double stranded DNA (ssDNA, dsDNA).[20,21] Upon reduction with β-mercaptoethanol (BME) under anaerobic conditions, the 2'-deoxyuridin-1'-yl (**1**) radical gives rise to a mixture of β- and α- deoxyuridines (**2** and **3** respectively, **Scheme 1.1**). The β:α ratios are (4.1:1) in ssDNA and (6.2:1) in dsDNA with the restoration of the naturally occurring β-anomer dominate over the premutagenic α-anomer.[21] In addition to reduction products, the 2-deoxyribonolactone (**7**, **Scheme 1.1**) is formed in small amounts under these conditions. In the presence of oxygen, 2'-deoxyuridin-1'-yl (**1**) radical is trapped by oxygen at a diffusion-controlled rate to generate peroxyl radical **4**. Reduction of **4** by thiol produces ribonolactone **7**. In the absence of thiol, the peroxyl radical undergoes superoxide release to generate a carbocation which reacts with water to deliver ribonlactone **7**.[22,23,24] Under physiological conditions, the ribonolactone undergoes β-elimination to form butenolide species **9** which has a half-life of 20 hours in ssDNA and 32-54 hours in dsDNA.[25] Lesion **9** can undergo a second elimination to release 5-methylene-2-furanone (**10**), which is a strong electrophile that has the ability to react with cellular nucleophiles. 2-Deoxyribonolactone **7** can induce formation of crosslinks with DNA repair proteins such as polymerase β and endonuclease III, in which the lysine at the active site of these enzymes undergoes nucleophilic attack on the lactone to produce an amide linkage. Normally, during excision of an unmodified abasic site, the lysine

forms a Schiff's base with the C1-aldehyde in the open form of the native abasic site. The formation of an amide linkage results in the inhibition of DNA repair enzymes (**12**, **Scheme 1.2**).[26,27] Lesion **9** acts as a Michael acceptor that has been shown to be reactive toward sulfur and nitrogen nucleophiles.[28]

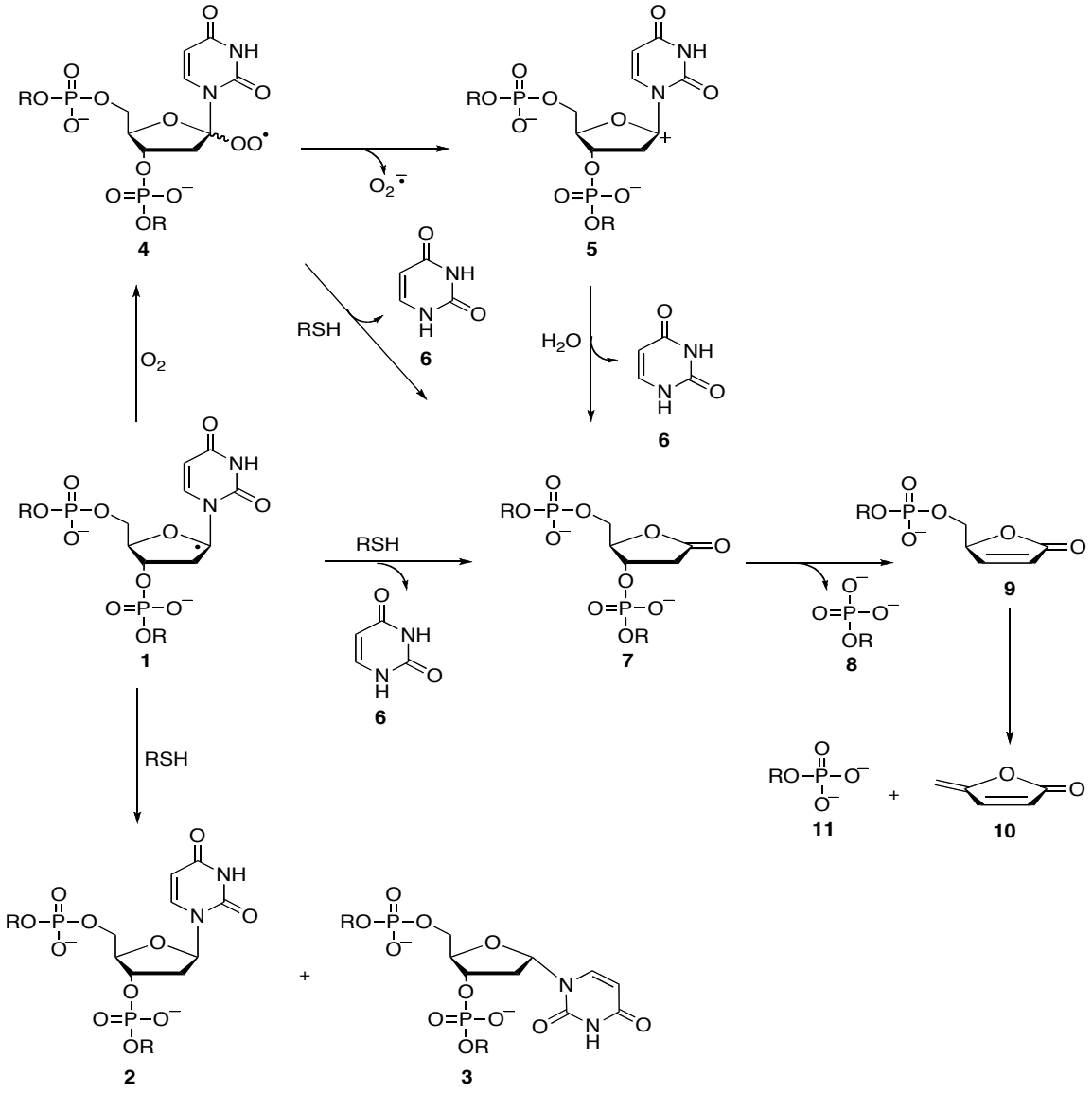

Scheme 1.1: Fate of the 2'-deoxyuridin-1'-yl (**1**) radical

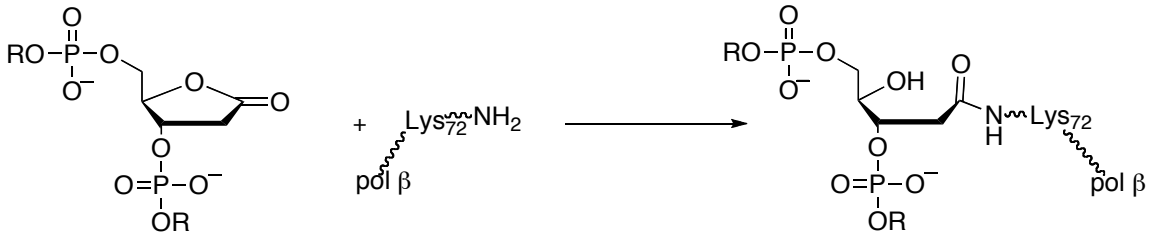

Scheme 1.2: 2-Deoxyribonolactone induced cross-link formation with human DNA polymerase β[27]

1.3.2.2 C2'-Radical

Oxidation at the C2'-deoxyribose moiety in DNA occurs through the abstraction of either one of the two hydrogen atoms. This carbon centered radical has been generated by γ-irradiation and by the abstraction of a 2'-hydrogen by the photochemically generated 5-uridinyl radical.[29] Trapping of C2'-radical **13** with oxygen leads to the formation of peroxyl radical **14**, (**Scheme 1.3**).[30] The fate of **13** depends on the conformation of DNA when its formed. For example, when **13** is formed in B-form DNA the erythrose abasic site **16** is the major product, while in Z-form DNA the primary product is ribonucleotide **17**.[30,31]The erythrose abasic site **16** is stable to hydrolysis in comparison to other abasic sites, with a half-life of 3 h in 0.1 M NaOH at 37 °C.[32]

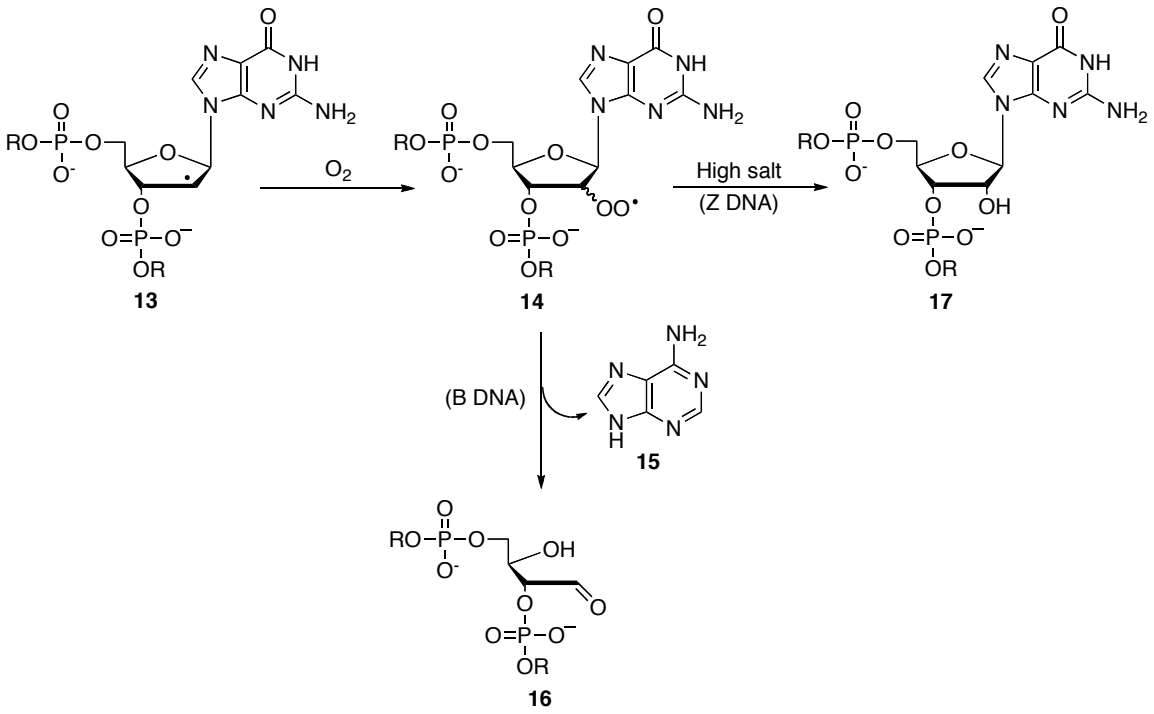

Scheme 1.3: Fate of the C2'-deoxyguanyl radical[33]

1.3.2.3 C3'-Radical

The C3'-deoxyribosyl radical (**18**) is an α-phosphatoxyalkyl radical generated by the abstraction of the C3'-hydrogen atom by the hydroxyl radical. The fate of this radical was investigated using Rh-phenanthrenequinone diimine complexes[34,35] and site-specific radical generation using photolabile groups at the C3' position.[36] Under anaerobic conditions, it has been suggested that **18** is oxidized to a carbocation **19** that undergoes solvolysis to yield **20**. Compound **20** undergoes elimination to yield 3'-ketonucleotide **21** and 5'-phosphorylated oligonucleotide **8**. Compound **21** can undergo a second elimination to release 3'-phosphate **11**, small sugar fragment **22** and nucleobase **23**. The decomposition of **18** under aerobic conditions results in formation of peroxyl radical **24** which converts to hydroperoxide **25** in the presence of thiol. The hydrogen peroxide (**25**) undergoes a Criegee-type rearrangement to generate intermediate **26**. Subsequent

decomposition leads to the formation of base propenoate **29**, 5'-Phosphate **8**, and 3'-phosphoglycolaldehyde (3'-PGA, **30**) (**Scheme 1.4**).[37]

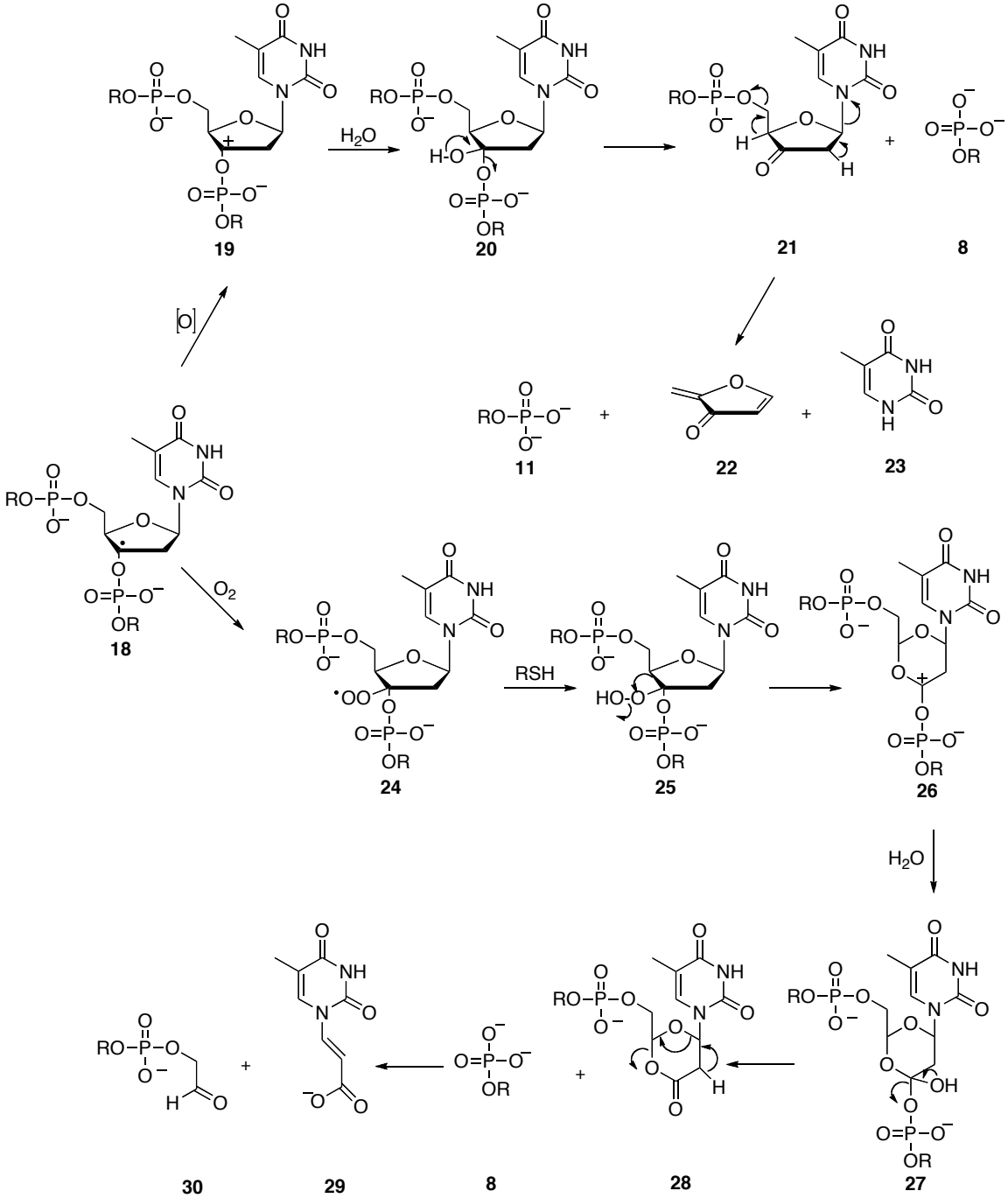

Scheme 1.4: Fate of C3'-deoxyribosyl radical proposed by Stubbe et.al.[37,34]

It was shown by Bryant-Friedrich that in the presence of thiol and in the absence of oxygen, the C-3' radical in single stranded DNA is reduced to give the repaired 2'-deoxyribose **31**, and possibly the pseudorepair 2-deoxyxylose **32** in oligomers (**Scheme 1.5**).[38] Under aerobic conditions, trapping of **18** results in formation of isomeric peroxyl radicals **33** and **34** which subsequently degrade to give rise to strand breaks 8 and 11 as the major products.[39] Lesions **30**, 3'-phosphoglycolate (3'-PG) **35**, and 5'-aldehyde **36** were also detected from experiments performed under aerobic conditions and confirmed by mass spec analysis. Formation of **30** can be explained, as mentioned above, through molecular rearrangement of the peroxyl radical formed at the C3'-position, while formation of **35** and **36** can be explained by oxidation of the C4' radicals of the same nucleotide and the oxidation of C5' radicals of the 3'-adjacent nucleotide, respectively. Compound **37** can undergo a second elimination step to release 3'-phosphate **11**, and small sugar fragment (**22**) (**Scheme 1.5**).

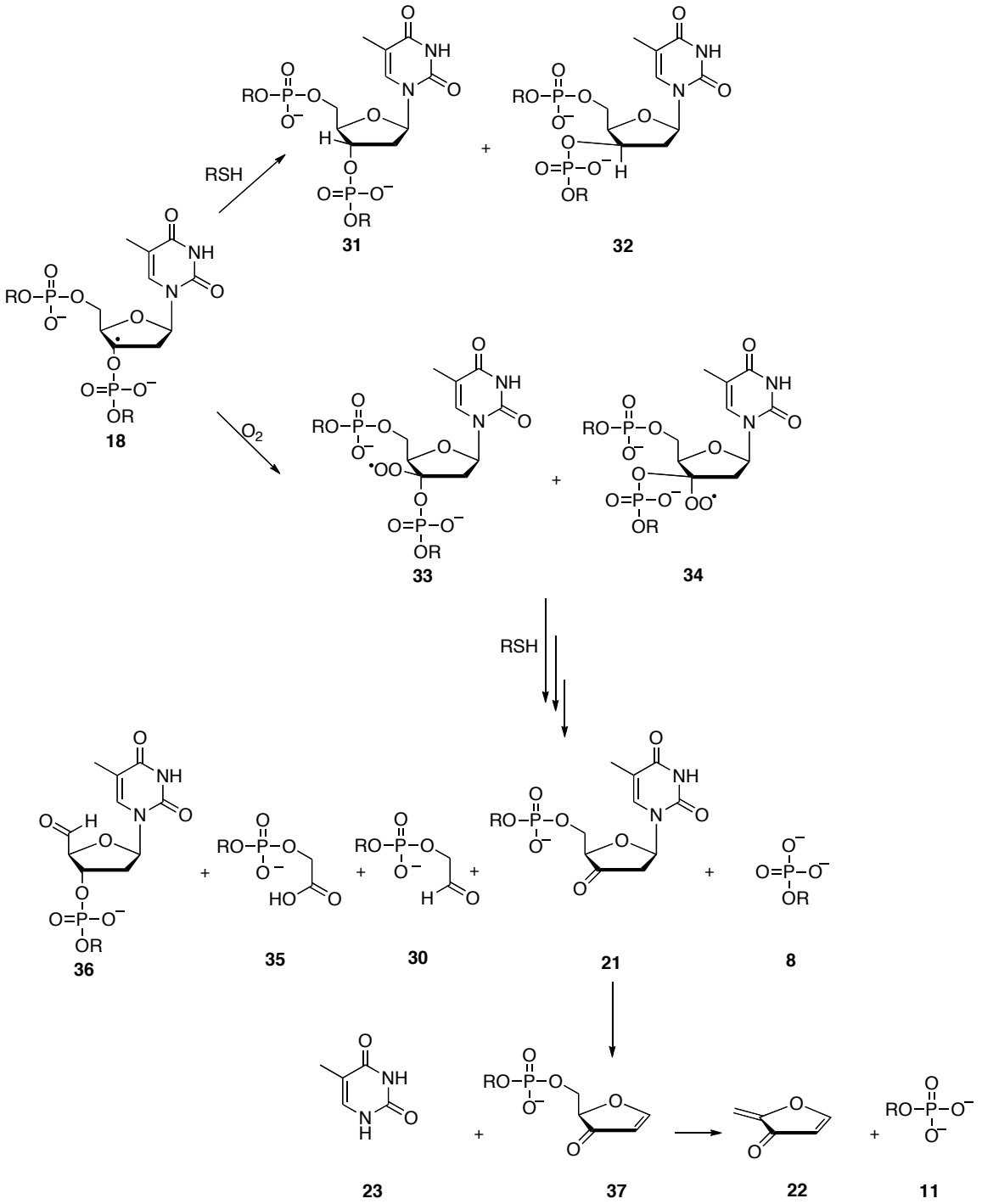

Scheme 1.5: Products of the degradation of the C3'-thymidinyl radical under anaerobic and aerobic conditions[39]

It was observed by Awada et al. that 2-phosphoglycolaldehyde (**38**), a model for 3'-PGA (**30**), decomposes to glyoxal under biological conditions and reacts with dG (**40**)

in DNA to form the diasteromeric 1,N2-glyoxal adducts of dG (**41** and **42**, **Scheme 1.6**).[40]

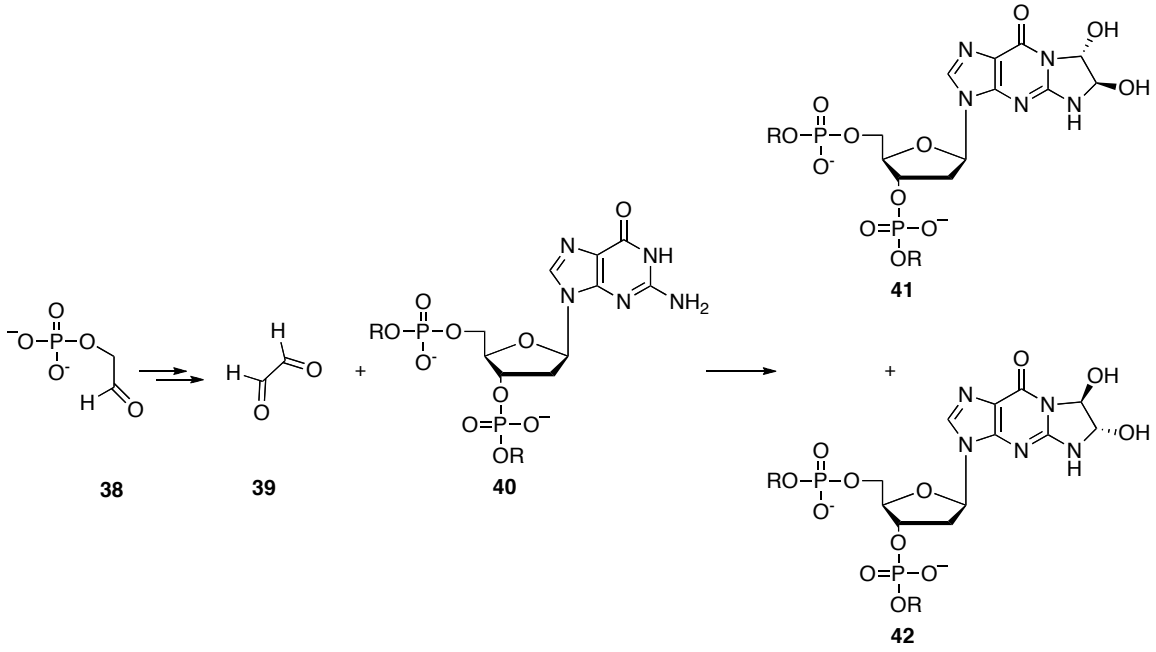

Scheme 1.6: DNA adducts derived from phosphoglycolaldehyde[40]

1.3.2.4 C4'-Radical

The C4'-radical has been the most studied sugar radical in DNA. The C4'-deoxyribosyl radical (**43**) is a β-phosphatoxyalkyl radical and α-oxy radical bearing two phosphate groups beta to the radical making the elimination of phosphate fast. C4'-deoxyribosyl radical **43** has been independently generated in nucleosides and oligonucleotides.[41,42] The fate of this radical under anaerobic and aerobic conditions has been investigated in detail.[43] Under anaerobic conditions and in the absence of reducing agent, the C4'-deoxyribosyl radical (**43**) in ss- or ds-DNA undergoes heterolytic cleavage to generate radical cation **44** and strand breaks (**8**) with a rate constant of about 10^3 s^{-1} in ssDNA (dsDNA is 10 times slower) (**Scheme 1.7**).[44] Trapping of radical cation **44** by a water molecule yields radical **45**, which undergoes a second β-phosphate elimination to

give 3'-phosphate containing oligonucleotide **11** and radical cation **46**. Radical **45** can abstract a hydrogen from GSH to generate **47**.[44] In the presence of GSH, there is competition between heterolytic cleavage of the C4'-deoxyribosyl radical (**43**) and hydrogen abstraction from GSH. Trapping of **43** with GSH occurs at a rate of 1.9×10^6 $M^{-1}s^{-1}$ giving rise to a mixture of repaired (**48**) and "pseudorepaired" (**49**) nucleotides.[44,45] The hydrogen trapping reaction is stereoselective in dsDNA resulting in formation of natural 2'-deoxyribonucleotides (ratio **48**:**49** = 9) while in ssDNA trapping is nonselective, producing **48** and **49** in a ratio of 1.5.[44]

Under aerobic conditions and in the presence of GSH, C4'-radical **43** is trapped by oxygen to form isomeric peroxyl radicals **50** with a rate constant of 2×10^9 $M^{-1}s^{-1}$. This reaction was found to be reversible. Peroxyl radicals (**50**) abstracts a hydrogen atom from GSH to form hydroperoxide **51**.[45,46] The hydroperoxide undergoes a Criegee-type rearrangement to generate intermediate **52** which subsequently decomposes to yield base propenal **55**, 5'-phosphorylated oligonucleotide (**8**), and 3'-phosphoglycolate (3'-PG) **35** (**Scheme 1.7**).

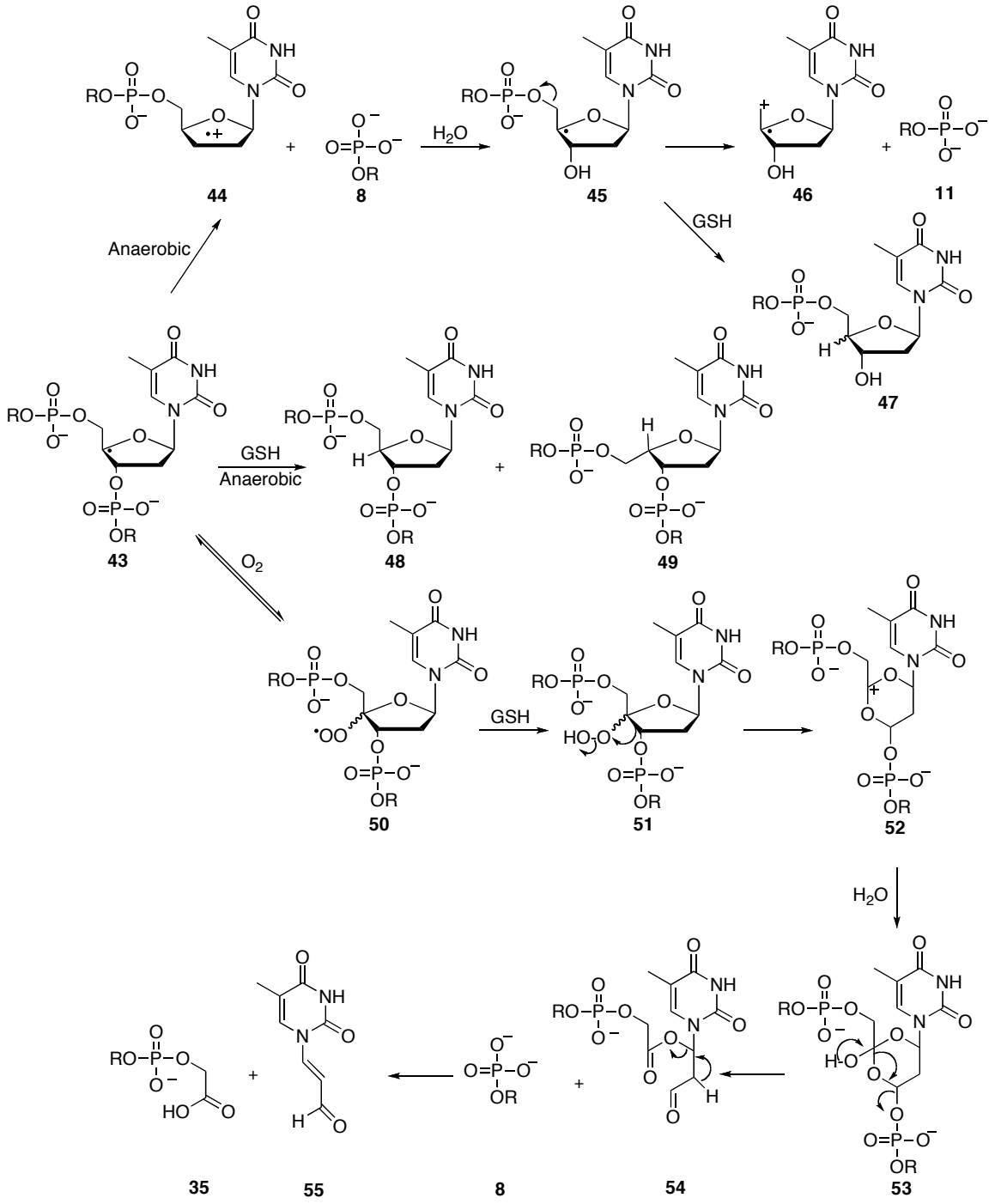

Scheme 1.7: Fate of C4'-thymidinyl radical

Base propenal **55** can react with deoxyguanosine in DNA to form the DNA adduct M_1dG (**56**) (**Scheme 1.8**).[47,48]

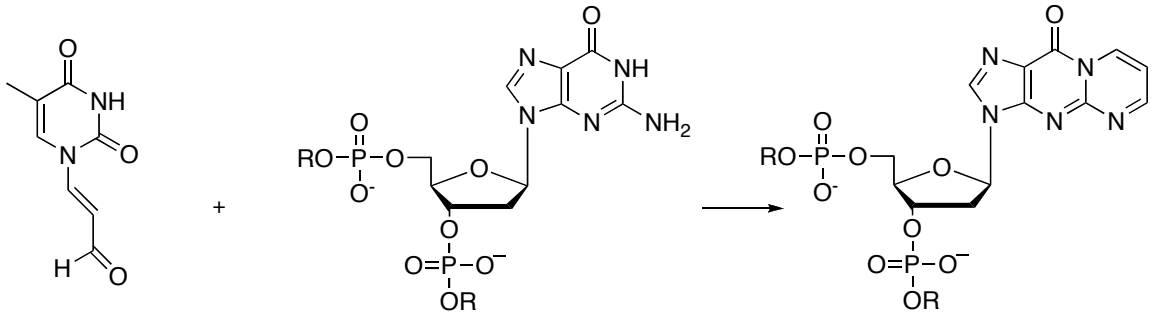

55 **40** **56**

Scheme 1.8: M_1dG adduct of base propenal with guanine

1.3.2.5 C5'-Radical

The C5'-deoxyribosyl radical (**57**) is an α-phosphatoxyalkyl radical generated by the abstraction of one C5'-hydrogen. Under anaerobic conditions, the C5' radical (**57**) attacks the C8-N7 double bond in purine bases of the same nucleoside leading to cyclization at C8. The outcome of this cyclization is the formation of both R and S diastereomers of 8,5'-cyclo-2'-deoxyguanosine (cdG) or 8,5'-cyclo-2'-deoxyadenosine (cdA, **59** and **60**, **Scheme 1.9**).[49,50] The rate constant of intramolecular cyclization of 2'-deoxyadenosine-5'-yl radical and 2'-deoxyguanosine-5'-yl is 1.6×10^5 s^{-1} and 1.0×10^6 s^{-1}, respectively.[49,51] In the presence of physiological concentrations of thiol, hydrogen trapping of the radical competes with the cyclization process. Trapping of the C5' radical with GSH results in formation of **58** and occurs at a rate of 4.9×10^7 $M^{-1}s^{-1}$.[52] In the presence of oxygen, C5' radical **57** reacts with oxygen at a diffusion-controlled rate (~1.9×10^9 $M^{-1}s^{-1}$) to form peroxyl radical **61**. The peroxyl radical decomposes by two pathways (**Scheme 1.9**), one yielding strand breaks with 3'-phosphate (**11**) and 5'-

aldehyde (**63**) end groups,[53] while the other delivers 5'-(2-phosphoryl-1,4-dioxobutane) **64** along with 3'-formyl oligonucleotide (**65**).[54]

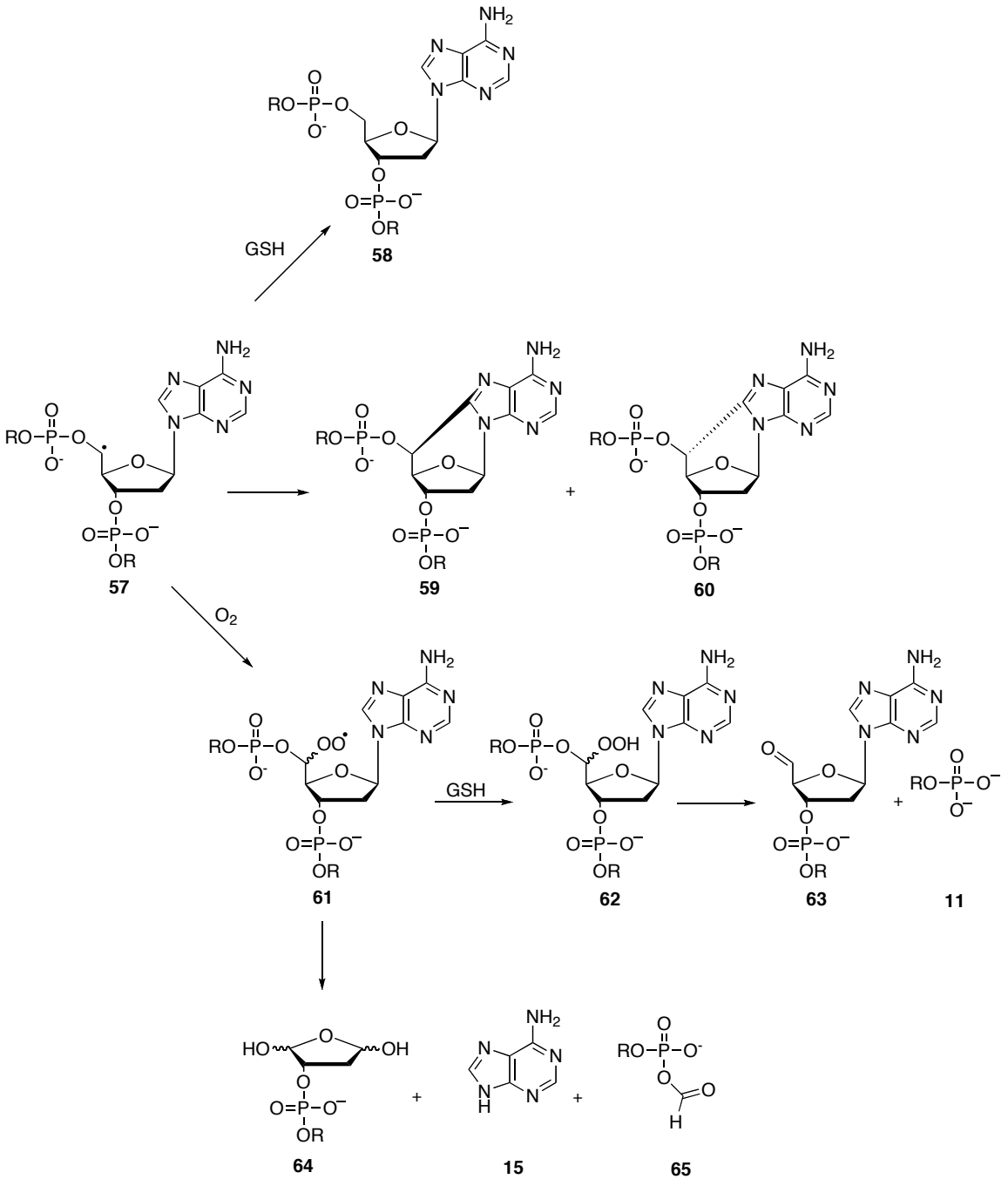

Scheme 1.9: Fate of C5 '-deoxyadenosyl radical

The 5'-aldehyde can undergo β-elimination to form unsaturated aldehyde **66** and 5'-phosphorylated oligonucleotide **8**. Unsaturated aldehyde **66** undergoes base elimination to deliver furfural **67** and ree base **23** (**Scheme 1.10**).[55,56]

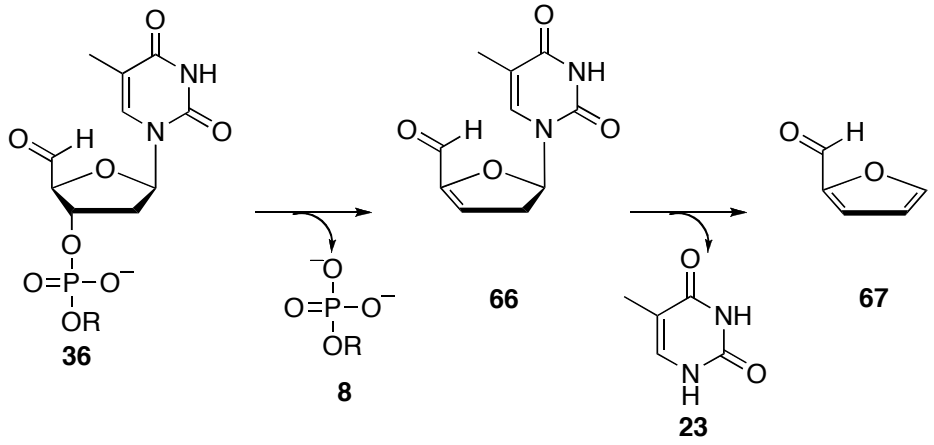

Scheme 1.10: Fate of 5'-thymidinylaldehyde

It was shown that furfural can form an adduct with adenine residues in DNA. This adduct subsequently undergoes deglycosylation to form kinetin (**68**) and an abasic site (**69**) (**Scheme 1.11**).[57]

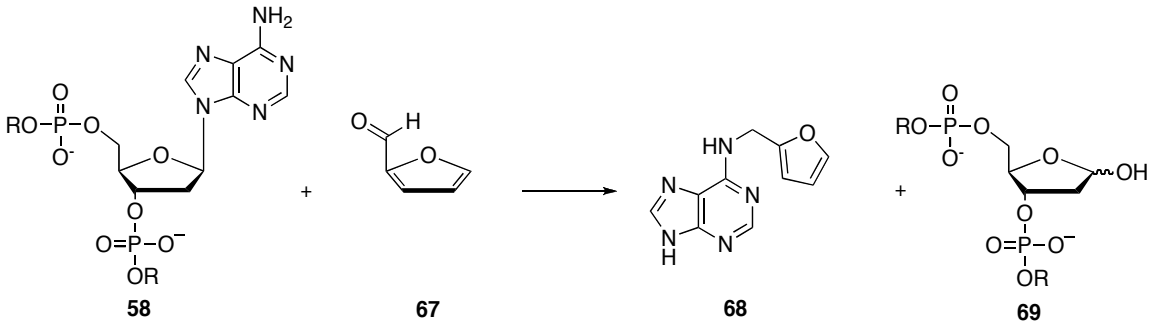

Scheme 1.11: Adduct formation between furfural and an adenine residue in DNA

5'-(2-Phosphoryl-1,4-dioxobutane) (**64**) in its cyclic form can exist in equilibrium with the open chain form (**Scheme 1.12**). This dialdehydic lesion undergoes β-elimination to form trans-1,4-dioxo-2-butene (**70**), a highly reactive α,β unsaturated dicarbonyl species.[54] It has been demonstrated that this electrophilic lesion can react with

nucleophiles in DNA to form stable oxadiazabicyclo (3.3.0)octamine adducts of dC, dA, and dG under biological conditions (reaction with dC, **Scheme 1.13**).[58,59]

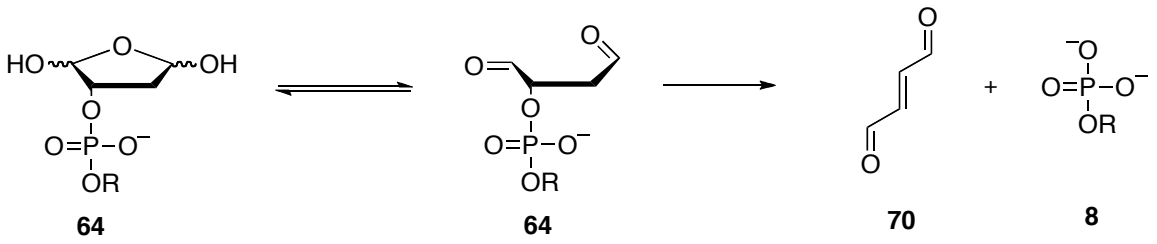

Scheme 1.12: Fate of 5'-(2-phosphoryl-1,4-dioxobutane)

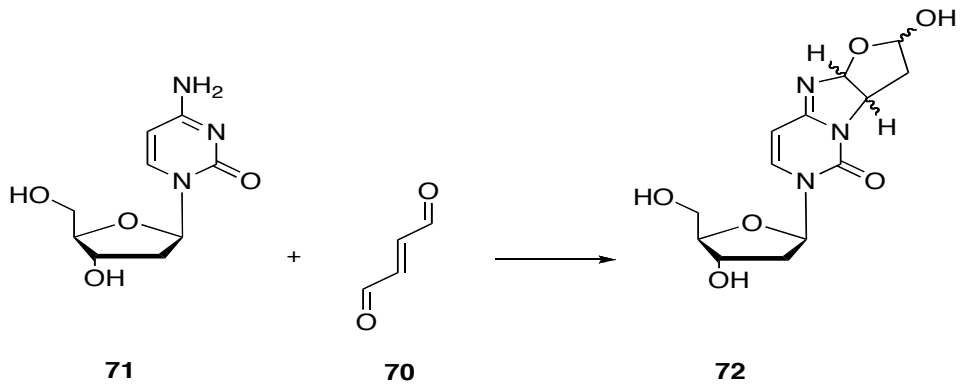

Scheme 1.13: Adduct formation by trans-1,4-dioxo-2-butene with deoxycytidine

1.4 DNA Damage by Hydrogen Atoms ($H^{\bullet}$)

The hydrogen atom ($H^{\bullet}$) is considered a reducing species generated from ionizing water molecules through the indirect effect of ionizing radiation.[3, 11] It can damage DNA through addition to the double bonds of the nucleobases resulting in formation of neutral nucleobase radicals that can react further to cause more damage.[60]

1.5 DNA Damage by Solvated Electrons (e^-_{aq})

Solvated electrons are generated from radiolysis of water molecules and are stronger reducing agents than the hydrogen atom.[3] Solvated electrons are highly reactive and damage biological molecules by one-electron transfer.[11] Hydrated electrons add to the nucleobases of DNA forming radical anions (**73**, **Figure 1-4**) that are easily protonated resulting in the formation of neutral radicals (**74** and **75**).[3]

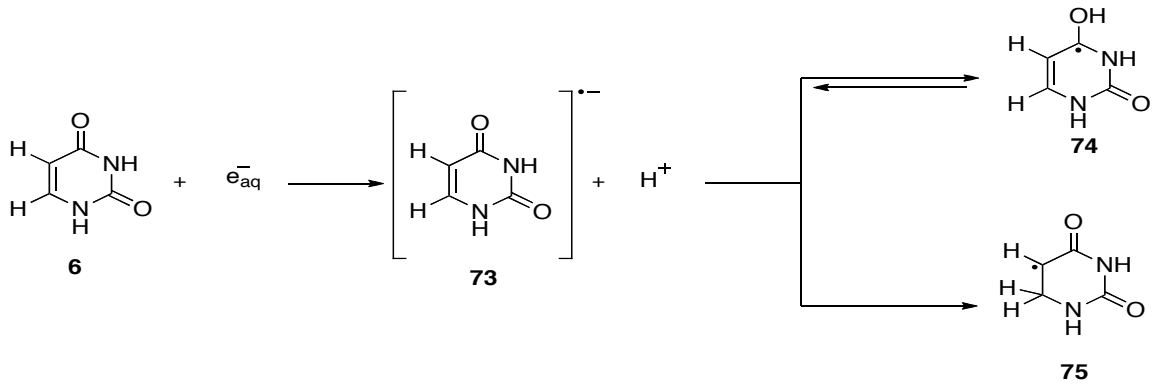

Figure 1-4: Reaction of a solvated electron with uracil[61]

1.6 Significance of the DNA Damage by IR

IR causes a variety of damage to DNA in living systems by randomly ionizing the DNA components and the surrounding water molecules producing a cascade of secondary electrons with LEE <15 eV. This damage can be in the form of base and sugar damage, single and double strand brakes, and clustered damage, which can be genotoxic, mutagenic, and lethal.[5,62,63,64,65] Although ionizing radiation is used as a therapeutic method to treat cancer, it can not distinguish between the DNA of healthy cells and cancerous cells. Understanding the mechanisms involved in IR induced damage to DNA will help in the development of more efficient radiotherapeutic methods.

1.6.1 Significance of the Investigation of the C-3' dideoxy Radical Generated by LEE-DNA interaction.

It has been established that DNA damage is mostly produced by secondary species generated along the radiation track. LEEs are produced in large quantities and have been established to induce both single and double strand brakes as well as base release.[9,66] This was supported through the investigation of the basic interaction of LEE with ribose derivatives,[67,68] nucleobases,[10,69,70] oligonucleotides,[71,72] and plasmid DNA.[5,73,74] It was determined that electrons below 15 eV break DNA bonds through a resonance process called dissociative electron attachment (DEA) producing stable anions and radicals fragments.[75] Although this process induces DNA strand breaks, the chemical steps leading to the formation of the final DNA modification remain to be established.

One proposed mechanism to explain the mechanism of LEE-induced strand breaks in DNA which involves dissociative electron attachment is seen in **Figure 1-5**.[66] It is believed that LEE are captured first by the π^* orbital of the nucleobases in DNA (**76**)[9] followed by electron transfer to the π^* orbital of the phosphate group resulting in the formation of transient molecular anions at the phosphate group (**77**), which dissociate via two possible pathways: Path A involves homolytical cleavage of the C-O σ bond at the 3' and/or 5' positions resulting in the formation of carbon-centered radicals **78** and **83**, respectively along with the corresponding phosphorylated oligonucleotides **79** and **82** (**Figure 1-5**), whereas path B involves homolytic cleavage of the P-O σ bond at the 3' and/or 5' positions resulting in the formation of phosphoryl radicals **81** and **84**, respectively along with the corresponding alkoxyl anions **80** and **85** (**Figure 1-5**).[66,4] It is believed that cleavage of the phosphodiester bond takes place primarily via C-O σ bond

cleavage as shown in pathway A. The formation of reactive intermediates **78** and **83** was confirmed through the identification of the dephosphorylated C3' sugar radical through electron spin resonance (ESR) studies of argon ion and γ- irradiated hydrated DNA.[76] Investigation of the reactivity and fate of this sugar radical intermediate will facilitate the elucidation of the structure of the final DNA lesions and establish the mechanism of DNA damage resulting from LEE.

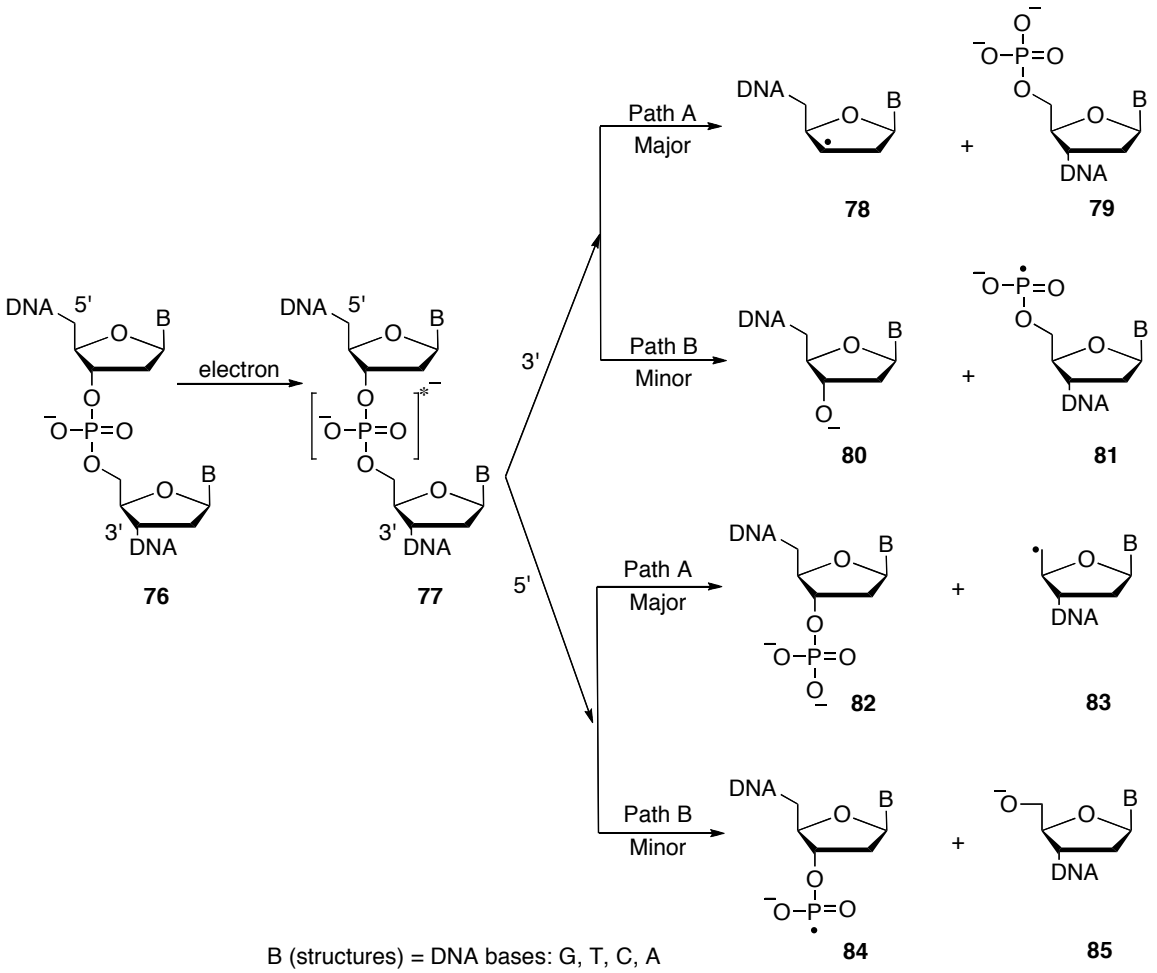

Figure 1-5: Proposed pathways for phosphodiester bond cleavage of DNA via LEE[66]

1.6.2 Independent Generation of the Deoxyribosyl Radical

Many investigations have been performed to understand the alterations in DNA induced by LEE.[3] However, DNA damage by IR and DNA damaging agents can be

complicated due to the generation of multiple reactive intermediates (nucleobase and sugar radicals) through random attack at biopolymers.[77] To facilitate the mechanistic investigation of DNA damage, reactive intermediates have been independently generated in a controlled manner at defined sites in DNA.[38,78] This strategy has allowed for the elucidation of reaction mechanisms and uncovered reaction pathways while improving the overall understanding of biologically important chemistry.[79,80,81] Independent generation of reactive intermediates involved in DNA damage facilitate separation of the chemical processes that generate this species from the effect of a damaging agent on the reactivity of the intermediate.[82] The use of photolabile groups such as phenylselenyl[83] or acyl groups[36,84] to generate the radical of interest at specific sites has been very successfully applied to the generation of pyrimidine nucleobase[84] radicals and sugar radicals at various positions in nucleosides[20] and nucleotides.[85] Acyl derivatives of modified nucleosides and oligonucleotides have been utilized as excellent radical precursors, undergoing Norrish Type I photocleavage processes at wavelengths above those that usually damage DNA. In Norrish Type I photocleavage, photoactivation of acyl groups (isopropyl, acetyl, or pivaloyl) result in excitation of electrons to the singlet state followed by bond scission at either side of the carbonyl group (**Figure 1-6**). Photocleavage of acyl derivatives of oligonucleotides (**86**) can undergo bond scission by two pathways: Path A, in which the homolytic cleavage occurs between the C-CO bond between ketone and 2'-deoxyribose moiety of the nucleotide resulting directly in formation of sugar radical **87** and acyl radical **88** fragment. Acyl radical **88** undergoes decarbonylation to deliver carbon monoxide (**89**) and a second alkyl radical (**90**). In path B, homolytic cleavage of R-CO results in formation of the acyl sugar radical **91** and alkyl

radical **90**. Compound **91** subsequently decarbonylate to release carbon monoxide **89** and sugar radical **87**.[86]

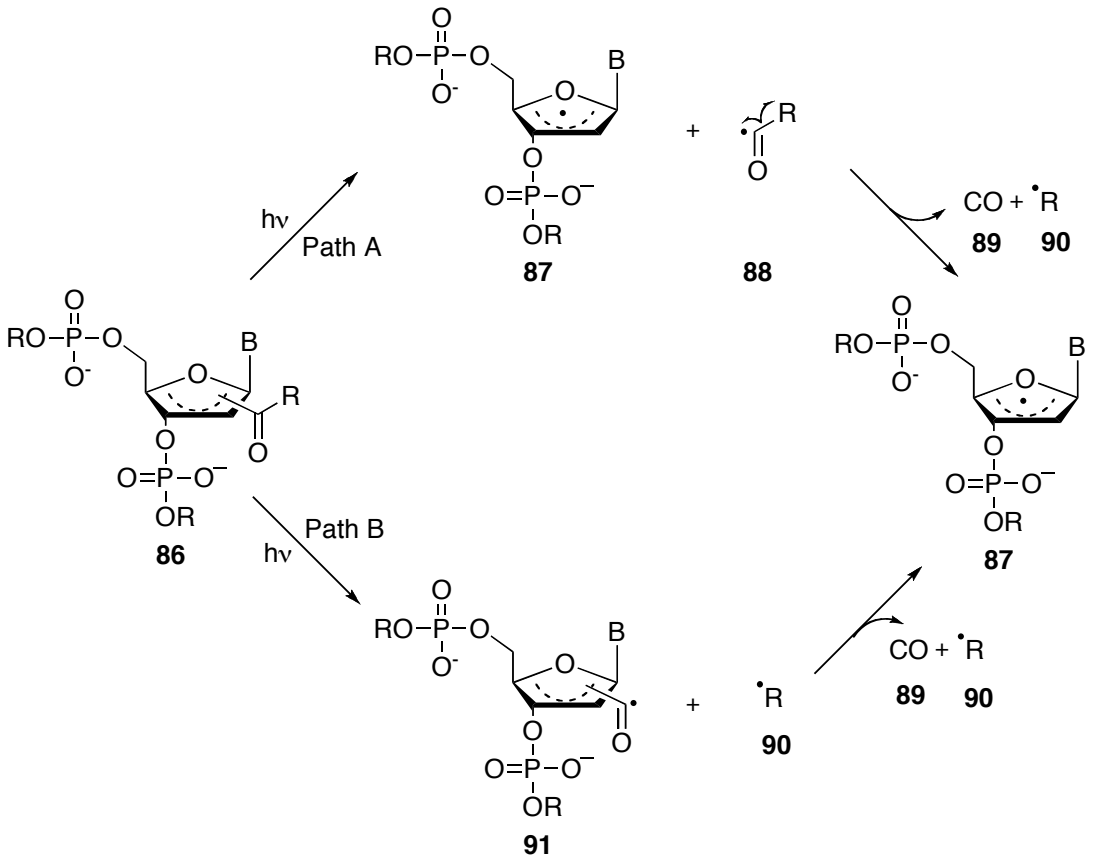

Figure 1-6: Norrish Type I photocleavage of oligonucleotide containing acyl groups

The pivaloyl group was chosen to be used as a radical precursor for the mechanistic investigation of LEE induced DNA damage. Since it is expected to undergo photocleavage through path B, forming an acyl sugar radical (**91**) which is expected to undergo fast decarbonylation ($\geq 10^5$ s^{-1}) rather than reduction by a hydrogen atom source process.[86,87,88] In addition, the *tert*-butyl radical (**90**) is believed to diffuse away from the site of radical generation without participating in secondary reactions.[45] On the other

hand, methyl and isopropyl ketones were shown to produce side products and cause lower yields. The pivaloyl group has been used successfully to site-specifically generate the radical of interest at a predetermined position on the base and sugar moieties of nucleosides and oligonucleotides. **Figure 1-7** shows examples of pivaloyl radical precursors (**92-100**) that have been used to efficiently generate nucleobase and sugar radicals in nucleosides and oligonucleotides.[89,90,91,92] These radical precursors helped in the elucidation of mechanisms involved in the fate of radicals induced from IR.

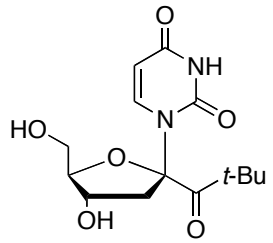

92

J.Org.Chem. **1996**, *61*, 2-3

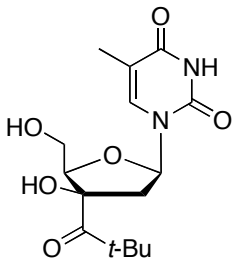

93

J.Org.Chem. **1999**, *64*, 1559-1564

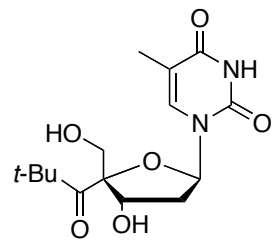

94

Helvetica Chimica Acta. **1996**, *79*, 1980-1994

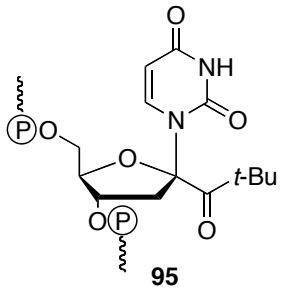

95

Chem. Biol. **1998**, *5*, 263-271

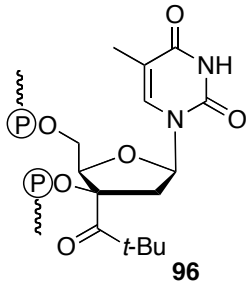

96

Chem. Res. Toxicol. **2006**, *19*, 1630-1636

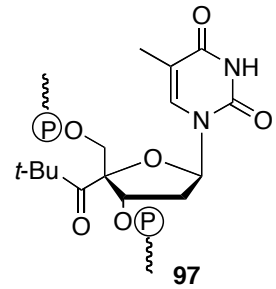

97

Chem. Biol. **1995**, *2*, 367-375

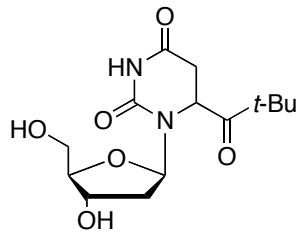

98

J.Org.Chem. **2003**, *68*, 4275-4280

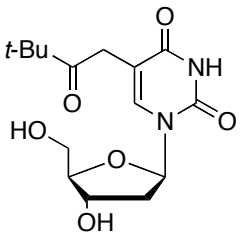

99

J.Org.Chem. **2000**, *65*, 4648-4654

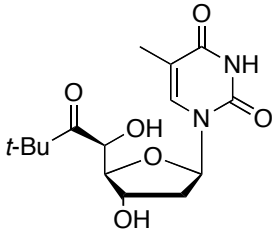

100

J.Org.Chem. **2007**, *72*, 3659-3666

Figure 1-7: Pivaloyl radical precursors designed to generate radicals at different positions in nucleosides and nucleotides

1.7 Relevance of the Investigation of the Oxidative Damage to C-5'

ROS, with hydroxyl radical being one of the most reactive species, can abstract hydrogen atoms from the deoxyribose moiety of DNA causing the formation of sugar radicals that degrade frequently to strand breaks accompanied by end modified DNA fragments.[17,53] Those fragments can degrade to small electrophilic fragments capable of reacting with cellular nucleophiles such as nucleobases and side chains of proteins forming DNA adducts and/or DNA-protein crosslinks. DNA adduct formation can be toxic, mutagenic, and carcinogenic. Therefore identification of adducts formed through 2'-deoxyribose oxidation in DNA has the potential to reveal biomarkers suitable for early detection of many diseases with cancer being one of the most important. Biomarker discovery will aid in the early detection of cancer and its treatment.

Several DNA adducts were found to form as a result of oxidative damage to the sugar moiety in DNA (**Figure 1-8**). The formation of these adducts were explained in the above sections. Oxidation at the C5' position of 2'-deoxyribose results in formation of strand breaks terminated with a 5'-aldehyde group (**36**).[17,77] Degradation of this lesion results in formation of furfural (**67**), a compound known to form adducts with adenine to give kinetin (**68**).[55,57] Investigation of the ability of 5'-aldehyde containing oligonucleotides and its degradation products **66** and **67** to form adducts with DNA at physiological conditions will be conducted. These investigations may reveal biomarkers to be used for early detection of diseases.

Although oxidative stress causeses damage to DNA components resulting in the formation of modified nucleobases and 2-deoxyribose lesions as seen above, but most of this damage can be repaired by DNA repair enzymes such as base excision repair

enzymes (BER) which can remove modified nucleotides including various types of abasic sites whereas bulkier lesions and cross-links are removed by nucleotide excesion repair enzymes (NER).

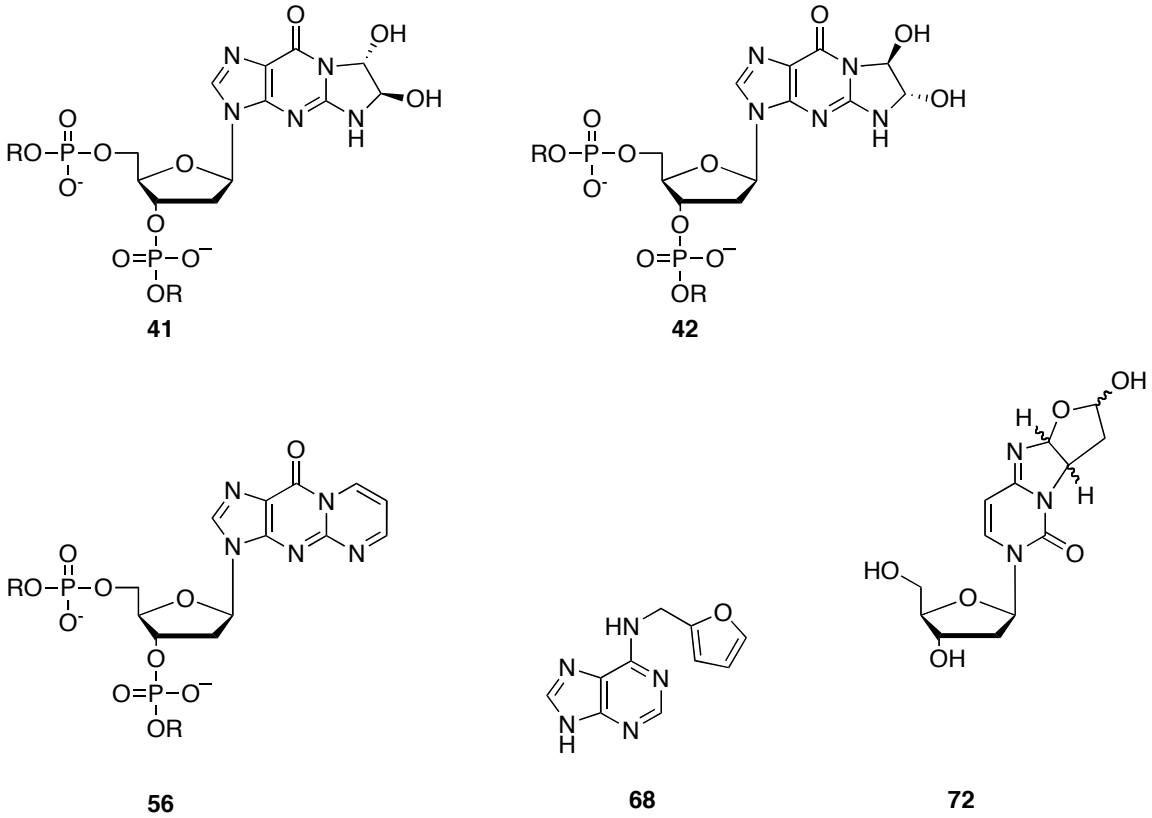

Figure 1-8: DNA adducts derived from 2'-deoxyribose oxidation

2 CHAPTER TWO

2.1 RESULTS and DISCUSSION: Synthesis and Photolysis of C3'-Modified Nucleosides

DNA damage caused by ionizing radiation and DNA damaging agents is a complex process involving the generation of multiple reactive intermediates through random attack at biopolymers.[77] In order to overcome multiple radical formation and a lack of control over the site of radical generation, organic chemistry has been used to independently generate reactive intermediates in a controlled manner at defined sites in biopolymers.[82] This approach has clarified reaction mechanisms and identified new DNA damage pathways.[38,78] These studies often use photolabile groups such as phenylselenyl[83] or acyl groups[36] to generate the radical of interest. Pivaloyl derivatives of modified nucleosides[82,84] and oligonucleotides[39,28] have been utilized as precursors for site-specific generation of nucleobase and sugar radicals. With the goal to investigate the fate of the C2',3'-dideoxy-C3'-thymidinyl radical in DNA, a proposed intermediate of DNA-LEE interactions,[66] C2',3'-dideoxy-C3'-pivaloyl modified thymidines (**101** and **103**) were synthesized and their suitability as precursors of the C2',3'-dideoxy-C3'-thymidinyl radical (**102**) investigated (**Figure 2-1**).

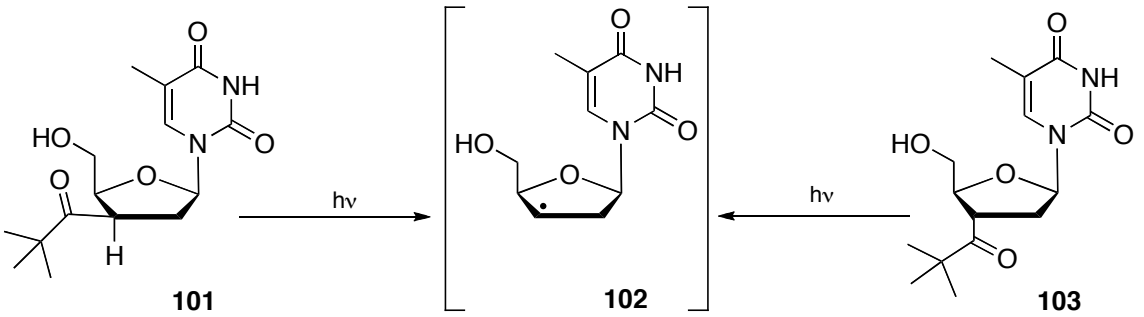

Figure 2-1: Photochemical generation of C2',3'-dideoxy-C3'-thymidinyl radical (**102**) from precursors **101** and **103**

2.2 Design and Synthesis of Photochemical Precursors for the C2',3'-Dideoxy-C3'-thymidinyl Radical (**102**).

Designing efficient photoactive or photolabile radical precursors requires consideration of a set of factors. The stability of photolabile groups during synthesis, and the ability of these groups to generate the radical of interest upon exposure to ultraviolet (UV) light must be utilized. Norrish Type I photochemical reactions have proven to be very effective for generating DNA radicals at different positions at the monomer and polymer levels.[38, 78, 84] The pivaloyl moiety was chosen as a photolabile group based upon its demonstrated successes in the generation of nucleoside-based radical intermediates.[93-90] The pivaloyl group has a carbonyl moiety that absorbs light outside the range that usually damages DNA and subsequently undergoes Norrish Type I photocleavage. This photochemical process involves the generation of a *tert*-butyl and an acyl radical. The acyl radical subsequently undergoes decarbonylation to form a second alkyl radical. The *tert*-butyl radical is belived to diffuse away from the site of radical generation without participating in secondary reactions.[45] To investigate the mechanistic pathway of DNA damage through the formation of the C2',3'-dideoxy-C3'-thymidinyl radical (**102**), α- and

β-C2',3'-dideoxy-C3'-pivaloylthymidines (**101** and **103**) were synthesized. The isomeric precursors were synthesized to investigate the effect of the stereochemistry of the C3'-radical precursors on product formation.

The synthesis β-C2',3'-dideoxy-C3'-pivaloylthymidine (**101**) started with the conversion of commercially available thymidine (**104**) to C3'-methylene thymidine (**107**) according to published literature procedures (**Scheme 2.1**).[94]

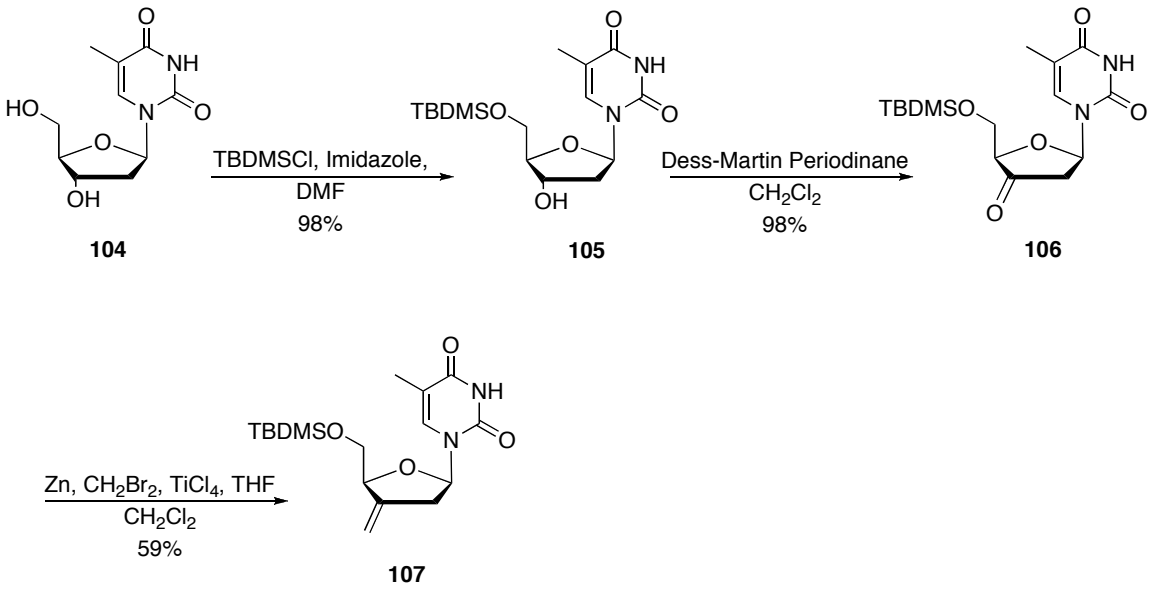

104 **105** **106** **107**

Scheme 2.1: Synthesis of compound **107**[94]

Compound **107** was subjected to hydroboration-oxidation to afford primary alcohol **108** as the β-isomer in 89% yield. Oxidation of the hydroxymethyl using the Dess-Martin periodinane at low temperature gives only the β-isomer of aldehyde **109** in 100% yield. The aldehyde was then subjected to nucleophilic addition using *tert*-butyllithium in the presence of cerium (III) chloride to deliver alcohol **110** in 67% yield as a diasteromeric mixture. Oxidation of secondary alcohol **110** using the Dess-Martin Reagent afforded the β-isomer of ketone **111** in 96% yield. Subsequent deprotection of

the 5'-hydroxyl with THF/TFA/H_2O (8:1:1) afforded nucleoside **101** in 91% yield. (**Scheme 2.2**).[95]

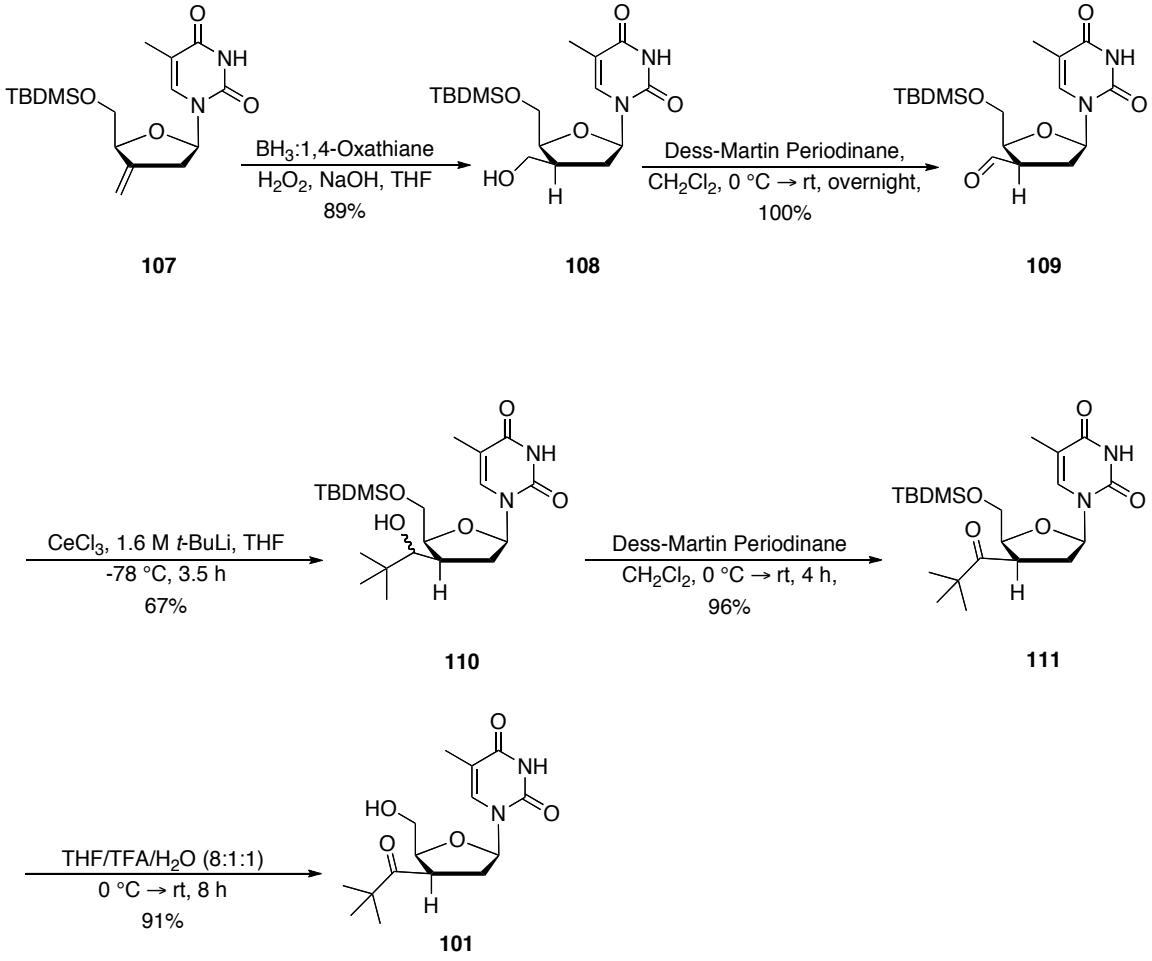

Scheme 2.2: Synthesis of β-C2',3'-dideoxy-C3'-pivaloylthymidine **101**[95]

In order to obtain α-isomer **103** a different strategy was employed. Commercially available thymidine (**104**) was converted to α-aldehyde (**115**) according to published protocols (**Scheme 2.3**).[96,97] The key step in the stereoselective formation of the α-isomer was the conversion of *tert*-butyldiphenylsilyl protected C3'-O-phenoxythiocarbonylthymidine (**113**) to *tert*-butyldiphenylsilyl protected C3'-styrylthymidine (**114**). The reason for stereoselectivity is attribute to the presence of the

C5' bulky protecting group that stericly blocks the top face of the nucleoside forcing the incoming styryl group to approach from the least hindered α-face of the C3'-radical.

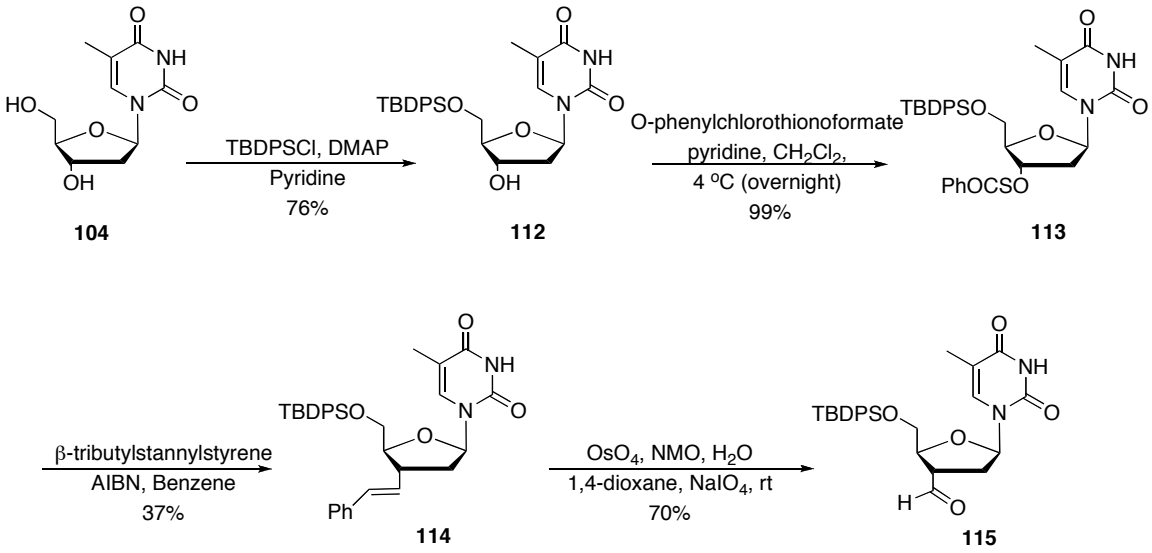

Scheme 2.3: Synthesis of compound **115**[96,97]

Conversion of compound **115** to *tert*-butyl alcohol **116** as a diasteromeric mixture employing the same synthetic strategic as used in the case of the β-isomer proceeded in low yield (13%). Extending the reaction time to 8 hours, however increased the yield to 30%. The lower yield of this reaction compared to the same reaction for the β-isomer may be due to the presence of the bulky 5'-*tert*-butydiphenylsilyl protecting which decreases the reactivity of the formyl group to nucleophilic addition. Oxidation of **116** using the Dess-Martin periodinane delivered the desired ketone (**117**) in 100% yield. Removal of the TBDPS with TBAF resulted in the formation of α-isomer **103** in 44% yield (**Scheme 2.4**).[95] The absolute configuration of these substrates was confirmed through Nuclear Overhauser Effect Spectroscopy (NOESY NMR) analysis. In NOESY experiments the correlation between nuclei that are physically close to each other in space regardless of whether there is a bond between them are detected. Thus, atoms that

are in close proximity to each other display an NOE effect. In our experiments, a strong NOE effect between the 3'-H, 4'-H and 2'-H were used to determine the absolute configuration of these modified substrates. Spectral data for (**108-111**) and (**115-103**) is available in (**Figure 1-14**, Appendix **C**), and NOESY spectra is available in supporting information of the cited reference.[95]

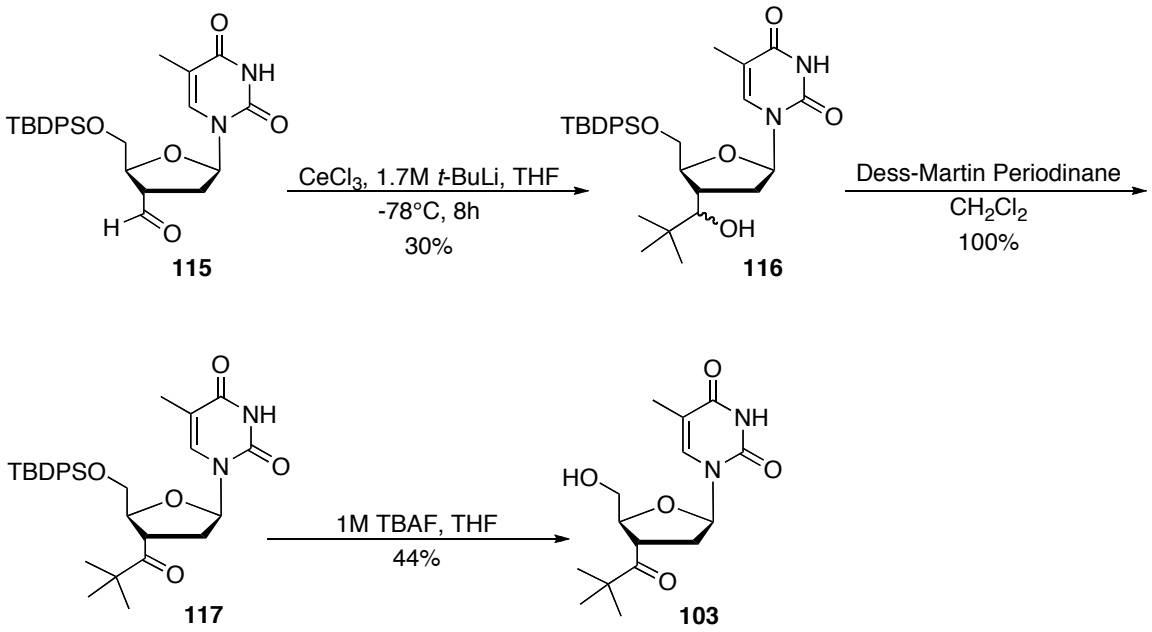

Scheme 2.4: Synthesis of α-C2',3'-dideoxy-C3'-pivaloylthymidine (**103**)[95]

2.3 Investigation of the suitability of α and β-Pivaloylketone Precursors **101** and **103** for the Generation of C3' Radical **102**.

The use of photolabile precursors to independently generate the C2',3'-deoxy-C3'-thymidinyl radical in nucleic acids will help to elucidate the reactivity of the radical and facilitate the identification of the damage products generated from this intermediate in nucleosides and nucleotides. The suitability of α and β-pivaloylketone precursors **101** and **103** for site specific generation of C2',3'-dideoxy-C3'-thymidinyl radical **102** under

anaerobic conditions and in the presence of different hydrogen atom donors was explored.

2.3.1 Photochemical Generation of the C2',3'-Dideoxy-C3' Radical in the Presence of *tri-n*Butyltin Hydride.

Initial photolysis experiments were carried out in order to determine whether the C2',3'-dideoxy-α-C3'-pivaloylthymidine (**103**) and C2',3'-dideoxy-β-C3'-pivaloylthymidine (**101**) are capable of generating the C2',3'-dideoxy-C3'-thymidinyl radical (**102**). Their efficiencies as radical precursors were determined through trapping of **102** with a hydrogen atom donor. The formation of reduction product **118** provides proof for the suitability of **101** and **103** as precursors of the C2',3'-dideoxy-C3'-thymidinyl radical (**102**) **Figure 2-2**.

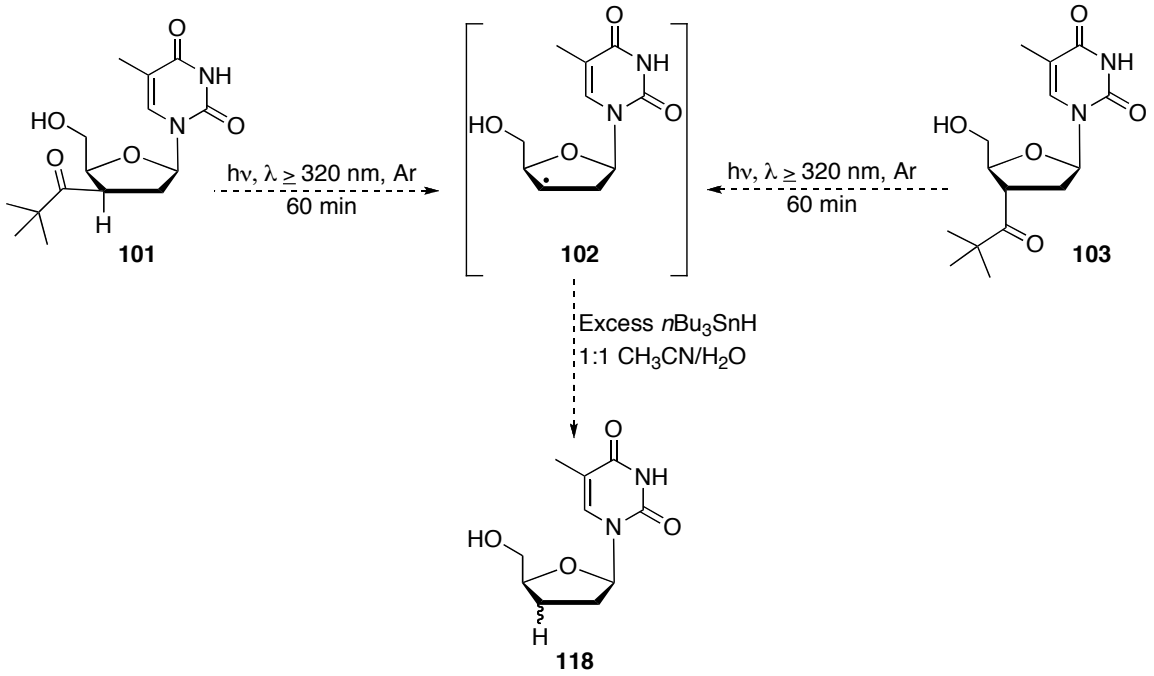

Figure 2-2: Strategic approach to determine the feasibility of **101** and **103** as photochemical precursors of the C2',3'-dideoxy-C3'-thymidinyl radical

Photolysis of **103** (1 mM) was performed, using a 500 W high pressure mercury arc lamp fitted with an IR filter, focusing lens, and 320 nm cutoff filter, in 1:1 acetonitrile/water containing excess *tri-n*butyltin hydride (**Scheme 2.5**).

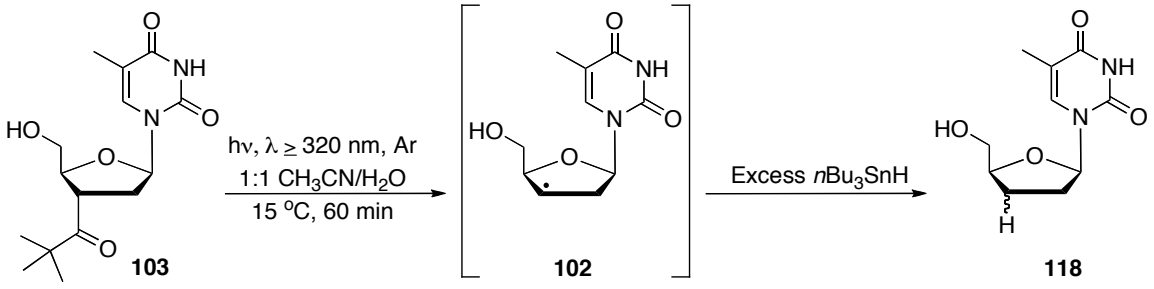

Scheme 2.5: Photochemical generation of the C2',3'-dideoxy-C3'-thymidinyl radical (**102**) from **103** in the presence of *tri-n*butyltin hydride

The photolysate was analyzed directly without workup using high performance liquid chromatography (HPLC) employing a C18 reversed-phase column with detection

at 254 nm. The products were isolated and identified by electrospray ionization mass spectrometry (ESI-MS) and by comparison with authentic samples. **Figure 2-3** shows the reversed-phase HPLC chromatogram of the crude photolysate (green), the control (red), and the standards (blue). Irradiation of **103** under the above conditions resulted in 62% conversion of **103** to reduction product **118** as the sole product. The formation of the reduction product indicates that **103** is a viable precursor of radical **102**. In order to confirm formation of the reduction product, a standard was synthesized[95] and injected along with the precursor **103** and their retention times were compared to the photolysate (blue). In addition, the identities of photoproduct **118** and precursor **103** were confirmed with ESI-MS. The mass spectrum shows a molecular weight of 249.2 m/z corresponding to the sodium adduct of **118** and a molecular weight of 333.4 m/z corresponding to the sodium adduct of **103** (Appendix **A**, Figure **1** and **2**, respectively). A control experiment was done in which the precursor (**103**) was prepared as described with the exclusion of exposure to UV light. From the HPLC chromatogram, we see only the presence of **103** indicating the formation of the reduction product in the photolysate results only from trapping of **102** with a hydrogen atom confirming the viability of **103** as a precursor of **102**.

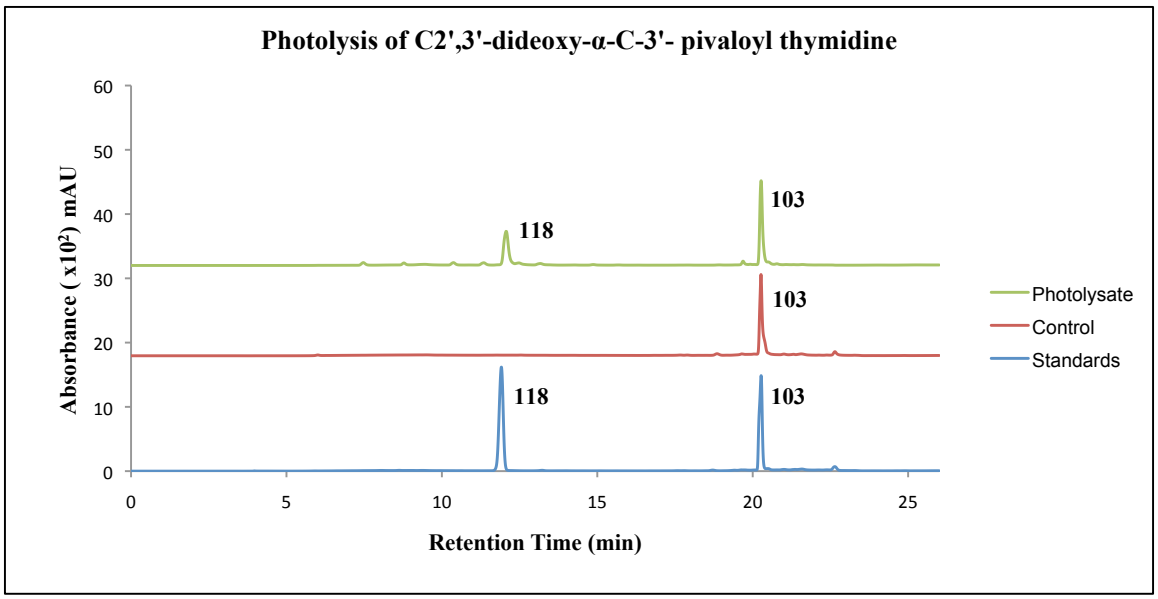

Figure 2-3: Reversed-phase HPLC analyses of the photolysate resulting from photolysis of **103** (green), Controls (red), Standard **118** along with radical precursors **103** (blue) were injected separately

In contrast, β-C3'-pivaloylthymidine (**101**) was photolyzed under the same conditions as used for α-precursor **103** (**Scheme 2.6**).

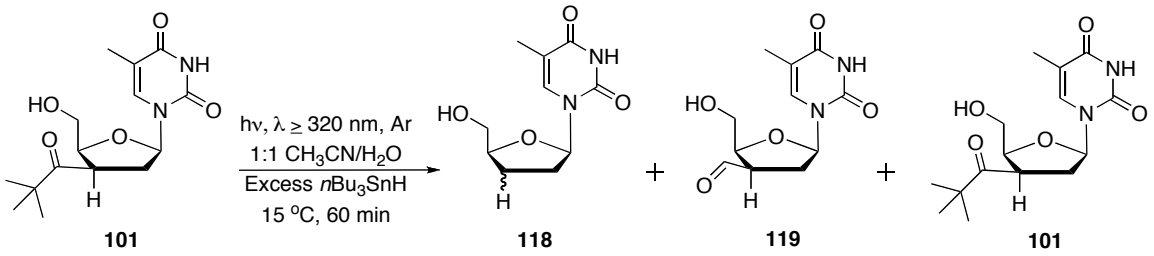

Scheme 2.6: Product identification from photochemical generation of the C2',3'-dideoxy-C3'-thymidinyl radical (**102**) from **101** in 1:1 acetonitrile/water in the presence of *tri-n*butyltin hydride

The crude sample was analyzed by HPLC on a C8 reversed-phase column without any workup and detection at 254 nm. Unfortunately, reduction product **118** was detected in very small amount (peak at 13.580 min, **Figure 2-4**). Fractions eluting at 13.580 min

and 13.740 min were collected together and concentrated. Analysis by MALDI-ToF MS indicated *m/z* values of 249.092 and 265.058 corresponding to the monoisotopic masses of the sodium and potassium adducts of **118**, respectively, and a monoisotopic mass of 277.090 corresponding to the sodium adduct of aldehyde **119** (Appendix **A**, **Figure 3**). Aldehyde **119** is a side product resulting from homolytic cleavage of the *tert*-butyl-acyl bond followed by subsequent trapping with *tri-n*butyltin hydride. This implies that there is competition between trapping of the acyl radical and liberation of carbon monoxide to generate the C2',3'-dideoxy-C3'-thymidinyl radical (**102**). In addition to MALDI-ToF analysis, the retention time of the aldehyde was compared to that of independently synthesized aldehyde (**119**) and both were identical. The major component of the mixture eluting at 14.860 min could not be analyzed by either ESI-MS or MALDI-ToF MS. Analysis of fractions eluting at 9.900 and 12.787 min with MALDI-ToF also failed. The fraction eluting at 20.533 min was confirmed to be the precursor **101** by MALDI-ToF MS (333.151 and 349.114 monoisotopic masses of sodium and potassium adducts, respectively (Appendix **A**, **Figure 4**).

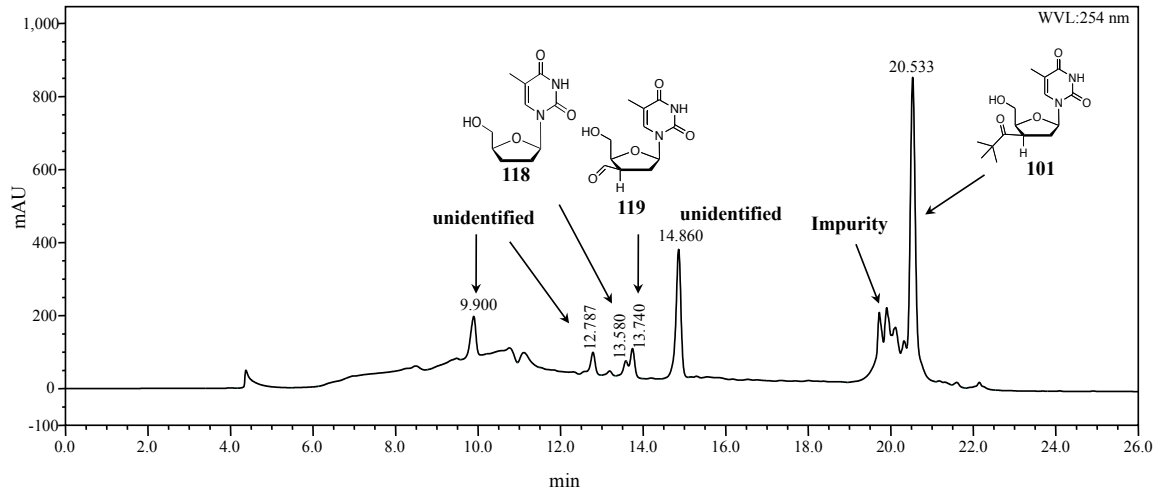

Figure 2-4: Reversed-phase HPLC chromatogram of the photolysate resulting from photolysis of **101** (1 mM) in 1:1 acetonitrile/water in the presence *tri-n*butyltin Hydride

Since the photolysis of the β-C3'-pivaloylthymidine **101** in 1:1 CH_3CN/H_2O did not afford the reduction product as the major product, the photolysis solvent was changed to absolute acetonitrile, as a polar aprotic organic solvent, to determine if elimination of solute-solvent hydrogen bonding would have any effect on product distribution. Photolysis of β-C3'-pivaloylthymidine **101** was performed in acetonitrile containing an excess of *tri-n*butyltin hydride for 1 h at 15 ºC after degassing with argon for 20 minutes (**Scheme 2.7**).

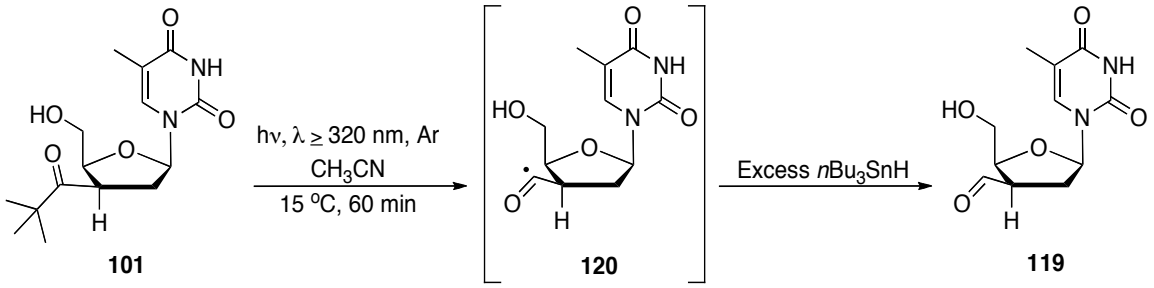

Scheme 2.7: Photochemical generation of the C2',3'-dideoxy-C3'-acylthymidinyl radical (**120**) from **101** in acetonitrile in the presence of *tri-n*butyltin hydride

The crude sample was analyzed by reversed-phase HPLC (**Figure 2-5**). The chromatogram shows the presence of fractions eluting at 13.887 and 20.593 min which were collected, concentrated, and analyzed by MALDI-ToF MS. The MALDI data shows monoisotopic masses equal to 255.235 and 277.073 which corresponds to the hydrogen and sodium adducts of aldehyde (**119**), respectively and a monoisotopic mass of 333.109 which corresponds to the sodium adduct of recovered starting material **101**, the potassium adduct of **101** was also observed (*m/z* 349.080) (Appendix **A**, **Figure 5** and **6**, respectively). This result indicates that acetonitrile as solvent makes trapping of the acyl radical (**120**) by a hydrogen atom faster than decarbonylation. This may be due to the formation of a hydrogen bond between the oxygen of the acyl group and the hydrogen of the 5'-hydroxyl group forming a seven member ring causing the decarbonylation to be slow and the trapping with hydrogen atom donor faster. Additionally, it was reported that decarbonylation of acyl radicals decreases with increasing solvent polarity due to a decrease in the dipole moment during the bond scission process. This causes the exothermicity of the cleavage to decrease. Thus, the activation energy increases which cause slower decarbonylation.[98]

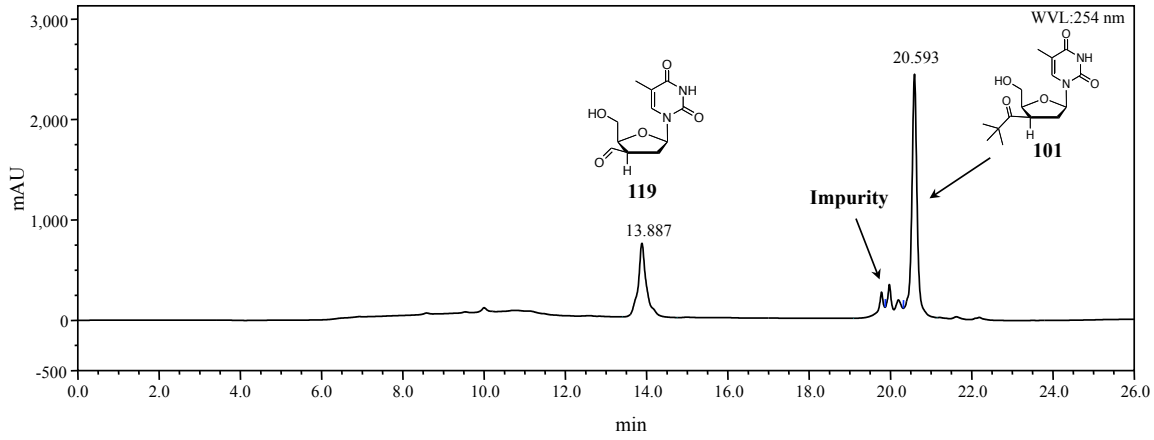

Figure 2-5: Reversed-phase HPLC chromatogram of the photolysate resulting from photolysis of **101** (1 mM) in acetonitrile in the presence *tri-n*butyltin hydride

Since acetonitrile resulted in acyl radical trapping, we investigated the photochemical reactivity of **101** in the presence of a polar protic solvent. Photolysis of β-C3'-pivaloylthymidine (**101**) was performed in water with 0.1 % acetonitrile containing an excess *tri-n*butyltin hydride for 1 h at 15 ºC after degassing with argon for 20 minutes (**Scheme 2.8**). Additionally, the same experiment was performed in methanol with 0.1 % acetonitrile containing an excess *tri-n*butyltin hydride for 1 h at 15 ºC after degassing with argon for 20 minutes (**Scheme 2.9**).

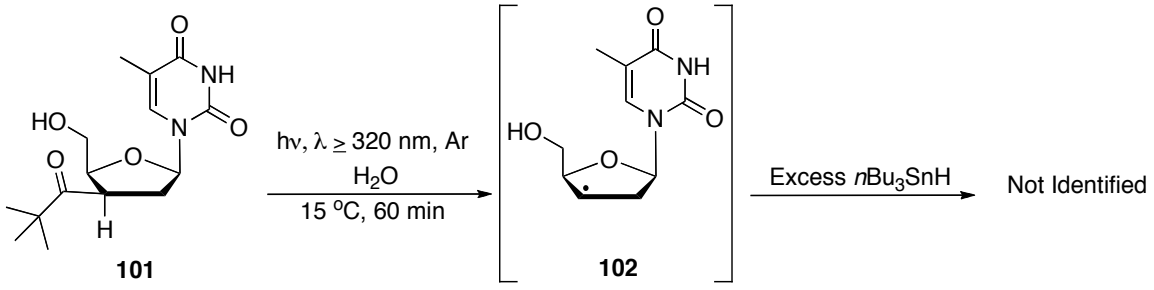

Scheme 2.8: Photochemical generation of the C2',3'-dideoxy-C3'-thymidinyl radical (**102**) from **101** in water in the presence of *tri-n*butyltin hydride

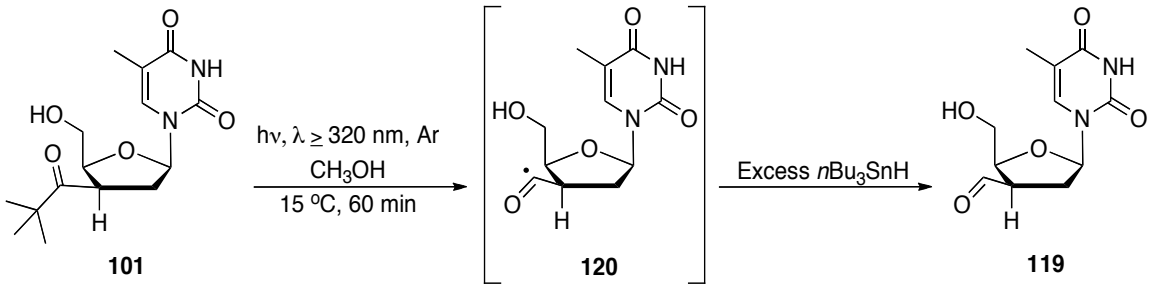

Scheme 2.9: Photochemical generation of the C2',3'-dideoxy-C3'-acylthymidinyl radical (**120**) from **101** in methanol in the presence of *tri-n*butyltin hydride

The crude sample from the photolysis in water was analyzed as described above (**Figure 2-6**). The chromatograph shows no signs of reduction product **118**. The chromatograph shows the presence of components at 9.967, 14.987, and 20.587 minutes, which were collected, concentrated, and analyzed by MALDI-ToF MS. Unfortunately, compounds eluting at 9.967 and 14.987 min were not identified using this technique. A substance eluting at 20.587 min gave a monoisotopic mass of 333.161 which corresponds to the sodium adduct of starting material **101** (Appendix **A**, **Figure 7**).

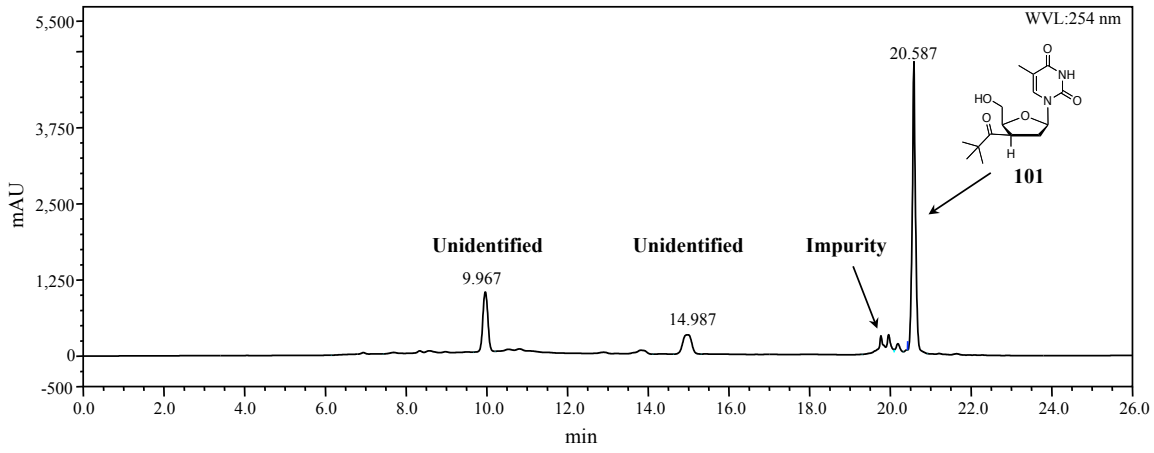

Figure 2-6: Reversed-phase HPLC chromatogram of the photolysate resulting from photolysis of **101** (1 mM) in water in the presence *tri-n*butyltin hydride

In contrast, the analysis of the photolysate in methanol indicated the presence of a major component at 13.673 min, which was determined to be aldehyde **119** (**Figure 2-7**). These results indicate that both protic and aprotic polar solvents do not facilitate the generation of the C2',3'-Dideoxy-C3'-thymidinyl Radical (**102**) from precursor **101**. We conclude that organic polar solvents facilitate the trapping of the acyl radical generating aldehyde **119** and inorganic solvents result in formation of unidentified products. In the case of the photolysis of **101** in water, the unidentified products may be the result of the involvement of the Norrish Type II instead of Type I photocleavage in which the excited carbonyl compound undergoes intramolecular abstraction of a γ-hydrogen to produce a 1,4-biradical as a primary photoproduct **121**, followed by either intramolecular recombination of the two radicals to form cyclic compound **122** or fragmentation to form **123** which may undergo subsequent degradation to form **124** and **39** (**Figure 2-8**).

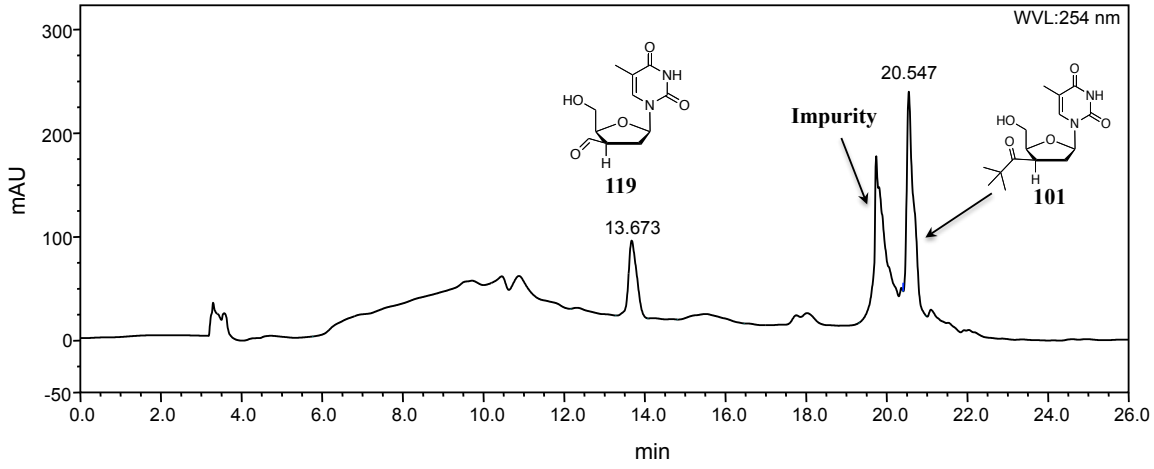

Figure 2-7: Reversed-phase HPLC chromatogram of the photolysate resulting from photolysis of **101** (1 mM) in methanol in the presence *tri-n*butyltin hydride

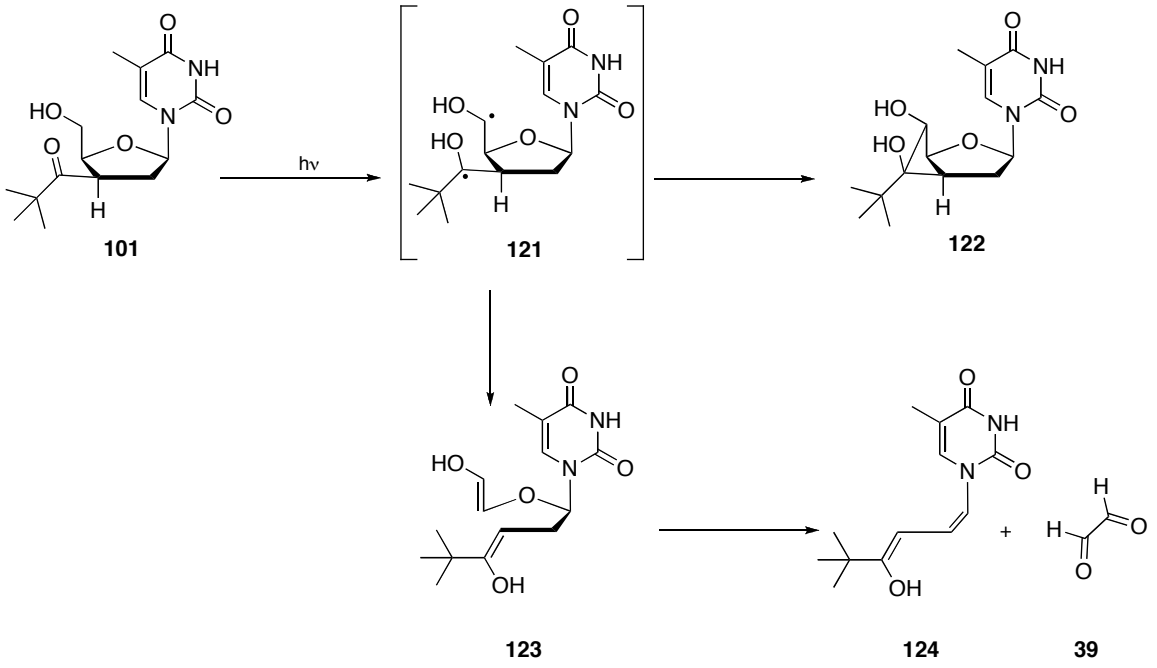

Figure 2-8: Proposed mechanism for Norrish Type II photocleavage for **101**

Based on the results obtained from the photolysis of both C2',3'-dideoxy-α-C3'-pivaloylthymidine (**103**) and C2',3'-dideoxy-β-C3'-pivaloylthymidine (**101**) in the presence of a strong hydrogen atom donor, we conclude that precursor **103** is suitable to generate the C2',3'-dideoxy-C3'-thymidinyl Radical (**102**). In order to fully evaluate these precursors, we examined their photochemical conversion in the presence of the more biologically relevant hydrogen atom donor glutathione (GSH).

2.3.2 Photochemical Generation of the C2',3'-Dideoxy-C3'-Radical in the Presence of Glutathione.

Glutathione is a reducing agent produced by cells as a defense mechanism against radicals. The physiological concentration of GSH in cells is 6 mM.[99] Therefore photolysis of precursor **103** (1 mM) in 1:1 acetonitrile/water in the presence of 6 mM GSH as a hydrogen atom donor (**Scheme 2.10**).

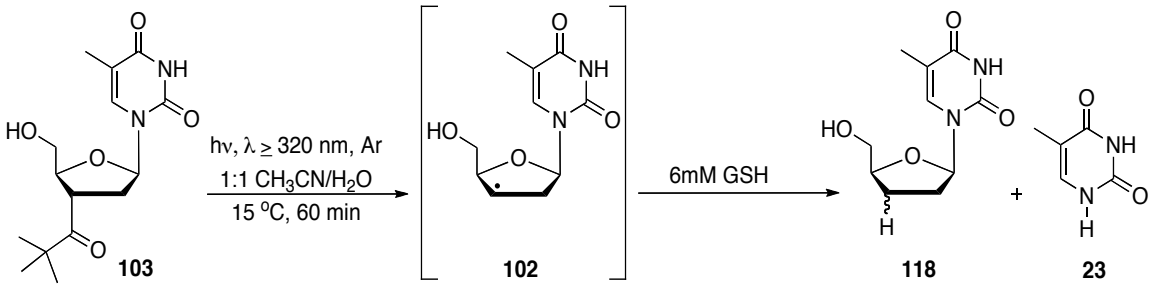

Scheme 2.10: Photochemical generation of the C2',3'-dideoxy-C3'-thymidinyl radical (**102**) from **103** in 1:1 acetonitrile/water in the presence of GSH

The crude sample was analyzed directly by HPLC and MALDI-ToF MS as described above (**Figure 2-9**). The chromatogram shows the presence of substances eluting at 3.973, 6.647, 8.560, 9.733, 10.367, 12.320, 13.740, and 20.327 minutes. The compound with a retention time of 3.973 min corresponds to the sodium adduct of GSH. Compounds eluting at 6.647, 9.733, 10.367, 12.320 min could not be identified. The component eluting at 8.560 min corresponds to thymine (**23**). The component eluting at 13.740 min gives monoisotopic masses of 249.085 and 265.059 corresponding to the sodium and potassium adducts of reduction product **118**, respectively (Appendix **A**, **Figure 8**) and that at 20.327 min gives monoisotopic masses of 333.153 and 349.125 corresponding to the sodium and potassium adducts of starting material **103** (Appendix **A**, **Figure 9**).

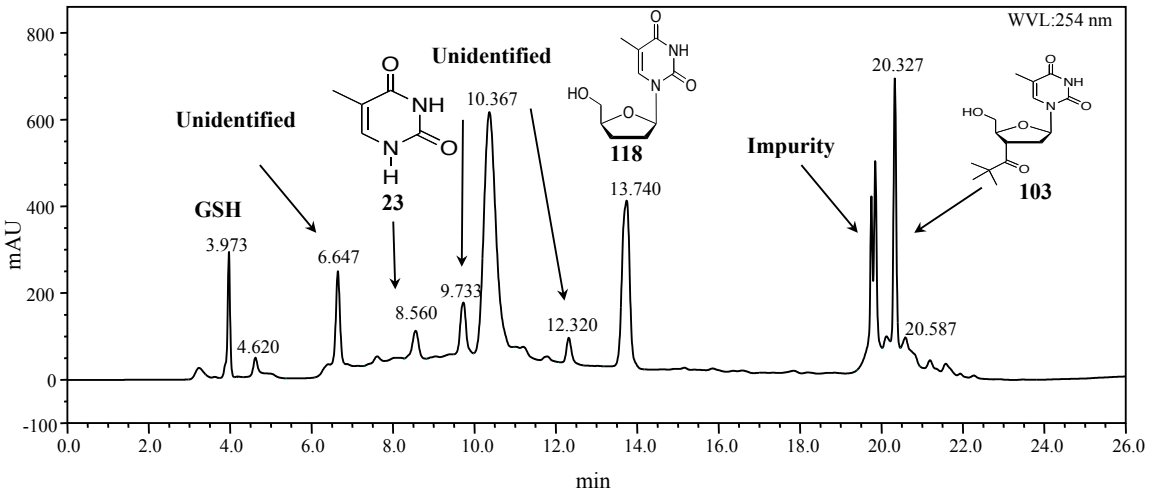

Figure 2-9: Reversed-phase HPLC chromatogram of the photolysate resulting from photolysis of **103** (1 mM) in 1:1 acetonitrile/water in the presence 6 mM GSH

In contrast the photolysis of precursor **101** (1 mM) was carried out using the same methodology as described for **103** (**Scheme 2.11**).

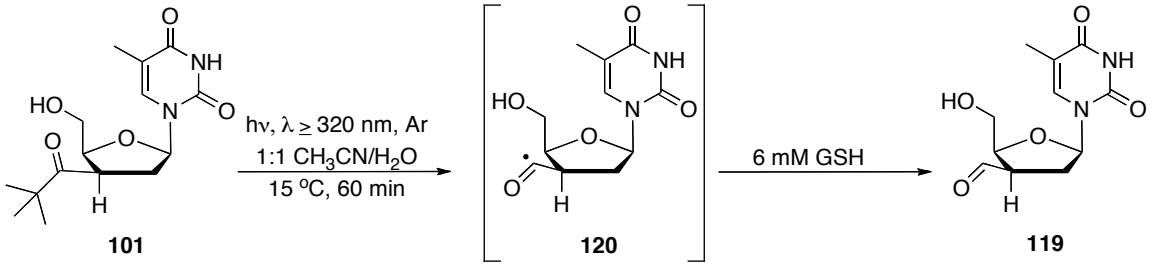

Scheme 2.11: Photochemical generation of the C2',3'-dideoxy-C3'-acylthymidinyl radical (**120**) from **101** in 1:1 acetonitrile/water in the presence of GSH

The crude photolysate was analyzed in the same manner as described above (**Figure 2-10**). Through HPLC analysis aldehyde **119** (13.653 min) and the starting material (20.553 min) were identified (Appendix **A**, **Figure 10**). The absence of reduction product **118** indicates that GSH traps the acyl radical preventing decarbonylation.

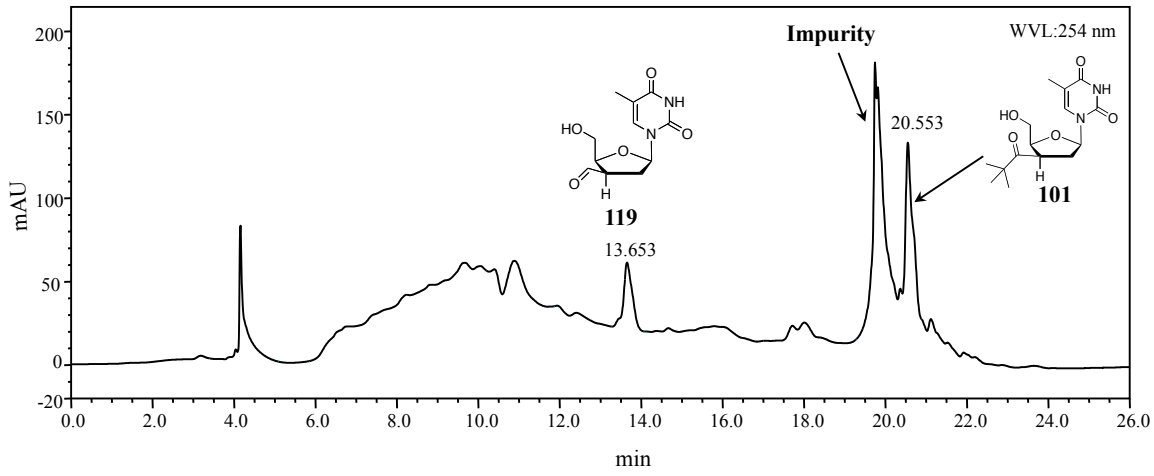

Figure 2-10: Reversed-phase HPLC chromatogram of the photolysate resulting from photolysis of **101** (1 mM) in 1:1 acetonitrile/water in the presence 6 mM GSH

2.3.3 Photochemical Generation of the C2',3'-Dideoxy-C3'-Radical in the Absence of Hydrogen Atom Donor.

Photolysis of both **103** and **101** was performed using the same method as described above except no hydrogen atom donor was added. The crude photolysates were injected without any workup and the photoproducts were detected at 254 nm (**Figure 2-11** and **2-12**, respectively).

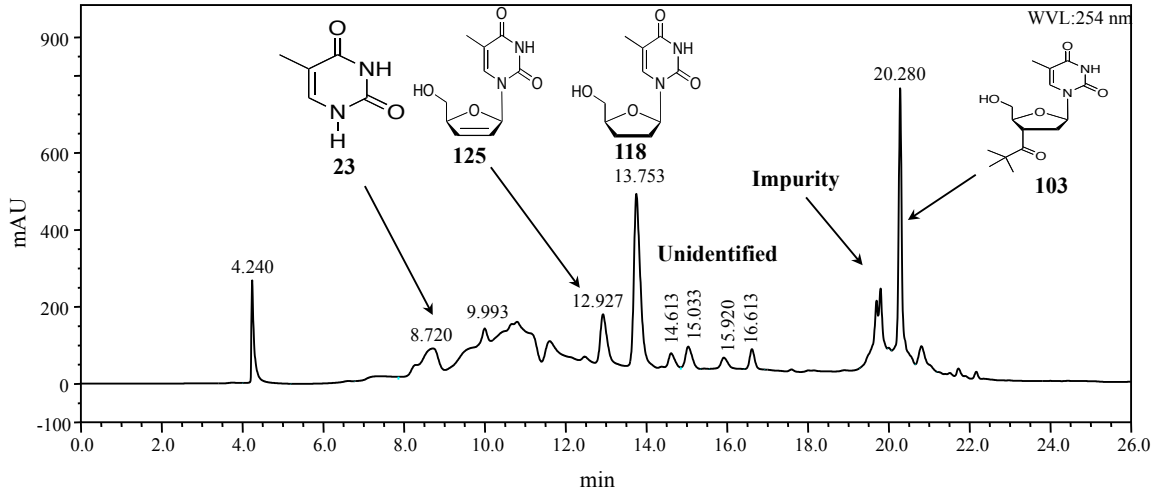

Figure 2-11: Reversed-phase HPLC chromatogram of the photolysate resulting from photolysis of **103** (1 mM) in 1:1 acetonitrile/water in the absence of hydrogen atom donor

The analysis of the crude photolysate **103** (**Figure 2-11**) indicated the formation of the reduction product **118** (13.753 min) (Appendix **A**, Figure **11**, **12**), C2',3'-didehydro-2',3'-dideoxythymidine (**125**) (12.927 min) (Appendix **A**, Figure **13**, **14**) and thymine (**23**) (8.720 min) plus other unidentified peaks (**Scheme 2.12**).

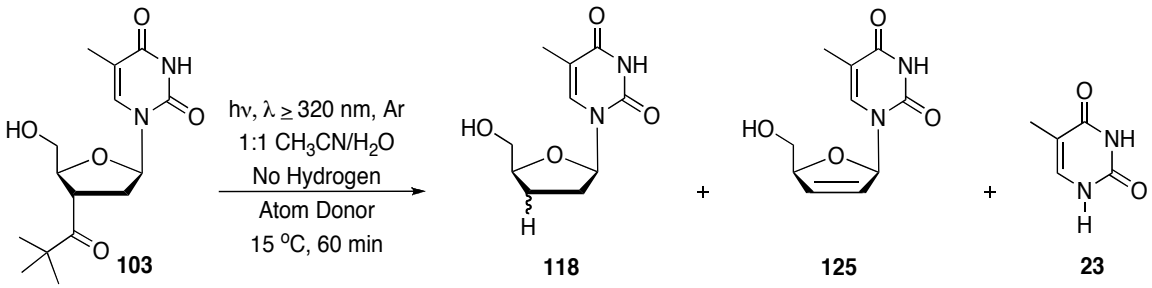

Scheme 2.12: Product identification from photochemical generation of the C2',3'-dideoxy-C3'-thymidinyl radical (**102**) from **103** in 1:1 acetonitrile/water in the absence of hydrogen atom donor

In contrast, the HPLC chromatogram of the photolysate of **101** indicates the presence of a very small amount of photoproducts as seen by **Figure 2-12**. This indicates that precursor **101** is not efficient at generation of the C2',3'-dideoxy-C3'-radical (**102**).

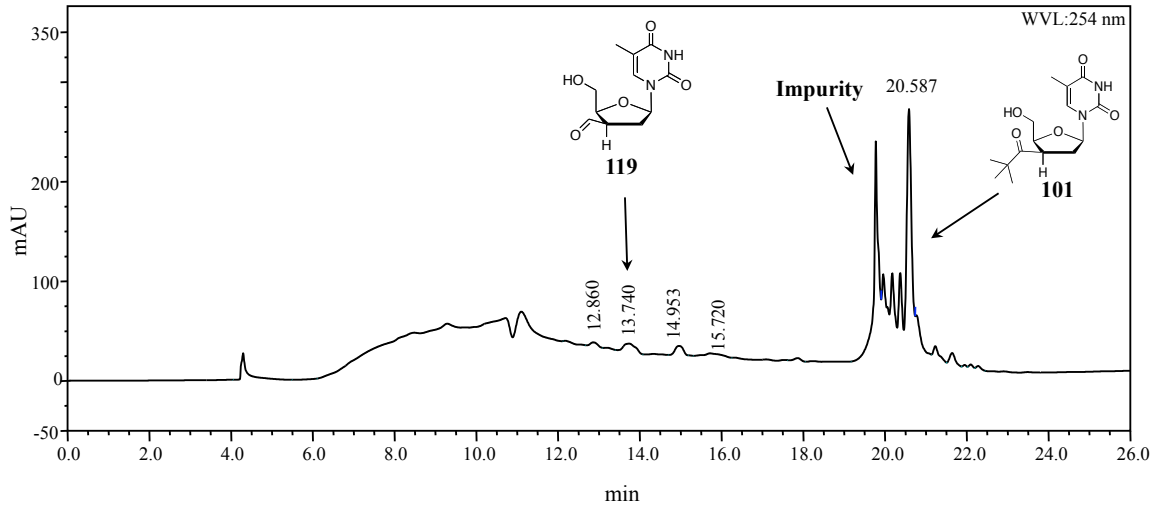

Figure 2-12: Reversed-phase HPLC chromatogram of the photolysate resulting from photolysis of **101** (1 mM) in 1:1 acetonitrile/water in the absence of hydrogen atom donor

In conclusion, photochemical generation of the C2',3'-dideoxy-C3'-thymidinylradical (**102**) from β-C2',3'-dideoxy-C3'-pivaloylthymidine **101** and α-C2',3'-dideoxy-C3'-pivaloylthymidine **103** precursors were investigated under different conditions and based on the results obtained, precursor **103** was found to generate the reduction product **118** under all conditions. In the absence of a hydrogen atom donor the formation of C2',3'-didehydro-2',3'-dideoxythymidine (**125**) was detected which indicates a radical disproportionation mechanism between two alkyl radicals of either the C2',3'-dideoxythymidinyl radical **102** and *tert*-butyl radical or the two C2',3'-dideoxythymidinyl radicals to generate compounds **118** and **125** (**Scheme 2.13** and **2.14**, respectively).[84]

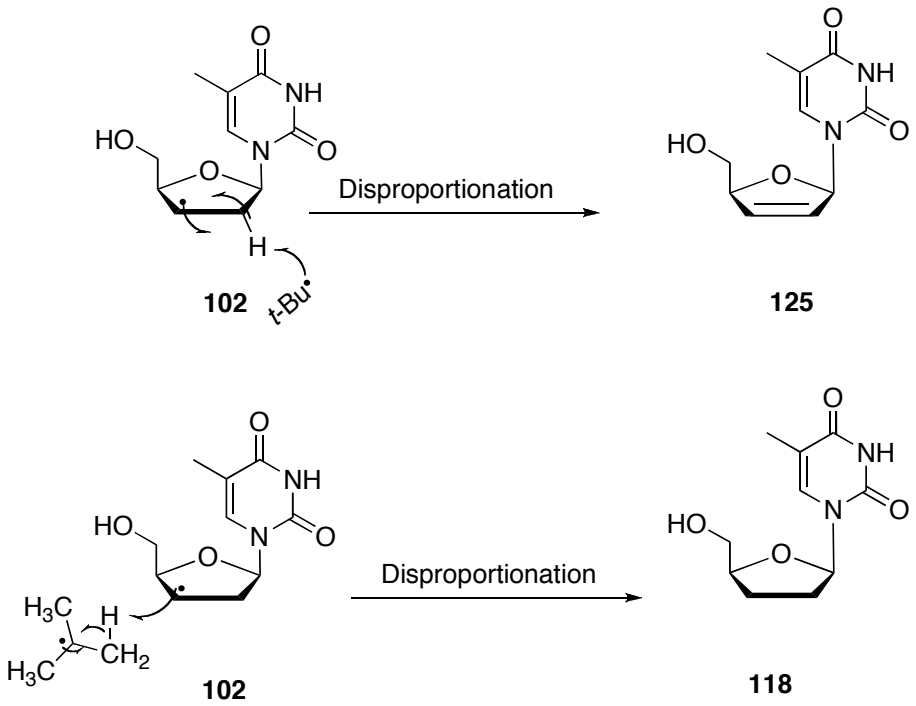

Scheme 2.13: Disproportionation between the C2',3'-dideoxy-C3'-thymidinyl radical (**102**) and *tert*-butyl radical, a proposed mechanism for formation of the reduction product **118** and the unsaturated product **125** in the absence of a hydrogen atom donor

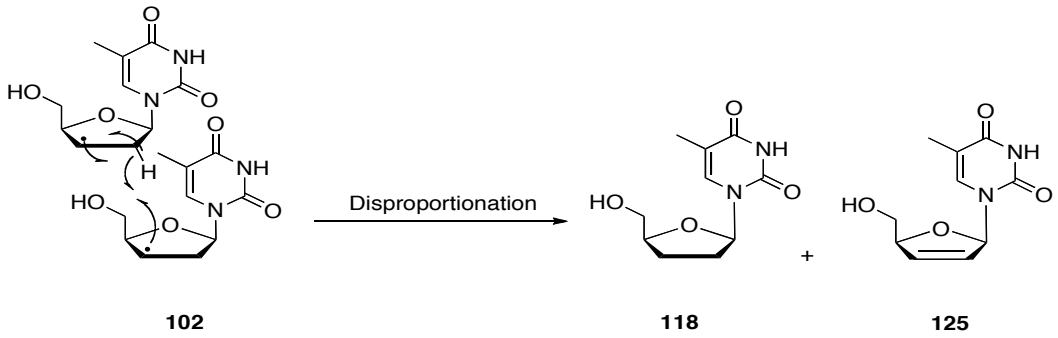

Scheme 2.14: Disproportionation between the C2',3'-dideoxy-C3'-thymidinyl radical (**102**), a proposed mechanism for formation of the reduction product **118** and the unsaturated product **125** in the absence of a hydrogen atom donor

On the other hand precursor **101** was unable to generate reduction product **118** under all conditions and resulted in the formation of products that could not be identified using our present methods. Therefore, based on the results obtained precursor **103** will be used to investigate the fate of the C2',3'-deoxy-C3'-thymidinyl radical in oligonucleotides.

3 CHAPTER THREE:

3.1 Results and Discussion: Investigation of the 5'-Aldehyde Lesion

Oxidative damage to DNA caused by the indirect effect of ionizing radiation leads to the formation of single and double strand breaks.[3] At sites of strand cleavage, oxidized electrophilic fragments[17] are formed that are capable of reacting with local nucleophiles to form adducts.[40,58,48] Oxidation of 2-deoxyribose at the 5'-position in DNA leads to the formation of strand breaks containing 3'-phosphate (**11**) and 5'-aldehyde residues (**36**) under aerobic conditions. Oligonucleotides containing a 5'-aldehyde moiety such as **36** are unstable and are proposed to undergo β-elimination to form electrophilic fragment **66** followed by loss of the nucleobase **23** to deliver the aromatic compound furfural and free base (**67**, **Scheme 1.10**)[56] as shown in chapter one. It was shown that furfural can form an adduct with adenine in DNA which is undergoes subsequent deglycosylation to deliver kinetin (**Scheme 1.11**).[100] With the goal to investigate the stability and reactivity of oligonucleotides containing a 5'-aldehyde lesion, and its degradation products, fragments believed to be produced upon C5'-oxidation, and oligonucleotides containing the 5'-aldehyde moiety were independently synthesized.

3.2 Overview of DNA synthesis

Oligonucleotides were synthesized using standard automated solid phase techniques. Two types of chemistries are employed in automated DNA synthesis, the phosphoramidite and H-phosphonate methods. Automated DNA synthesis is a cyclic, stepwise process carried out by the addition of nucleotide residues to the 5'-terminus of the growing chain until the desired sequence is assembled. The first step of the synthetic cycle is treatment of the derivatized solid support (**126**) with acid to remove the DMT group to yield the 5'-hydroxyl nucleotide (**127**, step **1**, **Figure 3-1**). The next step is coupling the free 5'-hydroxyl group of **127** with the incoming 5'-protected 3'-phosphoramidite (**128**) using an activator such as tetrazole or 0.25 M 5-ethylthio-1H-tetrazole (step **2**, **Figure 3-1**). The phosphite triester linkage (**129**) usually carries a protecting group that prevents any side reactions that could result in branched oligomers, which would interfere with coupling yields. A capping step is introduced following the coupling reaction to terminate any chains that did not couple (**130**); therefore it is designed to minimize the presence of oligomeric impurities and facilitate the purification of the final product (step **3**, **Figure 3-1**). Finally, the phosphite triester linkage in **129** is oxidized to a stable phosphate triester (**132**) using iodine as an oxidizing agent and water as the oxygen donor, producing a chain that has been lengthened by one nucleotide **132** (step **4**, **Figure 3-1**). The 5'-end protecting group of the added nucleotide is then removed, and the cycle is repeated until the desired length is achieved. Final deprotection of the bases and the phosphate groups and cleavage of the oligonucleotides from the solid support liberates the desired oligonucleotide with a DMTr group on its 5'-end **133** (step **5**, **Figure 3-1**).

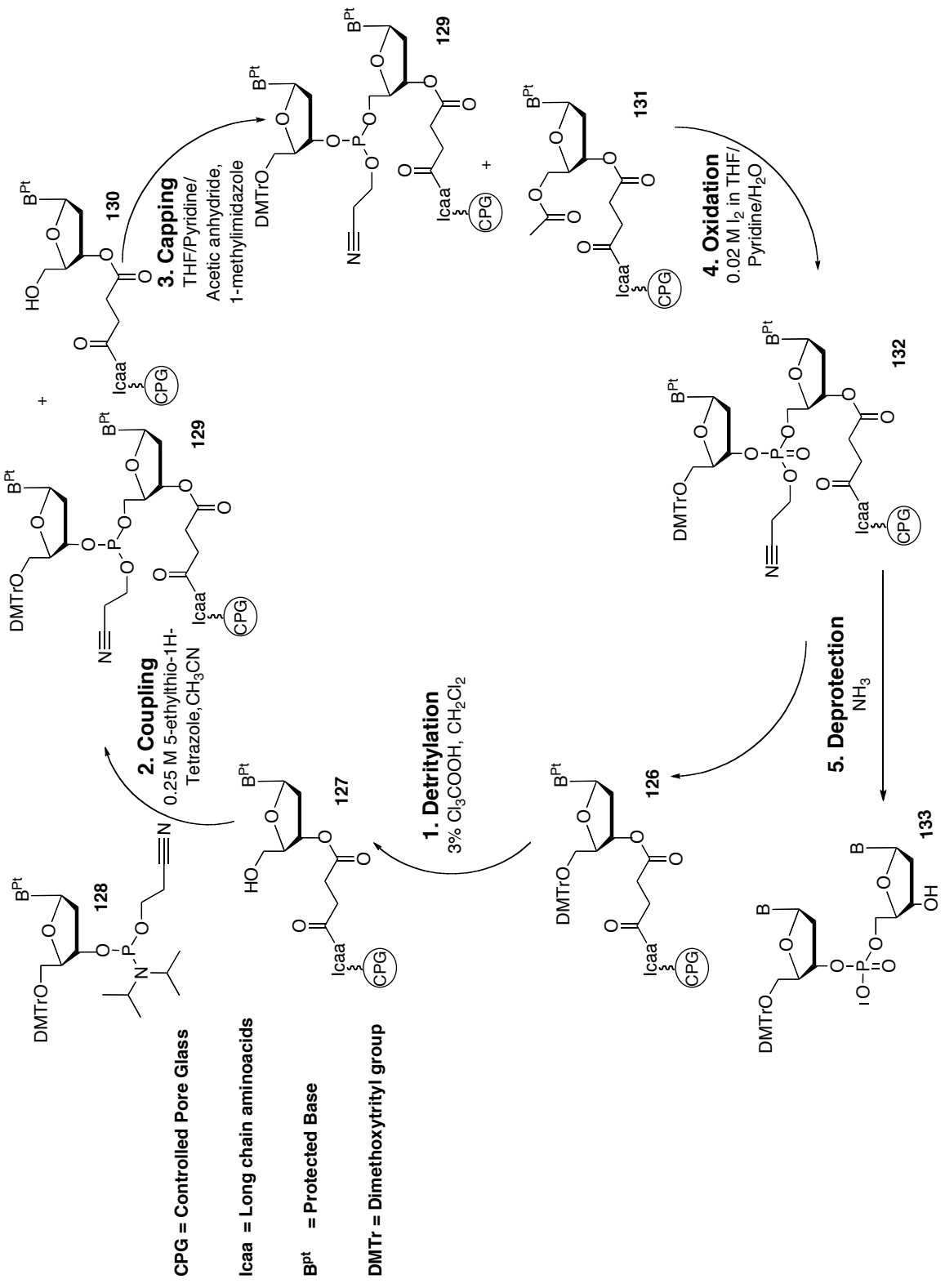

Figure 3-1: Steps involved in solid-phase oligonucleotide synthesis

3.3 Oligonucleotides Synthesis

Syntheses of standard oligonucleotides were carried out using the phosphoramidite method as described in **Figure 3-1**. Modified oligonucleotides were partially synthesized with the phosphoramidite method, followed by manual coupling of the 5'-modified nucleoside using H-phosphonate chemistry. The feasibility of this methodology for incorporation of modified nucleosides into DNA oligomers has been demonstrated previously in our laboratory employing modified 3'-H-phosphonate derivatives.[101] This approach allows the use of two types of chemistries in one synthesis providing the flexibility needed for optimization of the synthesis of modified oligonucleotides.

3.3.1 Synthesis of 5'-Modified Thymidine Building Blocks for Oligonucleotide Synthesis

Oligonucleotides containing 5'-aldehyde nucleosides at their 5'-termini are labile to alkaline conditions and temperatures normally used to deprotect oligonucleotides synthesized on solid supports; therefore, we introduce the aldehyde into the oligonucleotide postsynthetically through oxidative cleavage of the diol containing oligonucleotides. The 5'-aldehyde moiety in nucleotides is unstable due to its electrophilic character and acidic proton at the α-position to the carbonyl group. These factors contribute to the ease of β-elimination to form electrophilic fragment **66** followed by loss of the nucleobase (**23**) to deliver the aromatic compound furfural (**67**). This aldehyde is also reactive towards many nucleophiles, therefore, the need to mask its reactivity is required. This was achieved by introducing a diol at the 5'-position of the nucleoside. The synthesis of oligonucleotides containing a 5'-aldehyde was previously

reported by Greenberg[102] through the oxidative cleavage of the oligonucleotides containing a 5'-diol. Greenberg introduced the 5'-diol nucleoside into oligonucleotides using phosphoramidite chemistry.[102] In this work, the synthesis of the 5'-diol nucleoside was done based on methods developed by Greenberg and introduced into oligonucleotides was using the H-phosphonate method (**135**). We determined that the diol was compatibile with the use of this methodology (**134**). The synthesis of 3'-H-phosphonate derivative **135** began with the synthesis of compound **134** in 92% using published literature protocols.[102] Compound **134** was converted to **135** using a published procedure[101] in which the phosphorus tris(imidazole) was generated *in-situ* by reacting phosphorus trichloride with imidazole and triethylamine in dichloromethane at -10 °C (**Scheme 3.1**). After the completion of the reaction, the product was hydrolyzed using 1 M triethylammonium bicarbonate to give **135** in 34% yield as a diasteromeric mixture. Purity and identity were confirmed by NMR and MS (Appendix **B**, **Figure 1-4**).

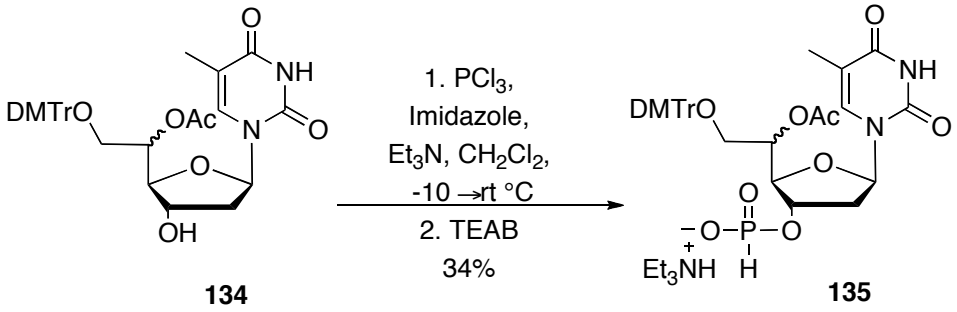

134 **135**

Scheme 3.1: Synthesis of building block **135** for DNA synthesis

3.3.2 Incorporation of **135** into Oligonucleotides

Oligonucleotides containing 5'-modified nucleosides at their 5'-termini were synthesized utilizing monomer building block **135**. The syntheses were performed using

semi-automated techniques in which the unmodified part of the oligomer was synthesized on an Applied Biosystems 391 DNA synthesizer using the phosphoramidite method on a 0.2 μmol scale, followed by manual coupling of 5'-modified nucleoside **135** using H-phosphonate chemistry. **Scheme 3.2** shows the synthesis of modified oligonucleotide **138** ($T^dCTATCTATCT$, where T^d = **134**) as an example of the strategy used in the manual incorporation of H-phosphonate **135** into oligonucleotides. The 5'-hydroxyl of **136** was deprotected during automated synthesis in order to facilitate coupling with the incoming H-phosphonate. Modified nucleoside **135** was then incorporated into oligonucleotides using a manual syringe technique. Briefly, **135** was dissolved in a mixture of acetonitrile/pyridine (1:1) to a final concentration of 0.1 M. The solution was transferred into a 1 mL syringe purged with argon. In another purged syringe was placed 5 μL of freshly distilled pivaloyl chloride in 305 μL of acetonitrile/pyridine (1:1). Each syringe was then attached to either end of the CPG column containing the polymer-bound unmodified oligomer **136**.

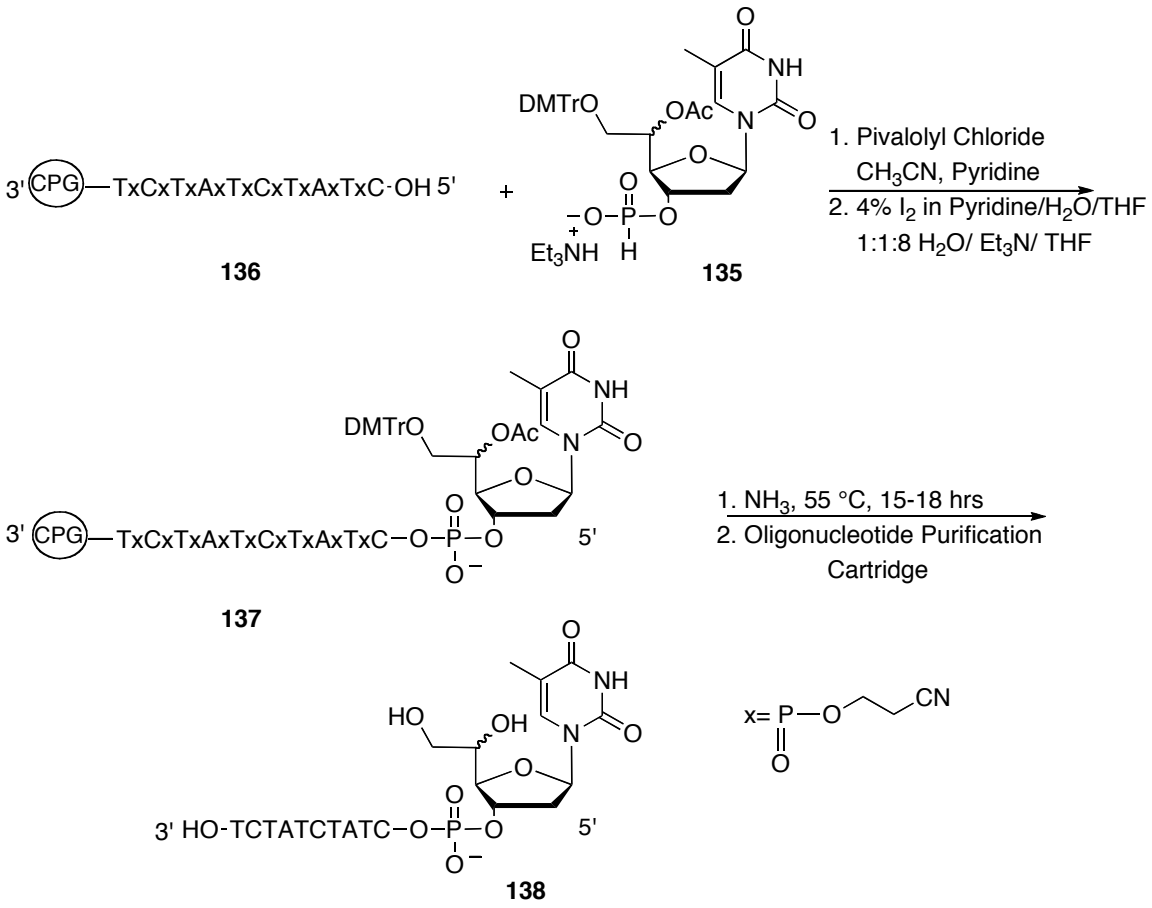

Scheme 3.2: Incorporation of **135** into oligonucleotide using a manual coupling strategy

The activator was delivered first followed by the monomer and after repetitive mixing for 20 minutes, the reagents were then removed and the oligomer was washed with 5 mL acetonitrile. The H-phosphonate linkage was oxidized to the corresponding more stable phosphodiester linkage by attaching the column to two 1 mL purged syringes, one containing 300 µL of 4% iodine in pyridine/H_2O/THF (1:1:8) and the other containing 300 µL of THF/H_2O/triethylamine (8:1:1) for 20 minutes. The column was then washed with 10 mL of anhydrous acetonitrile. Oligonucleotides were deprotected and cleaved from the solid support using concentrated ammonium hydroxide for 15-18 hours at 55 °C. The cleaved oligonucleotides have DMT groups on the 5'-termini, which allows the use of Oligonucleotide Purification Cartridges (OPC) for purification to yield

138. Purity and identity of all oligonucleotides was confirmed by analytical ion-exchange HPLC (**Figure 3-2**) and MALDI-MS (**Figure 3-3**) respectively.

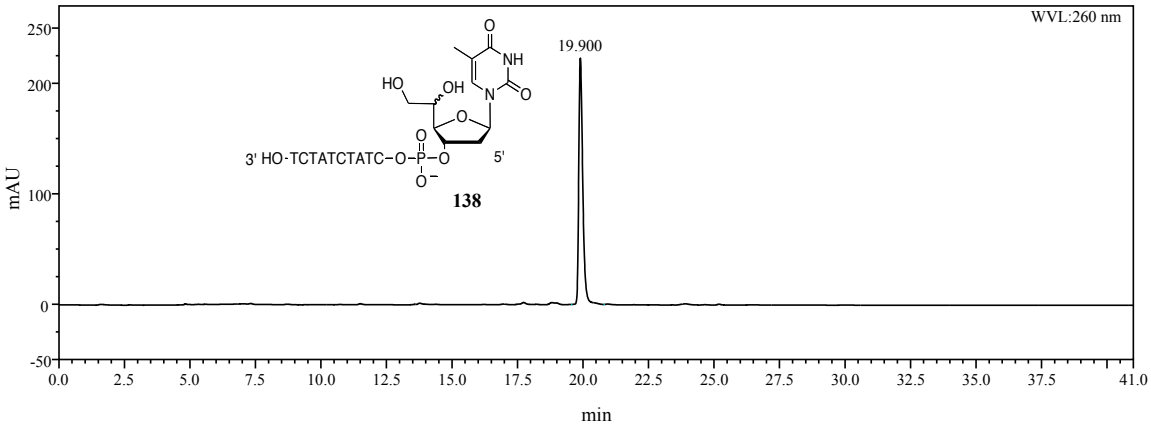

Figure 3-2: Ion-exchange HPLC chromatogram of modified oligonucleotide **138**

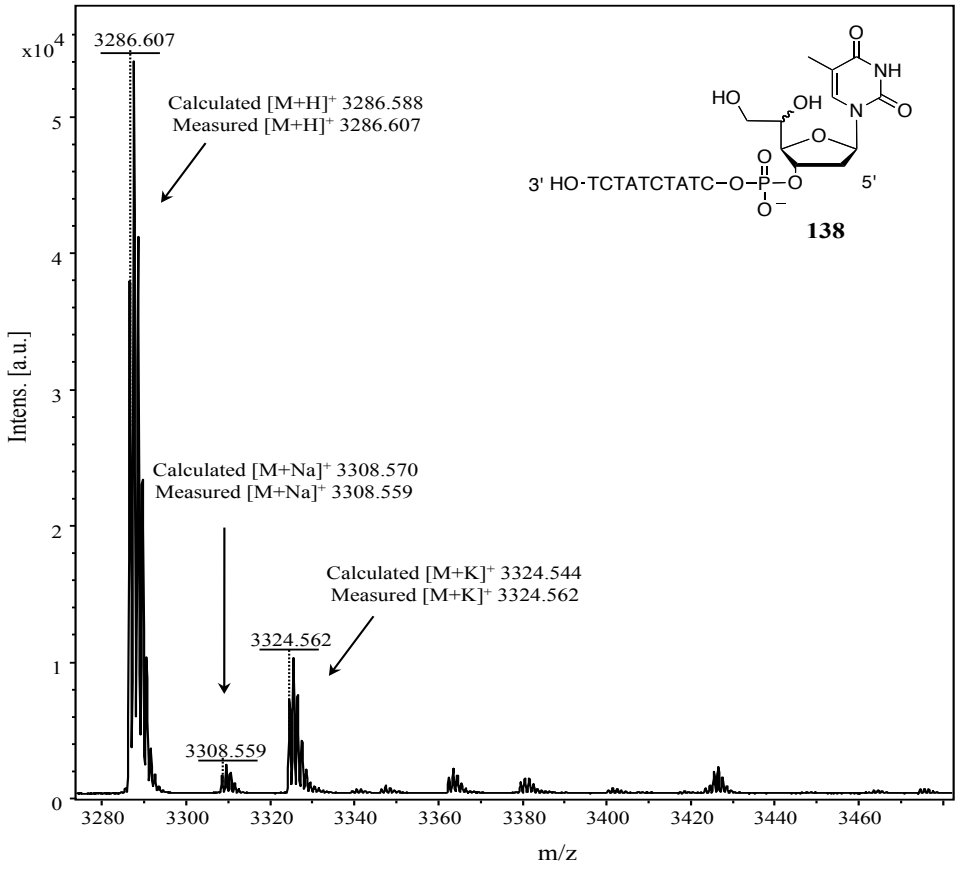

Figure 3-3: MALDI-ToF MS of modified oligonucleotide **138**

Attempts to use 1-Adamantanecarbonyl chloride as an activator in manual coupling failed to incorporate modified nucleoside **135** into oligonucleotides, which may be due to the bulkiness of this activator and the presence of bulky groups on the 5' end of **135**.

Modified oligonucleotides with different base context were synthesized and analyzed by analytical ion-exchange HPLC and MALDI-ToF MS (**Table 3.1**) (Appendix **B**, **Figure 5-14**). Quantification of these oligonucleotides was performed using UV absorbance (λ_{max} = 260 nm). Collectively, the results from these analyses confirmed the formation of the desired modified oligonucleotides with high purity and high coupling yields.

Table 3.1: Modified oligonucleotides containing diol and MALDI-ToF analyses

Sequence #	Sequences	Calculated $[M+H]^+$	Measured $[M+H]^+$	nmole
138	T^dCTATCTATCT	3286.588	3286.607	202
139	T^dATCTCTCTCT	3262.577	3262.485	214
140	T^dGTCTCTCTCT	3278.572	3278.403	202
141	T^dATCTCTGTCT	3302.583	3302.449	215
142	T^dTTCTCTCTCT	3253.565	3253.461	213
143	T^dCTCTCTCTCT	3238.566	3238.286	230

3.3.3 Synthesis of Modified Oligonucleotides Containing a 5'-Aldehyde Lesion (**144**)

The vicinal diol at the 5'-terminus in oligonucleotide **138** was converted to aldehyde **144** via oxidative cleavage using sodium periodate[103] (**Scheme 3.3**). The 5'-aldehye containing oligomer was isolated by desalting using a G-25 sephadex column.

Analyses were performed using analytical ion-exchange HPLC (**Figure 3-4**) and MALDI-ToF MS (**Figure 3-5**). The product was quantified using UV absorbance measurements at λ_{max} = 260 nm.

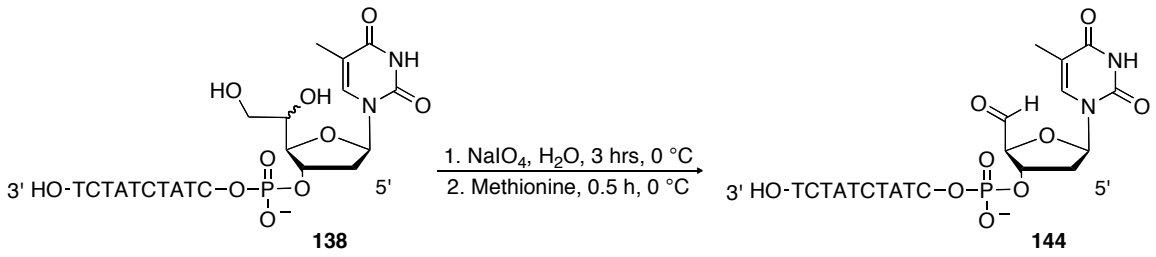

Scheme 3.3: Synthesis of 5'-aldehyde containing oligomer **144**

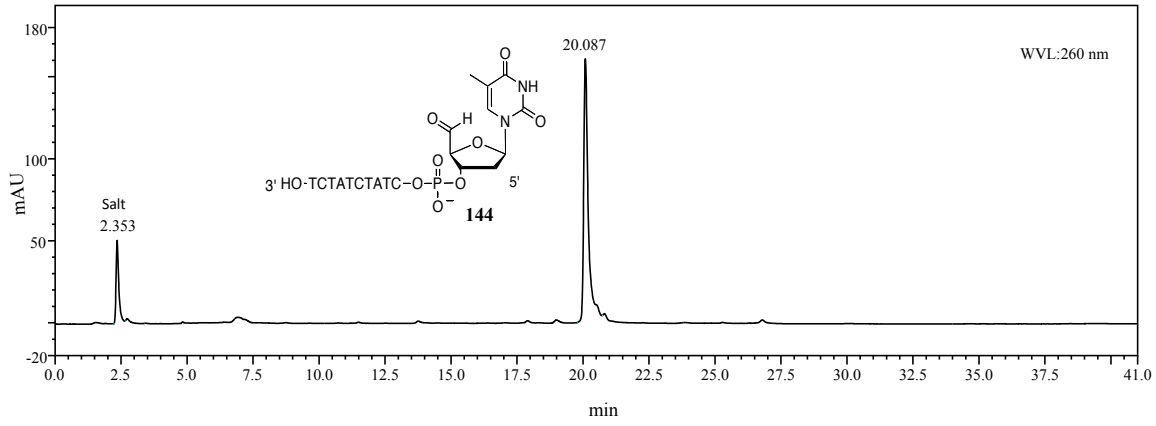

Figure 3-4: Ion-exchange HPLC chromatogram of 5'-aldehyde containing oligomer **144**

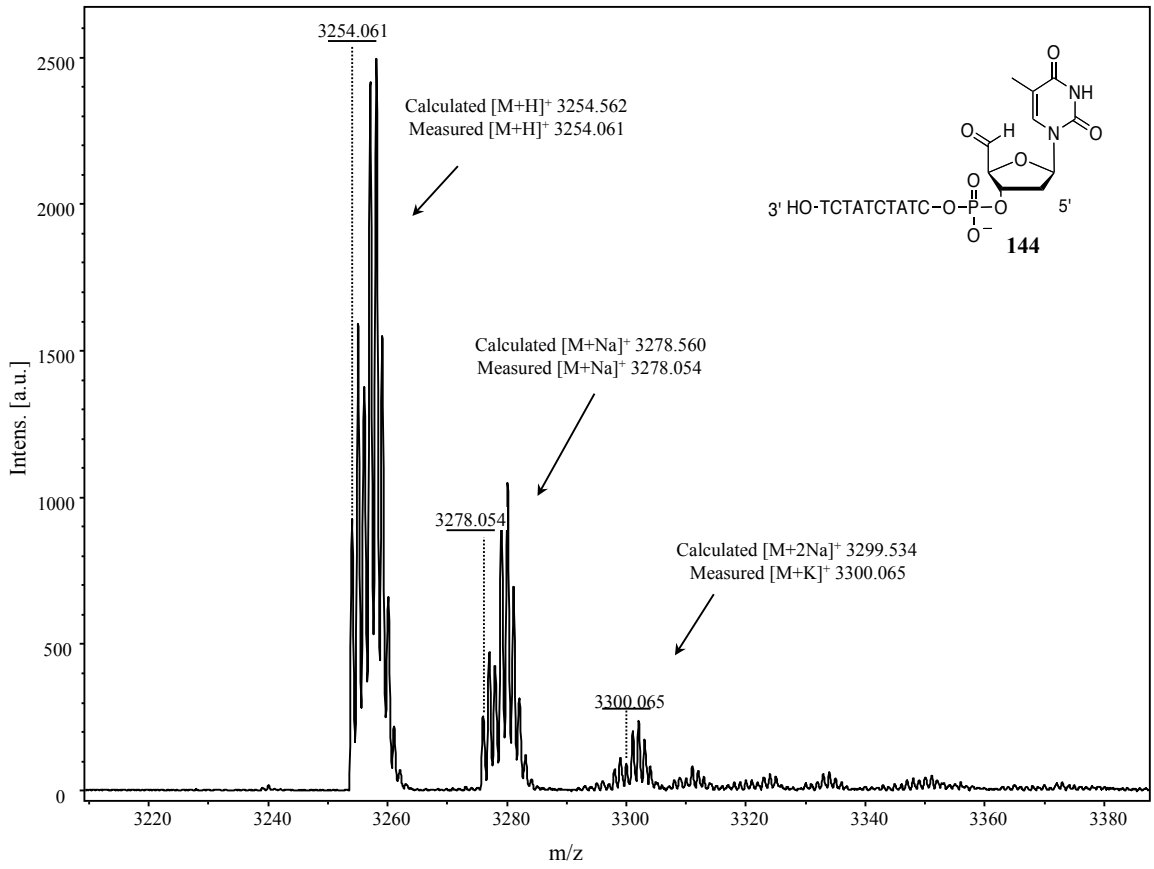

Figure 3-5: MALDI-ToF MS of 5'-aldehyde containing oligomer **144**

3.3.3.1 Storage of Modified Oligonucleotide Containing 5'-Aldehyde (**144**)

As mentioned above, oligonucleotides containing a 5'-aldehyde are unstable, therefore, the need to determine the proper conditions to isolated and investigate its reactivity is important. In order to determine the stability of **144** during long term storage, the aldehyde was synthesized and stored in water at 4 °C in pH = 7 after desalting with a G-25 sephadex column. The decomposition of the 5'-aldehyde to the corresponding 5'-phosphorylated ODN was monitored by MALDI-ToF over 10 days (**Scheme 3.4**). The presence of small amount of the elimination product **145** was observed after 10 days of storage.

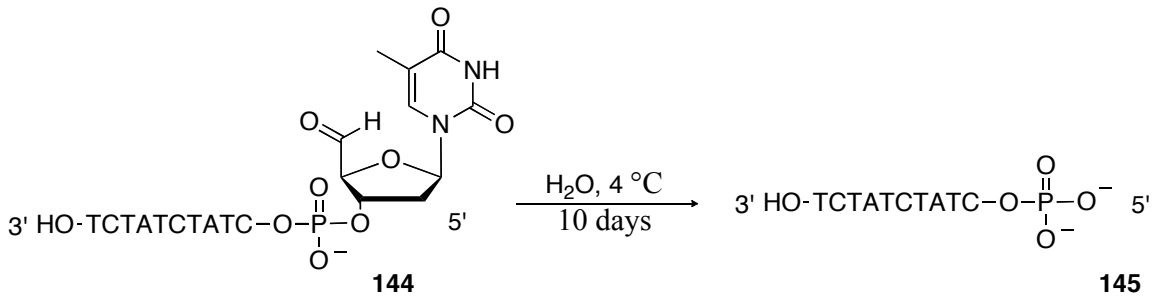

Scheme 3.4: Decomposition of **144** to **145**

3.3.3.2 Stability of 5'-Aldehyde Containing Oligomer (**144**) under Physiological Conditions

To determine the half-life of the 5'-aldehye in single-stranded oligonucleotides, oligonucleotide **144** was incubated in 100 mM phosphate buffer (pH = 7.4) at 37 °C and the conversion of **144** to **145** was measured by analytical ion-exchange chromatography. The half-life was determined to be 96 hours (**Figure 3-6**), which is similar to that found in the literature (100.7 hours) for ternary complexes (10 mM phosphate buffer at pH = 7.2 at 37 °C).

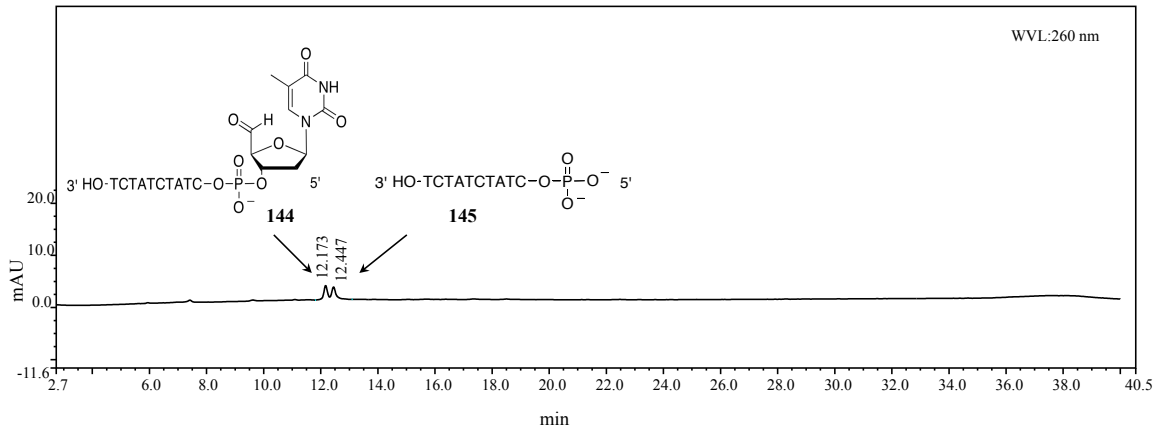

Figure 3-6: Ion-exchange HPLC chromatogram of 5'-aldehyde containing oligomer **144** after 96 hrs at pH 7.4 and 37 °C

3.4 Synthesis of the Nucleoside Resulting from β-Elimination of 5'-Aldehyde Containing Oligomers

Oligonucleotides containing 5'-aldehyde moiety **36** (**Scheme 1.10**) are unstable and can undergo β-elimination to form highly reactive electrophilic fragments 3',4'-didehydro-2',3'-dideoxy-5'-oxothymidine (**66**), followed by loss of nucleobase (**23**) to deliver aromatic compound furfural (**67**, **Scheme 1.10**) under both basic and acidic conditions. Compound **66** was synthesized to investigate its stability and reactivity under physiological conditions.

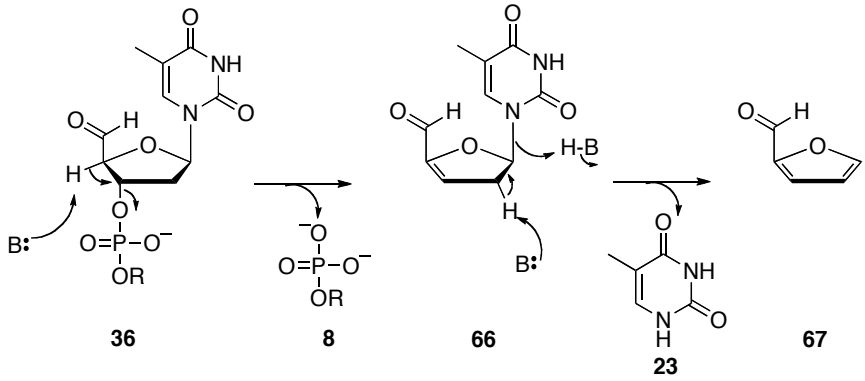

Scheme 3.3.5: Mechanism for the decomposition of **36** to **67**

3.4.1 Synthesis of 3',4'-Didehydro-2',3'-dideoxy-5'-oxothymidine (**66**)

The synthesis of **66** started with the conversion of commercially available thymidine (**104**) to 5'-O-*tert*-butyldimethylsilyl-3'-O-benzoyl-thymidine (**146**)[104-105] according to published literature procedures. Although compound **146** was previously synthesized, full characterization was not reported. Compound **147** is also known, however the synthesis was reported through regioselective acylation of thymidine (**104**) using an enzymatic reaction in the presence of an oxime ester. In our approach, the deprotection of the 5'-hydroxyl was done using a modified published literature protocol[104]

in which THF/TFA/H_2O was used to afford **147** in 95% yield compared to the reported yield of 59%. The reaction was over night as compared to 72 hours.[106] Oxidation of primary alcohol **147** with the Dess-Martin Reagent afforded 3'-O-benzoyl-5'-oxothymidine (**148**) which was used directly in the next reaction. Subsequent benzoyloxy elimination leading to **66** was performed under mildly basic conditions by treatment of **148** with 4 molar equivalents of triethylamine (TEA) at room temperature to afford **66** in 21% yield. The lower yield is due to the low solubility of **147** in solvents used for the Dess-Martin reaction and the fast elimination of thymine when treating **148** with TEA (**Scheme 3.5**). Compound **148** was obtained in the literature using a modified Moffat procedure in higher yield.[107] However, due to the convenience of using the Dess-Martin reagent, the reaction was accomplished using this reagent. Purity and identity were confirmed by NMR and ESI-MS, respectively (Appendix **B**, **Figure 15-23**).

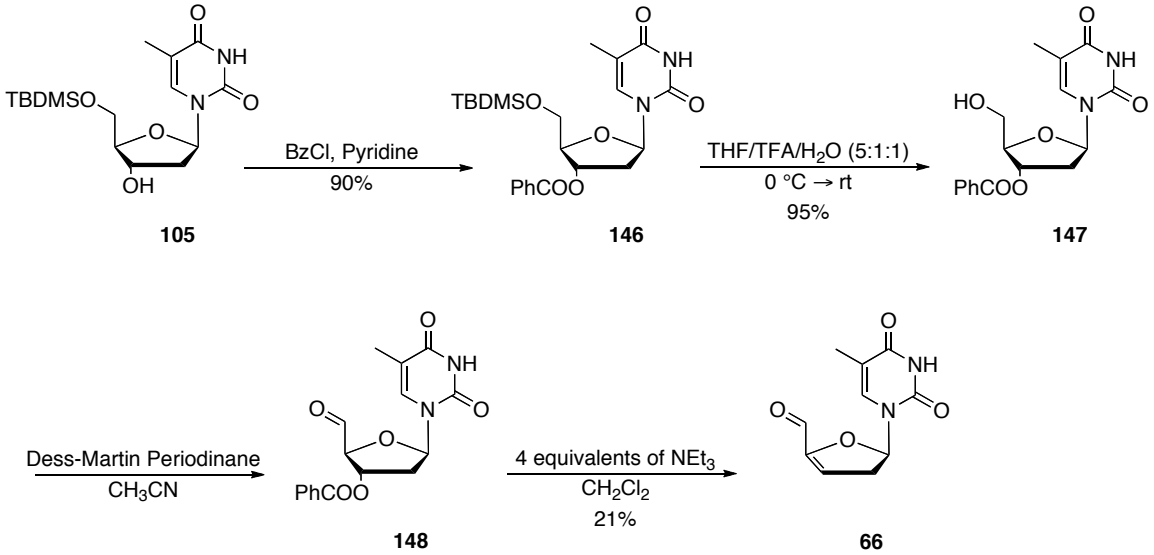

105 **146** **147** **148** **66**

Scheme 3.6: Synthesis of 3',4'-didehydro-2',3'-dideoxy-5'-oxothymidine (**66**)

3.4.1.1 Stability of 3',4'-Didehydro-2',3'-dideoxy-5'-oxothymidine (**66**)

Modified nucleoside **66** was incubated in 100 mM phosphate buffer (pH = 7.4) at 37 °C (**Figure 3-7**). The decomposition of **66** to furfural and thymine was monitored by analytical reversed-phase HPLC chromatography (**Figure 3-8**).

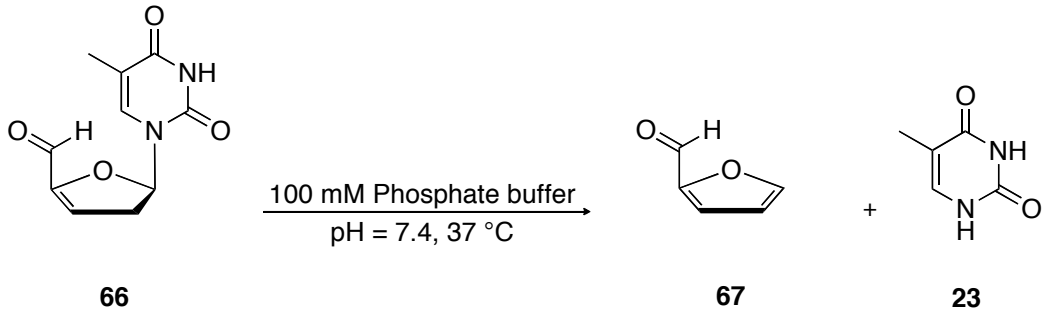

Figure 3-7: Incubation of **66** in 100 mM phosphate buffer pH = 7.4 at 37 °C

The chromatogram shows the presence of fractions eluting at 5.380, 10.140, and 12.073 min corresponding to thymine, furfural, and starting material **66**, respectively. The identity of each component was confirmed by comparison of the elution times as compared to the elution times of authentic samples. The half-life of **66** was found to be 13 hours based on the amount of **66** recovered (**Figure 3-9**)

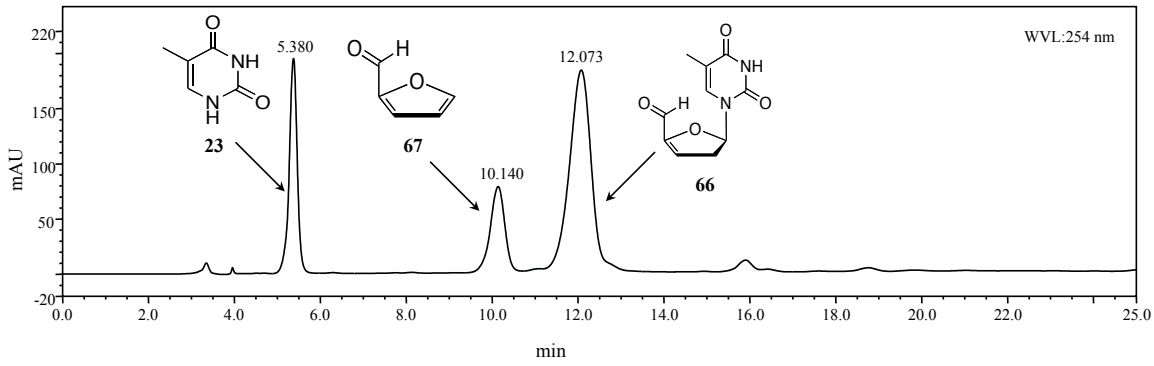

Figure 3-8: Reversed-phase HPLC chromatogram of incubation of **66** in 100 mM phosphate buffer pH = 7.4 at 37 °C at 12 hours

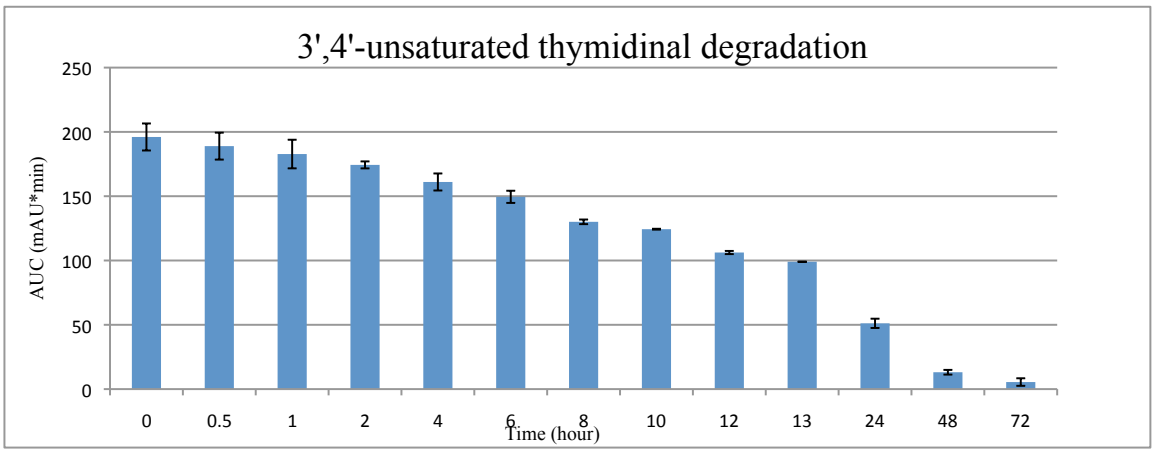

Figure 3-9: Incubation of **66** in 100 mM phosphate buffer pH = 7.4 at 37 °C

Compound **66** is a Michael acceptor and is a highly reactive electrophilic. It has been shown in the literature that the releated compound, ribonolactone **9**, generated as a result of C1'-oxidation undergoes β-elimination and can produce an electrophile capable of reaction with sulfur and nitrogen nucleophiles. Based on these observation the stability of **66** was determined in the presence of glutathione. Compound **66** was incubated in 100 mM phosphate buffer (pH = 7.4) at 37 °C in the presence of 6 mM GSH. An aliquot of the reaction mixture were analyzed by analytical reversed-phase HPLC chromatography. **Figure 3-10** shows a chromatogram after 30 minutes of incubation. All fractions were

collected and analyzed by MALDI-ToF or ESI MS. MALDI data from compounds eluting at 3.320 min shows monoisotopic masses equal to 308.108 and 346.048 which corresponds to the protonated and sodium adducts of GSH, respectively (**Figure 24**, Appendix **B**), while the fraction eluting at 5.380 min has a monoisotopic mass of 127.038 corresponding to protonated thymine (**Figure 25**, Appendix **B**). Unfortunately, all other fractions could not be identified by MALDI-ToF MS. The presence of glutathione accelerates the degradation of **66** and results in the formation of new compounds. Furfural (**67**) was not a major product although thymine release was observed. This may be due either to the formation of adducts between furfural and GSH or the formation of adducts between GSH and **66** that also facilitate thymine release. **Figure 3-11** shows the consumption of more than 75% of **66** in 30 minutes.

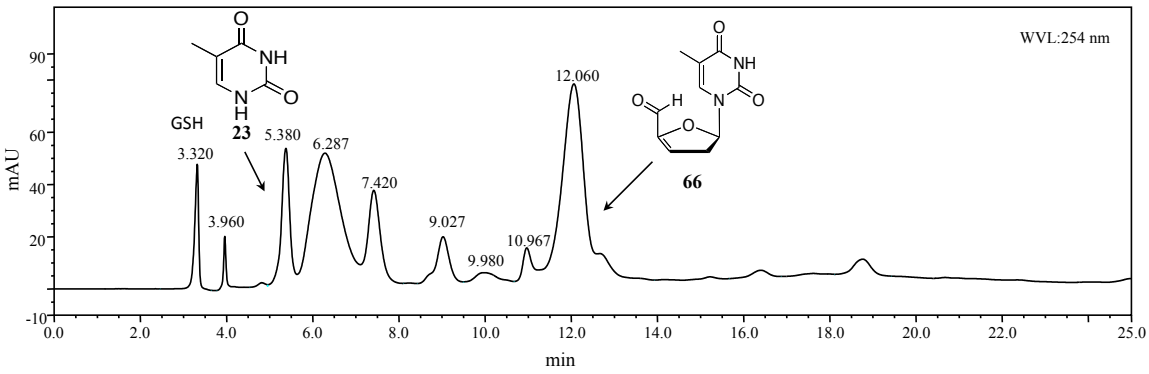

Figure 3-10: Reversed-phase HPLC chromatogram after incubation of **66** in 100 mM phosphate buffer pH = 7.4 at 37 °C in the presence of 6 mM GSH after 30 minutes

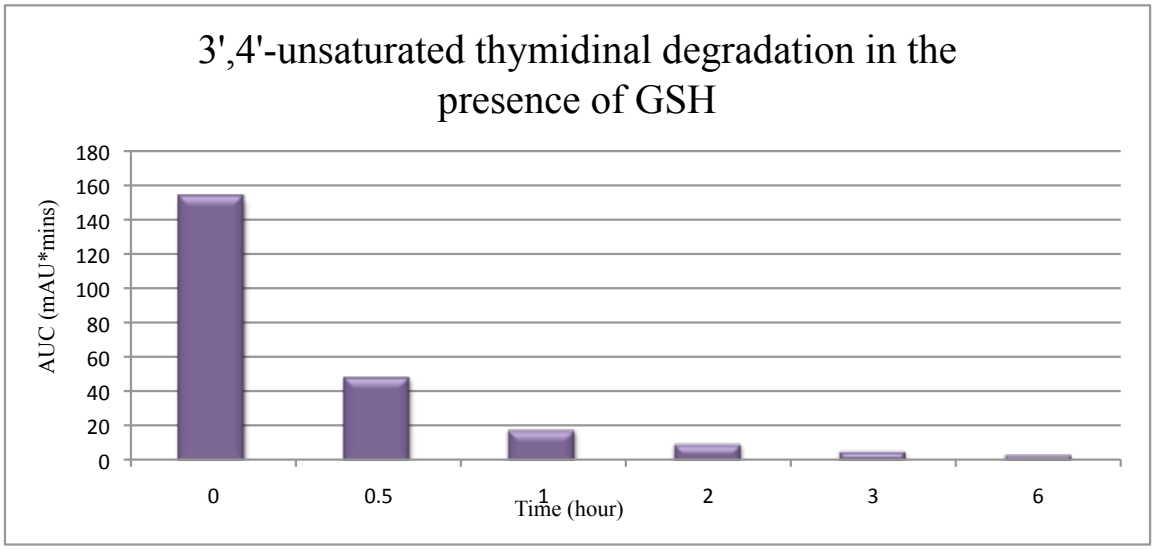

Figure 3-11: Incubation of **66** in 100 mM phosphate buffer pH = 7.4 at 37 °C in the presence of 6 mM GSH

3.4.1.2 Reactivity of 3',4'-Didehydro-2',3'-dideoxy-5'-oxothymidine (**66**) in the Presence of Deoxyadenosine

3',4'-Didehydro-2',3'-dideoxy-5'-oxothymidine (**66**) is an unsaturated aldehyde that is a highly reactive electrophile which may result in the formation of DNA adducts. To explore the reactivity of this electrophilic fragment towards the nucleobases found in DNA, incubation of **66** in 100 mM phosphate buffer (pH = 7.4) at 37 °C in the presence of excess 2-deoxyadenosine (dA) (**149**) was performed. An aliquot of the reaction mixture was analyzed by analytical reversed-phase HPLC (**Figure 3-12**). The chromatogram shows the decomposition of **66** to furfural (**67**) and thymine (**23**). The formation of adducts was however not observed, although the degradation of 66 to furfural and thymine was accelerated. The half-life of **66** in the presence of dA was found to be 3 hours based on recovered **66** compared to 13 hours in the absence of dA under the same conditions of incubation (**Figure 3-13**).

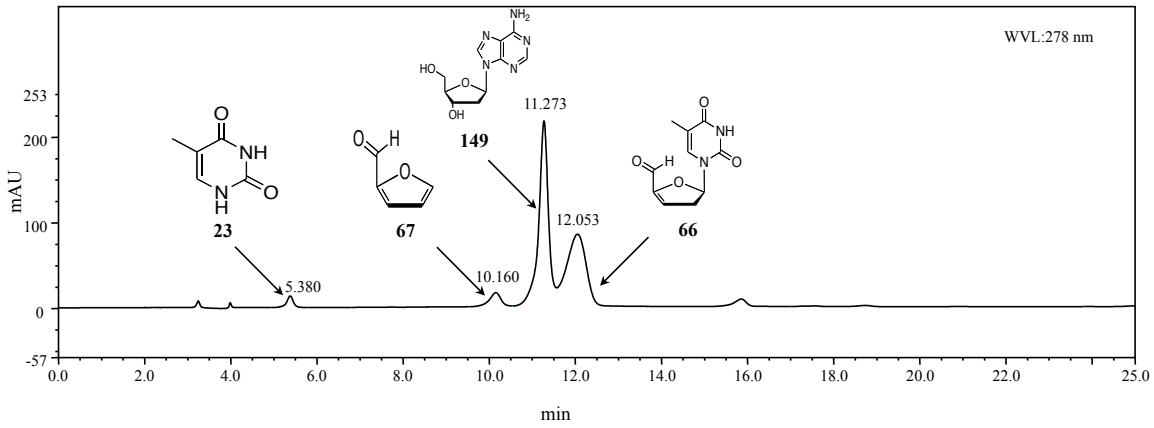

Figure 3-12: Reversed-phase HPLC chromatogram after incubation of **66** in 100 mM phosphate buffer pH = 7.4 at 37 °C in the presence of excess deoxyadenosine for 3 hours

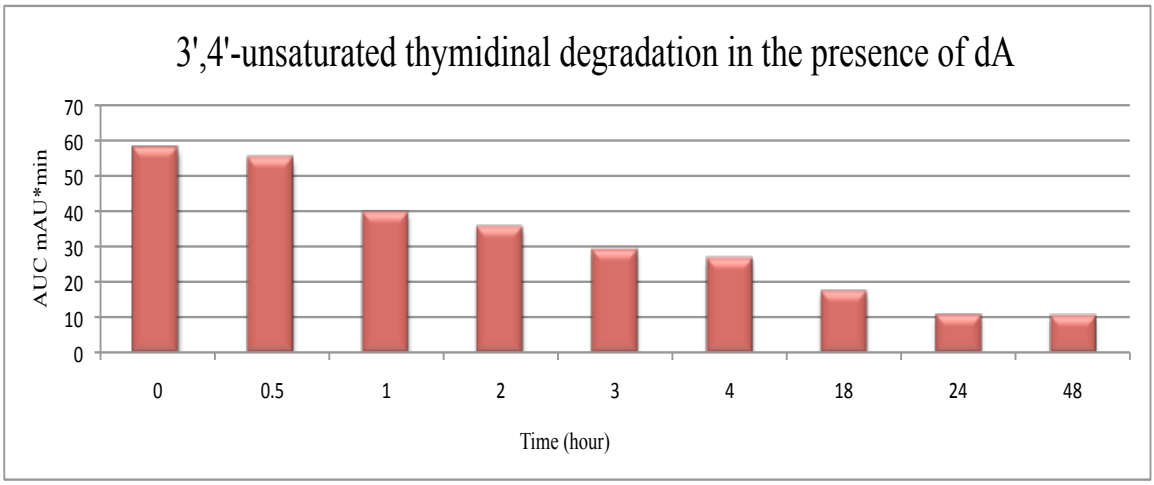

Figure 3-13: Incubation of **66** in 100 mM phosphate buffer pH = 7.4 at 37 °C in the presence of excess dA

3.4.1.3 Reactivity of 3',4'-Didehydro-2',3'-dideoxy-5'-oxothymidine (**66**) in the Presence of a dA Containing Oligonucleotide

To investigate the reactivity of **66** towards adenine in oligonucleotides, the incubation of **66** in 100 mM phosphate buffer (pH = 7.4) at 37 °C in the presence of

excess unmodified oligonucleotide (**150**) was performed (**Figure 3-14**). An aliquot of the reaction mixture was analyzed by analytical reversed-phase HPLC (**Figure 3-15**). As was the case with dA (**149**), the chromatogram shows the decomposition of **66** to furfural (**67**) and thymine (**23**). The formation of adducts was not observed.

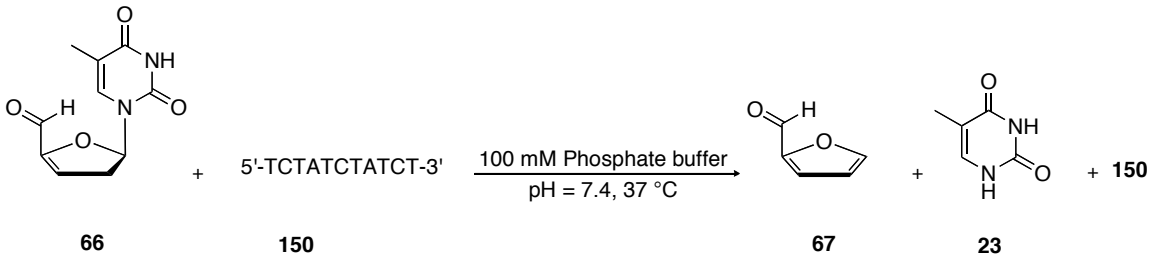

Figure 3-14: Incubation of **66** in 100 mM phosphate buffer pH = 7.4 at 37 °C in the presence of excess unmodified oligonucleotide 5'-TCTATCTATCT-3'

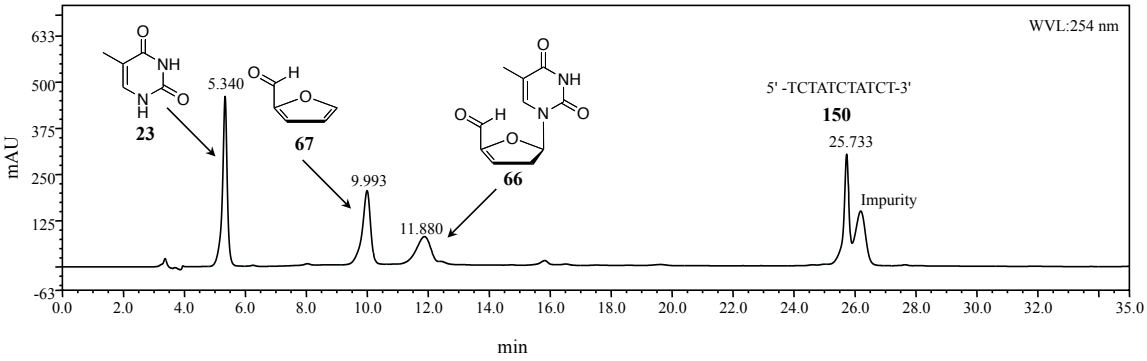

Figure 3-15: Reversed-phase HPLC chromatogram after the incubation of **66** in 100 mM phosphate buffer pH = 7.4 at 37 °C in the presence of an excess of unmodified oligonucleotide (TCTATCTATCT) for 24 hours

3.5 Reactivity of Furfural

Oxidation at the 5' position of DNA has been shown to lead to the formation of furfural,[55,56] which is believed to form adducts with the amino group of adenine in oligonucleotides. Upon heating or treatment with base, an intramolecular rearrangement occur. Under acidic conditions the resulting adduct is undergoes deglycosylation to form

kinetin (**Scheme 1.11**).[100] To investigate the reactivity of furfural toward 2-deoxyadenosine, incubation of furfural with dA was performrd under non-physiological (pH 2 and 50 °C) conditions to mimic the conditions for the proposed mechanism of kinetin formation,[100] as well as under physiological conditions (pH 7.4 and 37 °C) to determine its reactivity toward 2-deoxyadenosine.

3.5.1 Reactivity of Furfural (**67**) in the Presence of an Excess of dA at pH = 7.4 and 37 °C

To explore the reactivity of **67** toward 2-deoxyadenosine under physiological conditions, incubation of **67** in 100 mM phosphate buffer (pH=7.4) at 37 °C in the presence of excess deoxyadenosine (dA) (**149**) was performed. An aliquot of the reaction mixture were analyzed by analytical reversed-phase HPLC (**Figure 3-16**). The chromatogram shows no sign of adduct formation under these conditions.

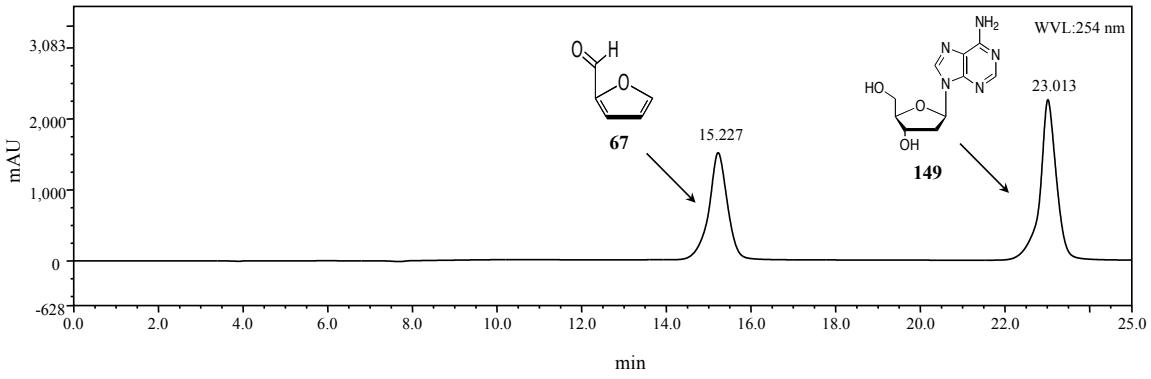

Figure 3-16: Reversed-phase HPLC chromatogram after incubation of **67** in 100 mM phosphate buffer pH = 7.4 at 37 °C in the presence of excess deoxyadenosine (dA) for 65 hours

Since incubation of furfural under these conditions did not yield adduct formation, the incubation of furfural with dA was performed under acidic conditions and at elevated temperatures to mimic the conditions reported for the formation of kinetin.[100]

3.5.2 Reactivity of Furfural (**67**) in the Presence of Excess dA at pH = 2 and 37 °C

To investigate the reactivity of **67** toward 2-deoxyadenosine under acidic conditions, **67** was incubated in 100 mM phosphate buffer (pH = 2.0) at 37 °C in the presence of excess deoxyadenosine (dA) (**Figure 3-17**). An aliquot of the reaction mixture were analyzed by analytical reversed-phase HPLC (**Figure 3-18**). The chromatogram shows, the deglycosylation of deoxyadenosine (**149**) resulting in the formation of adenine. The formation of adducts was not observed. The same result was obtained in the case of incubation of dA with an excess of furfural at the same pH of 2. Increasing the temperature of incubation from 37 °C to 50 °C did not yield to any adduct formation (**Figure 3-19**).

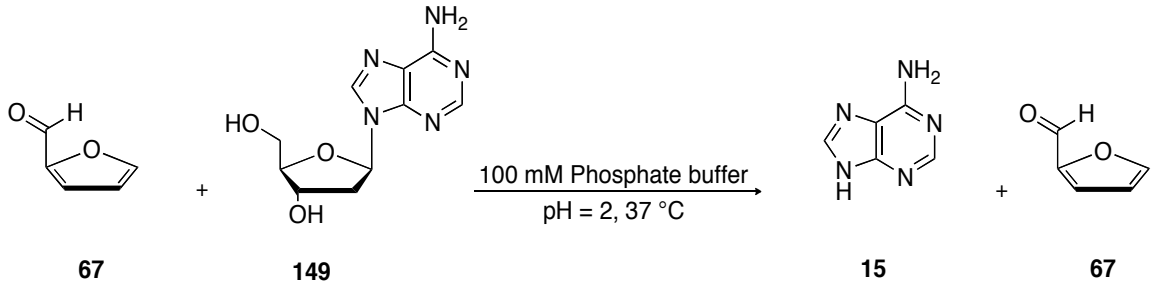

67 **149** **15** **67**

Figure 3-17: Incubation of **23** in 100 mM phosphate buffer pH = 2.0 at 37 °C in the presence of excess deoxyadenosine (dA, **149**)

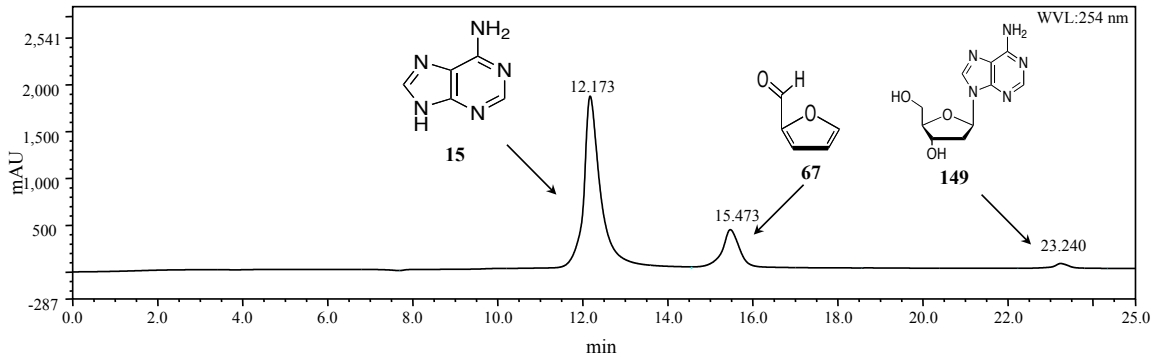

Figure 3-18: Reversed-phase HPLC chromatogram after incubation of **67** in 100 mM phosphate buffer pH = 2.0 at 37 °C in the presence of excess deoxyadenosine (dA) for 49 hours

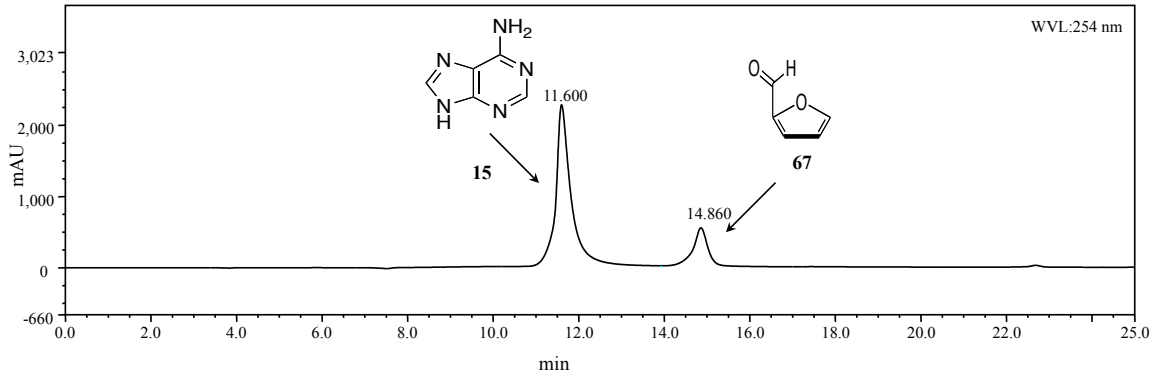

Figure 3-19: Reversed-phase HPLC chromatogram after the incubation of **67** in 100 mM phosphate buffer pH = 2.0 at 50 °C in the presence of excess deoxyadenosine (dA) after 2 hours

In conclusion, oligonucleotides containing a 5'-aldehyde moiety were successfully synthesized and stored at 4 °C for 10 days before β-elimination to form a 5'-phosphate oligonucleotide could be detected. The half-life was determined to be 96 hours in ssDNA under physiological conditions which is similar to what was reported in the literature[102] for ternary complexes (100.7 h). 3',4'-Didehydro-2',3'-dideoxy-5'-oxothymidine (**66**), a proposed product resulting from the β-elimination of the oligonucleotide containing 5'-aldehyde, was successfully synthesized and the half-life of this lesion was determined to

be under physiological conditions (pH 7.4 and 37 °C) 13 hours. The presence of GSH has a great impact on the stability of **66** and resulted in the formation of new compounds that are still under investigation. 2-Deoxyadenosine accelerated the degradation of **66** to thymine and furfural with a half-life of 3 hours compared to 13 hours in the absence of dA. No adduct formation was observed in the incubation of **66** with unmodified oligonucleotides containing dA. Moreover, incubation of furfural with dA did not result in adduct formation.

4 CHAPTER FOUR

4.1 Conclusion and Future Research Directions

4.1.1 Synthesis and Photolysis of C3'-Modified Nucleosides

Oxidative damage to DNA by IR induces mutagenesity, genotoxicity and cell death, which contributes to the development of many diseases with cancer being one of the most important. DNA damage has also been implicated in aging.[17,108] IR produces large amounts of LEEs with energy < 15 eV. These species have been established to cause SSBs and DSBs as well as base release.[66] It was determined that LEEs break DNA bonds through a resonance process called dissociative electron attachment producing stable anions and radical fragments (**Figure 1-5**). One of the intermediates postulated to form is the C2',3'-dideoxy-C3'-thymidinyl radical (**102**). The goal of this work was to synthesize stable and efficient phtolabile radical precursors for the generation of the C2',3'-dideoxy-C3'-thymidinyl radical (**102**) to elucidate the mechanism involved in LEE induced DNA damage. In order to understand the mechanisms involved in LEE induced damage to DNA, the fate of **102** was determined through its independent generation and elucidation of the structures of final DNA damage products. To facilitate this investigation, site-specifically modified nucleosides containing acyl photolabile groups were synthesized and proven to selectively generate the reactive intermediate of interest in a controlled manner at defined sites.[39,36]

The synthesis of α- and β-C2',3'-dideoxy-C3'-pivaloylthymidine (**103** and **101**, respectively) was successfully achieved employing organic chemistry. The efficiency of **103** and **101** for the generation of C2',3'-dideoxy-C3'-thymidinyl radical (**102**) photochemically was investigated under anaerobic conditions using excess *tri-n*butyltin hydride as a hydrogen atom donor. The formation of reduction product **118** provides proof for the suitability of **103** and **101** as precursors of the C2',3'-dideoxy-C3'-thymidinyl radical (**102**). The results showed that when α-isomer **103** is photolyzed in the presence of excess *tri-n*butyltin hydride the reduction product was obtained as the sole product, which indicates the suitability of this precursor for radical generation. On the other hand, photolysis of the β-isomer in the presence of excess *tri-n*butyltin hydride did not generate the reduction product **118** but instead resulted in the formation of products that could not be identified using our present methods. Attempts of changing the solvents in the case of β-isomer **101** were made to determine if the solvent plays any role in product formation. When the photolysis was done in absolute acetonitrile, as a polar aprotic organic solvent, aldehyde **119** was observed indicating trapping of the acyl radical (**120**) with a hydrogen atom faster than liberating carbon monoxide, this is may be due to the formation of a hydrogen bond between the oxygen of the acyl group and the hydrogen of the 5'-hydroxyl group forming a seven membered ring causing the decarbonylation to be slow and the trapping with a hydrogen atom donor to be faster. A second attempt using methanol as a polar protic organic solvent was carried out, Aldehyde **119** was also the only product observed. This also can be explained in the same way as seen in the case of acetonitrile. Additionally, it was reported that decarbonylation of acyl radicals decreases with increasing solvent polarity due to a decrease in the dipole moment during

the bond scission process since the exothermicity of the cleavage decreases with increasing solvent polarity. Thus the activation energy increases which causes slower decarbonylation.[98] Using water as a solvent for photolysis was examined and it resulted in formation of products that could not be identified which could be due to the involvement of a Norrish Type II reaction as seen in **Figure 2-8**.

In order to fully evaluate these precursors, we examined their photochemical conversion in the presence of the more biologically relevant hydrogen atom donor glutathione (GSH). Photolysis of α-isomer **103** was performed in the presence of 6 mM GSH and resulted in the formation of reduction product **118** in addition to other products that could not be identified using our present methods. In contrast, photolysis of β-isomer **101** in the presence of 6 mM GSH resulted in the formation of aldehyde **119** as the sole product. When the photolysis of both isomers was performed in the absence of a hydrogen atom donor, the α-isomer **103** resulted in formation of the reduction product **118** and 2',3'-didehydro-2',3'-dideoxythymidine (**125**), which indicates the involvement of a radical disproportionation mechanism between two alkyl radicals. These radicals are either the C2',3'-dideoxy-C3'-thymidinyl radical (**102**) and the *tert*-butyl radical or two C2',3'-dideoxy-C3'-thymidinyl radical (**102**) to generate compounds **118** and **125** (**Scheme 2.13** and **2.14**, respectively). Additional products were formed such as free base and small amounts of unidentified products, but in case of the β-isomer **101** the photolysis resulted in formation of a very small amount of photoproducts that could not be identified.

Collectively, photochemical generation of the C2',3'-dideoxy-C3'-thymidinylradical (**102**) from β-C2',3'-dideoxy-C3'-pivaloylthymidine **101** and α-C2',3'-

dideoxy-C3'-pivaloylthymidine **103** precursors were investigated under different conditions and based on the results obtained, precursor **103** was found to generate the reduction product **118** under all conditions. In the absence of a hydrogen atom donor the formation of C2',3'-didehydro-2',3'-dideoxythymidine (**125**) was detected which indicates the involvement of a radical disproportionation mechanism as explained. On the other hand precursor **101** was unable to generate the reduction product **118** under any conditions and resulted in the formation of products that could not identified using our present methods in addition to aldehyde **119** resulting from trapping of the acyl radical. Therefore, based on the results obtained precursor **103** will be used to investigate the fate of the C2',3'-dideoxy-C3'-thymidinyl radical (**102**) in oligonucleotides.

In order to incorporate **103** into oligonucleotides, the phosphoramidite or the H-phosphonate building block of α-C2',3'-dideoxy-C3'-pivaloylthymidine **103** will be synthesized and incorporated into DNA using automated reversed DNA synthesis in the case of the phosphoramidite building block, or semi-automated synthesis in the case of the H-phosphonate building block. In the case of the H-phosphonate monomer the unmodified portion of the oligonucleotides will be synthesized using automated reversed DNA synthesis. The identity and purity of both modified and unmodified oligonucleotides will be established using MALDI-ToF and IEX- and RP-HPLC. Quantification will be done using UV-Vis spectroscopy. The photochemical generation of the C2',3'-dideoxy-C3'-thymidinylradical (**102**) in oligonucleotides will be conducted under anaerobic and aerobic conditions in the presence of GSH at physiological conditions. The identification of the damage products will be performed using MALDI-

ToF and IEX- and RP-HPLC. This will help elucidate the mechanistic pathway in which LEE induce DNA damage.

Analysis of the unknown products could be carried out by LC-MS spectrometry which otherwise were difficult to be observed by ESI and MALDI MS techniques. Changing the photolysis conditions for the β-isomer **101** from neutral to mild basic may result in the formation of the radical of interest **102**. This prevents the formation of intramolecular hydrogen bonding between the acyl and the 5'-hydroxy groups that can helps in faster decarbonylation.

4.1.2 5'-Oxidative Damage

Oxidative damage to DNA caused by ROS leads to the formation of single and double strand breaks.[3] Oxidation of 2-deoxyribose at the 5'-position in DNA leads to the formation of strand breaks containing 3'-phosphate (**11**) and 5'-aldehyde residues (**36**) under aerobic conditions. Oligonucleotides containing a 5'-aldehyde moiety such as **36** are unstable and are proposed to undergo β-elimination to form electrophilic fragment **66** followed by loss of the nucleobase **23** to deliver the aromatic compound furfural and free base (**67**, **Scheme 1.10**)[56]. With the goal to investigate the stability and reactivity of oligonucleotides containing a 5'-aldehyde lesion, and its degradation products, fragments believed to be produced upon C5'-oxidation, and oligonucleotides containing the 5'-aldehyde moiety were independently synthesized. The synthesis of the H-phosponate of the modified 5'- nucleoside **135** was successfully achieved and used toward the synthesis of modified oligonucleotides (**138-143**) with high coupling yields. The 5'-diol containing oligonucleotides were successfully converted to the corresponding 5'-aldehyde through oxidative cleavage. Storage of the 5'-aldehyde containing oligonucleotide (**144**) at 4 °C

was stable for 10 days before β-elimination to form a 5'-phosphate oligonucleotide could be detected. The half-life of the 5'-aldehyde lesion in single-stranded DNA under physiological conditions (pH 7.4, 37 °C) was determined to be 96 hours which is agreement to what is reported in the literature[102] for ternary complexes (100.7 h). The 3',4'-didehydro-2',3'-dideoxy-5'-oxothymidine (**66**), a proposed product resulting from the β-elimination of the oligonucleotide containing 5'-aldehyde, was successfully synthesized and the half-life of this lesion was determined to be under physiological conditions (pH 7.4 and 37 °C) 13 hours. The presence of GSH has a great impact on the stability of **66** and resulted in the formation of new compounds that are still under investigation. 2-Deoxyadenosine accelerated the degradation of **66** to thymine and furfural with a half-life of 3 hours compared to 13 hours in the absence of dA. No adduct formation was observed in the incubation of **66** with unmodified oligonucleotides containing dA. Moreover, incubation of furfural with dA under physiological condition (pH 7.4 and 37 °C) did not result in adduct formation. Moreover, incubation of furfural with dA under (pH 2 and 37 °C) resulted in deglycosylation of dA.

In order to investigate stability and reactivity of oligonucleotides containing a 5'-aldehyde toward cellular nucleophile, incubation with GSH, nucleosides such as dA, dG, and dC as well as small DNAs and amino acids such as lysine and arginine and small peptides be investigated to determine adduct formation.

In order to identify electrophilic fragment such as **66,** we could try to use derivatization methods to convert the aldehyde to more stable compound that can be detected by MS or NMR techniques. For example, compound **66** can be reacted with

ethyl thiol in the similar way as was performed by stubbe to identify the 2-Methylene-3(2H)-furanone[109].

5 CHAPTER FIVE

5.1 EXPERIMENTAL PROCEDURES

All experiments were performed with standard laboratory instruments under an argon atmosphere using oven-dried glassware where water and oxygen exclusion were necessary.

5.2 Materials

All chemicals, reagents and solvents were purchased from the following commercial suppliers: Acros Organics, Sigma-Aldrich, EMD Chemicals, PHARMCO-AAPER and Fisher Scientific, and used without further purification unless otherwise stated. Deuterated solvents for NMR were purchased from Cambridge Isotope Laboratories. For chromatographic separation, HPLC grade solvents were used. Deionized water was purified with a PURELAB® Ultra Water Purification System. Anhydrous THF was dried over activated alumina. Triethylammonium acetate buffer (1 M) was purchased from Calbiochem. Pivaloyl chloride (Acros Organic) was distilled according to standard techniques. The Dess-Martin Reagent was synthesized according to published literature.[110] β-*tri*-Butylstannylstyrene was synthesized according to published literature.[111-112]

5.3 Structural Analysis

All synthesized products were characterized by NMR spectroscopy and mass spectrometry.

5.3.1 NMR Spectroscopy

5.3.1.1 ^{1}H-NMR

All ^{1}H-NMR spectra were acquired on a Varian VXR-400, Varian Unity Inova-600 NMR, or Bruker-Avance III-600 Nuclear Magnetic Resonance spectrometer in $CDCl_3$, CD_3CN, or DMSO. Chemical shifts are reported in parts per million downfield from tetramethylsilane (TMS) in $CDCl_3$, residual CD_3CN, or DMSO as internal references. Coupling constants (*J)* are reported in hertz (Hz). Multiplicity is as follows: s = singlet, d = doublet, dd = doublet of doublet, t = triplet, q = quartet, m = multiplet. The protons of the carbons of the furanose ring and the nucleobase thymine are designated as shown in **Figure 5-1**.

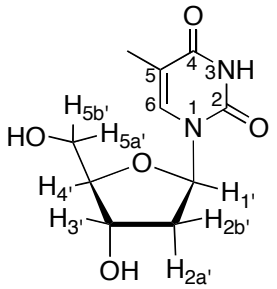

Figure 5-1: The proton assignment of the deoxyribose sugar and the nucleobase moieties in thymidine

5.3.1.2 ^{13}C-NMR

All ^{13}C-NMR were performed on a Varian VXR-400, Varian Unity Inova-600, or Bruker-Avance III-600 Nuclear Magnetic Resonance spectrometer in $CDCl_3$ using the triplet centered at δ 77.23 for $CDCl_3$ as an internal standard. The spectra are ^{1}H-broadband-decoupled.

5.3.1.3 ^{31}P-NMR

^{31}P NMR data was obtained on a Varian VXRS-400 Nuclear Magnetic Resonance spectrometer. All chemical shifts were reported in ppm relative to the external reference 5% H_3PO_4 in $CDCl_3$. The spectra are ^{1}H-broadband-decoupled.

5.3.1.4 ^{1}H-NOESY-NMR

^{1}H-NOESY NMR spectra were acquired on a Varian Unity Inova-600 Nuclear Magnetic Resonance spectrometer.

5.3.2 Mass Spectrometry

Mass spectrometric analyses of the synthesized products were performed using ESI and MALDI-ToF MS.

5.3.2.1 ESI-MS

Mass spectra were performed on an Esquire electrospray ionization (ESI) mass spectrometer (Bruker Daltonics, Bremen, Germany) operated in the positive ion mode and equipped with a quadrupole ion-trap mass analyzer. The samples were dissoved in Methanol to make final concentration of 0.1 μg/μL. The signals obtained correspond to the $[M+H]^+$ or $[M+Na]^+$ ions of the analyte.

5.3.2.2 MALDI-ToF MS

MALDI-ToF MS analyses were conducted using a MALDI-TOF UltrafleXtreme (Bruker Daltonics, Billerica, MA) operating in positive-ion, reflectron mode. Ions were formed by a pulsed UV laser beam, (Nd-YAG laser, wavelength 355 nm), with pulse duration of 1-5 ns. Spectra were recorded by accumulating 500-2500 shots per individual measurement. The pulse ion extraction delay was 100 ns. The acceleration voltage was varied from 22 to 25 kV. The samples were desalted either by reversed-phase HPLC or

by solid phase extraction using C18 ZipTip^{TM}. Sample spotting procedures are as follows:

A: for small molecules, the matrix solution employed was 2,5-dihydroxybenzoic acid (DHB) (20 mg/mL in 30% acetonitrile: 0.1% TFA in H_2O). The matrix (1 μL) was spotted on the MALDI plate. After evaporation to dryness, 1 μL of sample (1 μL each, ≥100 pmole) was spotted on top of the matrix and let dry at room temperature. The signals obtained correspond to the $[M+H]^+$ or $[M+Na]^+$ ions of the analyte, and isotopic peaks were recorded as well.

B: For oligonucleotides, samples, the matrix solution employed was composed of 90% of 3-hydroxypicolinic acid (HPA) (50 mg/mL in 50% acetonitrile: H_2O) and 10% of ammonium citrate (50 mg/mL in H_2O). The matrix (1 μL) was spotted on the MALDI plate. After evaporation to dryness, 1 μL of sample (1 μL each, ≥30 pmole) was spotted on top of the matrix and let dry at room temperature. The signals obtained correspond to the $[M+H]^+$ ions of the analyte, and isotopic peaks were recorded as well. Calibration was conducted before each measurement using external standards. For small molecules, the standard mass range was from 0-500 m/z. The reference mixture contained 1 μL of 10 μM clonidine, 1 μL of 10 μM propranolol, 1 μL of 10 μM hexamethoxyphosphazene, 1 μL of 10 μM papaverine, 1 μL of 10 μM verapamil, 10 μL of Electrospray tuning mix (Hewlett packard product # G2431A), and 26 μL of H_2O. For oligonucleotides the standard mass range was from 1000-4000 Da. To calibrate the MALDI-Tof MS instrument in this mass range, calibration mixture (Bruker, oligonucleotide calibration standard low molecular weight) was used.

5.3.2.3 High Resolution Mass Spectrometry

High resolution mass spectrometry (HRMS) was performed on a Micromass Q-ToF II mass spectrometer located at the Mass Spectrometry and Proteomics Facility, The Ohio State University.

5.3.3 Chromatographic Methods

5.3.3.1 Thin Layer Chromatography

Thin layer chromatography (TLC) was used to monitor all organic reactions, and to monitor the elution of compounds from flash chromatography. TLC was performed using Silicycle silica gel 60 F254 aluminum backed plates. Compound spots were visualized by UV light (254 nm) and stained with an anisaldehyde dip composed of the following: 180 mL of absolute ethanol, 10 mL concentrated sulfuric acid, 2 mL glacial acetic acid, and a few drops of p-anisaldehyde.

5.3.3.2 Flash Chromatography

Purification of all modified nucleosides was performed using an automated flash chromatography system unless otherwise stated. Purification was performed on a Biotage SP4 chromatography system equipped with an in-line variable wavelength detector. The nucleoside products were detected at 254 nm and monitored at 260 nm. TLC was used to determine the purity of chromatography eluents, and fractions containing pure compound were combined and evaporated under reduced pressure using a Heidolph Collegiate Brinkmann rotary evaporator.

5.3.3.3 HPLC

All high performance liquid chromatography (HPLC) analyses were performed on a Dionex Ultimate 3000 HPLC system equipped with an in-line variable wavelength

detector. Reversedd-phase HPLC was used in the analyses of the modified nucleoside in monomer and oligo experiments. The analyses include identification and quantification of the products. Two types of reversedd-phase columns were used:

Column 1: Thermo Hypersil-Keystone BDS Hypersil C-18 column, 4.6 x 250 cm, 5 μm.

Column 2: Agilent ZORBAX SB-C8 column, 4.6 x 250 cm, 5 μm.

The solvent systems used were:

Solvent A: 50 mM TEAA buffer pH = 7.0.

Solvent B: Acetonitrile.

Ion-exchange HPLC was used in the analyses of the modified oligonucleotides. The analytes are separated based on charge. In contrast to RP-HPLC, a n-1 resolution is obtained with this method. Ion-exchange column used: Dionex Pac PA-100 (13 μm), 4.6 x 250 cm.

The solvent systems used were:

Solvent A: 25 mM sodium acetate in 5% acetonitrile, pH = 6.0.

Solvent B: 25 mM sodium acetate in 5% acetonitrile, pH = 6.0, 1 M NaCl.

5.3.4 Other Equipment and Devices

Centrifuge - Thermo Electron Sorall Legend Micro21 centrifuge

High vacuum pump – Edwards RV3

pH meter – Fisher Accumet Basic AB15

Pipettes- Eppendorf Series 2100

Rotary evaporator – Heidolph Collegiate Brinkmann rotary evaporator

Solvent purification system – Innovative Technology PS-MD-2 Pure Solvent system

SpeedVac concentrator – Thermo Electron Savant DNA120

Thermal mixer – Eppendorf Thermomixer

Vortex mixer – Fisher Scientific

5.4 Synthesis of Nucleoside Radical Precursors

5.4.1 Synthesis of 3'-β-(pivaloyl)-3'-deoxythymidine (**101**)

5.4.1.1 5'-*O*-(*tert*-Butyldimethylsilyl)-3'-deoxy-*C*-methylenethymidine (**107**):

C3'-methylene thymidine was synthesized as reported by Wengel et al.[94]

5.4.1.2 1-[(5-*O*-*tert*-Butyldimethylsilyl)-3-*C*-(hydroxymethyl)-2,3-dideoxy-b-D-*threo*-pentofuranosyl]thymine (**108**):

To a solution of **107** (0.94 g, 2.66 mmol) in anhydrous THF (5.4 mL) under nitrogen, was added BH_3:1,4-oxathiane (0.33 mL of a 7.8 M solution in oxathiane, 2.87 mmol) at room temperature. After cooling of this mixture to 0 °C a 2 M solution of NaOH (1.5 mL) was slowly added followed by the dropwise addition of 30% aqueous H_2O_2 (0.38 mL). Stirring was continued for 1 h at room temperature. The reaction mixture was poured into ice-water (68 mL) and extracted with diethylether (80 mL). The combined organic phase was washed with water (68 mL) and saturated aqueous $NaHCO_3$ (2 x 68 mL), dried (Na_2SO_4) and evaporated to dryness *in vacuo*. The product was purified on a silica gel column (50:50 ethylacetate:pentane) to give **108** as a clear colorless oil. Yield: 0.88 g (89%). ^{1}H-NMR ($CDCl_3$, 400 MHz) δ: 0.15 (6H, s, $Si(CH_3)_2$), 0.94 (9H, s, $SiC(CH_3)_3$), 1.81 (1H, m, 2'-H_β), 1.93 (3H, s, CH_3), 2.44 (1H, m, 2'-H_α), 2.72 (1H, m, 3'-H), 3.34 (1H, t, J = 6.4 Hz, OH), 3.73-3.89 (3H, m, C$\underline{H_2}$OH, 5'-H), 4.00 (1H, m, 5'-H), 4.16 (1H, m, 4'-H), 6.06 (1H, dd, J = 8.2, 6.2 Hz, 1'-H), 7.48 (1H, s, 6-H), 9.44 (1H br s, NH). ^{13}C ($CDCl_3$, 100 MHz) δ: –5.3, 12.8, 18.4, 26.0, 34.0, 42.6,

61.8, 62.6, 79.8, 84.3, 111.0, 135.6, 150.8, 164.2. HRMS $[M + H]^+$: calc. for $C_{17}H_{31}O_5N_2Si$ 371.2002, found 371.2001.

5.4.1.3 1-[(5-*O*-*tert*-Butyldimethylsilyl)-3-*C*-(formyl)-2,3-dideoxy-β-D-*threo*-pentofuranosyl]thymine (**109**):

A solution of **108** (0.83 g, 2.24 mmol) in CH_2Cl_2 (8 mL) was cannulated into a solution of Dess-Martin periodinane (1.43 g, 3.37 mmol) in anhydrous CH_2Cl_2 (16 mL) at 0 °C. After stirring overnight at room temperature, diethyl ether (70 mL) was added and the solution was poured slowly into a solution of saturated $NaHCO_3$ (45 mL) containing $Na_2S_2O_3 \bullet 5H_2O$ (5.56 g). The organic layer was removed and the aqueous layer extracted with diethyl ether (95 mL). The combined organic phase was washed with saturated $NaHCO_3$ (95 mL) followed by H_2O (95 mL), dried (Na_2SO_4) and evaporated to dryness *in vacuo*. The product was isolated as a white amorphous solid. Yield: 0.83 g (100%). ^{1}H-NMR ($CDCl_3$, 600 MHz) δ: 0.10 (6H, s, $Si(CH_3)_2$), 0.91 (9H, s, $SiC(CH_3)_3$), 1.94 (3H, d, J = 1.2 Hz, CH_3), 2.43 (2H, m, 2'-H), 3.27 (1H, m, 3'-H), 3.95 (2H, m, 5'-H), 4.40 (1H, m, 4'-H), 6.14 (1H, dd, J = 7.2, 6.60 Hz, 1'-H), 7.44 (1H, d, J = 1.2 Hz, 6-H), 8.27 (1H, br s, NH), 9.85 (1H, s, CHO). ^{13}C ($CDCl_3$, 150 MHz) δ: –5.5, 12.7, 18.3, 26.0, 31.4, 51.0, 61.8, 80.3, 83.8, 111.4, 135.4, 150.9, 164.2, 199.5. HRMS $[M + H]^+$: calc. for $C_{17}H_{29}O_5N_2Si$ calc. 369.1846, found 369.1846.

5.4.1.4 1-[(5-*O*-*tert*-Butyldimethylsilyl)-3-*C*-(2,2-dimethyl-1-hydroxypropyl)-2,3-dideoxy-β-D-*threo*-pentofuranosyl]thymine (**110**):

Cerium chloride was dried as described by Kamiya.[113] To a suspension of dry $CeCl_3$ (16.7 g, 44.8 mmol) in THF (105 mL) at –78 °C was added a 1.6 M solution of *t*-butyllithium (28.0 ml, 44.8 mmol) in pentane. This was allowed to stir for 1.5 h before a

solution of **109** (0.83 g, 2.24 mmol) in THF (41 mL) was added dropwise at the same temperature. The reaction stirred at this temperature for 3.5 h, after which it was quenched by the addition of aqueous NH_4Cl (200 mL) and allowed to warm to room temperature. The product was then extracted with CH_2Cl_2 (6 x 250 mL), the organic layer dried over Na_2SO_4, and the solvent removed *in vacuo*. The crude product was purified on a silica gel column (40% ethyl acetate in hexane) to give **110** as a diasteromeric mixture of a clear colorless oil. Yield: 0.37 g (67%). ^{1}H-NMR ($CDCl_3$, 400 MHz) δ: 0.16 (6H, s), 0.94 (18H, 4s), 1.93 (3H, d, *J* = 1.2 Hz), 2.15 (1H, m), 2.27 (1H, m), 2.69 (1H, m), 3.47 (1H, d, *J* = 3.2), 3.60 (1H, d, *J* = 2.8 Hz), 3.90 (1H, m), 4.03 (2H, m), 6.08 (1H, dd, *J* = 9.0, 5.8 Hz), 7.50 (1H, d, *J* = 1.2 Hz), 8.8 (1H, br s). ^{13}C ($CDCl_3$, 100 MHz) δ: -5.2, 12.8, 18.5, 26.0, 27.0, 31.5, 35.5, 40.8, 63.0, 75.9, 80.5, 83.9, 111.1, 135.9, 150.8, 163.9. HRMS $[M + H]^+$: calc. for $C_{21}H_{39}O_5N_2Si$ 427.2628, found 427.2629.

5.4.1.5 1-[(5-*O*-*tert*-Butyldimethylsilyl)-3-*C*-(2,2-dimethyl-1-oxopropyl)-2,3-dideoxy-β-D-*threo*-pentofuranosyl]thymine (**111**):

To a solution of Dess-Martin periodinane (0.30 g, 0.71 mmol) in anhydrous CH_2Cl_2 (3 mL) was cannulated a solution of **110** (0.20 g, 0.47 mmol) in CH_2Cl_2 (2 mL) at 0 °C. Stirring was continued at 0 ºC for 15 minutes then at room temperature for 4 h. Diethylether (14 mL) was added and the solution was poured slowly into a solution of (1.16 g, 4.69 mmol) $Na_2S_2O_3.5H_2O$ in sat. $NaHCO_3$ (9 mL). The organic phase was washed with saturated $NaHCO_3$ (20 mL) followed by H_2O (20 mL), and saturated NaCl (20 mL), dried with $MgSO_4$ and evaporated to dryness *in vacuo*. The product was isolated as a white solid. Yield: 0.19 g (96%). ^{1}H-NMR ($CDCl_3$, 400 MHz) δ: 0.06 (6H, s, $Si(CH_3)_2$), 0.88 (9H, s, $SiC(CH_3)_3$), 1.16 (9H, s, $COC(CH_3)_3$), 1.96 (3H, d, *J* = 0.8 Hz,

CH_3), 2.06 (1H, m, 2'-H_β), 2.49 (1H, m, 2'-H_α), 3.68 (2H, m, 5'-H), 3.81 (1H, m, 3'-H), 4.20 (1H, m, 4'-H), 6.14 (1H, dd, *J* = 8.0, 6.0 Hz, 1'-H), 7.51 (1H, d, *J* = 0.8 Hz, 6-H), 9.23 (1H, br s, NH). ^{13}C ($CDCl_3$, 100 MHz) δ: –5.1, 12.9, 18.7, 26.0, 26.2, 36.7, 44.2, 45.0, 62.6, 80.8, 84.3, 111.4, 135.6, 150.8, 164.0, 214.1. HRMS $[M + H]^+$: calc. for $C_{21}H_{37}O_5N_2Si$ 425.2472, found 425.2473.

5.4.1.6 1-[2,3-dideoxy-3-*C*-(2,2-dimethyl-1-oxopropyl)-2,3-dideoxy-β-D-*threo*-pentofuranosyl]thymine (**101**):

To a stirred solution of **111** (0.12 g, 0.283 mmol) in THF (3 mL), was added aqueous trifluoroaceticacid (0.74 mL, 1:1, TFA/H_2O) at 0 °C. After stirring for 2 h at 0 °C, the reaction mixture was stirred at room temperature until completion. It was then neutralized with saturated aqueous $NaHCO_3$ (5 mL) and diluted with 10 mL of ethyl acetate. The aqueous layer was then extracted with ethyl acetate. The combined organic layers were dried over Na_2SO_4 and evaporated to dryness *in vacuo.* The crude product was purified on silica gel column (0-2% methanol in dichloromethane) to give **101** as a colorless foam. Yield: 0.08 g (91%). ^1H-NMR ($CDCl_3$, 400 MHz) δ: 0.99 (9H, s, $COC(CH_3)_3$), 1.91 (3H, s, CH_3), 2.20 (1H, m, 2'-H_β), 2.40 (1H, m, 2'-H_α), 2.97 (1H, m, 3'-H), 3.29 (1H, s, OH), 4.16 (2H, m, 5'-H), 4.63 (1H, m, 4'-H), 6.14 (1H, t, *J* = 7.2 Hz, 1'-H), 7.87 (1H, s, 6-H), 9.66 (1H, br s, NH). ^{13}C ($CDCl_3$, 100 MHz) δ: 12.8, 24.9, 32.3, 38.6, 47.0, 63.8, 71.3, 83.4, 87.1, 110.0, 110.8, 137.3, 150.9, 164.5, 216.9. ESI $[M + Na]^+$: calc. for $C_{15}H_{22}O_5N_2Na$ 333.1, found 333.2.

5.4.2 Synthesis of 3'-α-(pivaloyl)-3'-deoxythymidine (**103**)

5.4.2.1 1-[5-(*tert*-Butyldiphenylsilyl)-2,3-dideoxy-3-*C*-formyl-β-D-*erythro*-pentofuranosyl]thymine (**115**):

Compound **115** was synthesized as reported by Sanghvi, et al.[97]

5.4.2.2 1-[5-(*tert*-Butyldiphenylsilyl)-2,3-dideoxy-3-*C*-(2,2-dimethyl-1-hydroxypropyl)-β-D-*erythro*-pentofuranosyl]thymine (**116**):

Cerium chloride was dried as described by Kamiya.[113] To a suspension of dry $CeCl_3$ (8.32 g, 22.34 mmol) in THF (52 mL), was added dropwise 1.7 M *t*-butyllithium in pentane (13.14 mL, 22.34 mmol) at -78 ºC. The solution was allowed to stir at this temperature for 1.5 hours. Aldehyde **115** (0.55 g, 1.117 mmol) in THF (20 mL)**,** which was co-evaporated with dry THF, was added over 25 min and allowed to stir at the same temperature for 8 hours, before quenching by the addition of saturated NH_4Cl (101 mL) at -78 ºC. The reaction mixture was extracted with dichloromethane (x6), the organic layer was dried over Na_2SO_4, filtered, and the solvent was removed under reduced pressure to afford a brownish foam. The crude mixture was purified by column chromatography with 1:1 ethyl acetate:hexane to afford **116** as a diastereomeric mixture in the form of a colorless foam. Yield: 0.17 g (30%). ^{1}H-NMR ($CDCl_3$, 400 MHz) δ: 0.88-0.92 (18H, 2s), 1.1 (18H, s), 1.61 (6H, s), 1.85 (1H, m), 2.02 (1H, d, *J* = 5.6), 2.24 (1H, m), 2.45 (1H, d, *J* = 5.6 Hz), 2.71 (2H, m), 3.19 (1H, d, *J* = 5.2 Hz), 3.33 (1H, t, *J* = 4.99 Hz), 3.81, 3.88 (2H, 2 dd, *J* = 11.4, 2.8 Hz), 3.98 (1H, m), 4.07 (2H, m), 4.33 (1H, m), 6.13 (1H, t, *J* = 6.8 Hz), 6.23 (1H, t, *J* = 6.4 Hz), 7.36-7.69 (22H, m), 9.08 (1H, br s), 9.17 (1H, br s). ^{13}C ($CDCl_3$, 100 MHz) δ: 12.3, 19.6, 26.6, 26.7, 27.2, 32.8, 35.8, 36.1, 38.5, 40.1, 40.6, 63.3, 66.0, 77.4, 82.2, 82.9, 84.3, 85.4, 85.6, 111.0, 128.03, 128.07,

128.12, 130.11, 130.15, 130.19, 130.24, 132.74, 132.96, 133.27, 133.34, 135.57, 135.69, 135.75, 135.81, 150.6, 150.7, 164.2. HRMS $[M + Na]^+$: calc. for $C_{31}H_{42}O_5N_2SiNa$ 573.2761, found 573.2760.

5.4.2.3 1-[5-(*tert*-Butyldiphenylsilyl)-2,3-dideoxy-3-*C*-pivaloyl-β-D-*erythro*-pentofuranosyl]thymine (**117**):

A solution of **116** (0.17 g, 0.309 mmol) in anhydrous CH_2Cl_2 (1 mL) was added to a solution of the Dess-Martin periodinane (0.2 g, 0.472 mmol) in anhydrous CH_2Cl_2 (2.2 mL) at 0 ºC. Stirring was continued at 0 ºC for 15 minutes then at room temperature overnight. The reaction mixture was diluted with diethyl ether (10 mL), poured into ice-cold aqueous saturated $NaHCO_3$ (6.2 mL) containing $Na_2S_2O_3.5H_2O$ (0.77 g, 3.09 mmol), and stirred for 10 minutes. The organic layer was washed with sat. $NaHCO_3$, H_2O, and sat. NaCl, dried over Na_2SO_4, and the solvent was removed under reduced pressure to afford **117** as a colorless foam. Yield: 0.17 g (100%). ^{1}H-NMR ($CDCl_3$, 400 MHz) δ: 1.11 (18H, s, $SiC(C\underline{H}_3)_3$ & $COC(C\underline{H}_3)_3$), 1.62 (3H, d, J = 0.8, CH_3), 2.24 (1H, m, 2'-H_β), 2.43 (1H, m, 2'-Hα), 3.66 (1H, dd, J = 11.8, J = 2.6, 5'-H), 3.84 (1H, m, 3'-H), 4.09 (1H, dd, J = 12, J = 2, 5'-H), 4.25 (1H, dt, J = 6.8, J = 2.4, 4'-H), 6.22 (1H, dd, J = 6.8 Hz, J = 5.2 Hz, 1'-H), 7.37-7.47 (6H, m, Ar), 7.53 (1H, d, J = 0.8, 6-H), 7.64-7.68 (4H, m, Ar), 8.88 (1H, br s, NH). ^{13}C ($CDCl_3$, 100 MHz) δ: 12.3, 19.6, 26.0, 27.3, 30.5, 39.0, 43.7, 44.9, 63.5, 83.8, 85.6, 111.1, 128.2, 130.3, 132.8, 135.6, 150.3, 164.1, 215.3. HRMS $[M + Na]^+$: calc. for $C_{31}H_{40}O_5N_2SiNa$ 571.2604, found 571.2617.

5.4.2.4 1-(2,3-dideoxy-3-*C*-pivaloyl-β-D-*erythro*-pentofuranosyl)thymine (**103**):

To a solution of **117** (0.15 g, 0.27 mmol) in THF (2.3 mL) was added a 1M solution of TBAF in THF (0.41 mL) at room temperature. Stirring was continued for 1 h.

The solvent was removed *in vacuo* and the crude mixture was purified by column chromatography with ethyl acetate to afford **103** as a colorless foam. Yield: 0.04 g (44%). ^{1}H-NMR ($CDCl_3$, 400 MHz) δ: 1.18 (9H, s, $COC(C\underline{H}_3)_3$), 1.93 (3H, s, CH_3), 2.44 (2H, m, 2'-H), 2.65 (1H, dd, *J*= 6.2 Hz, *J* = 3.4, 5'-OH), 3.62 (1H, m, 3'-H), 3.97 (2H, m, 5'-H), 4.29 (1H, dt, *J* = 8 Hz, J = 2.4 Hz, 4'-H), 6.0 (1H, dd, *J* = 7.2 Hz, *J* = 4.4 Hz, 1'-H), 7.48 (1H, d, J = 0.8 Hz, 6-H), 8.67 (1H, br s, NH). ^{13}C ($CDCl_3$, 100 MHz) δ: 12.8, 25.8, 38.7, 43.3, 45.2, 61.9, 84.7, 88.2, 110.9, 137.6, 150.4, 164.1, 215.8. HRMS $[M + Na]^+$: calc. for $C_{15}H_{22}O_5N_2Na$ 333.1426, found 333.1419.

5.5 Synthesis of Damage products

5.5.1 Synthesis of C2',3'-Dideoxythymidine (**118**)

Compound **118** was synthesized as reported by Audat, et al.[95]

5.5.2 Synthesis of C2',3'-Didehydro-2',3'-dideoxythymidine (**125**)

Compound **125** was synthesized according to published literature.[114]

5.6 Photolysis Experiments

Photolysis experiments were performed in 4x10 mm quartz cuvettes (*Sigma Aldrich*, St. Louis, MO) using an *Oriel* 500 W High Pressure Mercury Arc Lamp (*Newport*, Irvine CA) fitted with an IR filter, focusing lens, and a 320 nm cut-off filter. The temperature of the photoreactions was maintained at 15 ^{0}C using a Peltier PTP-1 single cell temperature controller system (*Varian*, Palo Alto, CA). The irradiation mixtures were analyzed directly without workup by analytical reversed-phase HPLC with UV detection at 254 nm. HPLC analyses were carried out on either column mentioned in section 5.3.3.3 using solvent systems described in the same section. A stepwise gradient

was applied. 0-20% B over 15 min, 20-75% B over 3 min, 75-90% B over 4 min. Flow rate, 1.0 mL/min

5.6.1 Photochemical Generation of the C2',3'-Dideoxy-C3'-thymidinyl Radical from **103**

5.6.1.1 Photolysis of **103** in the Presence of *tri-n*Butyltin hydride as a Hydrogen Atom Donor

A solution of radical precursor **103** (600 nmole, 1 mM in 1:1 CH_3CN/H_2O) was transferred to a quartz cuvette and degassed by bubbling argon through the solution for 20 min. *tri-n*Butyltin hydride (1000 equivalents) was added under an argon atmosphere. The mixture was immediately photolyzed for 60 min at 15 °C. The irradiation mixture was analyzed directly without workup by analytical reversed-phase HPLC with UV detection at 254 nm using C18 column and the solvent system described above. Products were identified by ESI-MS and by comparison with authentic samples. Product yields were determined using standard curves.

5.6.1.2 Photolysis of **103** in the Presence of Glutathione as a Hydrogen Atom Donor

A solution of radical precursor **103** (600 nmole, 1 mM) and glutathione (6 mM in 1:1 CH_3CN/H_2O) was transferred to a quartz cuvette and degassed by bubbling argon through the solution for 20 min. The mixture was immediately photolyzed for 60 min at 15 °C under an argon atmosphere. After the photolysis was completed, the crude volume was adjusted to 600 µL by addition of acetonitrile. The irradiation mixture was analyzed directly without workup by analytical reversed-phase HPLC with UV detection at 254 nm using C8 column and the solvent system described above. The products were identified by ESI-MS and by spiking the photolysate with authentic samples.

5.6.1.3 Photolysis of **103** in the Absence of a Hydrogen Atom Donor

A photolysis sample containing **103** (600 nmol, 1 mM) in CH_3CN/H_2O (1:1 v/v) was transferred to a quartz cuvette and purged with argon for 20 minutes. The sample was immediately photolyzed for 60 min at 15 °C under an argon atmosphere. The irradiation mixture was analyzed directly without workup by analytical reversed-phase HPLC with UV detection at 254 nm using C8 column and the solvent system described above. The products were identified by ESI-MS and by spiking the photolysate with authentic samples.

5.6.2 Photochemical Generation of the C2',3'-Dideoxy-C3'-thymidinyl Radical from **101**

5.6.2.1 Photolysis of **101** in the Presence of *tri-n*Butyltin hydride as a Hydrogen Atom Donor

5.6.2.1.1 Photolysis of **101** in 1:1 CH_3CN/H_2O

A solution of radical precursor **101** (600 nmole, 1 mM in 1:1 CH_3CN/H_2O) was transferred to a quartz cuvette and degassed by bubbling argon through the solution for 20 min. *tri-n*Butyltin hydride (1000 equivalents) was added under an argon atmosphere. The mixture was immediately photolyzed for 60 min at 15 °C under an argon atmosphere. The irradiation mixture was analyzed directly without workup by analytical reversed-phase HPLC with UV detection at 254 nm using C8 column and the solvent system described above. Products were identified by ESI-MS and by comparison with authentic samples.

5.6.2.1.2 Photolysis of **101** in H_2O

A solution of radical precursor **101** (600 nmole, 1 mM in H_2O containing 0.1% acetonitrile) was transferred to a quartz cuvette and degassed by bubbling argon through the solution for 20 min. *tri-n*Butyltin hydride (1000 equivalents) was added under an argon atmosphere. The mixture was immediately photolyzed for 60 min at 15 °C under an argon atmosphere. The irradiation mixture was analyzed directly without workup by analytical reversed-phase HPLC with UV detection at 254 nm using C8 column and the solvent system described above. Products were identified by ESI-MS and by comparison with authentic samples.

5.6.2.1.3 Photolysis of **101** in CH_3CN

A solution of radical precursor **101** (600 nmole, 1 mM in CH_3CN) was transferred to a quartz cuvette and degassed by bubbling argon through the solution for 20 min. *tri-n*Butyltin hydride (1000 equivalents) was added under an argon atmosphere. The mixture was immediately photolyzed for 60 min at 15 °C under an argon atmosphere. The irradiation mixture was analyzed directly without workup by analytical reversed-phase HPLC with UV detection at 254 nm using C8 column and the solvent system described above. Products were identified by ESI-MS and by comparison with authentic samples.

5.6.2.2 Photolysis of **101** in the Presence of Glutathione as a Hydrogen Atom Donor

A solution of radical precursor **101** (600 nmole, 1 mM) and glutathione 6 mM in 1:1 CH_3CN/H_2O was transferred to a quartz cuvette and degassed by bubbling argon through the solution for 20 min. The mixture was immediately photolyzed for 60 min at 15 °C under an argon atmosphere. After the photolysis was completed, the crude volume was adjusted to 600 μL by addition of acetonitrile. The irradiation mixture was analyzed

directly without workup by analytical reversed-phase HPLC with UV detection at 254 nm using C8 column and the solvent system described above. The products were identified by ESI-MS and by spiking the photolysate with authentic samples.

5.6.2.3 Photolysis of **101** in the Absence of a Hydrogen Atom Donor

A photolysis sample containing **101** (600 nmol, 1 mM) in CH_3CN/H_2O (1:1 v/v) was transferred to a quartz cuvette and purged with argon for 20 minutes. The sample was immediately photolyzed for 60 min at 15 °C under an argon atmosphere. The irradiation mixture was analyzed directly without workup by analytical reversed-phase HPLC with UV detection at 254 nm using C8 column and the solvent system described above. The products were identified by ESI-MS and by spiking the photolysate with authentic samples.

5.7 Synthesis of C5'-modified thymidine

5.7.1 1-[5-*O*-(acetyl)-5-*C*-((4,4'-dimethoxytrityl)oxymethyl)-2-deoxy-β-D-*erythro*-pentofuranosyl]thymine (**134**)

Synthesis of **134** was performed as reported by Kodama, et al.[115]

5.7.2 1-[5-*O*-(acetyl)-5-*C*-((4,4'-dimethoxytrityl)oxymethyl)-3-H-phosphonateTriethylammonium Salt, 2-deoxy-β-D-*erythro*-pentofuranosyl]thymine (**135**)

Imidazole (0.30 g, 4.41 mmol) was coevaporated twice with anhydrous acetonitrile and dissolved in anhydrous CH_2Cl_2 (15 mL). While stirring at -10 °C, phosphorous trichloride (0.11 mL, 1.26 mmol) followed by a solution of anhydrous triethylamine (0.62 mL, 4.45 mmol) in CH_2Cl_2 (0.62 ml) was added dropwise with vigorous stirring. The mixture was allowed to stir for 30 min at this temperature. The

modified nucleoside (**134**) (0.23 g, 0.37 mmol) was coevaporated twice with anhydrous pyridine and dissolved in anhydrous CH_2Cl_2 (9.2 mL). The solution was added to the reaction mixture over 30 min. The reaction mixture was slowly warmed to room temperature and strirred for 8 hrs. The mixture was then hydrolyzed with 1 M triethylammonium bicarbonate TEAB (27 mL). The organic layer was separated and washed with an equal volume of 1 M TEAB. The organic layer was then concentrated under reduced pressure. The crude mixture was purified by column chromatography using a stepwise gradient of methanol (0-10%) in CH_2Cl_2 containing 1% triethylamine to afford **135** as a diasteromeric mixture in the form of a yellow foam. Yield: 0.10 g (34%). ^{1}H-NMR ($CDCl_3$, 400 MHz) δ: 1.27 (18H, t, J = 7.2 Hz, N($CH_2\underline{CH_3}$)$_3$), 1.84-1.87 (6H, 2s, CH_3), 1.96-2.04 (2H, m, 2'-H), 2.127-2.13 (6H, 2s, CO$\underline{CH_3}$), 2.52-2.62 (2H, m, 2'-H), 2.95-3.01 (12H, q, *J* = 7.2 Hz, N($\underline{CH_2}CH_3$)$_3$), 3.22-3.51 (4H, m, 3', 5'-H), 3.77 (12H, s, O$\underline{CH_3}$), 4.30-4.33 (2H, m, 4'-H), 4.70-4.86 (2H, m, 6'-H), 5.26-5.41 (2H, m, 6'-H), 6.04 (1H, d, *J* = 620.3 Hz, P-H), 6.09 (1H, d, *J* = 622.7 Hz, P-H), 6.24 (1H, dd, *J* = 8.4, 5.6 Hz, 1'-H), 6.31 (1H, dd, *J* = 7.2, 6.0 Hz, 1'-H), 6.80-7.42 (28H, m, Ar-H and 6-H). ^{13}C ($CDCl_3$, 100 MHz) δ: 7.8, 9.1, 12.7, 12.8, 21.2, 21.3, 39.3, 39.6, 45.7, 52.7, 55.3, 62.4, 62.5, 71.9, 72.5, 73.18, 73.2, 77.4, 84.0, 84.1, 84.17, 84.2, 84.5, 84.7, 86.3, 110.9, 111.2, 113.15, 113.2, 126.9, 127.87, 127.9, 128.1, 130.0, 134.6, 135.1, 135.7, 135.76, 135.8, 144.6, 150.6, 158.5, 164.0, 164.1, 169.6, 170.3. ^{31}P NMR ($CDCl_3$, 400 MHz) δ: 3.84, 4.20. HRMS $[M + Et_3NH]^+$: calc. for $C_{46}H_{68}O_{11}N_4P$ 883.46, found 883.54.

5.7.3 5'-*O*-(*tert*-Butyldimethylsilyl)-thymidine (**105**)

Compound **105** was synthesized according to published procedure.[104]

5.7.4 5'-*O*-(*tert*-Butyldimethylsilyl)-3'-*O*-benzoyl-thymidine (**146**)[105]

To a solution of **105** (4.96 g, 13.91 mmol) in anhydrous pyridine (14.3 mL) was added benzoyl chloride (1.9 mL, 16.38 mmol) at room temperature. Stirring was continued overnight. The solvent was removed *in vacuo* and the moist residue was triturated with water (100 mL). The resulting precipitate was filtered and air dried. The crude product was azeotropically dried with acetonitrile and then recrystallized from acetonitrile to afford **146** as white crystals. Yield: 5.77 g (90%). ^{1}H-NMR ($CDCl_3$, 600 MHz) δ: 0.18 (6H, s, $Si(CH_3)_2$), 0.96 (9H, s, $SiC(CH_3)_3$), 1.95 (3H, d, *J* = 0.6 Hz, CH_3), 2.23 (1H, m, 2'-H), 2.60 (1H, dd, *J* = 13.8, 5.4 Hz, 2'-H), 3.98 (1H, dd, *J* = 11.4, 1.8 Hz, 5'-H), 4.04 (1H, dd, *J* = 11.4, 1.8 Hz, 5'-H), 4.27 (1H, d, *J* = 1.8 Hz, 4'-H), 5.51 (1H, d, *J* = 6.0 Hz, 3'-H), 6.50 (1H, dd, *J* = 9.6, 5.4 Hz, 1'-H), 7.48 (2H, t, J = 7.8 Hz, 4-Ph), 7.61 (2H, m, 3-Ph and 6-H), 8.06 (2H, dd, *J* = 8.4, 1.2 Hz, 2-Ph), 8.86 (1H, br s, NH). ^{13}C ($CDCl_3$, 150 MHz) δ: -5.4, -5.3, 12.6, 18.4, 26.0, 38.2, 63.8, 76.2, 84.9, 85.7, 111.4, 128.6, 129.3, 129.8, 133.6, 135.2, 150.9, 164.4, 166.3. ESI $[M + Na]^+$: calc. for $C_{23}H_{32}O_6N_2SiNa$ 483.59, found 483.60.

5.7.5 3'-*O*-benzoyl-thymidine (**147**)[106]

To a stirred solution of **146** (3.73 g, 8.10 mmol) in THF (37 mL), was added aqueous trifluoroacetic acid (13.8 mL, 1:1, TFA/H_2O) at 0 °C. After stirring for 30 minutes at 0 °C, the reaction mixture was stirred at room temperature overnight. It was then neutralized with saturated aqueous $NaHCO_3$ (60 mL) and diluted with 46 mL of ethyl acetate. The resulting precipitate was formed then filtered to give **147** as white powder. Yield: 2.66 g (95%). ^{1}H-NMR (DMSO-d_6, 400 MHz) δ: 1.80 (3H, s, CH_3), 2.41 (2H, m, 2'-H), 3.70 (2H, m, 5'-H), 4.16 (1H, m, 4'-H), 5.28 (1H, t, *J* = 5.4 Hz, 5'-OH),

5.48 (1H, m, 3'-H), 6.29 (1H, t, *J* = 7.2 Hz, 1'-H), 7.56 (2H, t, J = 7.8 Hz, 4-Ph), 7.68 (1H, m, 3-Ph), 7.8 (1H, s, 6-H), 8.02 (2H, dd, *J* = 8.4, 1.2 Hz, 2-Ph), 11.38 (1H, br s, NH). ^{13}C (DMSO-d_6 100 MHz) δ: 12.4, 36.7, 61.4, 75.7, 83.8, 84.5, 109.8, 128.8, 129.4, 133.7, 135.9, 150.5, 163.7, 165.3. ESI $[M + Na]^+$: calc. for $C_{17}H_{18}O_6N_2Na$ 369.33, found 369.50.

5.7.6 3',4'-Didehydro-2',3'-dideoxy-5'-oxothymidine (**66**)[107]

To a solution of the Dess-Martin periodinane (0.92 g, 2.169 mmol) in anhydrous CH_3CN (17 mL) was added **147** (0.3 g, 0.866 mmol) at 0 ºC. Stirring was continued at 0 °C for 15 minutes then at room temperature overnight. The reaction mixture was diluted with diethyl ether (26 mL), filtered through a pad of celite, which was rinsed with acetonitrile. The organic layer was dried over Na_2SO_4, and the solvent was removed under reduced pressure to afford 3'-O-benzoyl-5'-oxothymidine (**148**) as a crude white powder 0.22 g. To a solution of the crude sample 148 in anhydrous CH_2Cl_2 (10 mL) was added triethylamine (0.36 mL), the reaction mixture was stirred at room temperature for 10 minutes, then the solvent was removed under reduced pressure at ambient temperature. The crude mixture was purified by column chromatography with ethyl acetate to afford **66** as white powder. Yield: 0.04 g (21%). ^{1}H-NMR (CD_3CN, 400 MHz) δ: 1.82 (3H, d, *J* = 0.8 Hz, CH_3), 2.92 (1H, ddd *J* = 20.4, 5.2, 3.6 Hz, 2'-H), 3.38 (1H, ddd *J* = 20.4, 10.4, 2.8 Hz, 2'-H), 6.30 (1H, t, *J* = 2.8 Hz, 3'-H), 6.75 (1H, dd, *J* = 10.4, 5.2 Hz, 1'-H), 7.06 (1H, d, *J* = 0.8 Hz, 6-H), 9.01 (1H, br s, NH), 9.43 (1H, s, CHO). ^{13}C (CD_3CN 100 MHz) δ: 12.5, 36.7, 86.8, 112.7, 121.3, 136.3, 151.1, 156.2, 164.5, 182.3. MALDI-Tof $[M + Na]^+$: calc. for $C_{10}H_{10}O_4N_2Na$ 245.054, found 245.051

5.8 Oligonucleotide Synthesis

All oligonucleotide synthesis was carried out on an ABI 391 DNA synthesizer (Applied Biosystem, Carlsbad, CA). All reagents for automated oligonucleotide synthesis were purchased from Glen Research. Pivaloyl chloride (Acros Organic) was distilled according to the standard techniques. All syntheses were performed on a 0.2 μmole scale using controlled pore glass (CPG) columns (500 Å pore size). Syntheses of the unmodified oligonucleotides were carried out in the 3'→5' direction using the phosphoramidite method. Modified oligonucleotides were partially synthesized in the 3'→5' direction with standard phosphoramidite chemistry, followed by manual coupling of the modified nucleoside with H-phosphonate chemistry. Deblocking was accomplished using 3% trichloroacetic acid in dichloromethane. 5-Ethylthio-1H-tetrazole (0.25 M) in acetonitrile was used as an activator in the coupling steps of unmodified oligonucleotides, and pivaloyl chloride was used as an activator for the manual coupling of the H-phosphonate. Capping of the unreacted nucleotides was performed using acetic anhydride in THF/pyridine and 10% 1-methylimidazole in THF. Unmodified oligonucleotides were oxidized with 0.02 M I_2 in pyridine/THF/H_2O, while the oxidation of modified oligonucleotides were executed through simultaneous exposure to 4% I_2 in pyridine/H_2O/THF (1:1:8) and THF/H_2O/triethylamine (8:1:1) for 20 min.

5.8.1 Purification of Oligonucleotides

Oligonucleotides were deprotected and cleaved from the solid support by treating the resin with 1 mL of concentrated ammonium hydroxide (28-30% in H_2O) for 15-18 hrs at 55 °C, followed by purification.

5.8.1.1 Oligonucleotide Purification Cartridges (OPC) (Trityl-on Method)

Oligonucleotides sequences were synthesized with trityl on at the 5' end in order to use OPC purification. Columns were activated by flushing with 2 mL acetonitrile, followed by 2 mL 2 M triethylammonium acetate (TEAA) buffer. The ammonia solution of the crude oligonucleotide was diluted (1:3) and applied directly to the column. All impurities and failure sequences were eluted with 3 mL of (1:20) ammonium hydroxide. Excess ammonium hydroxide was then removed with 2 mL water. Direct detritylation on the column occurred by passing 2 mL of 3% TFA through the cartridge. Excess acid is then removed with 2 mL water. The pure oligonucleotide is eluted with 1 ml 20% acetonitrile in water containing 0.5% ammonium hydroxide.

5.8.1.2 Desalting of Oligonucleotide

Oligonucleotides were desalted using either OPC or size exclusion G-25 Sephadex columns.

5.8.1.2.1 Oligonucleotide Purification Cartridges (OPC)

The OPC column was activated by flushing with 2 mL acetonitrile, followed by 2 mL 2 M TEAA buffer. The oligonucleotide sample was loaded onto the column followed by flushing the column with 3 mL of 0.1 M TEAA to remove the salt from the cartridge. The desalted oligonucleotide was then eluted using 1 mL 50% aqueous acetonitrile.

5.8.1.2.2 Size Exclusion G-25 Sephadex columns.

G-25 Sephadex columns were manually prepared through packing the Macro Spin column with activated G-25 Sephadex. The column was then equilibrated with water (x 4). Centrifuging at 800 x g for 3 min to remove the storage solution. The oligonucleotides

were then loaded onto the column. The desalted oligos were eluted by centrifugation at the same speed and time.

5.8.2 Quantification of Oligonucleotides

Oligonucleotide quantification was performed on an Agilent 8453 UV-Vis spectrometer. The oligonucleotides were diluted with water and transferred into a quartz cuvette and the absorbance was measured at λ_{max} = 260 nm. The millimolar extinction coefficient at λ_{max} = 260 nm for each oligo was obtained from the online oligonucleotide properties calculator. Modified oligonucleotides were attributed the extinction coefficient of the corresponding unmodified oligos. Using Beer's law, the concentration of the solutions and the absolute quantity of the oligos was calculated.

5.8.3 Synthesis of Modified Oligonucleotides

5.8.3.1 Modified Oligonucleotides Containing monomer (**134**)

A CPG-bound unmodified oligonucleotide was first synthesized on an ABI 391 DNA synthesizer using the phosphoramidite method on a 0.2 μmole scale. Incorporation of modified nucleoside **135** was achieved manually using H-phosphonate chemistry. Modified H-phosphonate **135** was coevaporated in anhydrous pyridine three times then dissolved in a mixture of acetonitrile: pyridine (1:1) to a final concentration of 0.1 M. This was transferred into a 1 mL syringe purged with argon. In another 1 mL purged syringe was placed a solution of 5 μL freshly distilled pivaloyl chloride in 305 μL acetonitrile: pyridine (1:1). Each syringe was then attached to either end of the CPG column containing the polymer-bound unmodified oligonucleotide. The activator was delivered first followed by the monomer and after repetitive mixing for 20 minutes, the reagents were then removed and the column was washed with 5 mL anhydrous

acetonitrile. The H-phosphonate linkage was oxidized to the corresponding more stable phosphodiester linkage by exposing the column to two 1 mL purged syringes, one containing 300 μL of 4% I_2 in pyridine/H_2O/THF (1:1:8) and the other contained 300 μL of THF/H_2O/triethylamine (8:1:1) for 20 min. The column was then washed with 10 mL anhydrous acetonitrile. Oligonucleotides were deprotected and cleaved from the solid support by treating the resin with 1 mL of concentrated ammonium hydroxide (28-30% in H_2O) for 15-18 hrs at 55 °C, followed by purification of oligonucleotides using OPC to afford the 5'-vicinal diol oligonucleotides (**138-143**).

5.8.3.2 Modified Oligonucleotides **144**

To a solution of oligonucleotides containing either one of (**138-143**) (10 nmol) in 100 μL H_2O was added 13.58 μL of 0.2 M sodium periodate ($NaIO_4$) at 0 ºC. The reaction mixture was stirred for 3 hours at this temperature. The reaction was then quenched at 0 ºC by addition of methionine (0.2 M, 19.56 μL) and stirred for an additional 30 minutes. The oligonucleotides were desalted using a G-25 Sephadex column as described above. The oligomers were quantified as described in section 5.8.2. The purity of the 5'-aldehyde oligos was determined using analytical ion-exchange (IEX) and reversed-phase (RP) HPLC.

5.9 Stability of Modified Oligonucleotides **144**

Oligonucleotides **144** (1 nmol) were incubated in (500 μL) of 100 mM phosphate buffer pH = 7.4 at 37 ºC. Aliquots of the reaction mixture of equal amounts were removed at specific time intervals and injected onto the IEX chromatography. Decomposition of the 5'-aldehyde to the 5'-phosphorylated ODNs was monitored to determine the half-life of the lesion.

5.10 Stability of 3',4'-Didehydro-2',3'-dideoxy-5'-oxothymidine (**66**) at pH = 7.4 at 37 ºC

Modified nucleoside **66** (1008 nmol) was incubated in 1000 μL of 100 mM phosphate buffer pH = 7.4 at 37 ºC. Aliquots of the reaction mixture of equal amounts were removed at specific times and analyzed by analytical RP-HPLC. Decomposition of 3',4'-Didehydro-2',3'-dideoxy-5'-oxothymidine was monitored to determine the half-life of the lesion.

5.11 Stability and Reactivity of **66** in Presence of GSH

Modified nucleoside **66** (4000 nmol) and 6 mM GSH were incubated in 1000 μL of 100 mM phosphate buffer pH = 7.4 at 37 ºC. Aliquots of the reaction mixture of equal amounts were removed at specific times and analyzed by analytical RP HPLC.

5.12 Reactivity of 3',4'-Didehydro-2',3'-dideoxy-5'-oxothymidine (**66**)

5.12.1 Reactivity of **66** in Presence of deoxyadenosine

Modified nucleoside **66** (12000 nmol) and deoxyadenosine (18000 nmol) were incubated in 1000 μL of 100 mM phosphate buffer pH = 7.4 at 37 ºC. Aliquots of the reaction mixture of equal amounts were removed at specific times and analyzed by analytical RP HPLC.

5.12.2 Reactivity of **66** in Presence of Oligonucleotides Containing dA

Modified nucleoside **66** (1008 nmol) was incubated in presence of (20 nmol) of unmodified oligonucleotide (TCT ATC TAT CT) in 1000 μL of 100 mM phosphate buffer pH = 7.4 at 37 ºC. Aliquots of the reaction mixture of equal amounts were removed at specific times were analyzed by analytical RP-HPLC.

5.13 Reactivity of Furfural

5.13.1 Reactivity of Furfural in Presence of dA at pH = 7.4 and 37 ºC

Furfural (4000 nmol) and deoxyadenosine (8000 nmol) were incubated in 1000 µL of 100 mM phosphate buffer pH = 7.4 at 37 ºC. Aliquots of the reaction mixture of equal amounts were removed at specific times and analyzed by analytical RP HPLC.

5.13.2 Reactivity of Furfural in Presence of Excess dA at pH = 2 and 37 ºC

Furfural (4000 nmol) and deoxyadenosine (8000 nmol) were incubated in 1000 µL of 100 mM phosphate buffer pH= 2 at 37 ºC. Aliquots of the reaction mixture of equal amounts were removed at specific times and analyzed by analytical RP HPLC.

5.13.3 Reactivity of Excess Furfural in Presence of dA at pH = 2 and 37 ºC

Furfural (8000 nmol) and deoxyadenosine (4000 nmol) were incubated in 1000 µL of 100 mM phosphate buffer pH = 2 at 37 ºC. Aliquots of the reaction mixture of equal amounts were removed at specific times and analyzed by analytical RP HPLC.

APPENDIX A

CHAPTER TWO

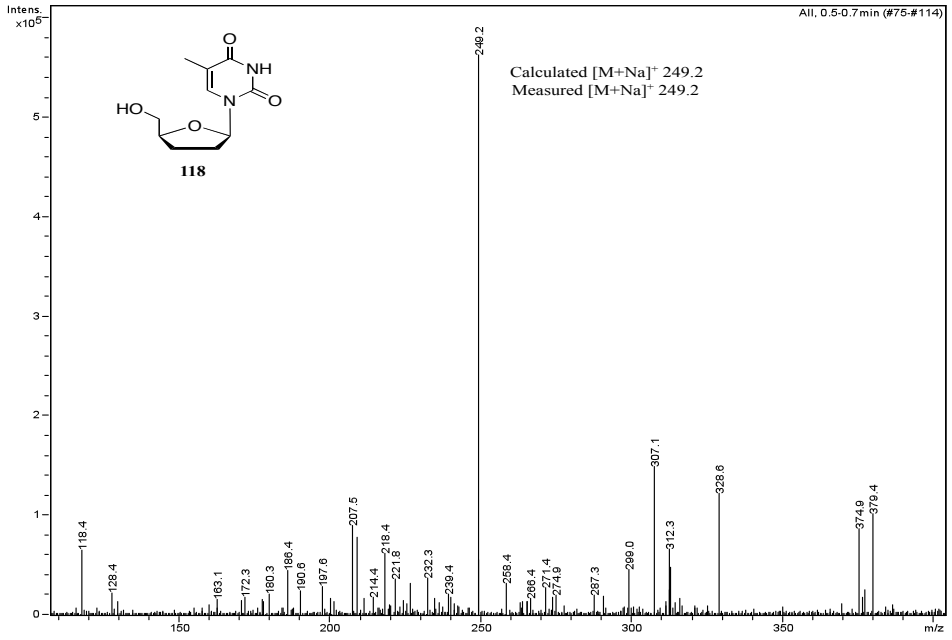

Figure 1: ESI-MS analysis of **118** from photolysis of **103** in presence of excess *tri-n*butyltin hydride under anaerobic conditions in 1:1 acetonitrile/water for one hour at 15 ºC

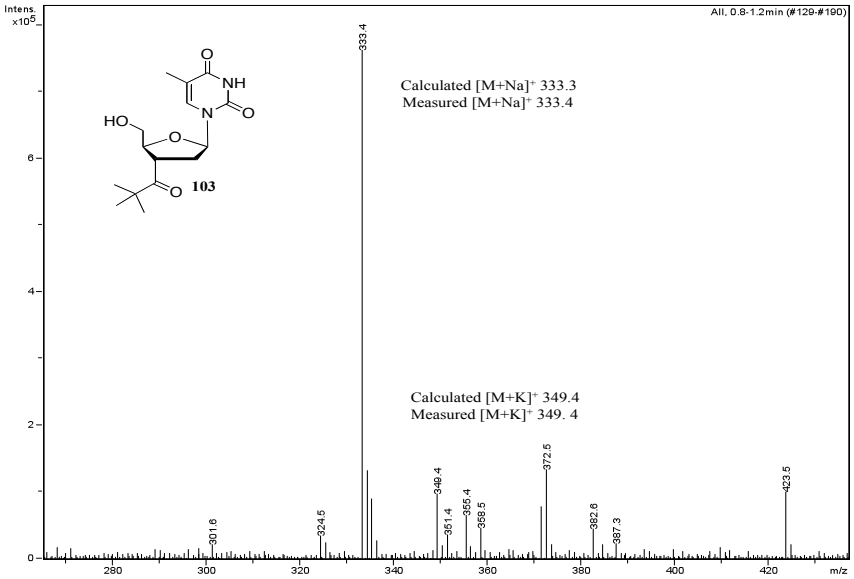

Figure 2: ESI-MS analysis of **103** from photolysis of **103** in presence of excess *tri-n*butyltin hydride under anaerobic conditions in 1:1 acetonitrile/water for one hour at 15 ºC

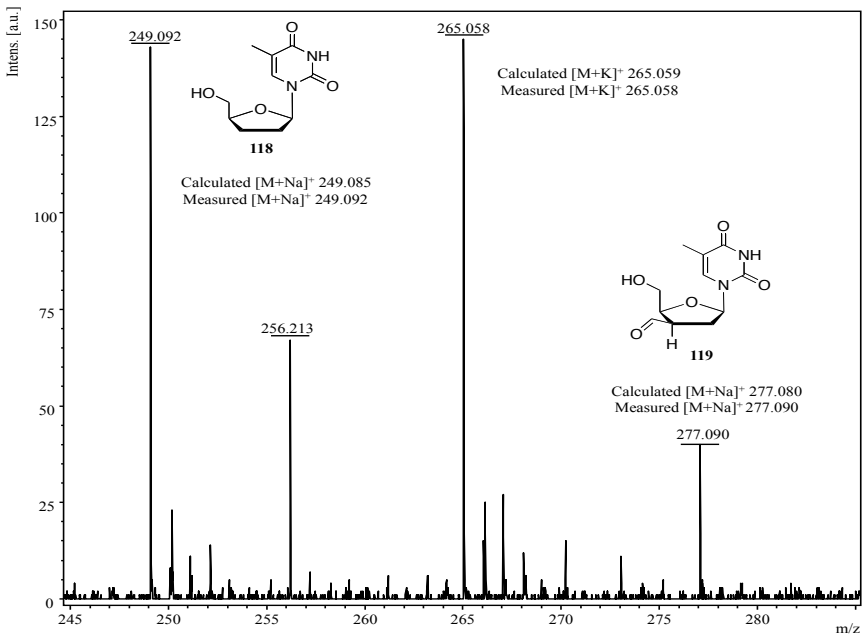

Figure 3: MALDI-ToF mass spectrum analysis of compounds eluted at 13.580 and 13.740 min from photolysis of **101** in presence of excess *tri-n*butyltin hydride under anaerobic conditions in 1:1 acetonitrile/water for one hour at 15 ºC

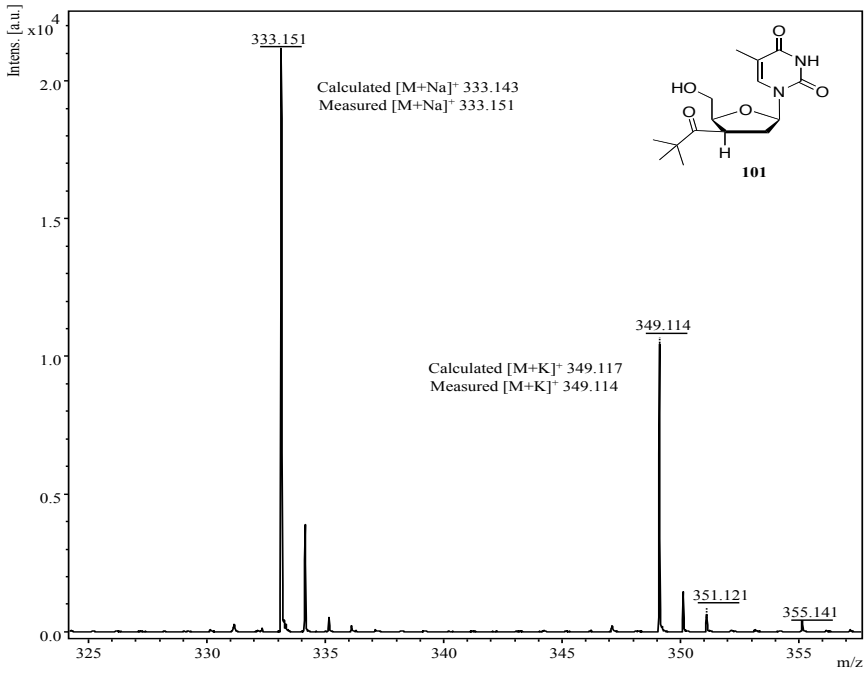

Figure 4: MALDI-ToF mass spectrum analysis of compound eluted at 20.533 min from photolysis of **101** in presence of excess *tri-n*butyltin hydride under anaerobic conditions in 1:1 acetonitrile/water for one hour at 15 ºC

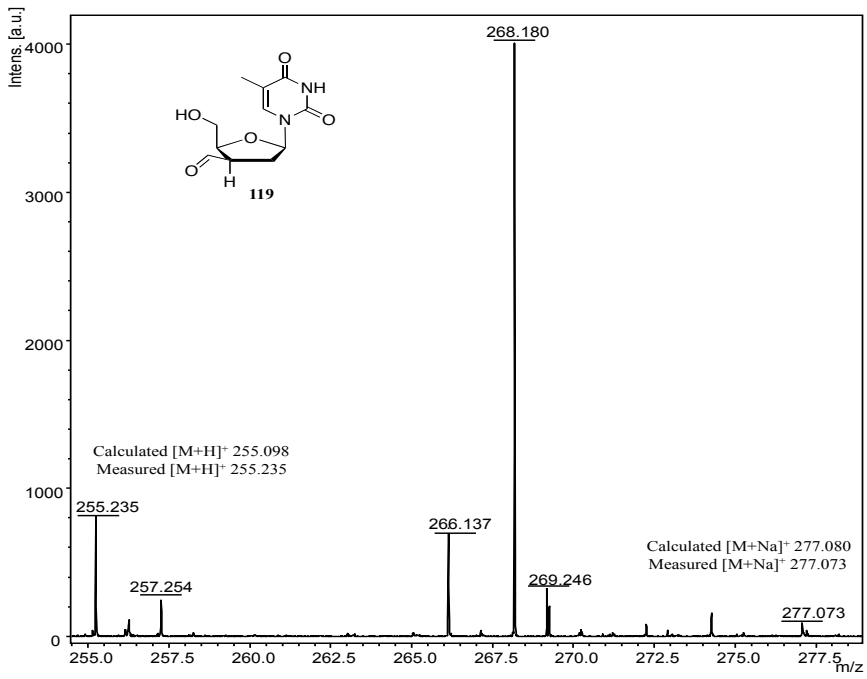

Figure 5: MALDI-ToF mass spectrum analysis of compound eluted at 13.887 min from photolysis of **101** in presence of excess *tri-n*butyltin hydride under anaerobic conditions in acetonitrile for one hour at 15 ºC

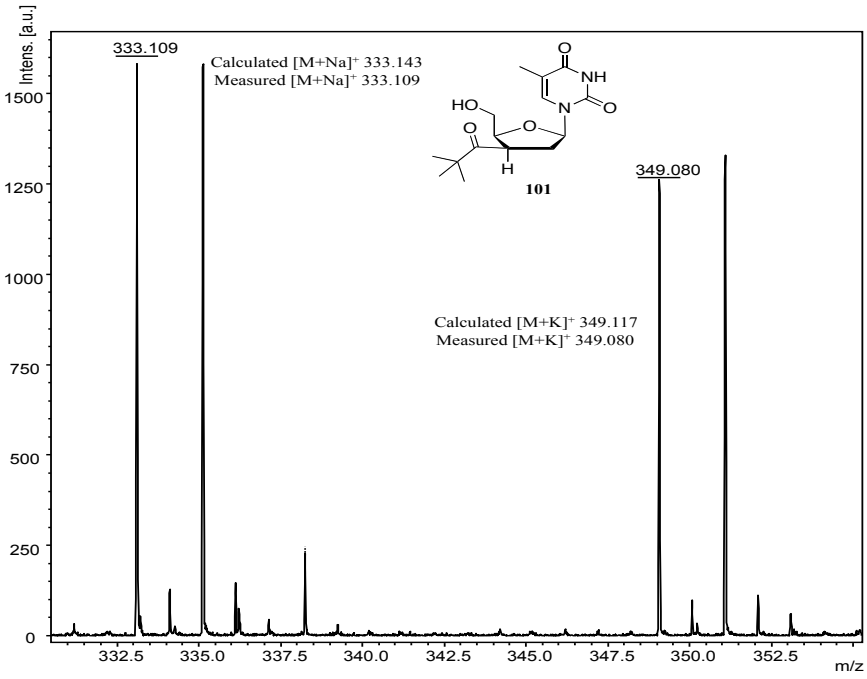

Figure 6: MALDI-ToF mass spectrum analysis of compound eluted at 20.593 min from photolysis of **101** in presence of excess *tri-n*butyltin hydride under anaerobic conditions in acetonitrile for one hour at 15 ºC

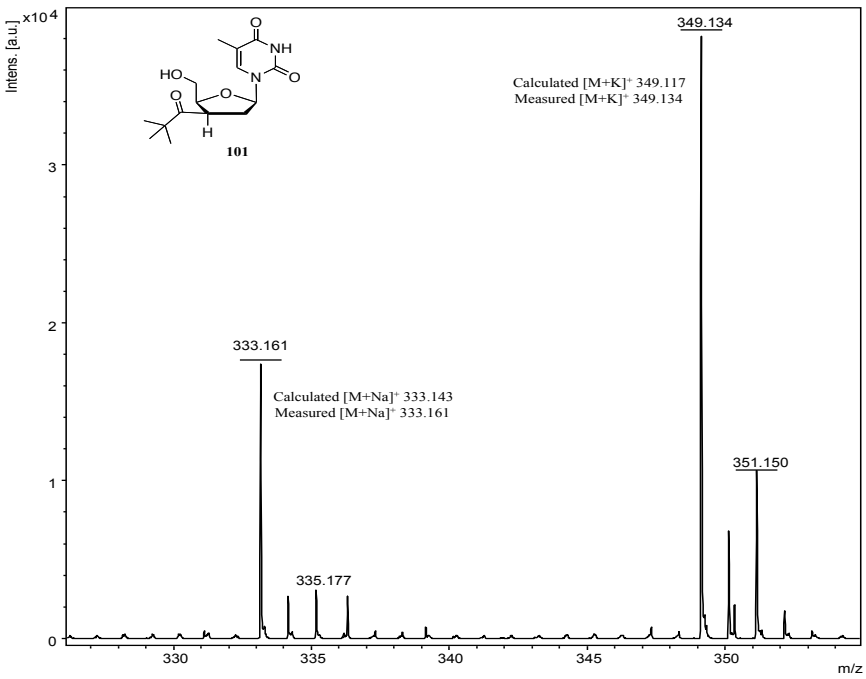

Figure 7: MALDI-ToF mass spectrum analysis of compound eluted at 20.587 from photolysis of **101** in presence of excess *tri-n*butyltin hydride under anaerobic conditions in water for one hour at 15 ºC

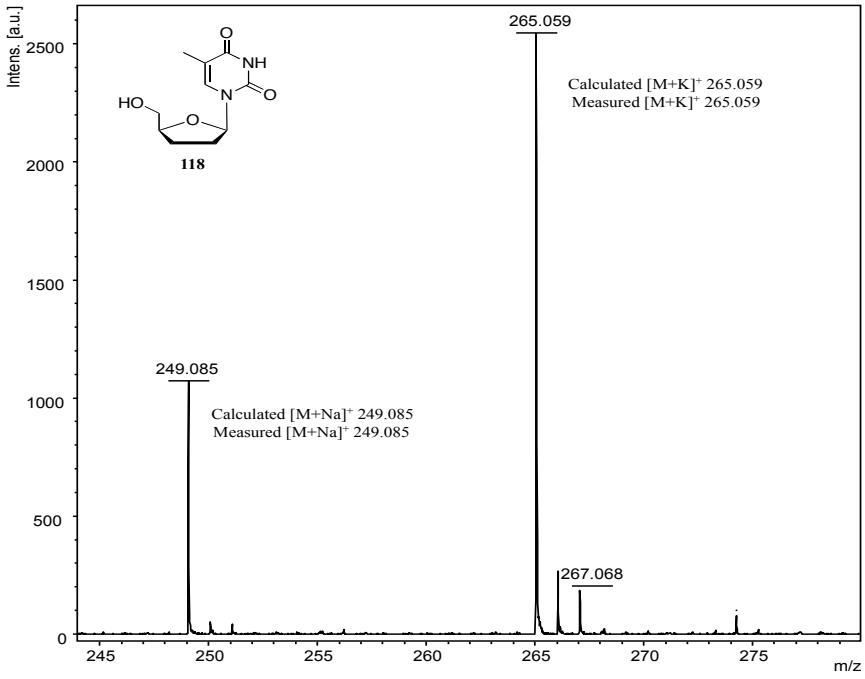

Figure 8: MALDI-ToF mass spectrum analysis of peak 13.740 from photolysis of **103** in presence of 6 mM GSH under anaerobic conditions in 1:1 acetonitrile/water for one hour at 15 ºC

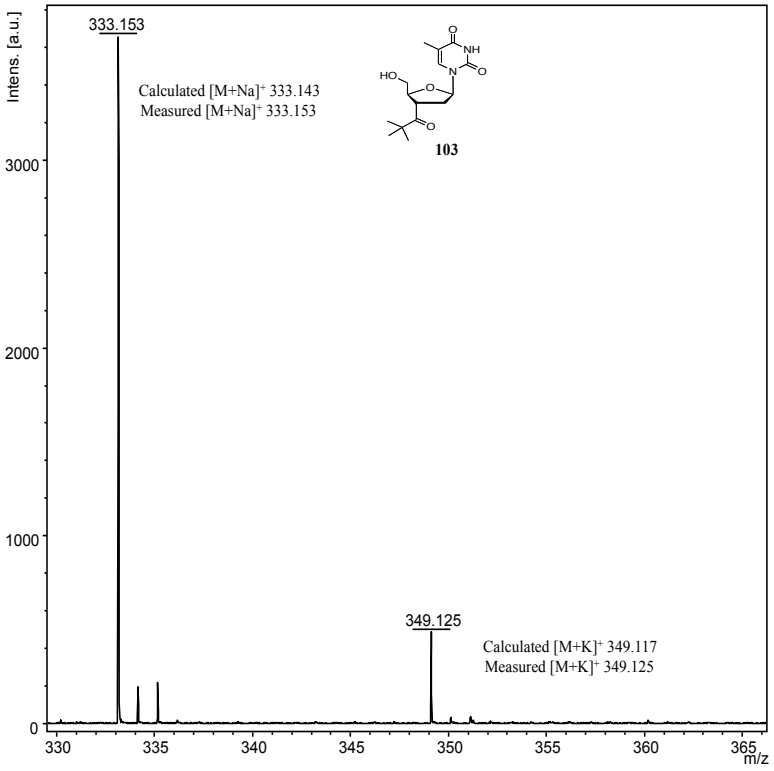

Figure 9: MALDI-ToF mass spectrum analysis of peak 20.327 from photolysis of **103** in presence of 6 mM GSH under anaerobic conditions in 1:1 acetonitrile/water for one hour at 15 ºC

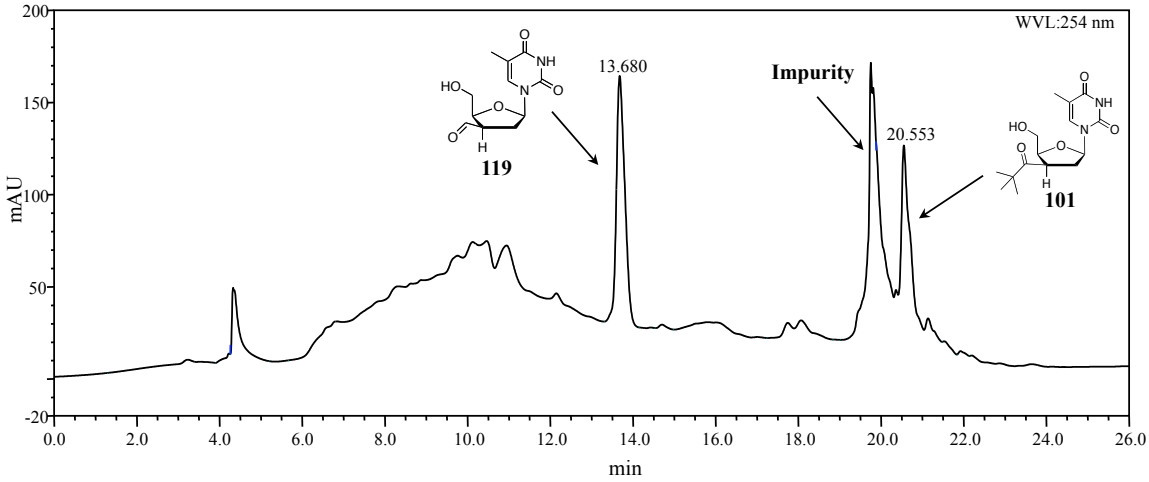

Figure 10: Reversed-phase HPLC chromatogram of spiking the photolysate sample with aldehyde **119** resulted in enhancement of peak at 13.680 min from photolysis of **101** in presence of 6 mM GSH under anaerobic conditions in 1:1 acetonitrile/water for one hour at 15 ºC

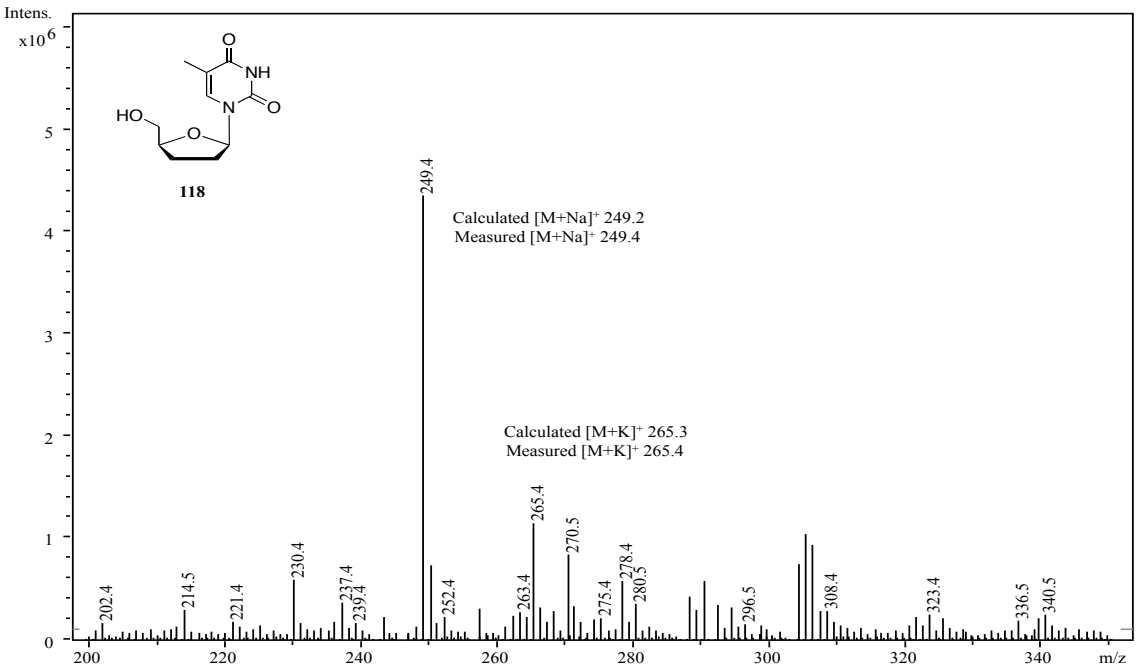

Figure 11: ESI-MS analysis of **118** from photolysis of **103** in absence of hydrogen atom donor under anaerobic conditions in 1:1 acetonitrile/water for one hour at 15 ºC

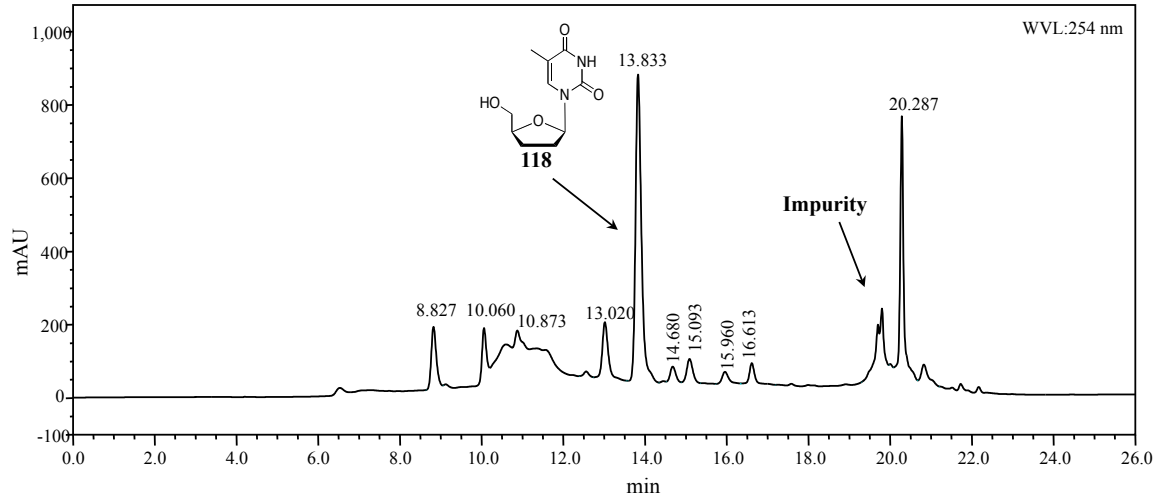

Figure 12: Reversed-phase HPLC chromatogram of spiking the photolysate sample with reduction product **118** resulted in enhancement of peak at 13.833 min from photolysis of **103** in presence of 6 mM GSH under anaerobic conditions in 1:1 acetonitrile/water for one hour at 15 ºC

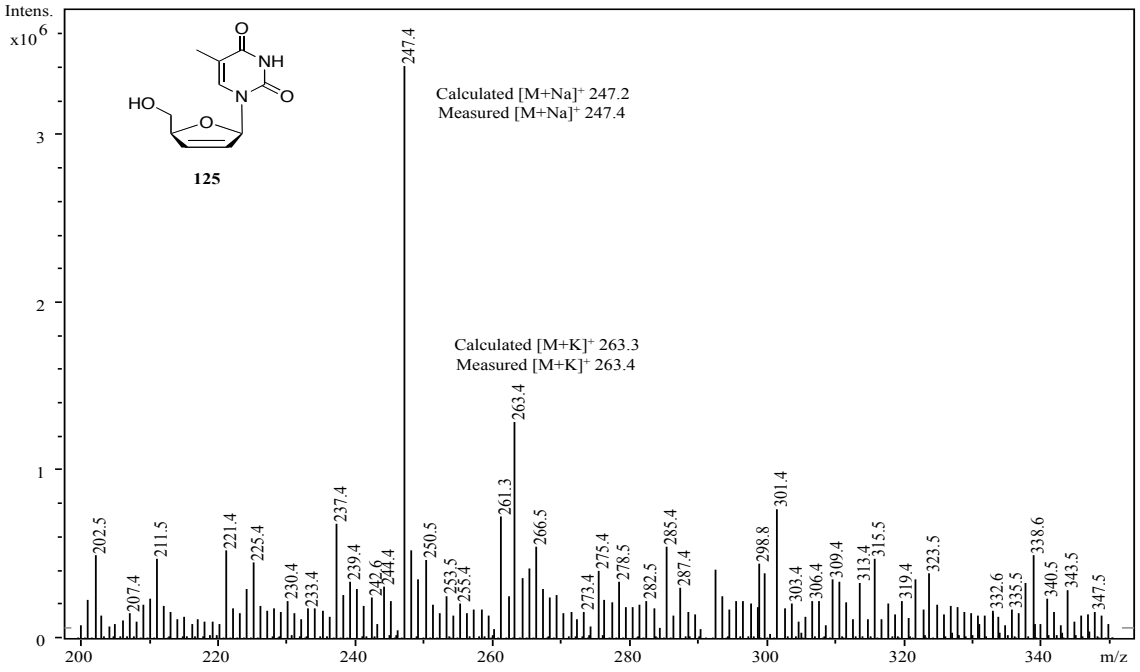

Figure 13: ESI-MS analysis of **125** from photolysis of **103** in absence of hydrogen atom donor under anaerobic conditions in 1:1 acetonitrile/water for one hour at 15 ºC

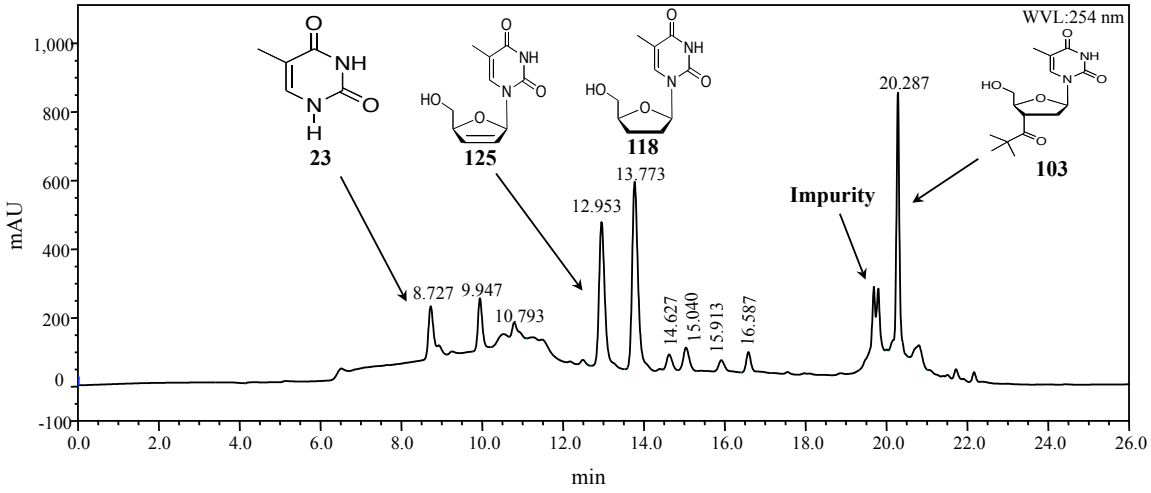

Figure 14: Reversed-phase HPLC chromatogram of spiking the photolysate sample with 2',3'-didehydro-2',3'-dideoxythymidine (**125**) resulted in enhancement of peak at 12.953 min from photolysis of **103** in presence of 6 mM GSH under anaerobic conditions in 1:1 acetonitrile/water for one hour at 15 ºC.

APPENDIX B

CHAPTER THREE

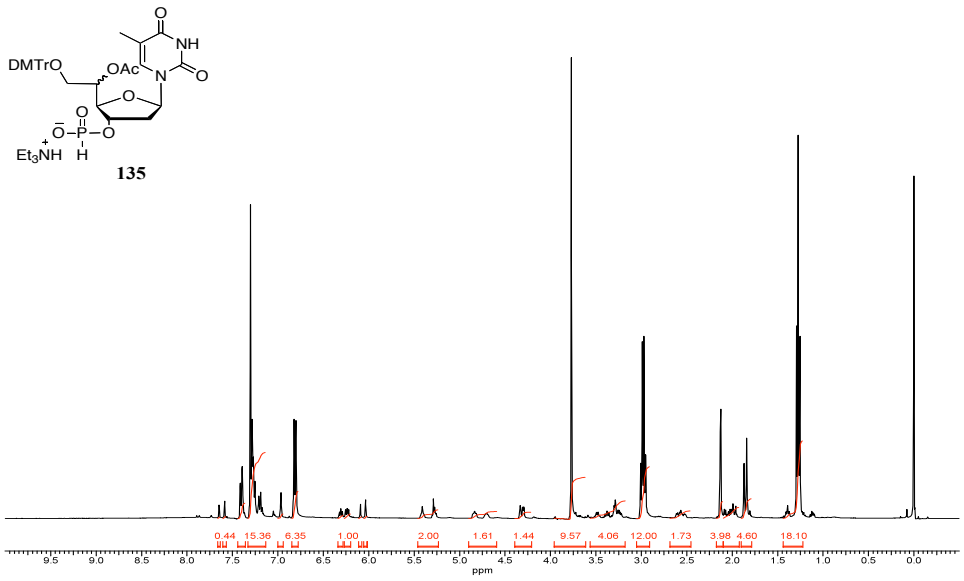

Figure 1: ^{1}H-NMR of compound **135** in $CDCl_3$ (400 MHZ)

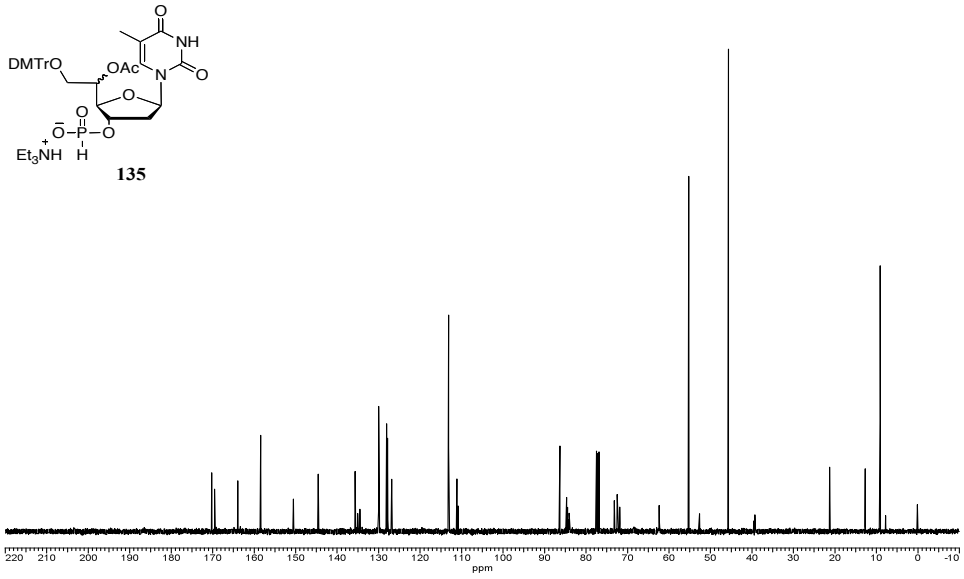

Figure 2: ^{13}C-NMR of compound **135** in $CDCl_3$ (100 MHZ)

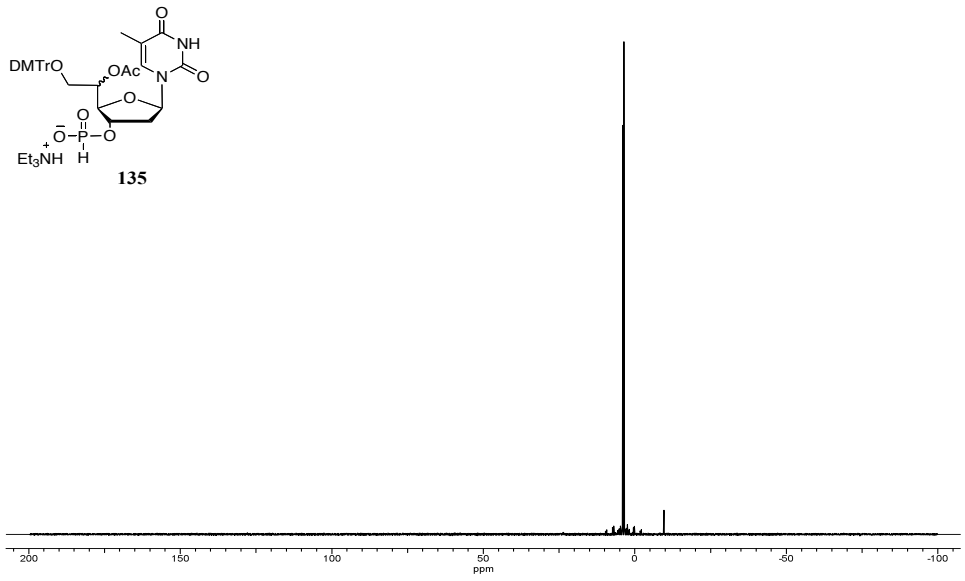

Figure 3: ^{31}P-NMR of compound **135** in $CDCl_3$ (400 MHZ)

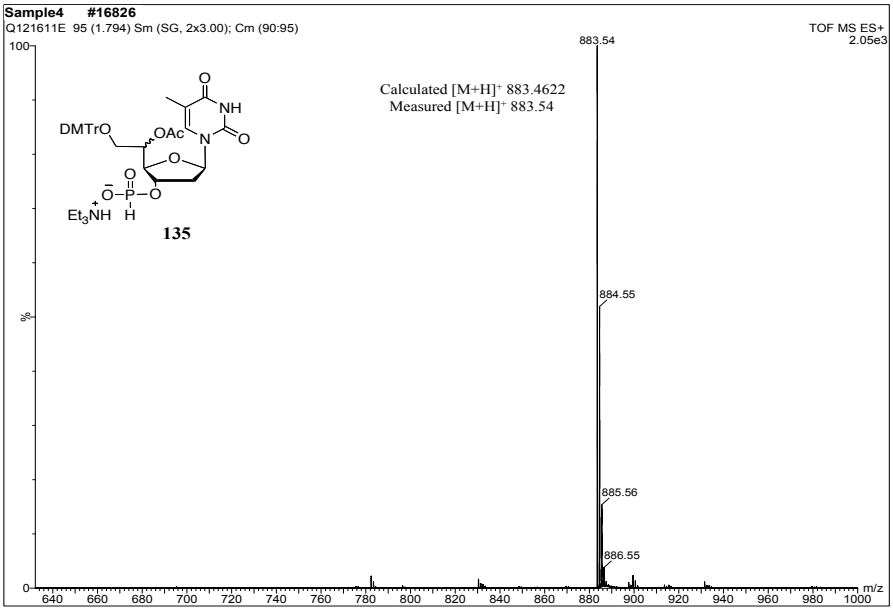

Figure 4: HRMS of compound **135**

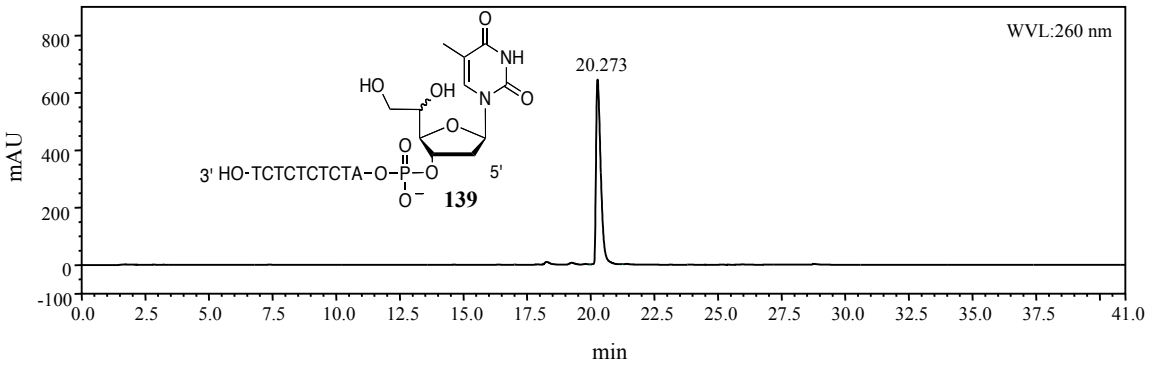

Figure 5: Ion-exchange HPLC chromatogram of modified oligonucleotide **139**

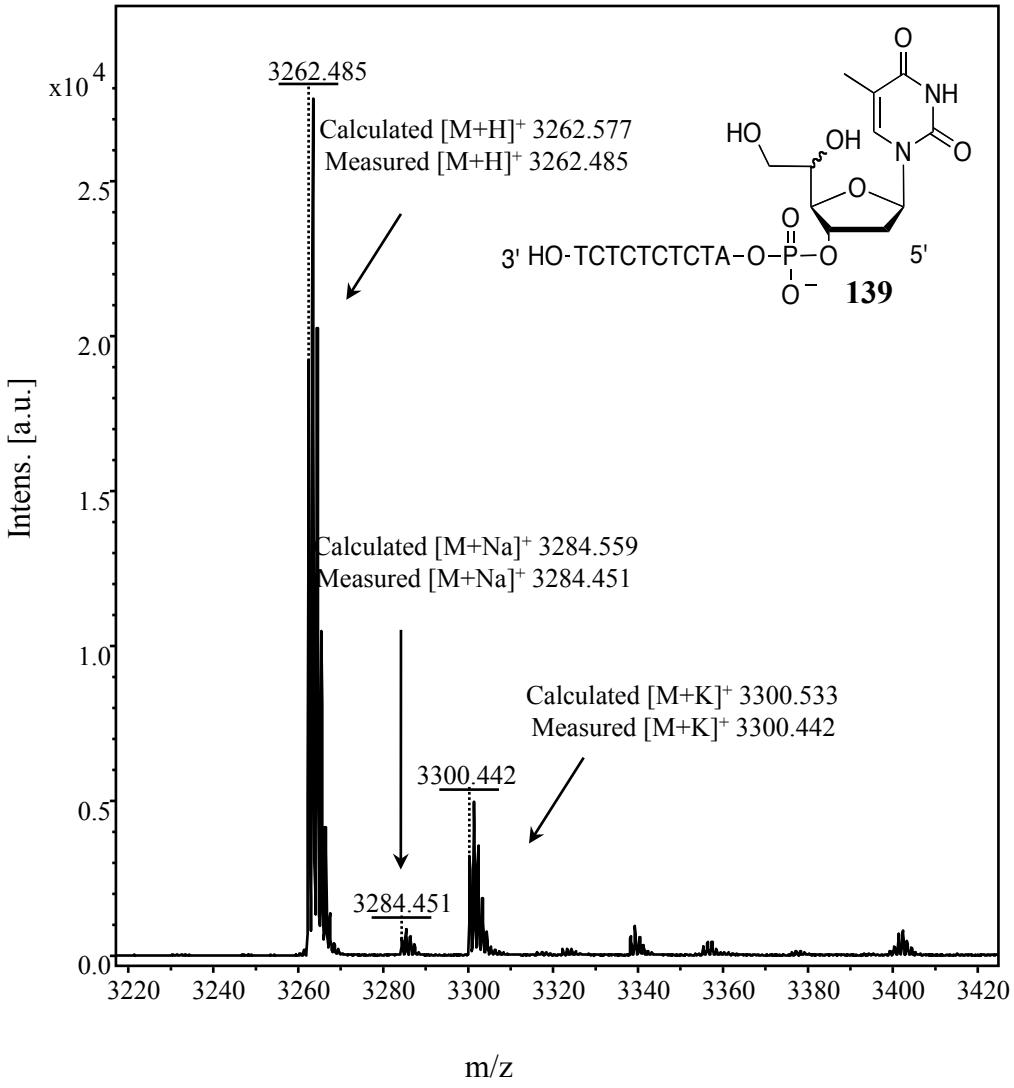

Figure 6: MALDI-ToF MS of modified oligonucleotide **139**

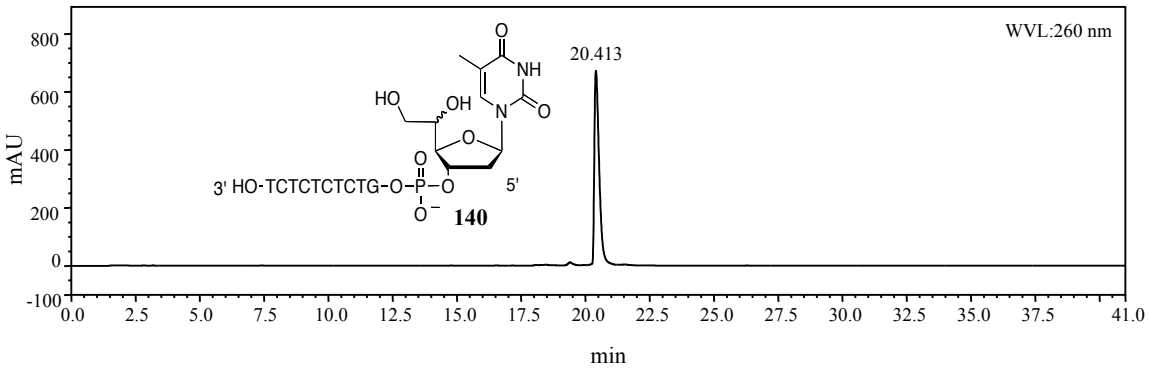

Figure 7: Ion-exchange HPLC chromatogram of modified oligonucleotide **140**

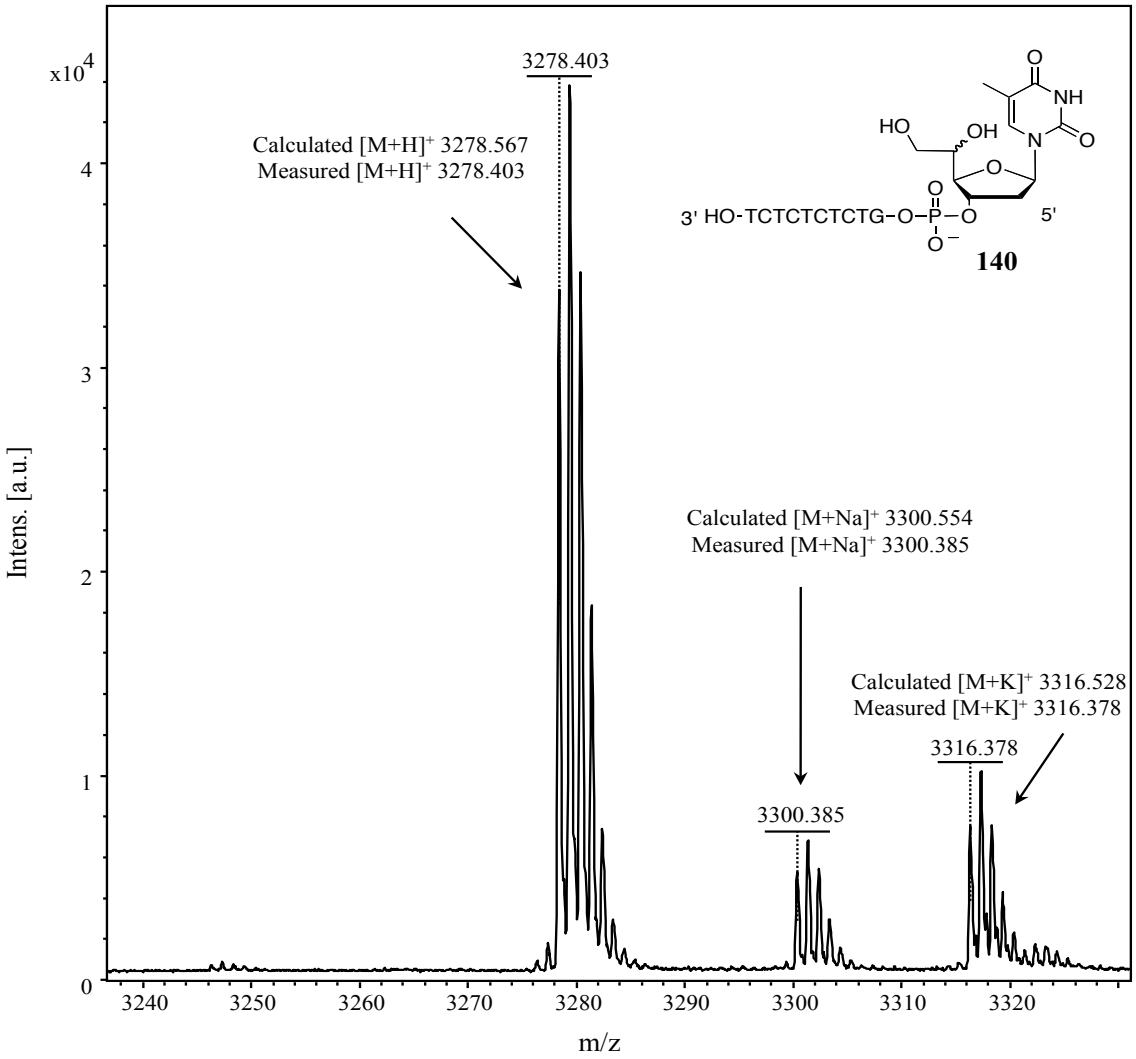

Figure 8: MALDI-ToF MS of modified oligonucleotide **140**

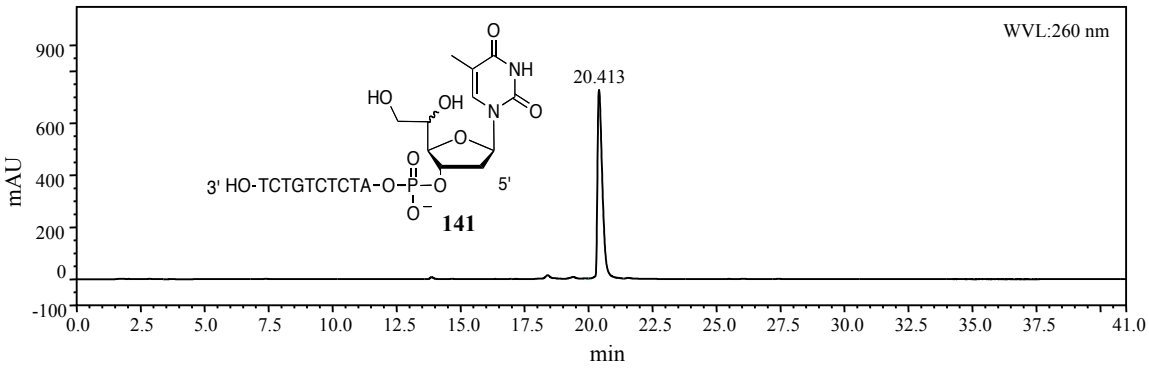

Figure 9: Ion-exchange HPLC chromatogram of modified oligonucleotide **141**

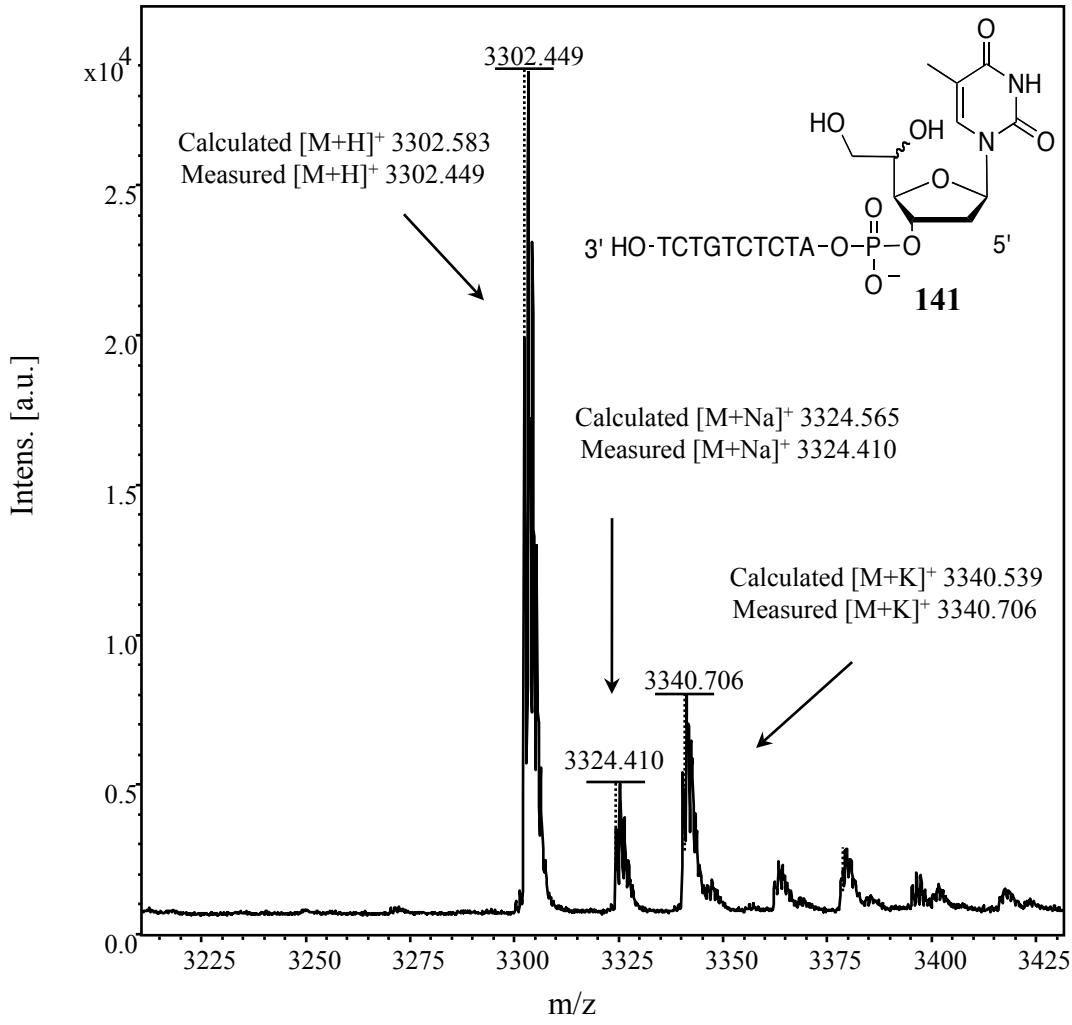

Figure 10: MALDI-ToF MS of modified oligonucleotide **141**

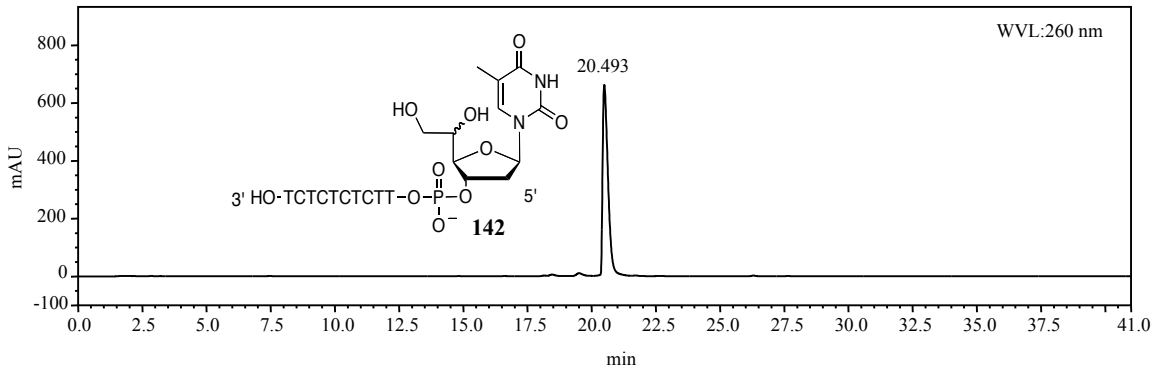

Figure 11: Ion-exchange HPLC chromatogram of modified oligonucleotide **142**

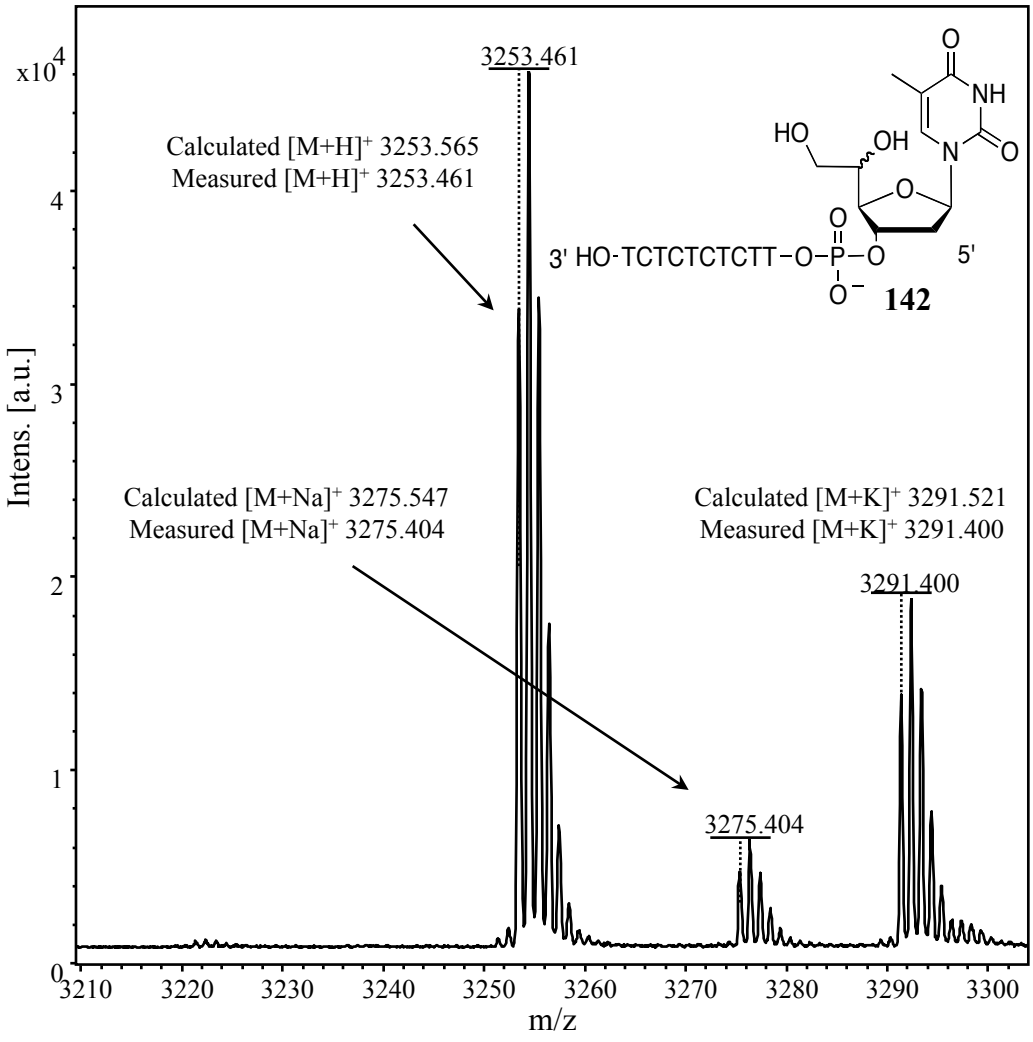

Figure 12: MALDI-ToF MS of modified oligonucleotide **142**

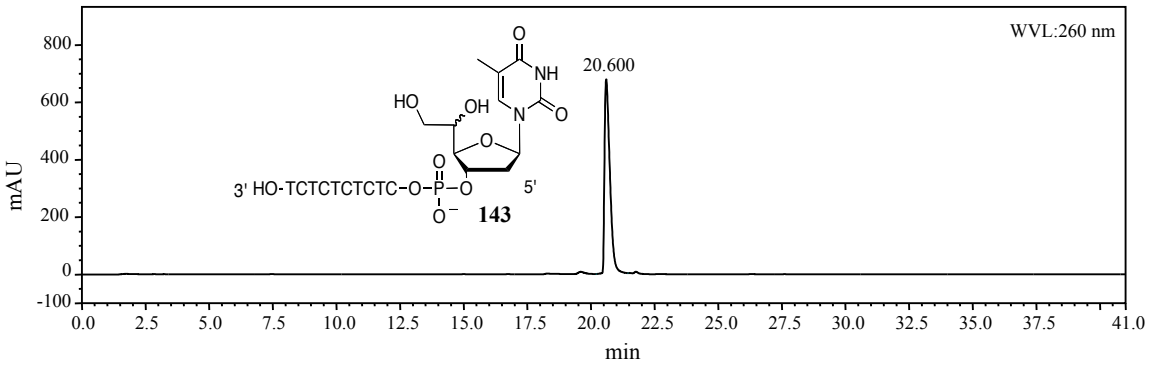

Figure 13: Ion-exchange HPLC chromatogram of modified oligonucleotide **143**

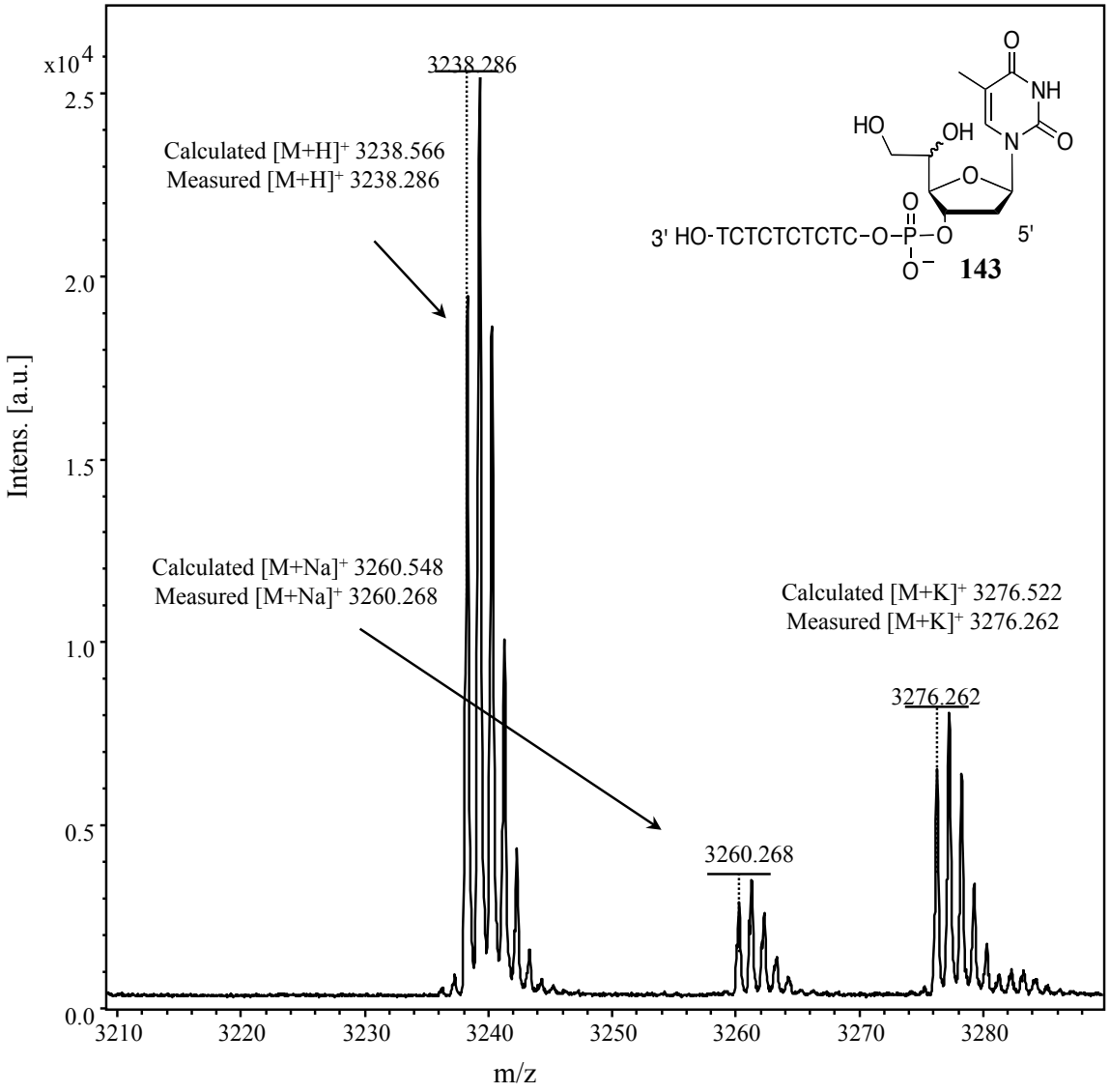

Figure 14: MALDI-ToF MS of modified oligonucleotide **143**

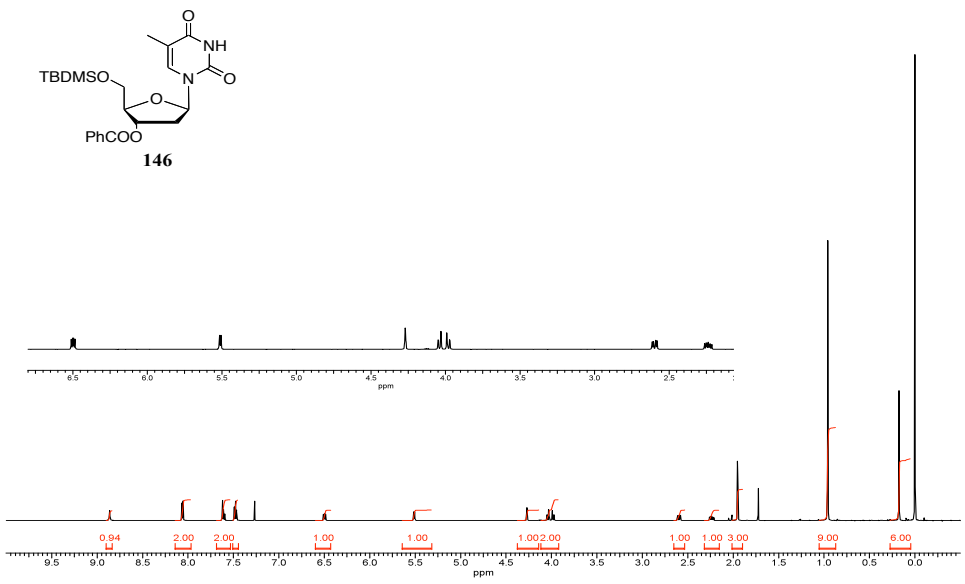

Figure 15: ^{1}H-NMR of compound **146** in $CDCl_3$ (600 MHZ)

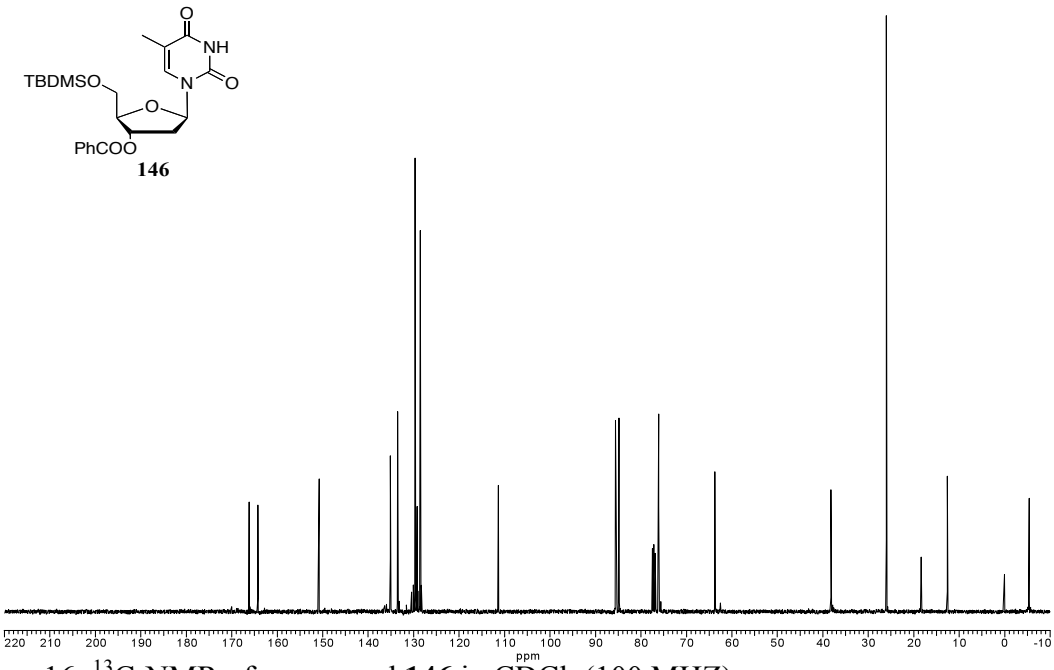

Figure 16: ^{13}C-NMR of compound **146** in $CDCl_3$ (100 MHZ)

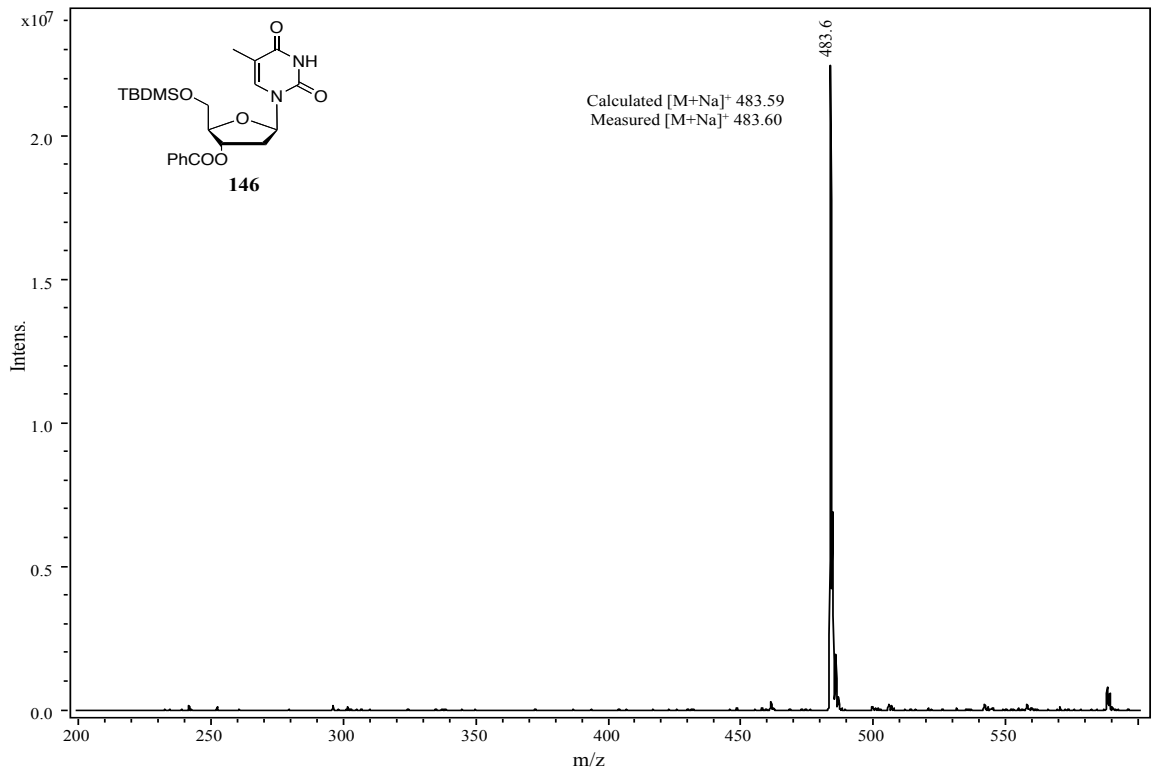

Figure 17: ESI-MS of compound **146**

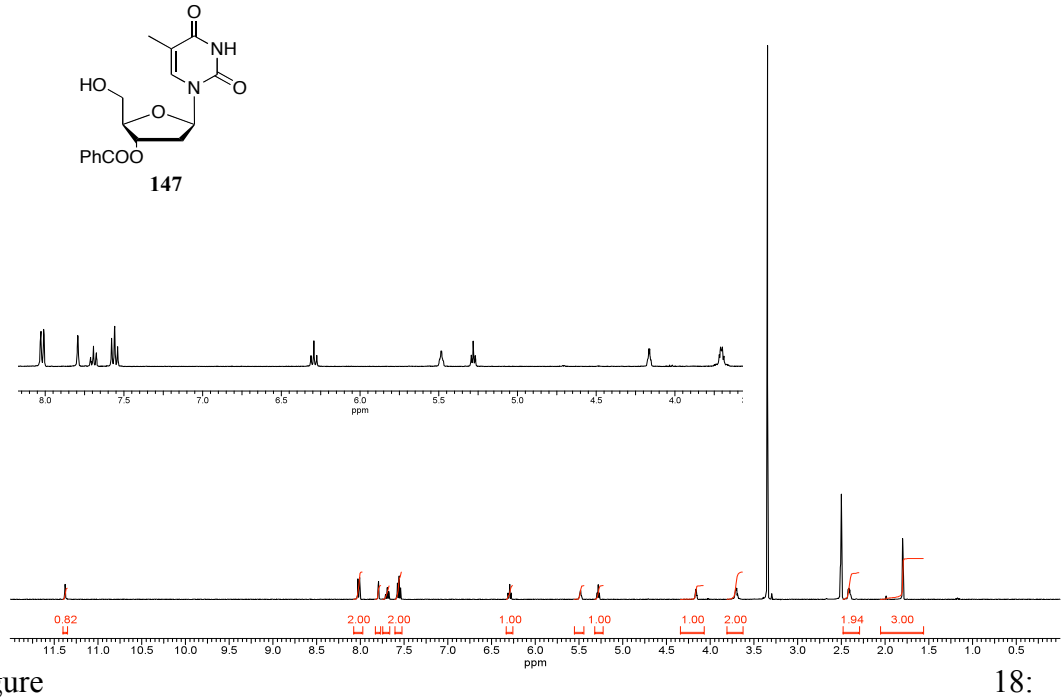

Figure 18: ^{1}H-NMR of compound **147** in DMSO (400 MHZ)

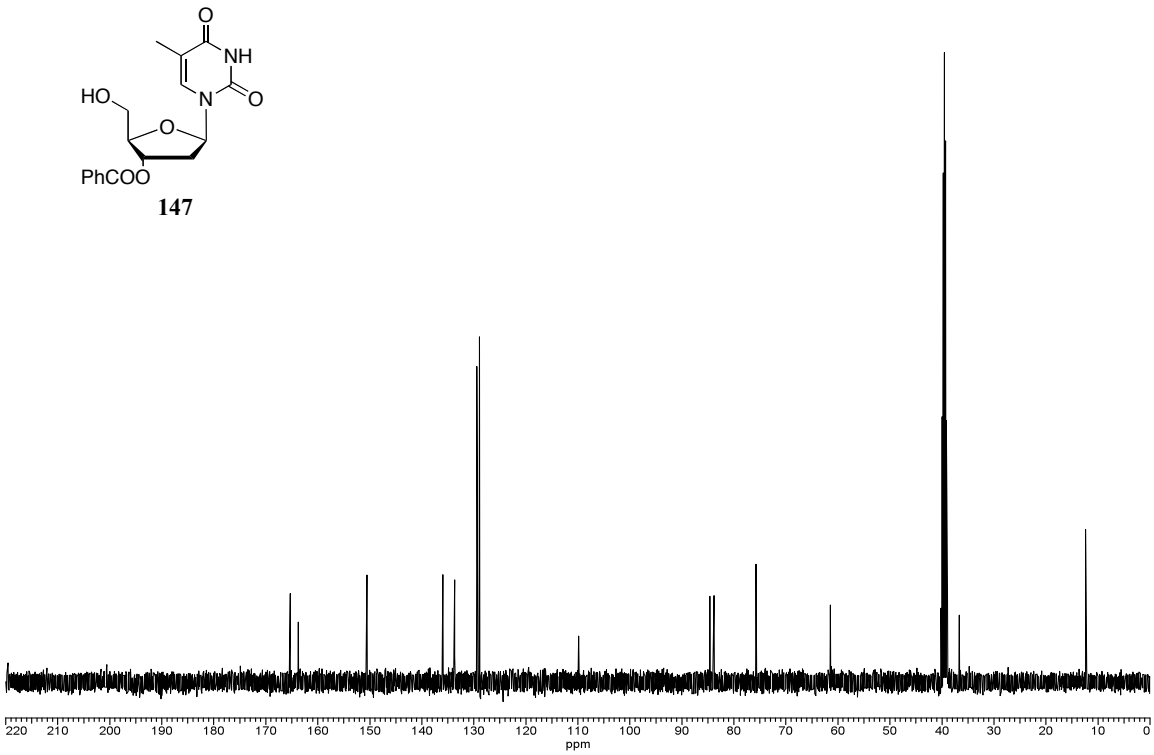

Figure 19: ^{13}C-NMR of compound **147** in DMSO (100 MHZ)

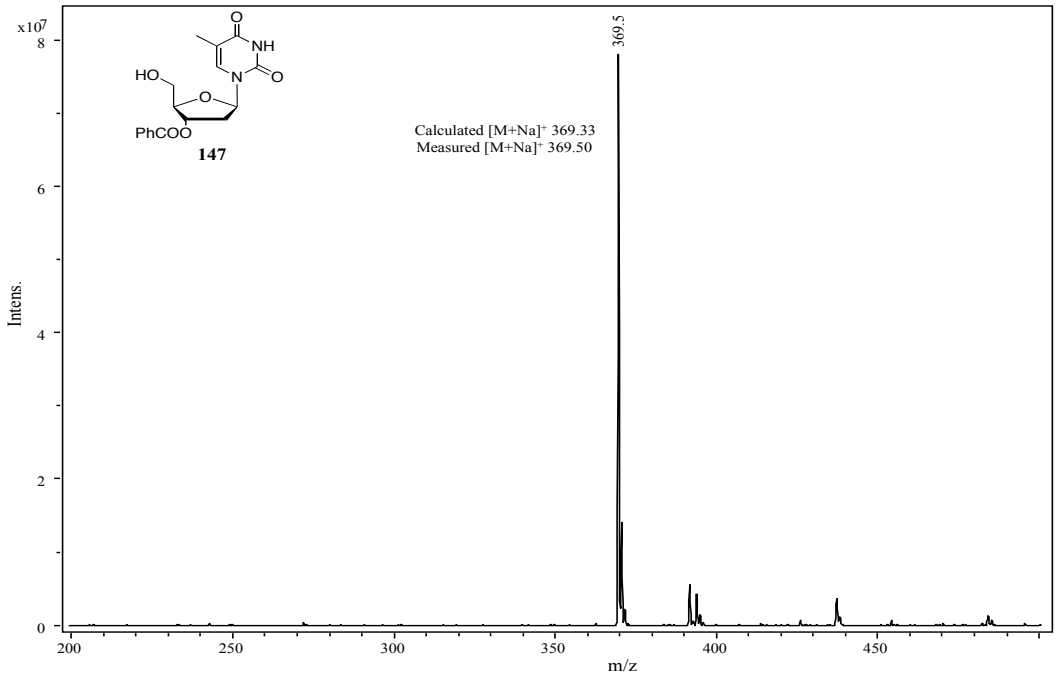

Figure 20: ESI-MS of compound **147**

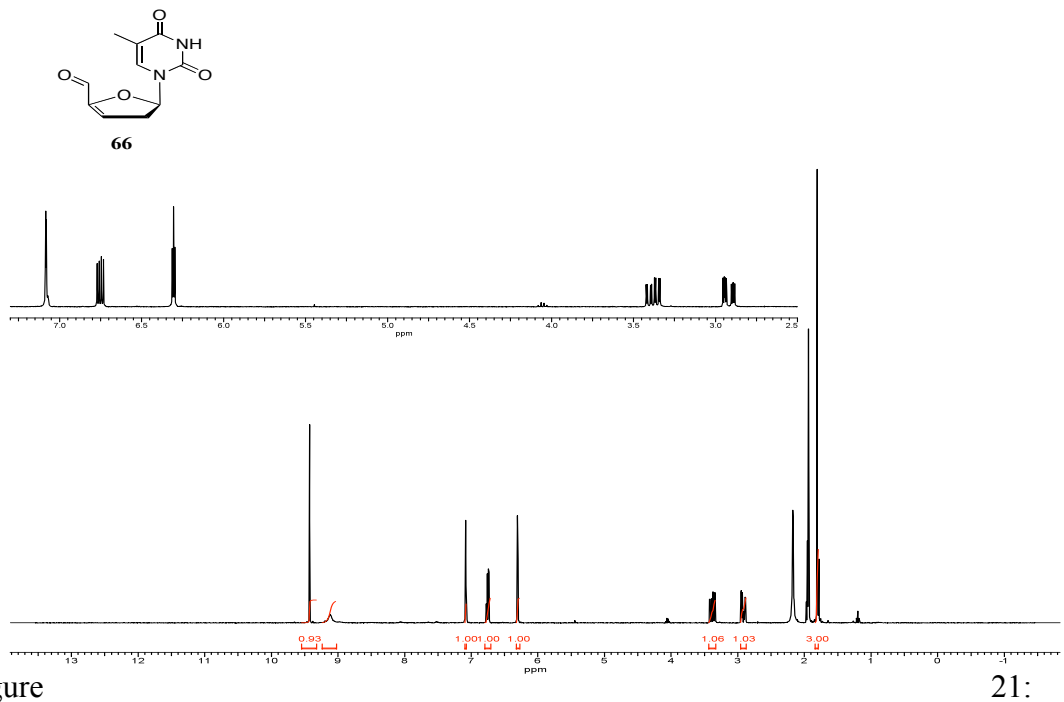

Figure 21: ^{1}H-NMR of compound **66** in CD_3CN (400 MHZ)

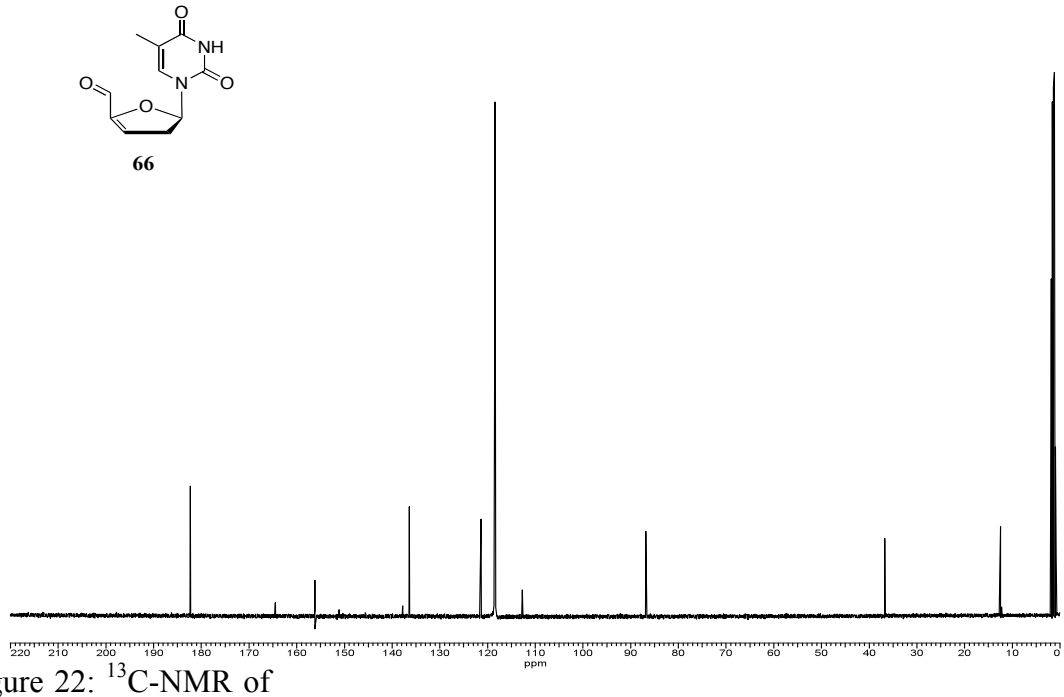

Figure 22: ^{13}C-NMR of compound **66** in CD_3CN (100 MHZ)

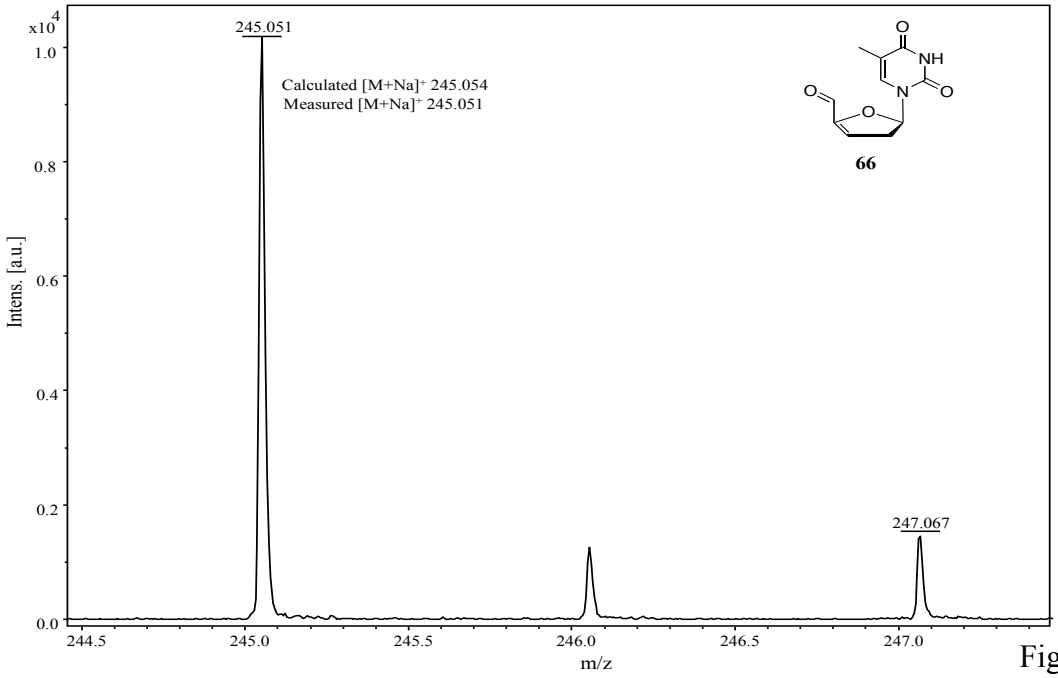

Figure 23: MALDI-ToF MS of compound **66**

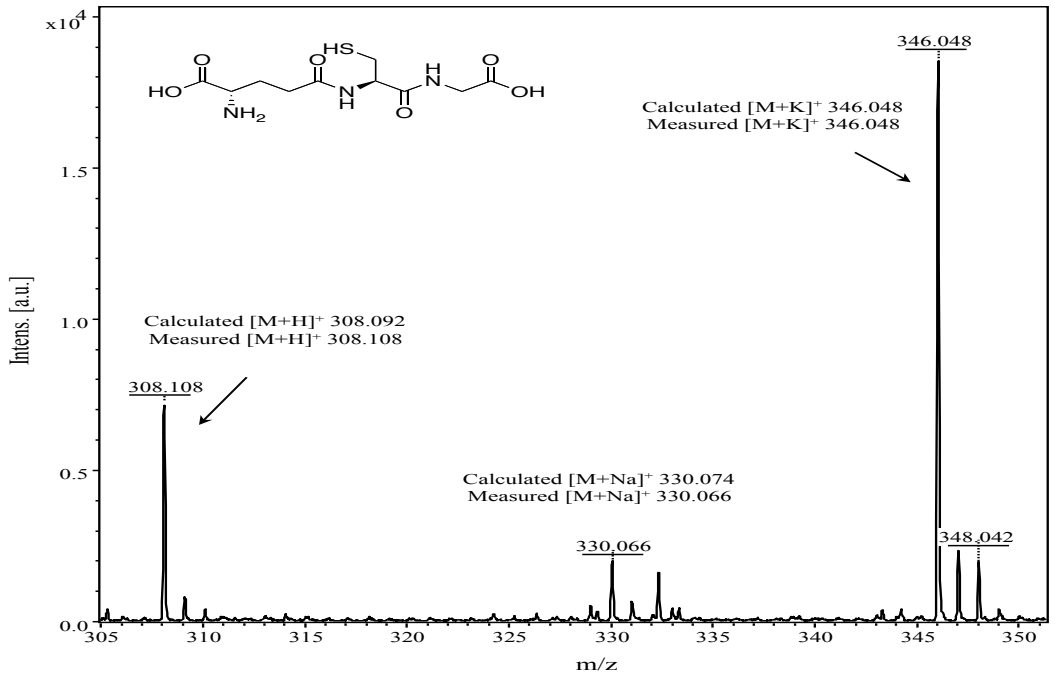

Figure 24: MALDI-ToF MS of compound eluted at 3.320 min after incubation of **66** in 100 mM phosphate buffer pH = 7.4 at 37 °C in presence of 6 mM GSH after 30 minutes

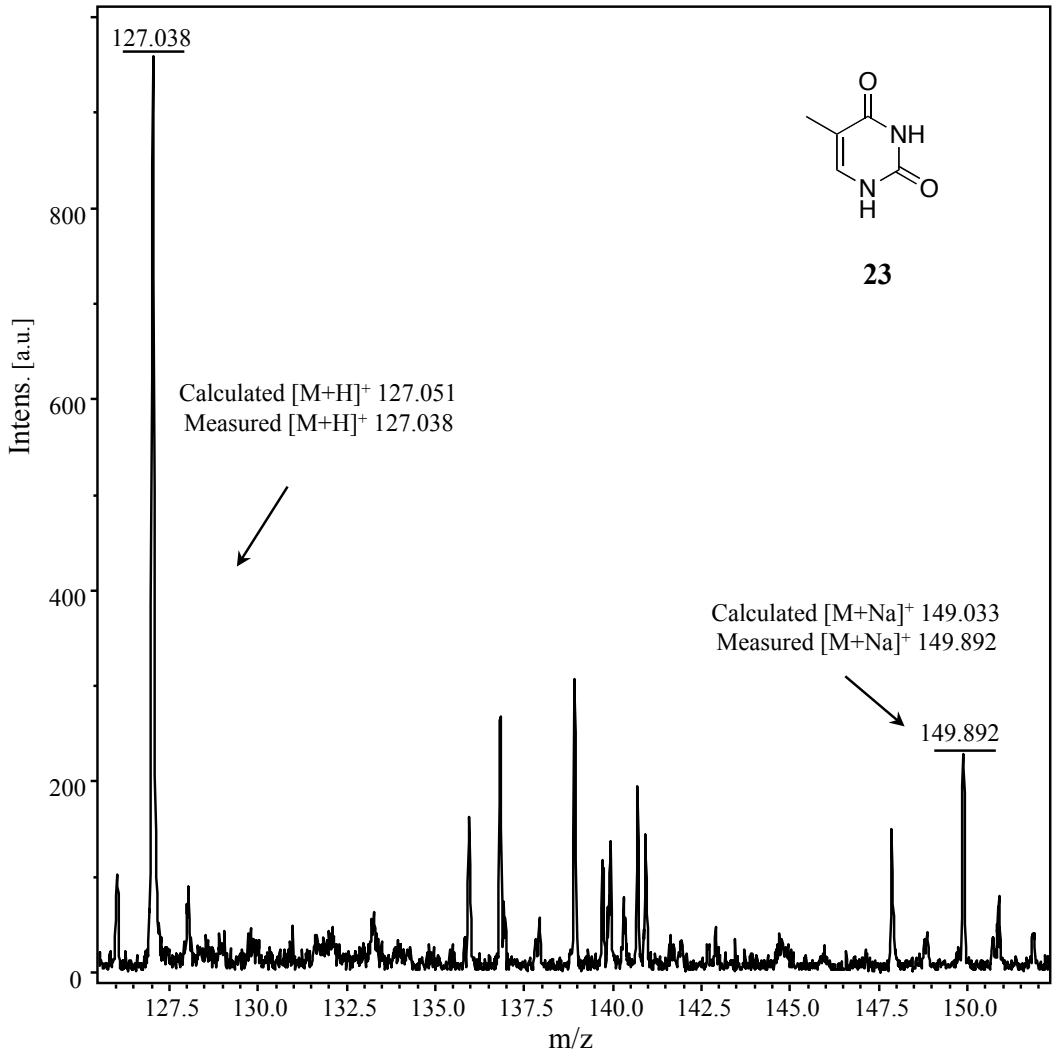

Figure 25: MALDI-ToF MS of compound eluted at 5.380 min after incubation of **66** in 100 mM phosphate buffer pH = 7.4 at 37 °C in presence of 6 mM GSH after 30 minutes

APPENDIX C

CHAPTER TWO

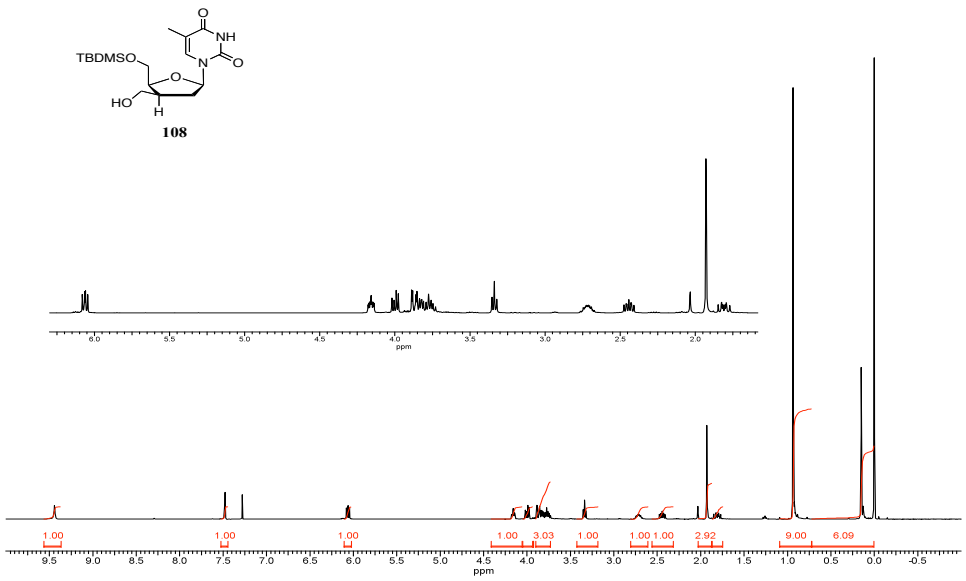

Figure 1: ^{1}H NMR spectrum of **108** in $CDCl_3$ (400 MHz)

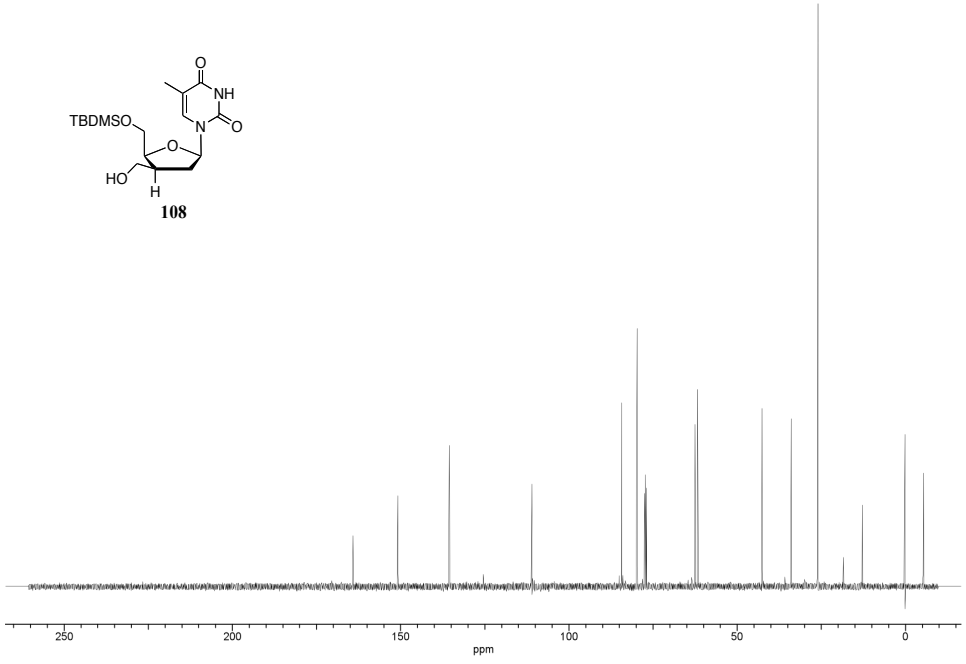

Figure 2: ^{13}C NMR spectrum of **108** in $CDCl_3$ (100 MHz)

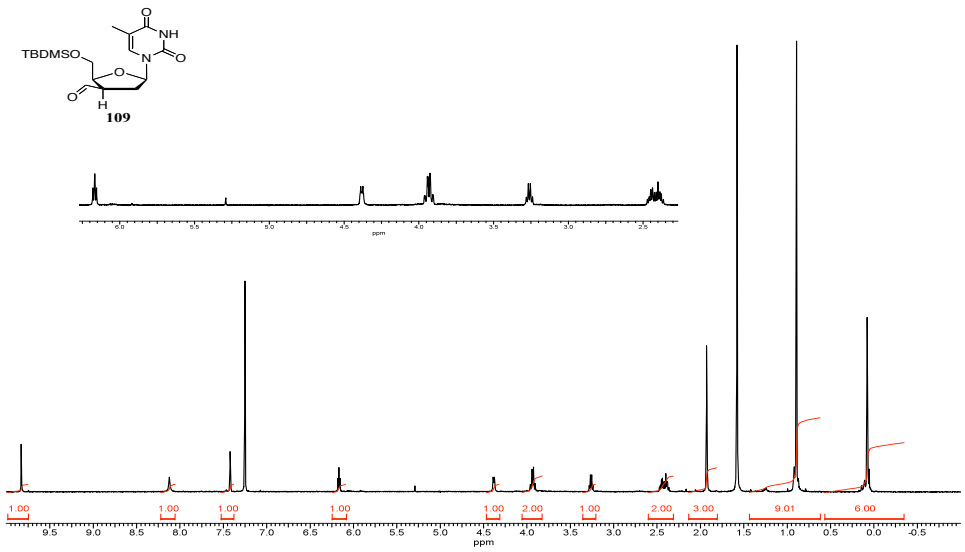

Figure 3: ^{1}H NMR spectrum of **109** in $CDCl_3$ (600 MHz)

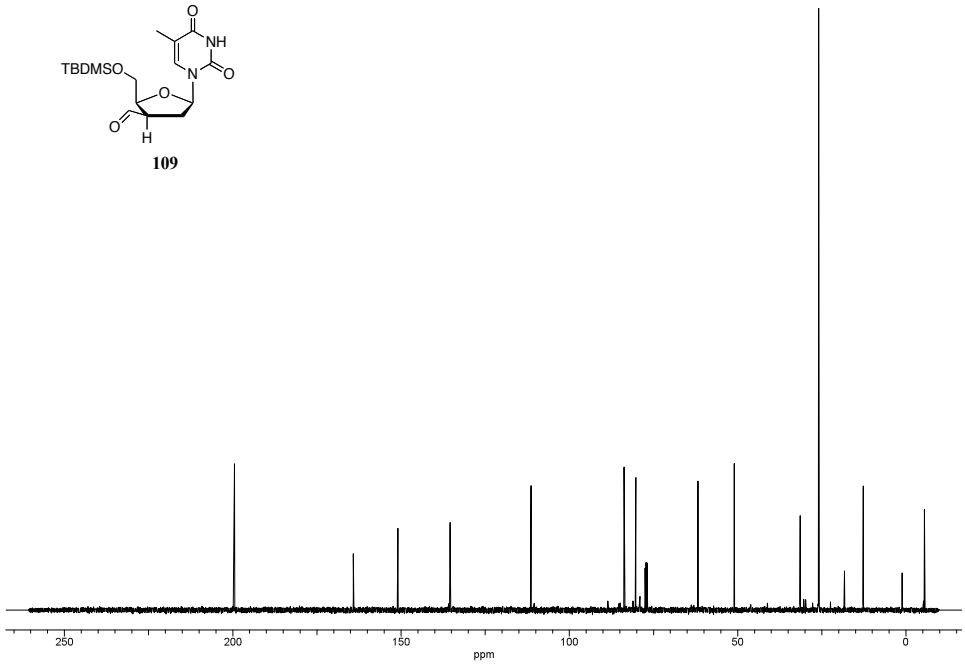

Figure 4: ^{13}C NMR spectrum of **109** in $CDCl_3$ (150 MHz)

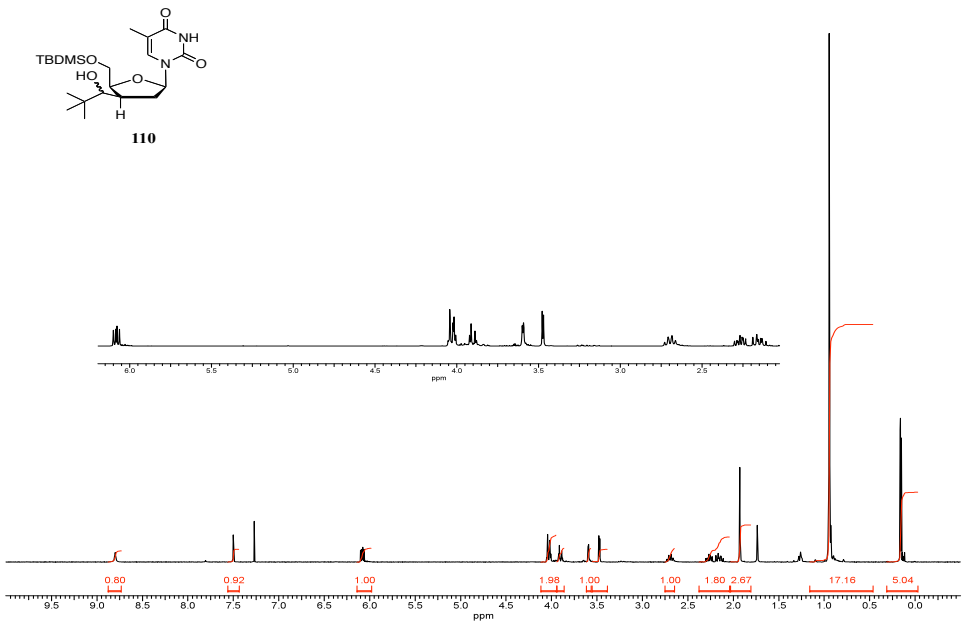

Figure 5: ^{1}H NMR spectrum of **110** in $CDCl_3$ (400 MHz)

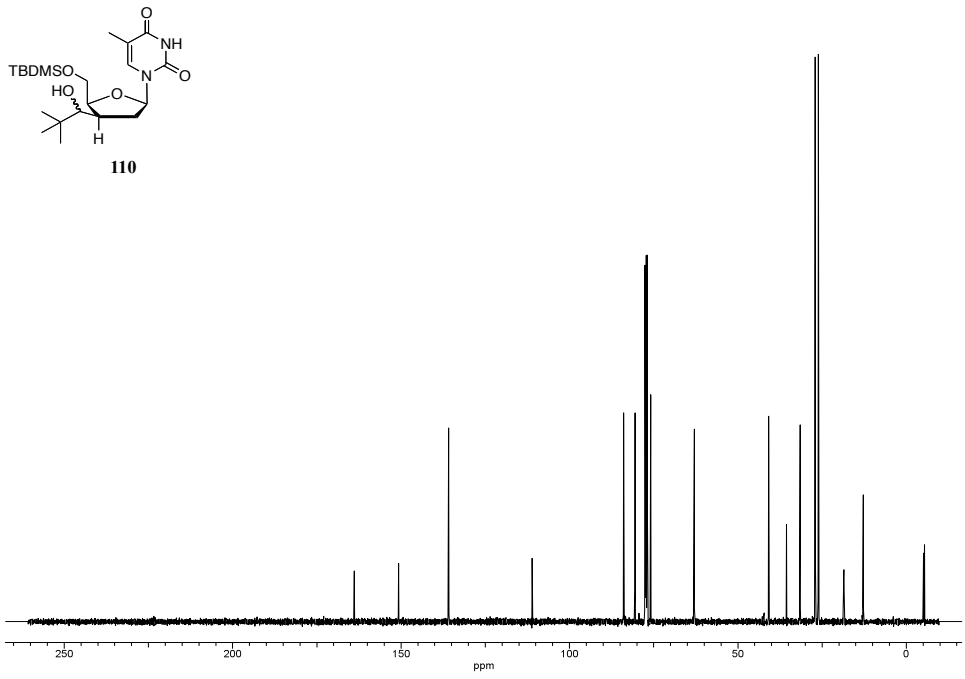

Figure 6: ^{13}C NMR spectrum of **110** in $CDCl_3$ (100 MHz)

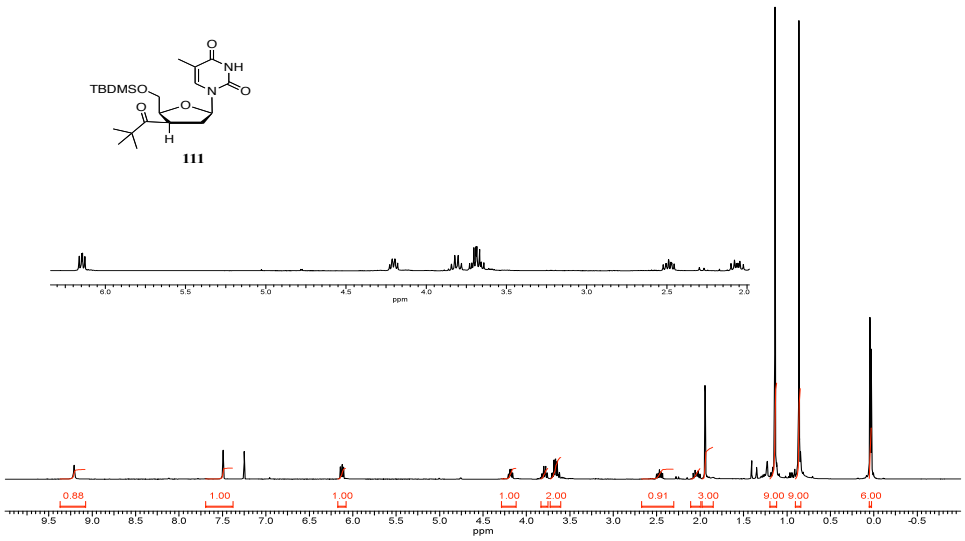

Figure 7: ^{1}H NMR spectrum of **111** in $CDCl_3$ (400 MHz)

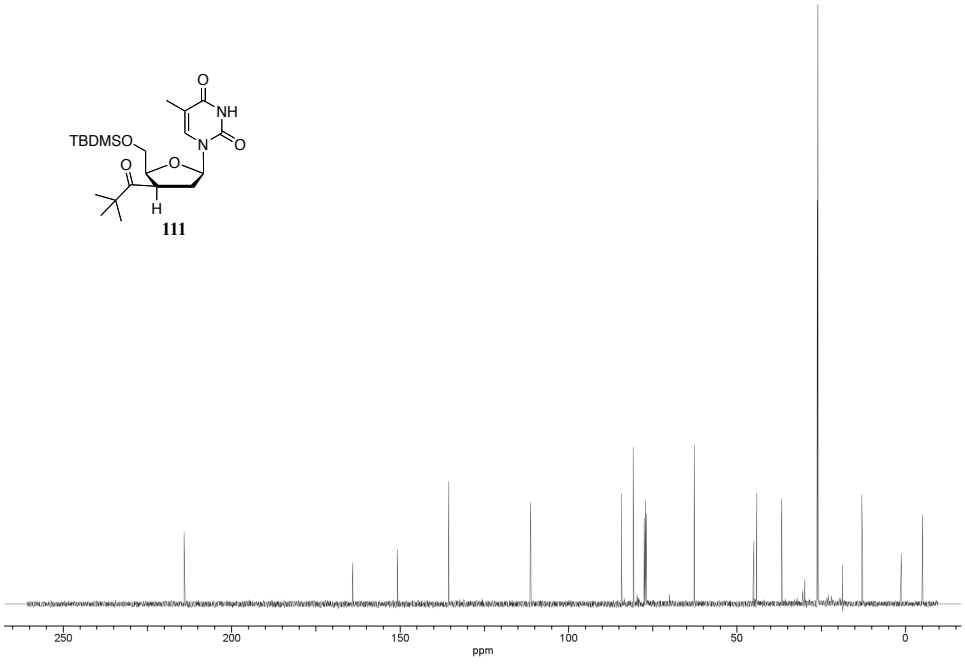

Figure 8: ^{13}C NMR spectrum of **111** in $CDCl_3$ (100 MHz)

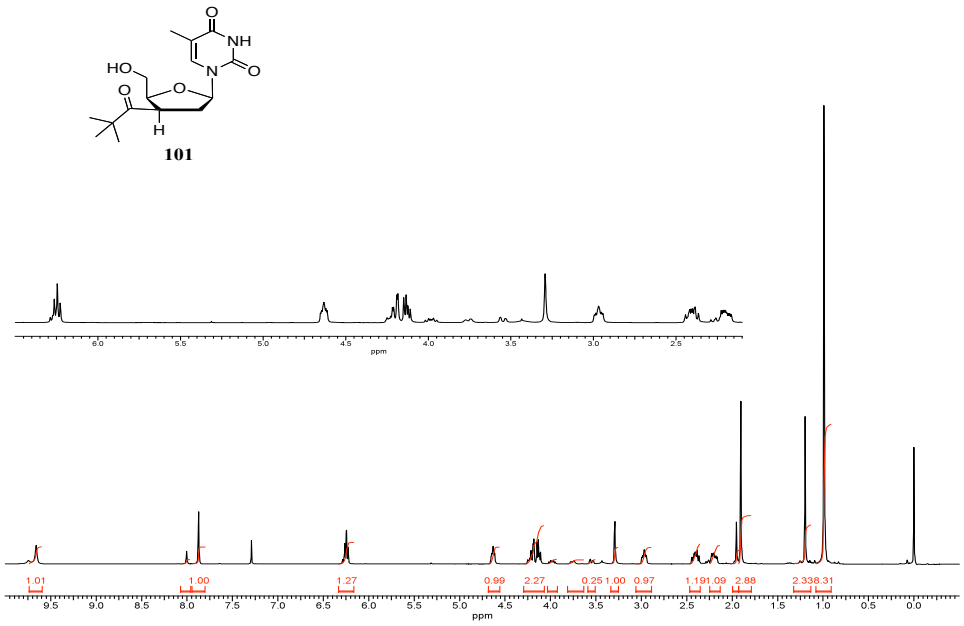

Figure 9: ^{1}H NMR spectrum of **101** in $CDCl_3$ (400 MHz)

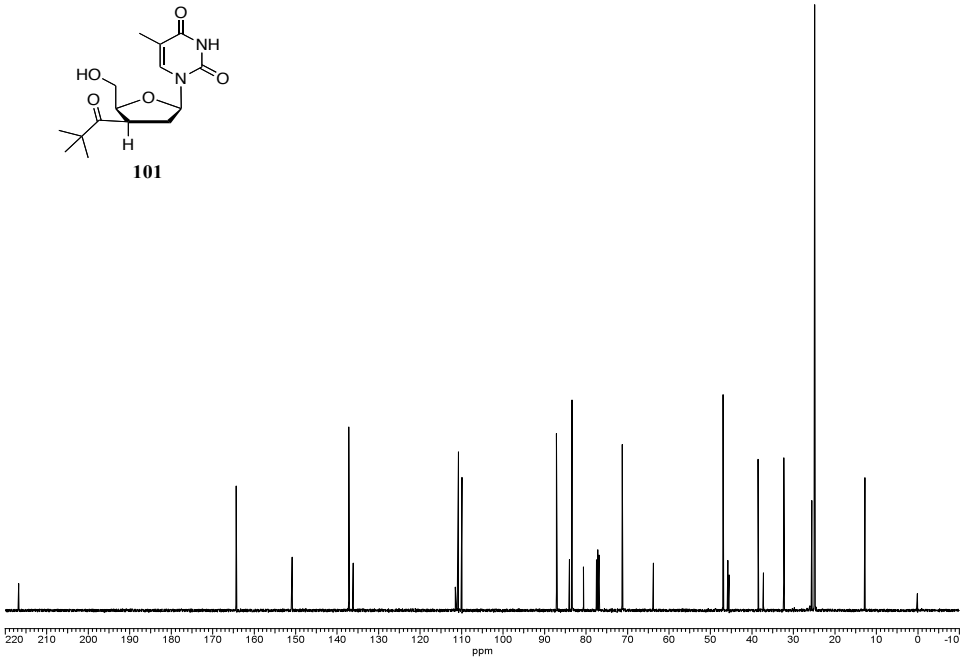

Figure 10: ^{13}C NMR spectrum of **101** in $CDCl_3$ (100 MHz)

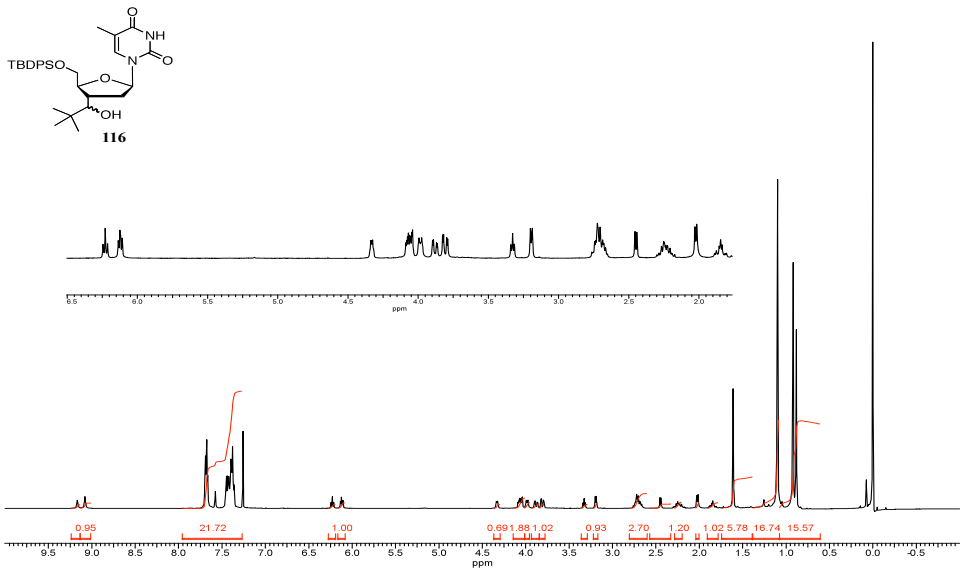

Figure 11: ^{1}H NMR spectrum of **116** in $CDCl_3$ (400 MHz)

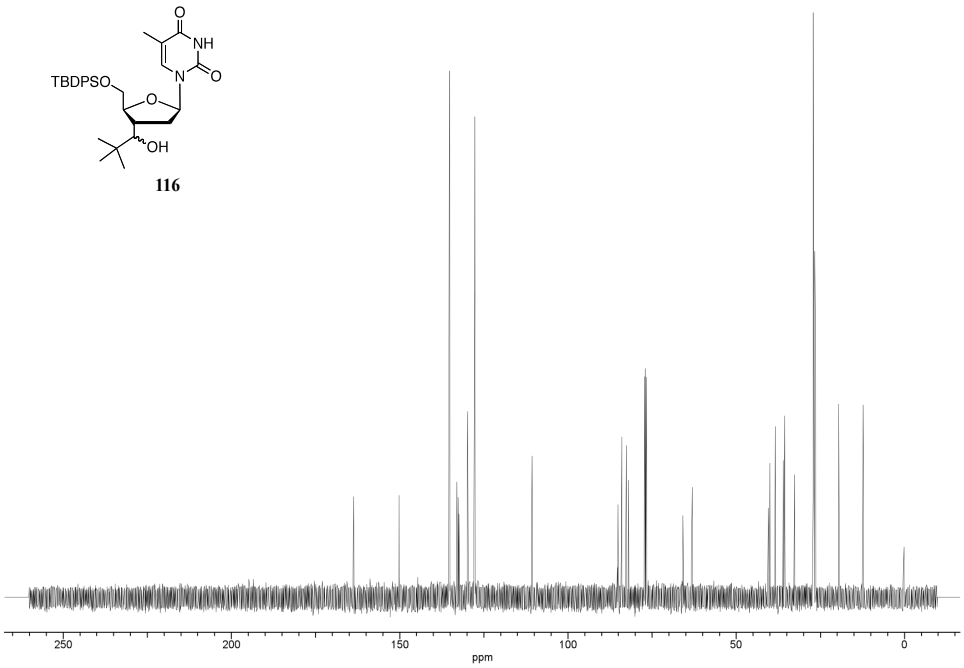

Figure 12: ^{13}C NMR spectrum of **116** in $CDCl_3$ (100 MHz)

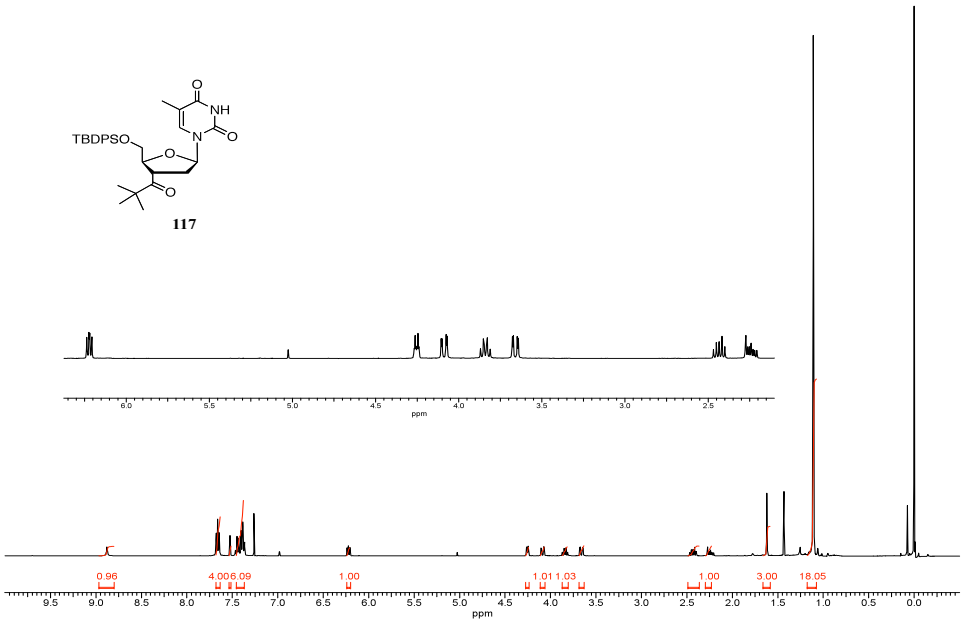

Figure 13: ^{1}H NMR spectrum of **117** in $CDCl_3$ (400 MHz)

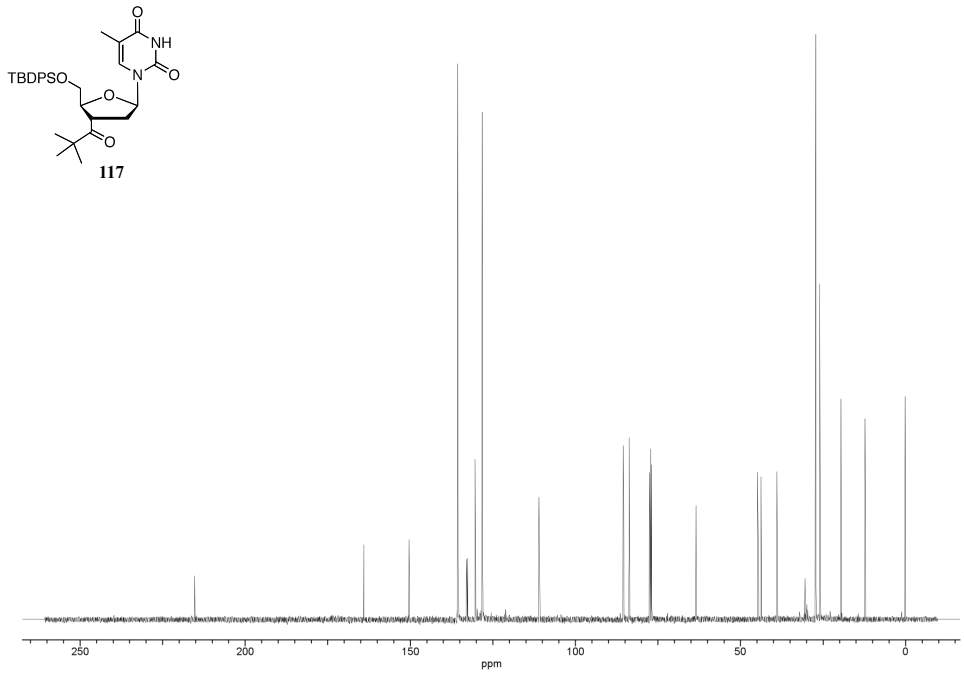

Figure 14: ^{13}C NMR spectrum of **117** in $CDCl_3$ (100 MHz)

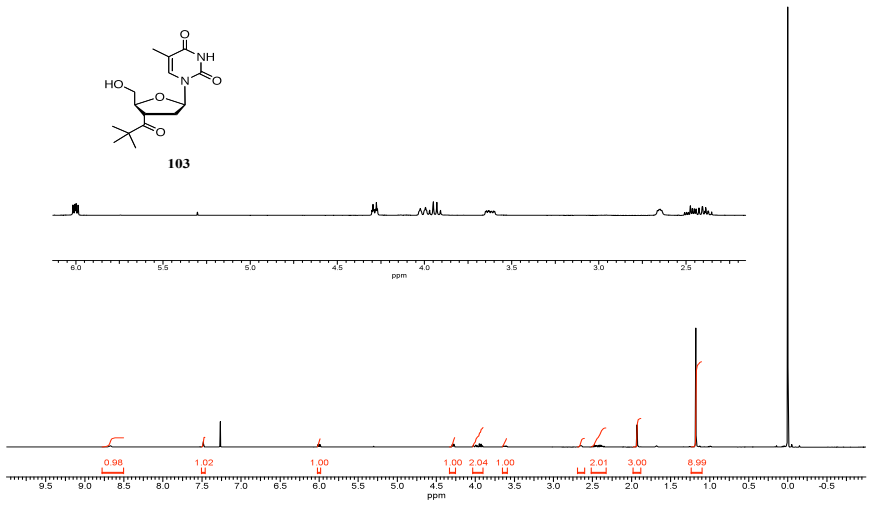

Figure 15: ^{1}H NMR spectrum of **103** in $CDCl_3$ (400 MHz)

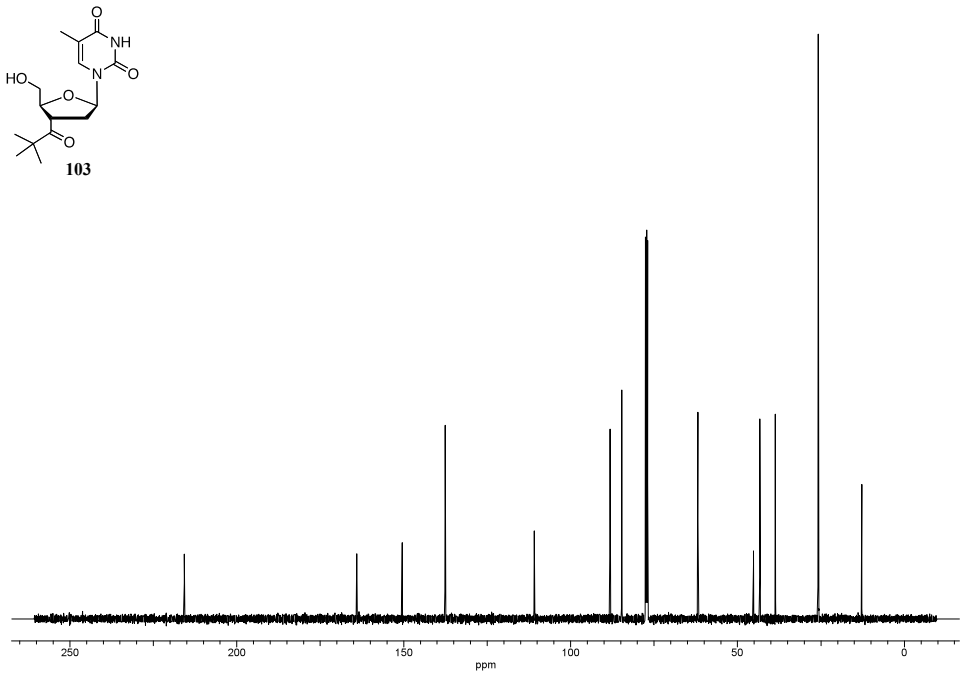

Figure 16: ^{13}C NMR spectrum of **103** in $CDCl_3$ (100 MHz)

References

1. *Radiation, People and the Environment*. International Atomic Energy Agency (IAEA), 2004.

2. *Ionizing Radiation Fact Book*. United States Environmental Protection Agency, 2007.

3. von Sonntag, C., *The Chemical Basis for Radiation Biology*. Taylor and Francis: London, 1987.

4. Sanche, L., Low-Energy Electron Interaction with DNA: Bond Dissociation and Formation of Transient Anions, Radicals, and Radical Anions. In *Radical and Radical Ion Reactivity in Nucleic Acid Chemistry*, Greenberg, M. M., Ed. A John Wiely & Sons, Inc.: Canada, 2009; pp 239-293.

5. Huels, M. A.; Boudaiffa, B.; Cloutier, P.; Hunting, D.; Sanche, L., Single, double, and multiple double strand breaks induced in DNA by 3-100 eV electrons. *Journal of the American Chemical Society* **2003,** *125* (15), 4467-4477.

6. Pimblott, S. M.; LaVerne, J. A., Production of low-energy electrons by ionizing radiation. *Radiat Phys Chem* **2007,** *76* (8-9), 1244-1247.

7. Moretto-Capelle, P.; Le Padellec, A., Electron spectroscopy in proton collisions with dry gas-phase uracil base. *Phys Rev A* **2006,** *74* (062705-062709).

8. Boudaiffa, B.; Cloutier, P.; Hunting, D.; Huels, M. A.; Sanche, L., Resonant formation of DNA strand breaks by low-energy (3 to 20 eV) electrons. *Science* **2000,** *287* (5458), 1658-1660.

9. Simons, J., How do low-energy (0.1-2 eV) electrons cause DNA-strand breaks? *Accounts Chem Res* **2006,** *39* (10), 772-779.

10. Zheng, Y.; Cloutier, P.; Hunting, D. J.; Wagner, J. R.; Sanche, L., Glycosidic bond cleavage of thymidine by low-energy electrons. *Journal of the American Chemical Society* **2004,** *126* (4), 1002-1003.

11. Buxton, G. V., The Radiation Chemistry of Liquid Water: Principles and Applications. In *Charged Particle and Photon Interactions With Matter: Chemical, Physicochemical, and Biological Consequences with Applications*, Mozumder, A., Hatano,Y, Ed. Marcel Dekker, Inc.: New York, 2004; pp 331-363.

12. Valko, M.; Izakovic, M.; Mazur, M.; Rhodes, C. J.; Telser, J., Role of oxygen radicals in DNA damage and cancer incidence. *Molecular and cellular biochemistry* **2004,** *266* (1-2), 37-56.

13. Hussain, S. P.; Hofseth, L. J.; Harris, C. C., Radical causes of cancer. *Nat Rev Cancer* **2003,** *3* (4), 276-285.

14. Federico, A.; Morgillo, F.; Tuccillo, C.; Ciardiello, F.; Loguercio, C., Chronic inflammation and oxidative stress in human carcinogenesis. *International Journal of Cancer* **2007,** *121* (11), 2381-2386.

15. von Sonntag, C., *Free-Radical-Induced DNA Damage and Its Repair: A Chemical Perspective*. Springer-Verlag Berlin: Germany, 2006.

16. Greenberg, M. M., Pyrimidine Nucleobase Radical Reactivity. In *Radical and Radical Ion Reactivity in Nucleic Acid Chemistry*, Greenberg, M. M., Ed. A John Wiely & Sons, Inc.: Canada, 2009; pp 135-162.

17. Dedon, P. C., The chemical toxicology of 2-deoxyribose oxidation in DNA. *Chemical research in toxicology* **2008,** *21* (1), 206-219.

18. Chatgilialoglu, C., Reactivity of Nucleic Acid Sugar Radicals. In *Radical and Radical Ion Reactivity in Nucleic Acid Chemistry*, Greenberg, M. M., Ed. A John Wiely & Sons, Inc.: Canada, 2009; pp 99-133.

19. Balasubramanian, B.; Pogozelski, W. K.; Tullius, T. D., DNA strand breaking by the hydroxyl radical is governed by the accessible surface areas of the hydrogen atoms of the DNA backbone. *Proceedings of the National Academy of Sciences of the United States of America* **1998,** *95* (17), 9738-9743.

20. Goodman, B. K.; Greenberg, M. M., Independent generation and reactivity of 2'-deoxyurid-1'-yl. *Journal of Organic Chemistry* **1996,** *61* (1), 2-3.

21. Hwang, J. T.; Greenberg, M. M., Kinetics and stereoselectivity of thiol trapping of deoxyuridin-1 '-yl in biopolymers and their relationship to the formation of premutagenic alpha-deoxynucleotides. *Journal of the American Chemical Society* **1999,** *121* (18), 4311-4315.

22. Tronche, C.; Goodman, B. K.; Greenberg, M. M., DNA damage induced via independent generation of the radical resulting from formal hydrogen atom abstraction from the C1'-position of a nucleotide. *Chemistry & biology* **1998,** *5* (5), 263-271.

23. Chatgilialoglu, C.; Ferreri, C.; Bazzanini, R.; Guerra, M.; Choi, S. Y.; Emanuel, C. J.; Horner, J. H.; Newcomb, M., Models of DNA C1 ' radicals. Structural, spectral, and chemical properties of the thyminylmethyl radical and the 2 '-deoxyuridin-1 '-yl radical. *Journal of the American Chemical Society* **2000,** *122* (39), 9525-9533.

24. Tallman, K. A.; Tronche, C.; Yoo, D. J.; Greenberg, M. M., Release of superoxide from nucleoside peroxyl radicals, a double-edged sword? *Journal of the American Chemical Society* **1998,** *120* (20), 4903-4909.

25. Zheng, Y.; Sheppard, T. L., Half-life and DNA strand scission products of 2-deoxyribonolactone oxidative DNA damage lesions. *Chemical research in toxicology* **2004,** *17* (2), 197-207.

26. Hashimoto, M.; Greenberg, M. M.; Kow, Y. W.; Hwang, J. T.; Cunningham, R. P., The 2-deoxyribonolactone lesion produced in DNA by neocarzinostatin and other damaging agents forms cross-links with the base-excision repair enzyme endonuclease III. *Journal of the American Chemical Society* **2001,** *123* (13), 3161-3162.

27. DeMott, M. S.; Beyret, E.; Wong, D.; Bales, B. C.; Hwang, J. T.; Greenberg, M. M.; Demple, B., Covalent trapping of human DNA polymerase beta by the oxidative DNA lesion 2-deoxyribonolactone. *Journal of Biological Chemistry* **2002,** *277* (10), 7637-7640.

28. Hwang, J. T.; Tallman, K. A.; Greenberg, M. M., The reactivity of the 2-deoxyribonolactone lesion in single-stranded DNA and its implication in reaction mechanisms of DNA damage and repair. *Nucleic acids research* **1999,** *27* (19), 3805-3810.

29. Sugiyama, H.; Tsutsumi, Y.; Fujimoto, K.; Saito, I., Photoinduced Deoxyribose-C2' Oxidation in DNA - Alkali-Dependent Cleavage of Erythrose-Containing Sites Via a Retroaldol Reaction. *Journal of the American Chemical Society* **1993,** *115* (11), 4443-4448.

30. Kawai, K.; Saito, I.; Sugiyama, H., Conformation-dependent photochemistry of 5-halouracil-containing DNA: Stereospecific 2 'alpha-hydroxylation of deoxyribose in Z-form DNA. *Journal of the American Chemical Society* **1999,** *121* (6), 1391-1392.

31. Oyoshi, T.; Kawai, K.; Sugiyama, H., Efficient C2 'alpha-hydroxylation of deoxyribose in protein-induced Z-form DNA. *Journal of the American Chemical Society* **2003,** *125* (6), 1526-1531.

32. Kim, J.; Weledji, Y. N.; Greenberg, M. M., Independent generation and characterization of a C2'-oxidized abasic site in chemically synthesized oligonucleotides. *Journal of Organic Chemistry* **2004,** *69* (18), 6100-6104.

33. Bryant-Friedrich, A. C., Fate of DNA Sugar Radicals. In *Advances in Molecular Toxicology*, Fishein, J. C., Ed. Elsevier B. V: 2010; Vol. 4, pp 127-155.

34. Sitlani, A.; Long, E. C.; Pyle, A. M.; Barton, J. K., DNA Photocleavage by Phenanthrenequinone Diimine Complexes of Rhodium(Iii) - Shape-Selective Recognition and Reaction. *Journal of the American Chemical Society* **1992,** *114* (7), 2303-2312.

35. Brunner, J.; Barton, J. K., Site-specific DNA photocleavage by rhodium intercalators analyzed by MALDI-TOF mass spectrometry. *Journal of the American Chemical Society* **2006,** *128* (21), 6772-6773.

36. Korner, S.; Bryant-Friedrich, A.; Giese, B., C-3'-Branched Thymidines as Precursors for the Selective Generation of C-3'-Nucleoside Radicals. *The Journal of organic chemistry* **1999,** *64* (5), 1559-1564.

37. Stubbe, J.; Kozarich, J. W., Mechanisms of Bleomycin-Induced DNA-Degradation. *Chemical reviews* **1987,** *87* (5), 1107-1136.

38. Bryant-Friedrich, A. C., Generation of a C-3'-thymidinyl radical in single-stranded oligonucleotides under anaerobic conditions. *Organic letters* **2004,** *6* (14), 2329-32.

39. Lahoud, G. A.; Hitt, A. L.; Bryant-Friedrich, A. C., Aerobic fate of the C-3'-thymidinyl radical in single-stranded DNA. *Chemical research in toxicology* **2006,** *19* (12), 1630-6.

40. Awada, M.; Dedon, P. C., Formation of the 1,N2-glyoxal adduct of deoxyguanosine by phosphoglycolaldehyde, a product of 3 '-deoxyribose oxidation in DNA. *Chemical research in toxicology* **2001,** *14* (9), 1247-1253.

41. Giese, B.; Imwinkelried, P.; Petta, M., Synthesis of a Modified Thymidine and Preparation of Precursors of Oligonucleotide Radicals. *Synlett* **1994,** (12), 1003-1004.

42. Giese, B.; Erdmann, P.; Schafer, T.; Schwitter, U., Synthesis of a 4'-Selenated 2-Deoxyadenosine Derivative - a Novel Precursor Suitable for the Preparation of Modified Oligonucleotides. *Synthesis-Stuttgart* **1994**, 1310-1312.

43. Giese, B.; Beyrich-Graf, X.; Erdmann, P.; Petretta, M.; Schwitter, U., The chemistry of single-stranded 4'-DNA radicals: influence of the radical precursor on anaerobic and aerobic strand cleavage. *Chemistry & biology* **1995,** *2* (6), 367-375.

44. Giese, B.; Dussy, A.; Meggers, E.; Petretta, M.; Schwitter, U., Conformation, lifetime, and repair of 4'-DNA radicals. *Journal of the American Chemical Society* **1997,** *119* (45), 11130-11131.

45. Dussy, A.; Meggers, E.; Giese, B., Spontaneous cleavage of 4 '-DNA radicals under aerobic conditions: Apparent discrepancy between trapping rates and cleavage products. *Journal of the American Chemical Society* **1998,** *120* (30), 7399-7403.

46. Giese, B.; Beyrichgraf, X.; Erdmann, P.; Giraud, L.; Imwinkelried, P.; Muller, S. N.; Schwitter, U., Cleavage of Single-Stranded 4'-Oligonucleotide Radicals in the Presence of O2. *Journal of the American Chemical Society* **1995,** *117* (22), 6146-6147.

47. Dedon, P. C.; Plastaras, J. P.; Rouzer, C. A.; Marnett, L. J., Indirect mutagenesis by oxidative DNA damage: Formation of the pyrimidopurinone adduct of deoxyguanosine by base propenal. *Proceedings of the National Academy of Sciences of the United States of America* **1998,** *95* (19), 11113-11116.

48. Zhou, X. F.; Taghizadeh, K.; Dedon, P. C., Chemical and biological evidence for base propenals as the major source of the endogenous M(1)dG adduct in cellular DNA. *Journal of Biological Chemistry* **2005,** *280* (27), 25377-25382.

49. Jaruga, P.; Dizdaroglu, M., 8,5 '-Cyclopurine-2 '-deoxynucleosides in DNA: Mechanisms of formation, measurement, repair and biological effects. *DNA Repair* **2008,** *7* (9), 1413-1425.

50. Flyunt, R.; Bazzanini, R.; Chatgilialoglu, C.; Mulazzani, Q. G., Fate of the 2 '-deoxyadenosin-5 '-yl radical under anaerobic conditions. *Journal of the American Chemical Society* **2000,** *122* (17), 4225-4226.

51. Chatgilialoglu, C.; Guerra, M.; Mulazzani, Q. G., Model studies of DNA C5 ' radicals. Selective generation and reactivity of 2 '-deoxyadenosin-5 '-yl radical. *Journal of the American Chemical Society* **2003,** *125* (13), 3839-3848.

52. Boussicault, F.; Kaloudis, P.; Caminal, C.; Mulazzani, Q. G.; Chatgilialoglu, C., The fate of C5 ' radicals of purine nucleosides under oxidative conditions. *Journal of the American Chemical Society* **2008,** *130* (26), 8377-8385.

53. Dedon, P. C.; Goldberg, I. H., Free-Radical Mechanisms Involved in the Formation of Sequence-Dependent Bistranded DNA Lesions by the Antitumor Antibiotics Bleomycin, Neocarzinostatin, and Calicheamicin. *Chemical research in toxicology* **1992,** *5* (3), 311-332.

54. Chen, B. Z.; Bohnert, T.; Zhou, X. F.; Dedon, P. C., 5 '-(2-phosphoryl-1,4-dioxobutane) as a product of 5 '-oxidation of deoxyribose in DNA: Elimination as trans-1,4-dioxo-2-butene and approaches to analysis. *Chemical research in toxicology* **2004,** *17* (11), 1406-1413.

55. Angeloff, A.; Dubey, I.; Pratviel, G.; Bernadou, J.; Meunier, B., Characterization of a 5 '-aldehyde terminus resulting from the oxidative attack at C5 ' of a 2-deoxyribose on DNA. *Chemical research in toxicology* **2001,** *14* (10), 1413-1420.

56. Pratviel, G.; Pitie, M.; Bernadou, J.; Meunier, B., Furfural as a Marker of DNA Cleavage by Hydroxylation at the 5' Carbon of Deoxyribose. *Angew Chem Int Edit* **1991,** *30* (6), 702-704.

57. Barciszewski, J.; Siboska, G. E.; Pedersen, B. O.; Clark, B. F.; Rattan, S. I., A mechanism for the in vivo formation of N6-furfuryladenine, kinetin, as a secondary oxidative damage product of DNA. *Febs Lett* **1997,** *414* (2), 457-60.

58. Chen, B. Z.; Vu, C. C.; Byrns, M. C.; Dedon, P. C.; Peterson, L. A., Formation of 1,4-dioxo-2-butene-derived adducts of 2 '-deoxyadenosine and 2 '-deoxycytidine in oxidized DNA. *Chemical research in toxicology* **2006,** *19* (8), 982-985.

59. Gingipalli, L.; Dedon, P. C., Reaction of cis- and trans-2-Butene-1,4-dial with 2'-deoxycytidine to form stable oxadiazabicyclooctaimine adducts. *Journal of the American Chemical Society* **2001,** *123* (11), 2664-2665.

60. Lyngdoh, R. H. D.; Schaefer, H. F., Elementary Lesions in DNA Subunits: Electron, Hydrogen Atom, Proton, and Hydride Transfers. *Accounts Chem Res* **2009,** *42* (4), 563-572.

61. Hayon, E., Optical-Absorption Spectra of Ketyl Radicals and Radical Anions of Some Pyrimidines. *J Chem Phys* **1969,** *51* (11), 4881-4892.

62. Berdys, J.; Skurski, P.; Simons, J., Damage to model DNA fragments by 0.25-1.0 eV electrons attached to a thymine pi* orbital. *J Phys Chem B* **2004,** *108* (18), 5800-5805.

63. Berdys, J.; Anusiewicz, I.; Skurski, P.; Simons, J., Theoretical study of damage to DNA by 0.2-1.5 eV electrons attached to cytosine. *J Phys Chem A* **2004,** *108* (15), 2999-3005.

64. Berdys, J.; Anusiewicz, I.; Skurski, P.; Simons, J., Damage to model DNA fragments from very low-energy (< 1 eV) electrons. *Journal of the American Chemical Society* **2004,** *126* (20), 6441-6447.

65. Sevilla, A. K. M. D., Theoretical Modeling of Radiation-Induced DNA Damage. In *Radical and Radical Ion Reactivity in Nucleic Acid Chemistry*, Greenberg, M. M., Ed. A John Wiely & Sons, Inc.: Canada, 2009; pp 1-40.

66. Zheng, Y.; Cloutier, P.; Hunting, D. J.; Sanche, L.; Wagner, J. R., Chemical basis of DNA sugar-phosphate cleavage by low-energy electrons. *Journal of the American Chemical Society* **2005,** *127* (47), 16592-16598.

67. Antic, D.; Parenteau, L.; Sanche, L., Electron-stimulated desorption of H- from condensed-phase deoxyribose analogues: Dissociative electron attachment versus resonance decay into dipolar dissociation. *J Phys Chem B* **2000,** *104* (19), 4711-4716.

68. Ptasinska, S.; Denifl, S.; Scheier, P.; Mark, T. D., Inelastic electron interaction (attachment/ionization) with deoxyribose. *J Chem Phys* **2004,** *120* (18), 8505-8511.

69. Abdoul-Carime, H.; Gohlke, S.; Illenberger, E., Site-specific dissociation of DNA bases by slow electrons at early stages of irradiation. *Phys Rev Lett* **2004,** *92* (16), 168103.

70. Abdoul-Carime, H.; Cloutier, P.; Sanche, L., Low-energy (5-40 eV) electron-stimulated desorption of anions from physisorbed DNA bases. *Radiation research* **2001,** *155* (4), 625-33.

71. Dugal, P. C.; Abdoul-Carime, H.; Sanche, L., Mechanisms for low-energy (0.5-30 eV) electron-induced pyrimidine ring fragmentation within thymine- and halogen-substituted single strands of DNA. *J Phys Chem B* **2000,** *104* (23), 5610-5617.

72. Abdoul-Carime, H.; Dugal, P. C.; Sanche, L., Damage induced by 1-30 eV electrons on thymine- and bromouracil-substituted oligonucleotides. *Radiation research* **2000,** *153* (1), 23-28.

73. Pan, X.; Cloutier, P.; Hunting, D.; Sanche, L., Dissociative electron attachment to DNA. *Phys Rev Lett* **2003,** *90* (20), 208102-1-208102-4.

74. Martin, F.; Burrow, P. D.; Cai, Z.; Cloutier, P.; Hunting, D.; Sanche, L., DNA strand breaks induced by 0-4 eV electrons: the role of shape resonances. *Phys Rev Lett* **2004,** *93* (6), 068101-1-068101-4.

75. Ptasinska, S.; Sanche, L., Dissociative electron attachment to abasic DNA. *Physical chemistry chemical physics : PCCP* **2007,** *9* (14), 1730-5.

76. Becker, D.; Bryant-Friedrich, A.; Trzasko, C.; Sevilla, M. D., Electron spin resonance study of DNA irradiated with an argon-ion beam: Evidence for formation of sugar phosphate backbone radicals. *Radiation research* **2003,** *160* (2), 174-185.

77. Pogozelski, W. K.; Tullius, T. D., Oxidative strand scission of nucleic acids: Routes initiated by hydrogen abstraction from the sugar moiety. *Chemical reviews* **1998,** *98* (3), 1089-1107.

78. Greenberg, M. M., Elucidating DNA damage and repair processes by independently generating reactive and metastable intermediates. *Organic & biomolecular chemistry* **2007,** *5* (1), 18-30.

79. Newman, C. A.; Resendiz, M. J. E.; Sczepanski, J. T.; Greenberg, M. M., Photochemical Generation and Reactivity of the 5,6-Dihydrouridin-6-yl Radical. *Journal of Organic Chemistry* **2009,** *74* (18), 7007-7012.

80. Giese, B., Long distance charge transport in DNA: The hopping mechanism. *Accounts Chem Res* **2000,** *33* (9), 631-636.

81. Giese, B., Long-distance electron transfer through DNA. *Annual review of biochemistry* **2002,** *71*, 51-70.

82. Greenberg, M. M., Investigating nucleic acid damage processes via independent generation of reactive intermediates. *Chemical research in toxicology* **1998,** *11* (11), 1235-1248.

83. Hong, I. S.; Greenberg, M. M., Mild generation of 5-(2'-deoxyuridinyl)methyl radical from a phenyl selenide precursor. *Organic letters* **2004,** *6* (26), 5011-5013.

84. Carter, K. N.; Greenberg, M. M., Independent generation and study of 5,6-Dihydro-2'-deoxyuridin-6-yl, a member of the major family of reactive intermediates formed in DNA from the effects of gamma-radiolysis. *The Journal of organic chemistry* **2003,** *68* (11), 4275-4280.

85. Carter, K. N.; Greenberg, M. M., Tandem lesions are the major products resulting from a pyrimidine nucleobase radical. *Journal of the American Chemical Society* **2003,** *125* (44), 13376-13378.

86. Greenberg, M. M.; Barvian, M. R.; Cook, G. P.; Goodman, B. K.; Matray, T. J.; Tronche, C.; Venkatesan, H., DNA damage induced via 5,6-dihydrothymid-5-yl in single-stranded oligonucleotides. *Journal of the American Chemical Society* **1997,** *119* (8), 1828-1839.

87. Lunazzi, L.; Ingold, K. U.; Scaiano, J. C., Absolute Rate Constants for the Decarbonylation of the Phenylacetyl Radical. *J Phys Chem-Us* **1983,** *87* (4), 529-530.

88. Hany, R.; Fischer, H., Absolute Chemically-Induced Nuclear Polarizations from the Photodissociation of Phenylsubstituted Ketones - Radical Pair Precursor States and Memory Effects. *Chem Phys* **1993,** *172* (1), 131-146.

89. Anderson, A. S.; Hwang, J. T.; Greenberg, M. M., Independent generation and reactivity of 2 '-deoxy-5-methyleneuridin-5-yl, a significant reactive intermediate produced from thymidine as a result of oxidative stress. *Journal of Organic Chemistry* **2000,** *65* (15), 4648-4654.

90. Manetto, A.; Georganakis, D.; Leondiadis, L.; Gimisis, T.; Mayer, P.; Carell, T.; Chatgilialoglu, C., Independent generation of C5'-nucleosidyl radicals in thymidine and 2'-deoxyguanosine. *The Journal of organic chemistry* **2007,** *72* (10), 3659-3666.

91. Giese, B.; Beyrichgraf, X.; Erdmann, P.; Petretta, M.; Schwitter, U., The Chemistry of Single-Stranded 4'-DNA Radicals - Influence of the Radical Precursor on Anaerobic and Aerobic Strand Cleavage. *Chemistry & biology* **1995,** *2* (6), 367-375.

92. Marx, A.; Erdmann, P.; Senn, M.; Korner, S.; Jungo, T.; Petretta, M.; Imwinkelried, P.; Dussy, A.; Kulicke, K. J.; Macko, L.; Zehnder, M.; Giese, B., Synthesis of 4'-C-acylated thymidines. *Helv Chim Acta* **1996,** *79* (7), 1980-1994.

93. Emanuel, C. J.; Newcomb, M.; Ferreri, C.; Chatgilialoglu, C., Kinetics of 2 '-deoxynridin-1 '-yl radical reactions. *Journal of the American Chemical Society* **1999,** *121* (12), 2927-2928.

94. Wengel, J. S., M.; Jorgensen, P.; Nielsen, C., Synthesis of Novel 3'-C-(Hydroxymethyl)thymidines and Oligodeoxynucleotide analogues containing Compressed 3'-C-Hydroxymethyl-Linked Phosphodiester Backbones. *Nucleosides & Nucleotides* **1995,** *14* (7), 1465-1479.

95. Audat, S. A.; Love, C. T.; Al-Oudat, B. A.; Bryant-Friedrich, A. C., Synthesis of C3' modified nucleosides for selective generation of the C3'-deoxy-3'-thymidinyl radical: a proposed intermediate in LEE induced DNA damage. *The Journal of organic chemistry* **2012,** *77* (8), 3829-37.

96. Chu, C. K.; Doboszewski, B.; Schmidt, W.; Ullas, G. V., Synthesis of Pyrimidine 3'-Allyl-2',3'-Dideoxyribonucleosides by Free-Radical Coupling. *Journal of Organic Chemistry* **1989,** *54* (11), 2767-2769.

97. Sanghvi, Y. S.; Bharadwaj, R.; Debart, F.; Demesmaeker, A., Efficient and Stereoselective Synthesis of 3'-Deoxy 3'-C-Branched-Chain Substituted Thymidine. *Synthesis-Stuttgart* **1994,** (11), 1163-1166.

98. Tsentalovich, Y. P.; Fischer, H., Solvent Effect on the Decarbonylation of Acyl Radicals Studied by Laser Flash-Photolysis. *J Chem Soc Perk T 2* **1994,** (4), 729-733.

99. Meister, A.; Anderson, M. E., Glutathione. *Annual review of biochemistry* **1983,** *52*, 711-60.

100. Barciszewski, J.; Siboska, G. E.; Pedersen, B. O.; Clark, B. F. C.; Rattan, S. I. S., A mechanism for the in vivo formation of N-6-furfuryladenine, kinetin, as a secondary oxidative damage product of DNA. *Febs Lett* **1997,** *414* (2), 457-460.

101. Lahoud, G.; Fancher, J.; Grosu, S.; Cavanaugh, B.; Bryant-Friedrich, A., Automated synthesis, characterization, and structural analysis of oligonucleotide C-3'-radical precursors. *Bioorganic & medicinal chemistry* **2006,** *14* (8), 2581-8.

102. Kodama, T.; Greenberg, M. M., Preparation and analysis of oligonucleotides containing lesions resulting from C5 '-oxidation. *Journal of Organic Chemistry* **2005,** *70* (24), 9916-9924.

103. Junker, H. D.; Hoehn, S. T.; Bunt, R. C.; Marathius, V.; Chen, J.; Turner, C. J.; Stubbe, J., Synthesis, characterization and solution structure of tethered oligonucleotides containing an internal 3'-phosphoglycolate, 5'-phosphate gapped lesion. *Nucleic acids research* **2002,** *30* (24), 5497-508.

104. Debarge, S.; Balzarini, J.; Maguire, A. R., Design and synthesis of alpha-carboxy phosphononucleosides. *The Journal of organic chemistry* **2011,** *76* (1), 105-126.

105. Grierson, J. R.; Brockenbrough, J. S.; Rasey, J. S.; Wiens, L. W.; Schwartz, J. L.; Jordan, R.; Vesselle, H., Evaluation of 5'-deoxy-5'-[F-18]fluorothymidine as a tracer of intracellular thymidine phosphorylase activity. *Nuclear medicine and biology* **2007,** *34* (5), 471-8.

106. Gotor, V.; Moris, F., Regioselective Acylation of 2'-Deoxynucleosides through an Enzymatic-Reaction with Oxime Esters. *Synthesis-Stuttgart* **1992,** (7), 626-628.

107. Navacchia, M. L.; Montevecchi, P. C., Sulfanyl radical promoted C4'-C5' bond scission of 5'-oxo-3',4'-didehydro-2',3'-dideoxynucleosides. *Organic & biomolecular chemistry* **2006,** *4* (20), 3754-3756.

108. Finkel, T.; Holbrook, N. J., Oxidants, oxidative stress and the biology of ageing. *Nature* **2000,** *408* (6809), 239-47.

109. Harris, G.; Ator, M.; Stubbe, J., Mechanism of Inactivation of Escherichia-Coli and Lactobacillus-Leichmannii Ribonucleotide Reductases by 2'-Chloro-2'-Deoxynucleotides - Evidence for Generation of 2-Methylene-3(2h)-Furanone. *Biochemistry* **1984,** *23* (22), 5214-5225.

110. Robert K. Boeckman, P. S., and Joseph J. Mullins THE DESS-MARTIN PERIODINANE: 1,1,1-TRIACETOXY-1,1-DIHYDRO-1,2-BENZIODOXOL-3(1H)-ONE. *Organic Syntheses* **Coll. Vol. 10, p.696 (2004); Vol. 77, p.141 (2000).**

111. Sanghvi, Y. S.; Ross, B.; Bharadwaj, R.; Vasseur, J. J., An Easy Access of 2',3'-Dideoxy-3'-Alpha-C-Formyl-Adenosine and 2',3'-Dideoxy-3'-Alpha-C-Formyl-Guanosine Analogs Via Stereoselective C-C Bond-Forming Radical Reaction. *Tetrahedron Lett* **1994,** *35* (27), 4697-4700.

112. Beauchard, A.; Phillips, V. A.; Lloyd, M. D.; Threadgill, M. D., Synthesis of 2-(4-carboxybutenyl)- and 2-(4-carboxybutynyl)-cyclopentene-1-carboxamides. *Tetrahedron* **2009,** *65* (39), 8176-8184.

113. Imamoto, T.; Takiyama, N.; Nakamura, K.; Hatajima, T.; Kamiya, Y., Reactions of Carbonyl-Compounds with Grignard-Reagents in the Presence of Cerium Chloride. *Journal of the American Chemical Society* **1989,** *111* (12), 4392-4398.

114. Negron, G.; Islas, G.; Diaz, Y.; Cruz, R.; Quicletsire, B., Straightforward Synthesis of 1-(2,3-Dideoxy-Beta-D-Glycero-Pent-2-Enofuranosyl)-Thymine. *Nucleosides & Nucleotides* **1994,** *13* (4), 1011-1013.

115. Kodama, T.; Greenberg, M. M., Preparation and analysis of oligonucleotides containing lesions resulting from C5'-oxidation. *The Journal of organic chemistry* **2005,** *70* (24), 9916-24.